

**BIOSYNTHESIS, CHARACTERIZATION AND ROLE OF EBOLA VIRUS
SECRETED GLYCOPROTEINS IN TARGET CELL ACTIVATION**

BY

**Victoria Jensen
B.S., University of New Hampshire, 1997
M.S., University of New Hampshire, 2000**

THESIS

**Submitted to the University of Manitoba
in Partial Fulfillment of
the Requirements for the Degree of**

Doctor of Philosophy

in

Medical Microbiology and Infectious Diseases

THE UNIVERSITY OF MANITOBA

FACULTY OF GRADUATE STUDIES

COPYRIGHT PERMISSION

**BIOSYNTHESIS, CHARACTERIZATION AND ROLE OF EBOLA VIRUS
SECRETED GLYCOPROTEINS IN TARGET CELL ACTIVATION**

BY

Victoria Jensen

A Thesis/Practicum submitted to the Faculty of Graduate Studies of The University of

Manitoba in partial fulfillment of the requirement of the degree

Of

DOCTOR OF PHILOSOPHY

Victoria Jensen © 2004

Permission has been granted to the Library of the University of Manitoba to lend or sell copies of this thesis/practicum, to the National Library of Canada to microfilm this thesis and to lend or sell copies of the film, and to University Microfilms Inc. to publish an abstract of this thesis/practicum.

This reproduction or copy of this thesis has been made available by authority of the copyright owner solely for the purpose of private study and research, and may only be reproduced and copied as permitted by copyright laws or with express written authorization from the copyright owner.

This Page is Intentionally Blank

This dissertation is dedicated to 6 wonderful women I have been fortunate enough to have in my life:

Mary Constantine taught me generosity and kindness.

Cornelia Dowd taught me to explore and love science.

Marylou Henn taught me to live my life with passion.

Carol Ann Nicholson for always seeing the best in people and always helping others. She had a gift of bringing beauty and light to everything she touched.

Adrienne LiCausi Vermilya for showing me that courage and determination can overcome any obstacle. Her peace, strength and dedication forever inspire me to do the best I can in my own life.

and my mom, **Erica Wahl**, who taught me to be a strong and confident woman by her example and to *always* reach for the stars! She gave me the opportunities she never had and I hope I will make her proud.

ACKNOWLEDGEMENTS

I am extremely thankful to the Department of Medical Microbiology for financial support and the Manitoba Health Research Council for 'Graduate Student Fellowships' in 2002-2004. I would like to thank all members of the department for their continued support and for always challenging me to develop into a better scientist. In particular, I want to thank Dr. Paul Hazelton for all his electron microscopy support and enthusiasm. It's nice to know someone loves Ebola particles as much as me! I am grateful to my committee members for their support and encouragement during the past 4 years.

I have been extremely fortunate to have the scientific opportunities afforded me. I am incredibly thankful to Heinz for inviting me to join his group. Throughout my studies he always encouraged me in the form of supporting my grants, conference presentations, and sending me to Dresden to pursue my endothelial studies and generally he always looked out for my well-being. I know he would say he is just doing his job and that's what makes him so great. I am also thankful to Dr. Hans-Joachim Schnittler and his group for welcoming me into their lab and teaching me so much. I will never forget the months I lived and worked in Dresden!

Thanks to everyone in Special Pathogens for helping me maintain my sanity, particularly my partner in crime, Allison Groseth. I guess I can tell you now that secretly I always thought Reston was cool. Thanks also to Alex "Mr. TLR/pDCs" Silaghi, Hideki Ebihara, Steve Jones, Lisa Fernando and Ricki Feldmann. Thanks to my friends in Dresden for many fun and crazy times: Jochen Seebach, Dirk Joachim, Michel Böckeler, and Gesine Haink.

To Chris, George, Cathy, Catherine, Jeff P., Justin, Jeff J., Robyn, Dade, Emma, Jim, Stacy and Grandma Jensen: thanks for your love and support. To the 'Goof Crew' for making me smile when I'm down: Jake, Ginger, Fat Mook & Sarah. To James: you are my love and my balance in life. No one can make me laugh like you do! To Uncle Len: for the childhood memories that always lift my spirits (John D., 7 lakes, Mets games, the garbage on the Whitestone Bridge and the list goes on). To my dad, Raymond Wahl: this is what happens when you buy your daughter microscopes and chemistry sets. And just for the record, the knee bone is connected to the shin bone.....

TABLE OF CONTENTS

	Page
Dedication.....	iv
Acknowledgement.....	v
Table of Contents.....	vi
List of Figures.....	x
List of Tables.....	xiii
ABSTRACT.....	xiv
SECTION	Page
1. Introduction	1
1.1 History of Filoviruses	1
1.2 Classification	3
1.2.1 Taxonomy and Nomenclature	3
1.2.2 Biohazard Classification	4
1.3 Genome Structure	5
1.4 Virion Morphology	7
1.5 Viral Proteins	8
1.5.1 Nucleoprotein	9
1.5.2 Virion Protein (VP) 35	10
1.5.3 Virion Protein (VP) 40	11
1.5.4 Glycoproteins	13
1.5.5 Virion Protein (VP) 30	20
1.5.6 Virion Protein (VP) 24	20
1.5.7 RNA-dependant RNA Polymerase (L)	22
1.6 Viral Replication Cycle	23
1.6.1 Growth Characteristics	23
1.6.2 Viral Attachment and Entry	23
1.6.3 Viral Replication in Susceptible Host Cells	27
1.7 Ebola Hemorrhagic Fever	29
1.7.1 Clinical Presentation of Ebola Hemorrhagic Fever	29
1.7.2 Transmission of Ebola Virus	30
1.7.3 Diagnosis	31
1.7.4 Therapy	32
1.7.5 Vaccine Developments	34

	Page
1.8 Pathogenesis	36
1.8.1 Projected Sequence of Infection	37
1.8.2 Viral Spreading and Role of the Endothelium	40
1.9 Objectives and Hypothesis	43
1.10 Significance of the Study	45
2. Materials and Methods	46
2.1 Cells	46
2.1.2 Eukaryotic Continuous Cell Lines	46
2.1.3 Isolation and Culture of Primary Human Monocytes- Macrophages	47
2.1.4 Isolation and Culture of Primary Human Umbilical Cord Endothelial Cells	47
2.1.5 <i>Escherichia coli</i> (<i>E.coli</i>)	49
2.2 Antibodies and Primers	49
2.3 Molecular Techniques	50
2.3.1 RNA Extraction	50
2.3.2 Polymerase Chain Reaction (PCR)	52
2.3.3 Reverse Transcriptase PCR (RT-PCR)	53
2.3.4 Real Time PCR-Relative Quantification of Transcript levels	54
2.3.5 Amplicon Analysis	55
2.4 Cloning	55
2.4.1 PCR Screen	56
2.4.2 Recombinant Vesicular Stomatitis Virus Plasmid	57
2.4.3 Soluble Glycoprotein Plasmids	58
2.4.4 ZEBOV Plasmids for Virus-Like Particle Production	60
2.5 Site-Directed Mutagenesis of ZEBOV Glycoproteins	60
2.6 Transfections	60
2.6.1 Optimization of Transfection Protocol	60
2.6.2 Expression and Purification of Recombinant Proteins	62
2.7 Protein Analysis	64
2.7.1 Harvesting of Cell Lysates	64
2.7.2 SDS-PAGE and Semi-Dry Transfer	65
2.7.3 Immunoblot	66
2.8 Production of Recombinant Vesicular Stomatitis Virus	66
2.8.1 Recombinant VSV-MARV GP ₁ Expression and Growth Characteristics	68
2.9 Characterization of Recombinant Proteins	68
2.9.2 Glycosylation	68
2.9.2 Oligomerization of Proteins	69
2.9.3 Characterization of GP ₁ Cysteine Mutants	69
2.10 Treatment of Macrophages with Secreted Glycoproteins and VLPs	70

	Page
2.10.1 Enzyme Linked Immunosorbant Assay	70
2.11 Treatment of HUVECs with Secreted Glycoproteins and VLPs	70
2.12 Immunofluorescence Assays (IFAs)	71
2.12.1 Activation of HUVECs	71
2.12.2 Junction proteins	71
2.12.3 Interaction of VLPs with Macrophages and HUVECs	72
2.13 Impedance Spectroscopy	72
2.14 Negative Stain and Immunoelectron Microscopy of VLPS	74
2.15 Atomic Force Microscopy	75
3. Results	78
3.1 Cloning of MARV GP ₁ into VSVXN2	76
3.1.2 Expression and Characterization of rVSV-MARV GP ₁	78
3.2 Cloning of Glycoproteins into a Mammalian Expression Vector	81
3.3 Optimization of Transfection Procedures	85
3.4 Generation of Recombinant Proteins	88
3.4.1 Expression and Purification from pDisplay Constructs	88
3.4.2 Expression and Characterization of rVSV-MARV GP ₁	92
3.5 Characterization of Proteins: Oligomerization and Glycosylation	94
3.6 Generation of Virus Like Particles	103
3.7 Activation of Macrophages by Secreted Glycoproteins and VLPs	113
3.7.1 Binding of VLPs to Macrophages	113
3.7.2 Transcriptional Activation	115
3.7.3 Secretion of Cytokines/Chemokines into Tissue Culture Supernatants	120
3.8 Activation of the Endothelium	124
3.8.1 Binding of Soluble Glycoproteins and VLPs to Endothelial Cells	124
3.8.1 Upregulation of Endothelial Cell Adhesion Molecules	125
3.8.2 Analysis of VE-cadherin and Actin Distribution Following Treatment with Soluble Glycoproteins and VLPs	130
3.8.3 Analysis of Transendothelial Electrical Resistance (TER)	132
4. Discussion	146
4.1 Project Background	142
4.2 Biosynthesis of Soluble Glycoproteins and VLPs	144
4.3 Characterization of Soluble Glycoproteins	146
4.4 Characterization of VLPs	149
4.5 Activation of Human Macrophages	151
4.6 Activation of the Endothelium	154

	Page
4.7 Alterations of VE-cadherin, Actin and Barrier Function	157
4.8 Summary	161
4.9 Future Studies	163
5. Bibliography	165
6. Appendix	180
A Primer List	180
B Protein Purification Scheme	185
C Buffers for Protein Purification	186
D Supporting Data for HUVEC Activation Studies	186
E Supporting data for VE-cadherin/actin staining of HUVECs	196

LIST OF FIGURES

		Page
Figure 1	Organization of filoviral genomes	6
Figure 2	Schematic representation of significant domains of GP _{1,2}	16
Figure 3	Orientation of mature sGP and delta peptide	18
Figure 4	Glycoprotein expression strategy for EBOV	19
Figure 5	Filovirus replication cycle in a susceptible host cell	29
Figure 6	Organization of endothelial junctions	41
Figure 7	Schematic representation of cloning strategy for recombinant proteins	59
Figure 8	Schematic drawing of the infectious clone system for vesicular stomatitis virus (VSV), Indiana serotype	67
Figure 9	Impedance spectroscopy electrode chambers	74
Figure 10	Cloning of MARV GP ₁ into the pVSVXN2 (full-length VSV genome)	77
Figure 11	Timecourse of MARV GP ₁ expression	78
Figure 11	Cloning of pDisplay constructs	79
Figure 12	Expression of rVSV proteins	79
Figure 13	Electron micrograph of rVSV MARV GP ₁	80
Figure 14	rVSV growth kinetics	81
Figure 15	Cloning of pDisplay constructs	83
Figure 16	Cloning of VP40 and GP _{1,2} into pCAGGS	80
Figure 17	Transfection Optimization	86
Figure 18	Optimization of FuGENE6 transfections and comparison to Lipofectamine 2000	87

	Page
Figure 19	Silver stained SDS-PAGE gel of ZEBOV GP ₁ 89
Figure 20	Purification steps for sGP 91
Figure 21	Expression of all secreted glycoproteins 92
Figure 22	Analysis of secreted glycoproteins by IFA 93
Figure 23	Oligomerization of sGP and delta peptide 95
Figure 24	Expression of GP oligomers 97
Figure 25	Expression of GP ₁ mutants 99
Figure 26	Expression of GP ₂ constructs 100
Figure 27	Expression of GP ₂ mutants 101
Figure 28	Deglycosylation of secreted glycoproteins 102
Figure 29	Expression of VLP proteins 104
Figure 30	Transmission electron micrographs of VLPs 106
Figure 31	Morphological comparison of VLPs following 4 months of storage at different temperatures 108
Figure 32	293T cells transfected with plasmids to generate VLPs 109
Figure 33	Immunogold labeling of VLPs 110
Figure 34	Atomic force microscopy of VLPs 112
Figure 35	Binding of VLPs to macrophages 114
Figure 36	Real time PCR analysis of IL-1 beta gene transcription 116
Figure 37	Real time PCR analysis of IL-6 gene transcription 117
Figure 38	Real time PCR analysis of IL-8 gene transcription 118
Figure 39	Real time PCR analysis of TNF-alpha gene transcription 119
Figure 40	IL-6 ELISA 121

		Page
Figure 41	TNF-alpha ELISA	122
Figure 42	IL-8 EIA	123
Figure 43	Binding of VLPs to HUVECs	125
Figure 44	HUVEC activation at 6h post treatment with soluble glycoproteins and VLPs	127
Figure 45	HUVEC activation at 12h post treatment with soluble glycoproteins and VLPs	128
Figure 46	HUVEC activation at 24h post treatment with soluble glycoproteins and VLPs	129
Figure 47	VE-cadherin and actin IFAs	131
Figure 48	TER results of HUVECs treated with 10µg/mL of soluble glycoproteins	134
Figure 49	Impedance spectroscopy: 50µg/mL sGP	135
Figure 50	Impedance spectroscopy: 50µg/mL delta peptide	136
Figure 51	Impedance spectroscopy: comparison of 50µg/mL GP ₁ and GP ₁ C53G mutant	137
Figure 52	Impedance spectroscopy: 50µg/mL GP _{1,2} ΔTM	138
Figure 53	Impedance spectroscopy: VLPs	139
Figure 54	Impedance spectroscopy: rhTNF-alpha titration	140
Figure 55	Impedance spectroscopy: protective effect of sGP	141
Figure 56	Pathogenesis model	154
Figure 57	Model of sGP protection	160

LIST OF TABLES

		Page
Table 1	Taxonomy for the family <i>Filoviridae</i>	4
Table 2	Summary of filoviral proteins	9
Table 3	Summary of EBOV vaccine candidates	35
Table 4	Summary of antibodies	51
Table 5	PCR master mix setup	52
Table 6	PCR cycling parameters	53
Table 7	Concentrations of purified recombinant proteins	90

ABSTRACT

BIOSYNTHESIS, CHARACTERIZATION AND ROLE OF EBOLA VIRUS SECRETED GLYCOPROTEINS IN TARGET CELL ACTIVATION

by

Victoria Jensen
University of Manitoba, June 2004.

Ebola virus, a member of the family *Filoviridae*, causes one of the most severe forms of viral hemorrhagic fever with mortality rates up to 90%. In the terminal stages of disease symptoms progress to hypotension, coagulation disorders, and hemorrhages and there is prominent involvement of the mononuclear phagocytic and reticuloendothelial systems. Cells of the mononuclear phagocytic system are primary target cells and producers of inflammatory mediators and their activation is independent of virus replication. Virus-induced dysfunction of the endothelium, including endothelial cell damage and increased permeability, may occur directly through virus infection that leads to activation and lytic replication as well as indirectly by mediator-induced inflammatory responses. Ebola efficiently produces 4 secreted glycoproteins during infection: sGP, delta peptide, GP₁ and GP_{1,2}ΔTM. While the presence of these glycoproteins has been confirmed in blood (sGP) and *in vitro* systems, it is hypothesized that they are of biological relevance in pathogenesis, particularly target cell activation. To gain insight into their function, I expressed the soluble glycoproteins in mammalian cells, characterized and subsequently purified them using immunoaffinity purification. The role of the transmembrane glycoprotein in the context of virus-like particles (VLPs) was also tested. Functional studies using proteins and VLPs were then performed on primary macrophages and

human umbilical vein endothelial cells (HUVECs). Cells were treated with increasing amounts of glycoproteins and subsequently tested for activation by detection of pro-inflammatory cytokines and chemokines (macrophages) and adhesion molecules (HUVEC). Furthermore, HUVECs were monitored for changes in morphology, trans-endothelial electrical resistance, and rearrangements of the endothelial junctions. The data clearly demonstrate VLPs, but not soluble glycoproteins, induce activation of macrophages and endothelial cells. VLPs and GP₁ cause an increase in endothelial permeability without visible changes in the cell junction proteins, however, VLPs do increase formation of actin stress fibers which may also contribute to permeability changes. Most unexpectedly, I found that sGP demonstrates a protective effect on endothelial barrier function when administered to TNF-alpha treated cells.

1.0 Introduction

1.1 History of Filoviruses

Filoviral disease was unknown to humankind until early August 1967 when simultaneous outbreaks of hemorrhagic fever disease occurred in both Marburg and Frankfurt, Germany, and later in Belgrade, Yugoslavia. The agent responsible for the outbreak was named Marburg virus for the town where illness was initially observed. This outbreak was linked to exposure to African green monkeys (*Cercopithecus aethiops*) imported from Uganda and in total there were 31 patients affected and a case fatality rate of 22% (Martini et al., 1968). This newly emergent virus would later be classified as the first recognized member of the family *Filoviridae* (Kiley et al., 1982). Since 1967 Marburg virus has only surfaced in sporadic outbreaks in South Africa (Gear et al., 1975), Kenya (Johnson et al., 1996; Smith et al., 1982) and the largest outbreak to date occurred among gold miners in the Democratic Republic of Congo (WHO, 1999).

It was not until simultaneous outbreaks of hemorrhagic fever occurred in Zaire and Sudan in 1976 that the second and perhaps more notorious member of the family *Filoviridae* was encountered, Ebola virus. In these two outbreaks there were upwards of 550 patients infected and mortality rates of 88% in Zaire and 53% in Sudan (WHO, 1976; WHO, 1978). This new member of the *Filoviridae* is the namesake of the Ebola river in Zaire where the 1976 outbreak occurred. Following the large outbreaks of 1976, there was a smaller outbreak in Sudan in 1979 (Baron, McCormick, and Zubeir, 1983), but then the human pathogenic species of virus remained silent for 15 years before emerging again in 1994 near the Tai Forest of Ivory Coast when a veterinarian was infected by a new species of Ebola, Ivory Coast Ebola virus (ICEBOV), after performing a necropsy

on a chimpanzee (Baron, McCormick, and Zubeir, 1983; Le Guenno, Formenty, and Boesch, 1999). During the 1990s there were several outbreaks of Ebola hemorrhagic fever (EHF) in Gabon (Georges-Courbot et al., 1997; Leroy et al., 2002b; 1997), a large outbreak in Kikwit, Zaire in 1995 (CDC, 1995; Prevention, 1995), and an epidemic in Uganda from August 2000 through January 2001 (CDC, 2001). There has also been an increase in frequency of outbreaks, particularly in Gabon and the Republic of Congo during 2002 and 2003 (WHO, 2002; WHO, 2003b). The most recent incidents of EHF were reported as recently as November 2003 from the Ministry of Health of the Republic of Congo with a total of 24 cases, including 12 deaths, in Mbomo (19 cases, 9 deaths) and Mbandza (5 cases, 3 deaths) villages located in Mbomo district, Cuvette Ouest Department (WHO, 2003a).

While the outbreaks of EHF mentioned above caused high mortality in humans the outbreaks were confined to the African continent. In 1989 this all changed when a new species of Ebola virus emerged in the United States of America (Jahrling et al., 1990). It was in Reston, Virginia, during late 1989 that a colony of cynomolgus macaques became ill with a hemorrhagic disease whose etiology would later be identified as co-infection with a novel Ebola virus, named *Reston ebolavirus* (REBOV), as well as simian hemorrhagic fever virus (SHFV). While REBOV was highly pathogenic for non-human primates, it did not initiate disease in humans despite the fact that several individuals who handled sick animals seroconverted but showed no signs of illness. The monkeys were traced to an exporter in the Philippines and in 1992 there was a similar outbreak among animals from the same Philippine exporter in Sienna, Italy (WHO, 1992) and in Alice, Texas in 1996 (Sanchez et al., 1999).

1.2 Classification

1.2.1 Taxonomy and nomenclature

After initial morphological observations of MARV it was proposed that this virus be classified in the family *Rhabdoviridae*. However, in 1982 this was challenged based on further characterization of distinctive morphological, morphogenetic, physiochemical, and biological features of MARV and EBOV. This marked the establishment of the family *Filoviridae* that contained the single genus *Filovirus* (Kiley et al., 1982). The family *Filoviridae* is a member of the order *Mononegavirales* that also contains three additional families of nonsegmented, negative sense, single stranded (NNS) RNA viruses: *Paramyxoviridae*, *Rhabdoviridae* and *Bornaviridae* (Sanchez, 2001). All members of *Mononegavirales* share similar genome organization, however, filovirus genomes align most closely with members of the genera *Paramyxovirus* and *Morbillivirus* (Feldmann and Kiley, 1999).

The family *Filoviridae* was restructured several times in the past few years. The most currently accepted taxonomy divides the family into two genera *Marburgvirus* and *Ebolavirus* (Feldmann, 2004). Within the genus *Marburgvirus* there is a single species *Lake Victoria marburgvirus* that is designated “MARV” and contains 6 strains with the prototype being Strain Musoke. The genus *Ebolavirus* is slightly more complicated with four recognized species: *Ivory Coast ebolavirus* (ICEBOV), *Reston ebolavirus* (REBOV), *Sudan ebolavirus* (SEBOV) and *Zaire ebolavirus* (ZEBOV). The prototype virus for the genus is ZEBOV Strain Mayinga. A detailed outline of the current taxonomy is listed in Table 1. There are a number of distinguishing features between the two genera including limited antigenic cross-reactivity between them, structural and

genome size differences as noted above, gene overlaps, glycoprotein expression strategy (only *Ebolaviruses* undergo RNA editing), and a nucleotide difference of 57% in the glycoprotein gene (Feldmann, 2004; Sanchez, 2001).

(Table 1)

Genus	Species	Strain	Location, Year Isolated
<i>Marburgvirus</i>	<i>Lake Victoria marburgvirus</i>	Musoke	Kenya, 1980
		Ratayczak	West Germany, 1967
		Popp	West Germany, 1967
		Voegel	Yugoslavia, 1967
		Ozolin	Zimbabwe, 1975
		Marburg Ravn	Kenya, 1987
<i>Ebolavirus</i>	<i>Ivory Coast ebolavirus</i>	Cote d'Ivoire	Tai Forest, 1994
	<i>Reston ebolavirus</i>	Reston	USA, 1989
		Phillipines	Phillipines, 1989
		Siena	Italy, 1992
		Texas	USA, 1996
	<i>Sudan ebolavirus</i>	Boniface	Sudan, 1976
		Maleo	Sudan, 1979
	<i>Zaire ebolavirus</i>	Mayinga	Zaire, 1976
		Zaire	Zaire, 1976
		Eckron	Zaire, 1976
		Tandala	Zaire, 1977
		Kikwit	DRC, 1995
Gabon		Gabon, 1994-1997	

Table 1. Taxonomy for the family Filoviridae. Strains seen in bold text represent the prototype for the genus. DRC: Democratic Republic of Congo.

1.2.2 Biohazard Classification

All members of the family *Filoviridae* are currently classified as 'Risk Group 4' agents by the Canadian Office of Laboratory Security (Artsob, 2001). Risk group classification is typically used to categorize the relative hazards of infective organisms and is based largely on characteristics of the organisms such as pathogenicity, infective dose, mode of transmission, host range, availability of preventative measures (vaccines)

and effective treatments. Risk group 4 agents are defined as possessing both a high individual as well as public health risk and are pathogens that produce very serious human and/or animal disease. These agents are often untreatable and are readily transmitted from person to person or animal to person or vice versa. Transmission may be direct or indirect or by casual contact (Artsob, 2001). Due to their high risk, work with infectious filoviruses must be performed in a certified Containment Level 4 (CL4) laboratory. A detailed description of biosafety aspects and work in a CL4 laboratory can be found in "*The Laboratory Biosafety Guidelines*" available through Health Canada (Artsob, 2001).

1.3 Genome Structure

The genome of all filoviruses consists of a non-segmented, single negative-stranded linear RNA molecule and contributes 1.1% of the total virion mass with a molecular mass of approximately 4.0×10^6 (Kiley et al., 1982; Regnery, Johnson, and Kiley, 1980). Regnery and colleagues were able to show lack of polyadenylation through a lack of virion RNA to bind oligodeoxythymidylic acid-cellulose under conditions known to bind RNAs rich in polyadenylic acid and were also able to demonstrate that the RNA was not infectious under conditions which yielded infectious RNA from Sindbis virus, suggesting that Ebola virus nucleic acid is negative-stranded RNA (Regnery, Johnson, and Kiley, 1980). The average size of a filoviral genome is 19kb with MARV being slightly larger than that of EBOV (MARV 19.1kb; EBOV 18.9kb). The complete nucleic acid sequence for three strains of MARV (Popp 1967, Musoke 1980, and M/S.Africa/Johannesburg/1975/Ozolin) and four EBOV strains (ZEBOV Zaire strain 1995, ZEBOV strain Mayinga, REBOV strain Pennsylvania, and REBOV strain

Phillipines) have been determined (Bowen, 2003; Bukreyev et al., 1995b; Chain, 2003; Feldmann et al., 1992; Groseth et al., 2002; Ikegami et al., 2001; Sanchez et al., 1993; Volchkov, 1993). The linear gene order for all members of the family *Filoviridae* is conserved, however, regions of genome organization on the genus level is shown in Figure 1.

(Figure 1)

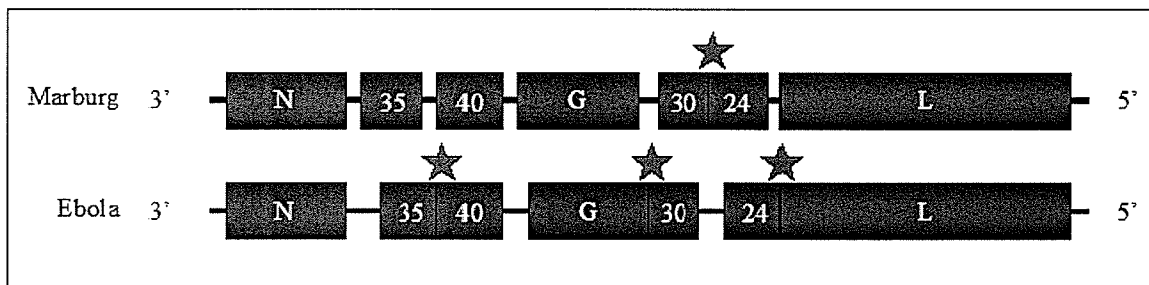


Figure 1. Organization of filoviral genomes. Regions of gene overlap are indicated by red stars. The linear gene order is conserved and shown here as nucleoprotein (NP), virion protein 35 (35), virion protein 40 (40), glycoprotein (G), virion protein 30 (30), virion protein 24 (24), and the RNA-dependent-RNA polymerase (L). Genome of Ebola is representative of ZEBOV.

The seven genes of filoviruses are flanked at their 3' and 5' ends by noncoding sequences that contain the signals for replication and encapsidation (Groseth et al., 2002; Muhlberger et al., 1998; Neumann et al., 2002; Volchkov et al., 2001). Filoviral genes possess highly conserved motifs for transcriptional start (3'-CUNCNUNUAAUU-5') and transcriptional stop (3'-UAAUUCUUUUU-5') signals (Feldmann and Kiley, 1999). Intergenic regions of variable length may exist between adjacent genes, however, some genes are known to overlap. This phenomenon is particularly evident within the genus *Ebolavirus* with three overlaps reported for ZEBOV, SEBOV and ICEBOV and 2 overlaps for REBOV (see Figure 1, representing ZEBOV). In the case when overlaps occur their length is limited to five highly conserved nucleotides within the

transcriptional signals (3'-UAAUU-5') (Feldmann et al., 1992; Groseth et al., 2002; Ikegami et al., 2001; Sanchez et al., 1993).

1.4 Virion morphology

The molecular mass of an average filoviral particle is $3-6 \times 10^8$ with a density in potassium tartrate of 1.14g/cm^3 (Elliott, Kiley, and McCormick, 1985; Kiley et al., 1988). Virions are filamentous but pleomorphic, often times occurring as U or 6-shaped, circular and branched in nature. The filamentous shape of particles gives rise to the name of the family *Filoviridae* (filo- means thread in Latin). Geisbert and Jarling were able to demonstrate quite nicely the ultrastructural details of morphology and morphogenesis of MARV and EBOV through electron microscopy studies (Geisbert and Jahrling, 1995). These studies showed that while all filoviral particles appeared to enter host cells by endocytosis and demonstrated a similar progression of morphogenic events, there were ultrastructural differences between MARV and other filoviruses. All filovirus particles appeared to have a uniform diameter of 80nm but MARV virions recovered from culture fluids were consistently shorter in mean unit length (795-828nm) than SEBOV (974-1063), ZEBOV (990-1086), or REBOV (1026-1083) particles. Virions are surrounded by a host cell, plasma membrane-derived lipid envelope. Surface glycoprotein spikes approximately 7nm in diameter and spaced 5-10nm apart are visualized on the envelope (Geisbert and Jahrling, 1995; Kiley et al., 1982). The lipid envelope provides the protection for the helical nucleocapsid also known as the ribonucleoprotein (RNP) complex (Elliott, Kiley, and McCormick, 1985).

1.5 Viral Proteins

The members of *Filoviridae* produce seven structural proteins from the seven genes encoded by the genome. Four of these seven proteins are associated with the genomic RNA to form the ribonucleoprotein complex (RNP): nucleoprotein (N), virion protein 30 (VP30), virion protein 35 (VP35) and the RNA-dependant RNA polymerase (L) (Elliott, Kiley, and McCormick, 1985). The remaining three structural proteins are all found in association with the lipid envelope. The glycoprotein, GP_{1,2}, is the major surface spike protein and virion protein 40 (VP40) is the major matrix protein while virion protein 24 (VP24) is believed to be a minor matrix protein also involved in the budding process (Elliott, Kiley, and McCormick, 1985; Han et al., 2003; Jasenosky et al., 2001). In addition to the structural proteins, several non-structural, secreted glycoproteins are also produced during viral infection including sGP, Δ peptide, GP₁ and GP_{1,2} Δ TM (Dolnik, 2003; Volchkov et al., 1998b; Volchkova et al., 1998; Volchkova, Klenk, and Volchkov, 1999). The complete list of filoviral proteins, their proposed functions and localization are listed in Table 2.

(Table 2)

Gene #	Protein Name	Present in EBOV	Present in MARV	Localization in virion	Function
1	NP	✓	✓	RNP complex	Encapsidation
2	VP35	✓	✓	RNP complex	Polymerase cofactor; IFN-antagonist
3	VP40	✓	✓	Membrane	Matrix protein; Viral egress
4	GP _{1,2}	✓*	✓	Membrane; Type 1 protein	Receptor binding and fusion
4	sGP & Δ peptide	✓	absent	nonstructural; secreted	Unknown
5	VP30	✓	✓	RNP complex	Encapsidation; Transcription
6	VP24	✓	✓	Membrane	Minor matrix protein; host specificity?
7	L	✓	✓	RNP complex	RNA-dependant RNA polymerase

Table 2. Summary of filoviral proteins. EBOV, Ebolavirus genus; MARV, Marburgvirus genus; RNP, ribonucleoprotein complex; NP, nucleoprotein; VP, virion structural protein; GP_{1,2}, surface glycoprotein, *expressed via RNA editing; sGP, secreted glycoprotein; peptide, delta peptide.

1.5.1 Nucleoprotein (NP)

The nucleoprotein gene (NP) is the first gene at the 3' end of the linear RNA genome and is the major structural phosphoprotein associated with nucleocapsids (Elliott, Kiley, and McCormick, 1985; Elliott et al., 1993; Kiley et al., 1988). When compared with other nucleoproteins within the order *Mononegavirales* that typically possess a M_r of 42 to 62 kDa, the NP of filoviruses possesses an unusually high M_r (Feldmann and Kiley, 1999). The M_r of filoviruses range from 95 kDa for MARV to 105 kDa for EBOV, while their estimated M_r based on amino acid sequence is only 78 kDa and 83 kDa, respectively (Feldmann et al., 1992; Sanchez et al., 1989; Sanchez et al., 1992). The size difference of the NP between MARV and EBOV is thought to be due to the less conserved COOH-

termini of the protein which is both hydrophilic and highly acidic in nature (Elliott, Kiley, and McCormick, 1985; Kiley et al., 1988). Based on sequence similarity to paramyxovirus NPs, it has been speculated that the 100 COOH- terminal amino acids of the filovirus NP may facilitate binding to the matrix protein (VP40) during virus budding (Sanchez, 2001). Expression studies using recombinant MARV NP demonstrated both phosphorylated and unphosphorylated forms of the protein, however, in virion particles NP was exclusively present in the phosphorylated form (Becker et al., 1994). It has also been recently reported by Huang et al. that EBOV NP, along with VP35 and VP24, were sufficient and necessary to spontaneously form nucleocapsids in 293T cells transfected with plasmids encoding all three proteins. Perhaps most interesting was the finding that O-glycosylation and sialation of NP were demonstrated and necessary for the association of all three proteins (Huang et al., 2002). Indeed, the COOH- terminal portion of NP has been recognized for its high antigenicity and potential use for both vaccine attempts as well as a target for diagnostic enzyme linked immunosorbent assays (ELISA) (Saijo et al., 2001; Sullivan et al., 2003; Wilson and Hart, 2001).

1.5.2 Virion protein 35 (VP35)

The second gene of filoviruses encodes a protein known as virion protein 35 (VP35). VP35 varies in length between 329 to 351 or 340 amino acids long for MARV and EBOV, respectively (Bukreyev et al., 1993b; Sanchez et al., 1993). The genomic position of VP35, when compared to paramyxoviruses and rhabdoviruses, has led to the hypothesis that it functions as a phosphoprotein and is involved in transcription and replication (Becker et al., 1998; Muhlberger et al., 1998; Muhlberger et al., 1999). The state of phosphorylation for this protein has not been fully elucidated but it is believed to

be weakly phosphorylated for filoviruses (Becker and Muhlberger, 1999). During the past 4 years a great deal of work on VP35 has been done and in 2000 Basler et al. made a major contribution to VP35 function by identifying its ability to function as a type 1 interferon antagonist (Basler et al., 2000). VP35 was able to block double-stranded RNA- and virus-mediated induction of an IFN-stimulated response element reporter gene and to block double-stranded RNA- and virus-mediated induction of the IFN-beta promoter (Basler et al., 2000). The mechanism for the VP35 effects were further elucidated 3 years later and it was shown that the blocking effect of VP35 was not due to an interaction with the IFN alpha/beta receptor but rather, the ability of VP35 to inhibit this virus-induced transcription correlates with its ability to block activation of IRF-3, a cellular transcription factor of central importance in initiating the host cell IFN response. Specifically, VP35 blocks virus-induced IRF-3 phosphorylation and subsequent IRF-3 dimerization and nuclear translocation (Basler et al., 2003). Therefore, in addition to its role in transcription and replication, VP35 likely plays an important role in virulence *in vivo* by downregulating expression of host antiviral genes such as the interferon beta gene.

1.5.3 Virion protein 40 (VP40)

Virion protein 40 (VP40) is the product of the third gene. VP40 is a membrane associated protein, possesses a slightly hydrophobic profile and is the most abundant viral antigen associated with virions (Elliott, Kiley, and McCormick, 1985; Feldmann et al., 1992; Sanchez et al., 1993). VP40 of EBOV is 326 amino acids in length, compared to the slightly smaller 303 amino acid protein found in MARV (Bukreyev et al., 1993b; Sanchez et al., 1993). Dessen et al. solved the crystal structure of VP40 and confirmed

that VP40 may be able to switch from a monomeric conformation to a hexameric form, as previously observed *in vitro* (Dessen et al., 2000). The function of VP40 had been assumed to be as a matrix protein and more recent studies have elucidated its role in formation of membrane-bound particles. When expressed independently of other viral proteins in a mammalian system, VP40 was sufficient to induce release of membrane-bound particles and this process most likely requires cellular WW domain-containing proteins that interact with the conserved PPXY motif of VP40 since mutation or loss of the PPXY motif resulted in reduced particle release (Jasenosky et al., 2001). Additionally, like retroviral Gag proteins, EBOV VP40 is capable of recruiting Tsg101, a factor involved in endosomal protein sorting, to sites of particle assembly (Martin-Serrano, Zang, and Bieniasz, 2001). In a more recent study by Timmins et al. it was demonstrated that for efficient budding, a full amino terminus of VP40 is required, which includes the proline-rich motifs PPXY and PTAP, both of which have been proposed to interact with cellular proteins. Furthermore, VP40 can interact with cellular factors human E3 ubiquitin ligase Nedd4 and Tsg101 *in vitro* (Timmins et al., 2003). Interestingly, these studies showed that the N-terminal hexameric domain of VP40 was in close contact with WW3 of Nedd4 but that the ubiquitin enzyme variant domain of Tsg101 was sufficient for binding to the PTAP motif of VP40, regardless of the oligomeric state. This, of course, implies that Nedd4 and Tsg101 may play complimentary roles at a late stage of the assembly process, by recruiting cellular factors of two independent pathways to the site of budding at the plasma membrane (Timmins et al., 2003; Yasuda et al., 2003). VP40 has also been implicated more specifically for inducing the characteristic filamentous morphology of filoviruses (Noda et al., 2002).

Expression of VP40 alone induced filamentous particle formation nearly identical to wildtype virus and when co-expressed with the surface glycoprotein, spikes were seen on the surface of particles, thereby suggesting an interaction of these proteins in morphogenesis (Bavari et al., 2002; Noda et al., 2002). The co-expression of VP40 and GP_{1,2} to form virus-like particles (VLPs) has received considerable attention in the past two years as a useful tool for the study of virus-host interactions, use as a vaccine candidate and in further studies regarding morphogenesis (Bavari et al., 2002; Licata et al., 2003; Warfield et al., 2003; Watanabe et al., 2004; Yasuda et al., 2003).

1.5.4 Glycoproteins

The fourth gene in the linear genome encodes the only surface glycoprotein, GP_{1,2}. The surface glycoproteins of filoviruses are type 1 transmembrane proteins that contain a COOH-terminal hydrophobic domain that anchors it to the membrane (Kiley, Regnery, and Johnson, 1980). The glycoprotein of MARV is 681 amino acids long, slightly larger than the 676 amino acid glycoprotein of EBOV (Sanchez et al., 1993; Volchkov, Blinov, and Netesov, 1992; Will et al., 1993). Synthesis of GP_{1,2} involves processing by the proprotein convertase furin, a subtilisin/kexin-like convertase localized in the trans Golgi, at a polybasic cleavage site and the mature protein consists of the amino-terminal fragment GP₁ and the carboxy-terminal fragment GP₂ that are linked by a disulfide bond (Jeffers, Sanders, and Sanchez, 2002; Volchkov et al., 1998a). Mutational analysis of cysteine residues in GP_{1,2} implicated cysteine 53 (in GP₁) as critical for binding of GP₁ to GP₂ and its mutation resulted in efficient secretion of GP₁ (Jeffers, Sanders, and Sanchez, 2002). Once fully processed the mature protein is present as homotrimers of the GP_{1,2} heterodimer complex on the surface of virions (Sanchez et al.,

1998b; Volchkov et al., 1998a). GP_{1,2} is heavily glycosylated with approximately 50% of its molecular mass attributed to N- and O- glycans (Geyer et al., 1992; Will et al., 1993). The molecular mass of GP_{1,2}, once fully processed, is approximately 140kDa for EBOV and 160kDa for MARV (Becker, Klenk, and Muhlberger, 1996; Sanchez et al., 1996). There is a reasonable degree of homology in both the amino- and carboxy-terminal regions of GP_{1,2} with the middle third of the protein representing a highly variable region, even within species of EBOV (Sanchez, 2001; Will et al., 1993). In comparison to the conserved regions that are quite hydrophobic in nature, the variable region is both hydrophilic and contains the bulk of the predicted N-linked glycosylation sites and nearly all the predicted O-linked sites. This region, rich in O-linked glycans, confers a mucin-like property to the variable region (Geyer et al., 1992; Sanchez et al., 1998a). In 2000, Yang et al. reported that the synthesis of the virion glycoprotein induced cytotoxic effects in human endothelial cells *in vitro* and *in vivo* and they mapped the observed effect to the serine-threonine-rich, mucin-like domain of GP_{1,2} (Yang et al., 2000). However, it is unlikely that the mucin-like domain is solely responsible for cytotoxic effects as others have demonstrated that detachment of cells (293T, endothelial, etc.) upon expression of GP_{1,2} was largely attributable to a domain within the extracellular region of GP₂ (Chan, Ma, and Goldsmith, 2000). Several studies in the past 5 years on EBOV GP_{1,2} have identified additional regions of the protein that may play critical roles in pathogenesis. In particular, a coiled-coil region of GP₂ is thought to play an important role in facilitating the entry of EBOV into host cells (Watanabe et al., 2000). The structural similarity between the EBOV GP₂ ectodomain and the core of the transmembrane subunit from oncogenic retroviruses was confirmed when the x-ray structure of a stable core of the GP₂

ectodomain was crystallized and it was determined at 1.9-Å resolution to resemble several other viral membrane-fusion proteins, including those from HIV and influenza (Malashkevich et al., 1999). It has been hypothesized that this coiled-coil region of GP₂ interacts with another region of GP₂ that was identified as a putative fusion domain based on the similarity of its topological position to that of the retroviral transmembrane domain (Gallaher, 1996; Ruiz-Arguello et al., 1998). Studies using a replication deficient Vesicular Stomatitis Virus (VSV) system provided additional evidence for the fusogenic function of that domain. In this system the fusion domain candidacy of amino acid positions 524 to 539 in the glycoprotein were tested by the ability of pseudotyped VSVs, bearing various mutations to these positions, to facilitate viral entry into cells (Ito et al., 1999). Indeed, most of the constructs lost at least 50% of their ability to confer infectivity to a VSV lacking its receptor binding protein (Ito et al., 1999). A schematic representation of GP_{1,2} is shown in Figure 2 and highlights significant domains within the protein.

(Figure 2)

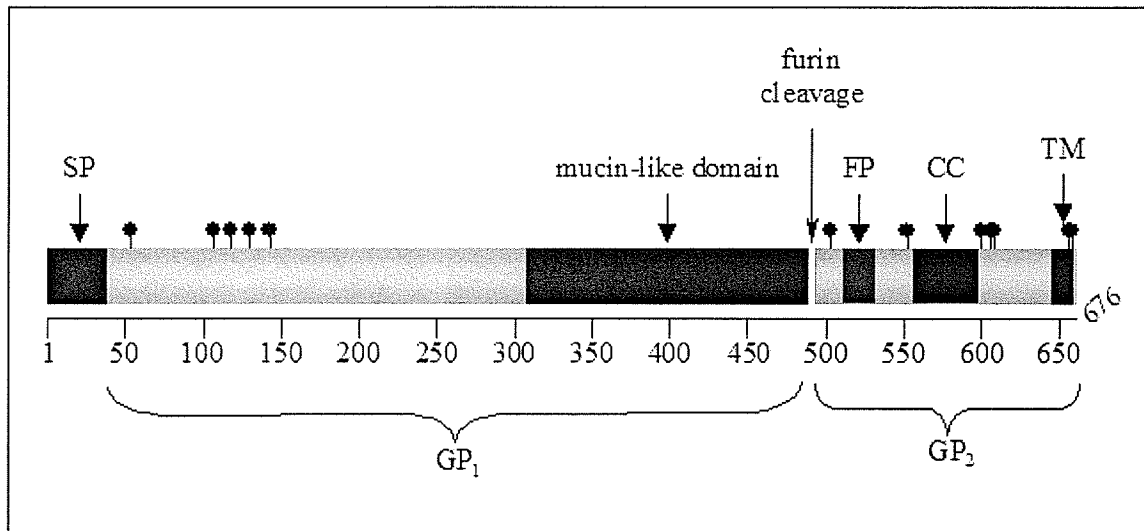


Figure 2. Schematic representation of significant domains of GP_{1,2}. A signal peptide (SP) is present at the amino-terminal portion of the protein and is cleaved off in the endoplasmic reticulum. The variable domain with mucin-like properties is shown in green. The protein is cleaved in the trans-golgi network by furin into GP₁ and GP₂. The subunits are linked through disulfide bonding. Conserved cysteines (shown as black lines with bulb at ends) are involved in inter- and intra-molecular bonding and proper folding of the protein. There are 3 significant domains in GP₂: the fusion peptide (FP), coiled-coil domain (CC), and the transmembrane domain (TM) that anchors the protein to the membrane. The number scale represents amino acid positions. This figure shows a single GP_{1,2} monomer, however, mature GP_{1,2} exists as trimers on the surface of virions.

While members of both *Ebolavirus* and *Marburgvirus* produce GP_{1,2} as the surface glycoprotein, the strategy they employ to do so differs. Members of the genus *Marburgvirus* produce their glycoprotein spike through authentic transcription of the viral RNA. The mechanism used for EBOV, however, is more complex and involves transcriptional editing by the RNA-dependant RNA polymerase (Volchkov et al., 1995). The editing event occurs approximately in the middle of the glycoprotein gene at a stretch of seven consecutive adenosine residues (plus sense). Upon editing an additional, non-template adenosine is inserted and this causes a shift in the reading frame thereby avoiding a translational stop codon that would be present in exact copies of the viral template (Volchkov et al., 1995). It has been estimated that 20% of all mRNA transcripts

from the glycoprotein gene encode the full-length GP_{1,2} (Sanchez et al., 1996; Volchkov et al., 1995). The remaining 80% of (unedited) transcripts encode a precursor protein known as pre-sGP, making it the primary product of the glycoprotein gene. This precursor protein is also glycosylated and cleaved at the multibasic amino acid motif RVRR at positions 321 to 324 of the open reading frame (Volchkova et al., 1998; Volchkova, Klenk, and Volchkov, 1999). The larger cleavage product is sGP, a 50kDa protein that is efficiently released as a homodimer (Volchkova et al., 1998). In addition to being observed *in vitro*, copious amounts of sGP have been detected in the blood of EBOV infected patients (Sanchez et al., 1999; Sanchez et al., 1996). The dimerization of sGP is due to an intermolecular disulfide linkage between cysteine residues at positions 53 and 306. Additionally, formic acid hydrolysis of sGP demonstrated that sGP dimers consist of monomers in antiparallel orientation (Volchkova et al., 1998). It is important to note that while sGP and GP_{1,2} share the 295 N-terminal residues, they are structurally distinct. sGP differs from GP_{1,2} in its 69 carboxy-terminal residues, however, only 29 of these amino acids are specific for sGP (Sanchez et al., 1996; Volchkov et al., 1995). The remaining 40 amino acids are specific for the smaller cleavage product of pre-sGP that has been designated delta (Δ) peptide (Volchkova, Klenk, and Volchkov, 1999). Delta peptide is sialylated and heavily O-glycosylated giving rise to a higher molecular mass (10-14kDa) than predicted (4.7kDa). Delta peptide is released as a monomer from infected or transfected cells (Volchkova, Klenk, and Volchkov, 1999). A schematic representation of mature sGP and Δ peptide is seen below in Figure 3.

(Figure 3)

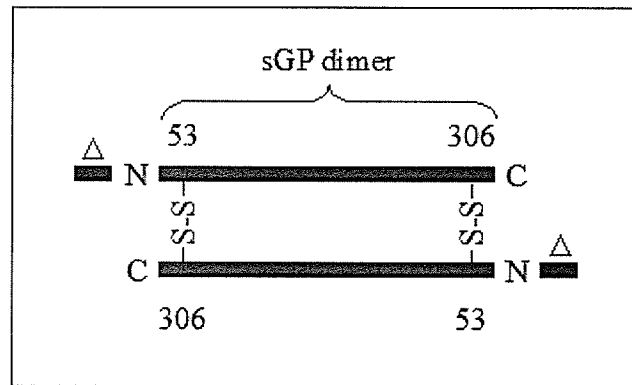


Figure 3. Orientation of mature sGP and delta peptide. Monomers of sGP are linked through disulfide bridging (S-S) between cysteines 53 and 306 to form dimers in anti-parallel orientation. Delta peptide is released as monomers following cleavage by furin.

In addition to both sGP and Δ peptide, EBOV produces two additional secreted glycoproteins but in these cases the secreted glycoproteins originate from full-length GP_{1,2}. Volchkov et al. were able to demonstrate significant amounts of glycoprotein in the culture medium in non-virion forms following EBOV infection. The major form represented the large subunit GP₁ that was shed after release of its disulfide linkage to the smaller transmembrane subunit GP₂. The minor form was intact GP_{1,2} complexes incorporated into virosomes (Volchkov et al., 1998b). More recently a truncated form of GP_{1,2}, designated GP_{1,2} Δ TM, was found to be released by proteolytic cleavage at amino acid position D637 thereby liberating a complex of GP₁ and a portion of the GP₂ ectodomain. Furthermore, the enzyme responsible for this cleavage was shown to be tumor necrosis alpha converting enzyme (TACE), which is a member of the ADAM family of zinc-dependant metalloproteases (Dolnik, 2003). Figure 4, shown below, summarizes the soluble glycoproteins of EBOV.

(Figure 4)

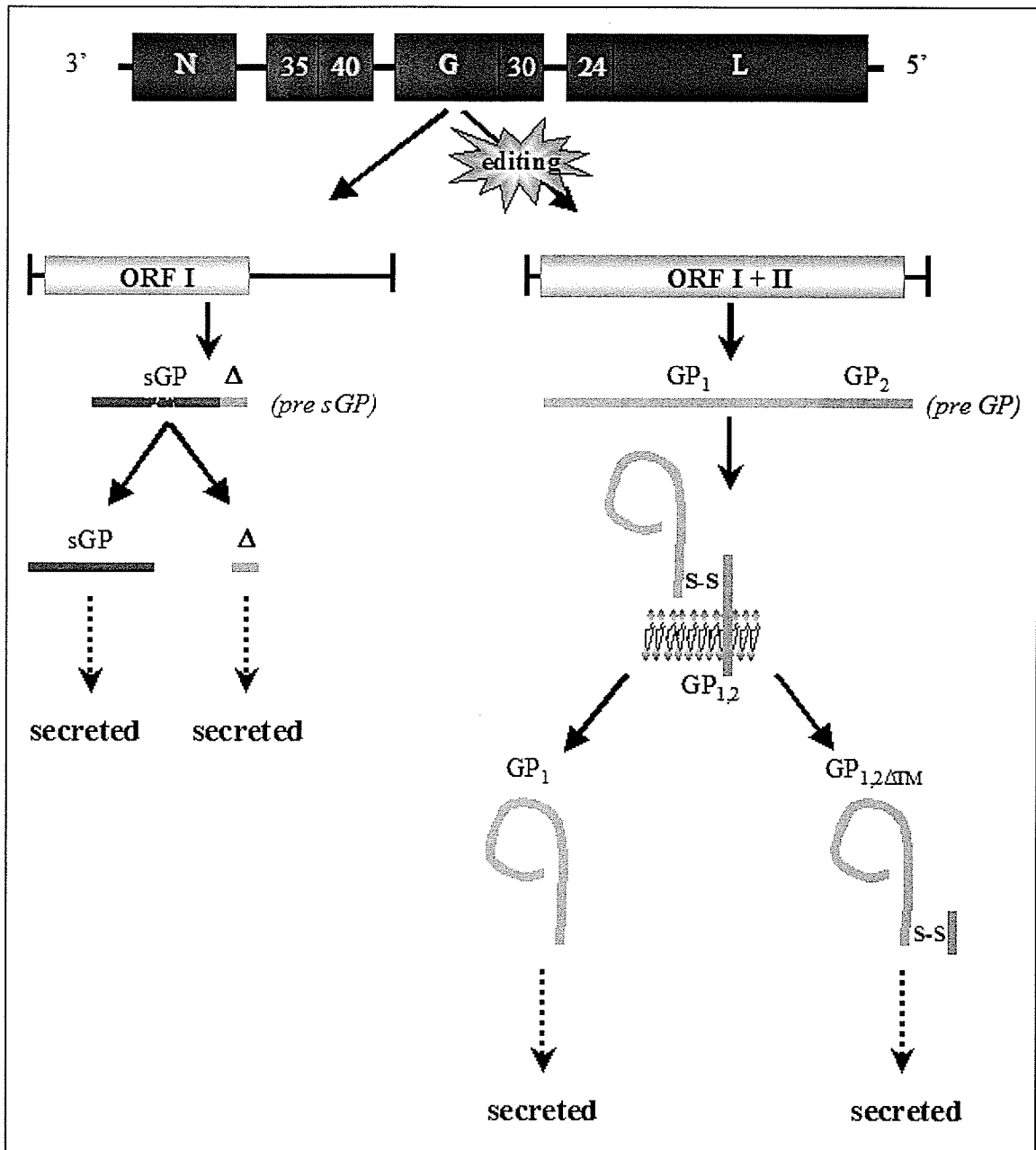


Figure 4. Glycoprotein expression strategy for EBOV. Direct transcription of viral RNA leads to production of pre-sGP which is posttranslationally modified and cleaved into sGP and delta peptide (both secreted). RNA editing leads to production of pre-GP and finally the mature GP1,2 on the surface of virions. GP1 is released when the disulfide bond between GP1 and GP2 becomes unstable. Through metalloprotease cleavage GP1,2deltaTM is released. GP1,2deltaTM contains a small portion of the GP2 ectodomain. S-S = disulfide bonds; ORF = open reading frame.

1.5.5 Virion protein 30 (VP30)

The fifth gene of filoviruses encode virion protein 30 (VP30), another integral component of the RNP complex (Elliott, Kiley, and McCormick, 1985; Feldmann et al., 1992). VP30 consists of 260 amino acids for EBOV and 281 for MARV (Bukreyev et al., 1995a; Sanchez et al., 1993). Whereas NP, L, and VP35 are functionally conserved within the order Mononegavirales, VP30 is thought to represent a filovirus-specific nucleocapsid protein (Modrof et al., 2001). VP30 is the minor phosphoprotein of virions (Elliott, Kiley, and McCormick, 1985; Elliott et al., 1993). The main phosphorylation sites of VP30 reside in the region of amino acid 40 to 51 at seven serine residues and it was shown by Modrof et al. that phosphorylation of serines at positions 40 and 42 is critical for VP30's interaction with NP inclusions (Modrof et al., 2001). Another region of VP30, amino acids 94 to 112, has also been identified as playing a critical role in proper oligomerization of the protein. In particular, a cluster of four leucine residues is critically important as mutation of any one of these residues results in oligomerization-deficient VP30 molecules that are no longer able to support EBOV-specific transcription (Hartlieb et al., 2003). Interestingly, if a 25-mer synthetic peptide that was shown to bind and block VP30 oligomerization was transfected into EBOV-infected cells, the peptide inhibited viral replication thereby suggesting that such a peptide may have potential as a therapeutic substance (Hartlieb et al., 2003). Further studies will need to be performed in animal models to further define the therapeutic potential of such a peptide.

1.5.6 Virion protein 24 (VP24)

Virion protein 24 (VP24) is the product of the sixth gene of filoviruses and is 253 and 251 amino acids in length for MARV and EBOV, respectively (Feldmann et al.,

1992; Sanchez et al., 1993). Like VP40, VP24 is localized to the viral membrane, however, unlike VP40 it could not be completely removed from the RNP complex under isotonic conditions (Elliott, Kiley, and McCormick, 1985; Kiley et al., 1988). Further studies have shown a specific biochemical interaction between VP24 and NP and VP35 (Huang et al., 2002). When transfected into 293T cells these three proteins are capable of spontaneously forming nucleocapsids as demonstrated by electron microscopy studies (Huang et al., 2002). VP24 is believed to be a minor matrix protein and based on current knowledge it is believed to link the membrane bound proteins (VP40 and/or GP_{1,2}) with the RNP, perhaps through interaction with VP35 and NP. VP24 might play a role in virus assembly and budding partially based on evidence that it strongly associates with lipid membranes (Han et al., 2003). The ability of VP24 to oligomerize was also demonstrated and progressive deletions at the N terminus of VP24 resulted in a decrease in oligomer formation and a concomitant increase in the formation of high-molecular-weight aggregates (Han et al., 2003). In addition to a role in viral budding VP24 is speculated to play a role in species adaption (Volchkov et al., 2000). Specifically, VP24 appears to be a hot spot for mutations leading to amino acid changes when EBOV was serially passaged and adapted to cause lethal infection in guinea pigs (Volchkov et al., 2000). Whilst a significant amount of research regarding the structure and function of VP24 has been performed in the past 4 years (Han et al., 2003; Huang et al., 2002; Leroy et al., 2002a; Volchkov et al., 2000; Watanabe et al., 2004; Wilson et al., 2001), the precise role that this protein plays in pathogenesis is still elusive.

1.5.7 RNA-dependant RNA Polymerase (L)

The RNA-dependant RNA polymerase, also known as the large (L) protein, is encoded at the most distal 5' end of the genome. The L gene encodes a polypeptide of 2212 amino acids for ZEBOV strain Mayinga (Volchkov et al., 1999) and 2330 amino acids for the Musoke strain of MARV (Muhlberger et al., 1992). Amino acid comparisons with ZEBOV strain Mayinga showed identities of about 73 and 44% to the L proteins of SEBOV strain Maleo and MARV strain Musoke, respectively (Volchkov et al., 1999). Early studies using computer assisted comparisons revealed three common conserved boxes (A, B, and C) among filo-, paramyxo-, and rhabdovirus L proteins, which are probably involved in the polymerase function. The L proteins can be divided into an N-terminal half, which seems to contain the common enzymatic sites, and a C-terminal half carrying virus specific idiosyncrasies (Muhlberger et al., 1992). The filoviral L protein shares many similarities with L proteins of other non-segmented, negative sense, single-stranded (NNS) RNA viruses. These are based on sequence similarity and include a high leucine and isoleucine content, a large positive net charge at neutral pH, and clusters of basic amino acids (Volchkov et al., 1999). The L protein functions as an RNA dependant RNA polymerase and expression of this protein, along with the other RNP complex proteins is sufficient to drive artificial replication of EBOV reverse genetics systems (Neumann et al., 2002; Volchkov et al., 2001). Whilst the majority of knowledge regarding L has been derived from sequence comparisons to other NNS RNA viruses, the advent of reverse genetics and minigenome systems will make it possible to directly test the functions of various domains.

1.6 Viral Replication Cycle

1.6.1 Growth characteristics

The most commonly used cell line for both isolation and propagation of filoviruses is the Vero (*Cercopithecus aethiops*, African green monkey kidney) cell line. The E6 clone of Vero cells is particularly susceptible to filovirus infection (Feldmann and Kiley, 1999). In addition to Vero cells, both MA-104, *Cercopithecus aethiops* African green monkey kidney cells (Whitaker and Hayward, 1985) and SW13, a human adrenal carcinoma cell line (Leibovitz et al., 1973) have proven useful in primary virus isolation (Jahrling et al., 1990; McCormick et al., 1983; Schnittler et al., 1993). In addition to their ability to infect a variety of continuous cell lines filoviruses have been shown to infect primary cell cultures, particularly monocytes, macrophages, and endothelial cells (Feldmann et al., 1996; Schnittler et al., 1993; Stroher et al., 2001).

Infection with either MARV or ZEBOV leads to lytic infection in cell culture (Feldmann and Kiley, 1999). Infection can be monitored in cell culture by indirect immunofluorescence assay (IFA) or by standard plaque assay. If plaques are not easily visualized a modified immunoplaque assay may be performed (Stroher, 2002) or reverse transcriptase-polymerase chain reaction (RT-PCR) on viral RNA either isolated from infected cells of cell culture supernatants (Schnittler et al., 1993).

1.6.2 Viral attachment and entry

The surface spike protein of filoviruses, GP_{1,2}, has long been suspected of mediating receptor binding and fusion to host cells. An asialoglycoprotein receptor (ASGP-R) found on hepatocytes has been shown to act as a receptor for Marburg virus (Becker, Spiess, and Klenk, 1995), however, this receptor is absent in a number of other

cells that support the growth of filoviruses. It is currently speculated that this may be a liver-specific receptor and that additional receptors must play a role in entry as well. The generation of pseudotype viruses expressing filovirus glycoproteins has proven to be a useful tool in studying interactions with cellular factors (ie: potential receptors). Early studies using these pseudotype viruses were able to demonstrate that while they exhibit certain functional similarities, MARV and EBOV GP_{1,2} interact with target cells by distinct processes, based largely on differential sensitivities to treatment of target cells with tunicamycin, endoglycosidase H, or protease (pronase) (Chan et al., 2000). Folate receptor (FR)- α was identified as a cofactor for filovirus cellular entry and its expression in Jurkat cells (normally resistant to filovirus infection) facilitated MARV or EBOV entry, and FR- α blocking reagents inhibited infection by MARV or EBOV (Chan et al., 2001). FR- α , a 38- to 39-kDa glycosyl phosphatidylinositol (GPI)-linked cell surface protein, normally binds and internalizes extracellular folic acid via vesicles (Antony, 1996). Additionally, although still somewhat controversial, FR- α is thought to be endocytosed via caveolae (Anderson, 1998). Briefly, caveolae are vesicles enriched with cholesterol and sphingolipids and are involved in a wide range of biological events such as transmembrane signaling, cellular cholesterol homeostasis, and cellular entry by certain bacteria, natural ligands, toxins, and viruses (Anderson, 1998; Kurzchalia and Parton, 1999). It is interesting to note that caveolae have been reported to be present in human cell types that are known to be major targets for wild-type ZEBOV and MARV, specifically, endothelial cells, hepatocytes, and macrophages (Calvo et al., 2001; Kiss et al., 2002; Kiss et al., 2000; Rizzo et al., 1998). The most direct evidence for a role of caveolae in filovirus entry was demonstrated by using human immunodeficiency virus

type 1 provirus, NL4-3 (that lacks envelope but carries a luciferase reporter gene) pseudotyped with ZEBOV or MARV GP_{1,2}. It was shown by confocal microscopy that pseudotype viruses were able to colocalize with caveolin-1 (CAV-1), a protein marker of caveolae (Empig and Goldsmith, 2002). The authors of this study then speculated that lipid rafts may be involved directly or indirectly in the filovirus entry process as well, since these membrane domains are precursors to caveolae (Empig and Goldsmith, 2002). Studies performed by Bavari et al. during the same time were able to provide the evidence that lipid rafts function as a gateway for the entry and exit of filoviruses (Bavari et al., 2002). The ability of EBOV and MARV to utilize rafts is not a unique ability of filoviruses. Indeed, HIV, Herpes simplex virus and Epstein–Barr virus are well-studied examples of viruses that have strategies to subvert raft-associated signalling and utilize rafts for viral entry (Bender et al., 2003; Manes, del Real, and Martinez, 2003). In an attempt to further characterize the role of FR- α in filovirus entry, Sinn et al. noted that polarized human airway epithelia expressed abundant FR- α on their apical surface (Sinn et al., 2003). Using feline immunodeficiency virus (FIV)-based vectors to pseudotype EBOV GP_{1,2} they were able to show FR- α -dependent and -independent entry by filovirus glycoprotein-pseudotyped FIV-based vectors in airway epithelia. This study was the first to raise questions regarding the necessity of FR- α , and indirectly, caveolae in filovirus entry. Further experiments later identified cell lines and primary cell types such as macrophages that were readily infected by GP_{1,2} pseudotypes despite lacking detectable surface FR- α , indicating that this receptor is not essential for Ebola virus infection (Simmons et al., 2003b). Furthermore, the authors report that T-cell lines stably expressing FR- α are not infectible, suggesting that FR- α is also not sufficient to mediate

entry. Due to the fact that T-cell lines lack caveolae (the predominant route of FR- α -mediated folate metabolism) it was thought that perhaps co-expression of FR- α with caveolin-1, the major structural protein of caveolae, would rescue infectivity in a T-cell line, however, this was unsuccessful (Simmons et al., 2003b). The current status regarding the role of FR- α and caveolae in filovirus entry remains controversial. While it appears that they do play a role in cellular entry, it is likely that other receptors are also utilized and it will require further studies to elucidate their identities.

Whilst a great deal of attention has been given to FR- α and caveolae in entry of filoviruses another type of cellular receptor has recently come to the forefront of filovirus receptor research. DC-SIGN (dendritic cell [DC]-specific ICAM-3 grabbing non-integrin, CD209) is a type II membrane protein with a C-type lectin extracellular domain. Expression of DC-SIGN is restricted to immature dendritic cells (Alvarez et al., 2002). L-SIGN (also known as DC-SIGN(R)), a homologue of DC-SIGN but expressed on the surface of liver and lymph node endothelial cells rather than DCs, has been shown to bind most lentiviruses of primates. The C-type lectins DC-SIGN and DC-SIGNR are known to efficiently bind human immunodeficiency virus (HIV) and simian immunodeficiency virus (SIV) strains and can transmit bound virus to adjacent CD4-positive cells (Turville et al., 2003). The pattern of DC-SIGN and L-SIGN expression in tissues and the ability of retroviral glycoproteins to bind these receptors were the precipitating factors that led investigators to study their interaction with filovirus glycoprotein (Alvarez et al., 2002). DC-SIGN and L-SIGN are indeed implicated in EBOV GP-mediated cell infection, however, the contribution and the specific molecular interactions of DC-SIGN and L-SIGN in Ebola virus cell entry were not completely elucidated. The current hypothesis

regarding these receptors is that they bind and concentrate EBOV to the cell membrane, thereby facilitating the interaction *in cis* with cofactors required for cell entry, the low density of which may be limiting for infection of certain cell types (Alvarez et al., 2002). DC-SIGN and L-SIGN have been coined “attachment factors” for EBOV and it is thought that they play a role in tissue tropism based on their expression *in vivo* and the fact that cells harboring these proteins are typically seen as early and major targets of EBOV infection (Simmons et al., 2003a).

Following attachment, filoviruses are believed to enter the cell by a process of endocytosis, acidification of the endocytic vesicle, and fusion of virus and host membranes that releases the nucleocapsid into the cell cytoplasm (Sanchez, 2001). GP₂ contains a putative fusion peptide near the N-terminal portion of the protein that is capable of inserting itself into membranes that contain phosphatidylinositol and resemble the lipid composition of hepatocyte plasma membranes (Ruiz-Arguello et al., 1998). The fusion peptide is thought to mediate the fusion of host and virus membranes as they are brought together by a conformational change in GP_{1,2} during the entry process (Ito et al., 1999).

1.6.3 Viral replication in susceptible host cells

The host cell cytoplasm is the location for replication of the filovirus genome. Once released into the cytoplasm the negative-sense genome must be transcribed. Encapsidated RNA acts as template for the generation of polyadenylated, monocistronic mRNA that is transcribed from the genes in a 3' to 5' manner (Sanchez, 2001). As early as 7 hours post infection NP mRNA can be detected and transcription peaks approximately 11 hours later (Sanchez and Kiley, 1987). The host cellular machinery

functions to transcribe and subsequently translate all the viral genes leading to their buildup within cells. Subsequent to the translation of viral proteins there is a switch from transcription to replication that leads to the synthesis and encapsidation of full-length positive-sense RNA (antigenome). The antigenome copy can serve as a template for the synthesis of full-length genomic RNA that is rapidly encapsidated by RNP complex proteins (Sanchez, 2001). As the newly transcribed RNP proteins are sequestered for encapsidation their depletion is thought to signal a switch back to transcription, eventually leading to a homeostatic balance between transcription and replication. As newly synthesized negative-sense nucleocapsids in the cytoplasm and membrane bound proteins (VP24, VP40 and GP_{1,2}) accumulate they amalgamate at the plasma membrane where viral egress occurs (Feldmann et al., 1996; Sanchez, 2001). A schematic representation of filovirus replication within a host cell is depicted below.

(Figure 5)

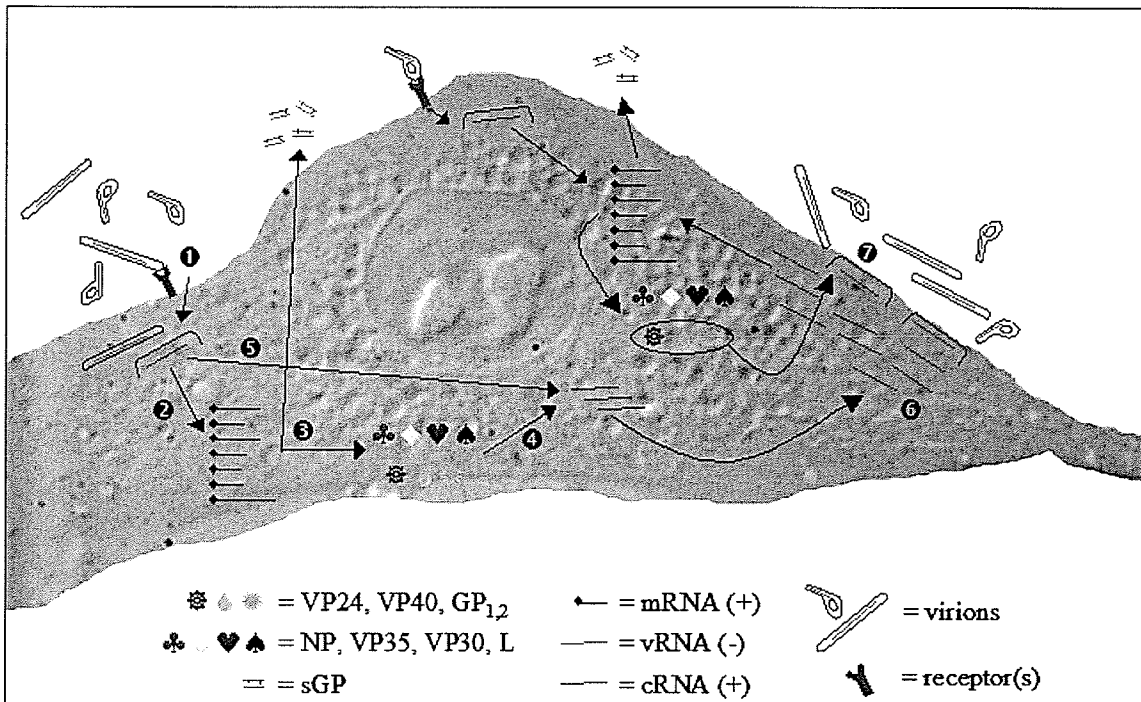


Figure 5. Filovirus replication cycle in a susceptible host cell. Viral replication begins with attachment to a host cell receptor (1). Viral particles enter the cell and the nucleocapsid is released into the cytoplasm. Primary transcription results in positive sense mRNA transcripts from viral genes (2). mRNA transcripts are then translated into viral proteins (3). In the case of EBOV a soluble glycoprotein, sGP, is secreted. The viral RNA (vRNA) is replicated with the aid of viral RNP proteins NP, VP30, VP35 and L into a positive sense, complementary RNA (cRNA), antigenome (5). The cRNA is used as template to generate progeny vRNA which are encapsided by RNP proteins (6). In the final step of replication the progeny nucleocapsids are united at the plasma membrane with VP24, VP40 and GP_{1,2} and mature viruses bud from the cell surface membrane (7).

1.7 Ebola Hemorrhagic Fever

1.7.1 Clinical presentation of Ebola Hemorrhagic Fever

Filovirus infection often results in fulminant hemorrhagic disease in human and non-human primates (Schnittler and Feldmann, 1999). Indeed, among all viral hemorrhagic fevers (VHFs) those caused by filoviruses are regarded as the most severe and are typically associated with hemorrhagic manifestations, coagulation disorders, generalized shock, and hepatic involvement (Feldmann et al., 2003; Feldmann and Klenk, 1996). Close observations during human cases of filovirus hemorrhagic fever (HF) have

generated important data regarding the clinical course of disease (Sanchez, 2001). The incubation period for filovirus HF is approximately 4 to 10 days and is followed by abrupt onset of non-specific flu-like symptoms including fever, chills, malaise, and myalgia. As disease progresses more severe and multi-system symptoms are noted such as gastrointestinal (anorexia, nausea, vomiting, abdominal pain, diarrhea), respiratory (chest pain, shortness of breath, cough), vascular (conjunctival injection, postural hypotension, edema), and neurologic (headache, confusion, coma) manifestations (Sanchez, 2001). Death is usually associated with fulminate shock which is characterized by fluid distribution problems (increased permeability), hypotension, coagulation disorders and widespread focal tissue destructions (Schnittler and Feldmann, 2003). A humoral antibody response in survivors is observed typically between days 7 and 11 which also marks a turning point to either death or an improvement in health (Ksiazek et al., 1999; Rowe et al., 1999). The small percentage of individuals that do not succumb to disease can expect a prolonged period of convalescence with varying degrees of sequelae including arthralgia (joint pain), uveitis (inflammation of the uvea, the part of the eye that collectively refers to the iris, the choroid of the eye, and the ciliary body), psychosocial disturbances, and orchitis (inflammation of the testis) (Rowe et al., 1999).

1.7.2 Transmission of Ebola virus

Outbreaks of filoviral HF in humans are propagated by person-to-person transmission involving close contact (Sanchez, 2001). The relative inefficiency of transmission is illustrated by somewhat low secondary attack rates of 10-15%, however, risk increases with respect to level of contact: from 23% for family members sleeping in the same room as the patient, to 81% for individuals providing active nursing care to a

patient during the 1976 Sudan outbreak (Baron, McCormick, and Zubeir, 1983; Sanchez, 2001). Perhaps one of the greatest risks for contracting disease is through nosocomial infection. The reuse of needles and syringes was identified as a transmission route during outbreaks (Sanchez, 2001). Health care providers are at a particularly high risk of infection. Indeed, 25% of the total infections during the 1995 ZEBOV outbreak in Kikwit were among health care professionals, however, once functional isolation wards to deal with EHF were established and protective supplies distributed to individuals who were involved with patient care the number of infections for these individuals dropped dramatically (Heymann et al., 1999; Kerstiens and Matthys, 1999). Utmost care should be taken with infected blood, secretions, excretions, tissues, and hospital materials and waste (Sanchez, 2001).

The ability of virus to be transmitted through the aerosol route remains controversial. Whilst virus was experimentally transmitted in non-human primates by aerosol route and virions have been identified in alveoli of infected monkeys, the actual role of this transmission route during human outbreaks is unclear (Geisbert et al., 1992; Johnson et al., 1995). Additional suggestive evidence for this transmission route was described during an outbreak of disease in non-human primates and was suspected to have been transmitted by droplets and perhaps small-particle aerosols (Sanchez, 2001).

1.7.3 Diagnosis

A differential diagnosis of an acute febrile illness with headache and diarrhea can be caused by a variety of different agents. Other causes of viral hemorrhagic fever include dengue, yellow fever, Lassa fever, South American arenaviral hemorrhagic fevers, Crimean Congo Hemorrhagic Fever, Rift Valley Fever, and hemorrhagic fever

with renal syndrome (Zaki and Peters, 1997). Both occupational and travel history are imperative in narrowing the diagnosis. Rural travel, jungle or cave exposure, contact with sick humans, or contact with sick or dead primates should all raise a flag for additional concern (Sanchez, 2001). More common causes of febrile illness that should be ruled out for travelers include malaria, typhoid fever, leptospirosis, borelliosis, septicemic plague, tick typhus, and dysentery (Peters and Khan, 1999).

An etiologic diagnosis should be sought at the earliest stages of illness. Virus, viral antigen, and viral RNA in serum or blood should be isolated during the acute phase of illness (Peters and Khan, 1999). Virus can be isolated on a variety of cell types as mentioned previously, however, Vero cells are typically the cell line of choice. Evidence of virus can be demonstrated directly by electron microscopic analysis of tissue culture supernatants, blood or serum, in addition to scanning of cell cultures for cytopathic effects and immunofluorescence assays (IFA) on infected cells (Peters, 1996). Detection of viral antigen from infected patients may be accomplished by enzyme linked immunosorbent assay (ELISA), however, if levels are low a more sensitive method to detect viral RNA such as reverse transcriptase polymerase chain reaction (RT-PCR) is more appropriate. In later stages of illness antibody capture ELISA tests can further support the diagnosis. IgM ELISA may only be positive during the early stages of convalescence and patients can be followed for rising IgG levels to further increase confidence in the diagnosis.

1.7.4 Therapy

There is currently no specific antiviral therapy for filovirus induced HF and patient care is supportive in nature (Slenczka, 1999). Supportive treatment should

include electrolyte balancing, particularly with respect to potassium substitution. Additionally, in several outbreaks antibiotics were administered (tetracycline, chloramphenicol, penicillin, cephalotin, and streptomycin) but did not alter the fever or course of disease. Often, however, antibioid treatment was continued in the hopes to avoid secondary bacterial infection (Slenczka, 1999). During various outbreaks and experimentally in animal models a number of treatments were administered in an attempt to reduce severity of disease. In particular neutralizing antibodies specific for the viral surface glycoprotein were shown to be both protective and therapeutic in rodent models (Maruyama et al., 1999a; Parren et al., 2002; Wilson et al., 2000). Baboons were successfully protected from EBOV challenge when administered a hyperimmune horse serum produced by Russian scientists (Krasnianskii et al., 1995). The use of horse serum in humans has been questioned, however, because horses produce a subclass of immunoglobulin (IgG_T) that is highly immunogenic in humans (Feldmann et al., 2003). The use of convalescence sera during an outbreak in Kikwit was reported as protective, however, the actual efficacy has been questioned since the severity of disease at that point in the outbreak was already somewhat reduced (Feldmann et al., 2003; Mupapa et al., 1999). The beneficial use of convalescence sera was also reported during MARV in Frankfurt, Germany (Slenczka, 1999; Stille et al., 1968). Since the coagulation cascade is dysregulated during EHF (leading to disseminated intravascular coagulation, DIC), treatments to alleviate microthrombi formation have been attempted. Heparin was used to successfully treat two MARV-infected patients (Peters and Khan, 1999). Most recently it has been shown that infection with EBOV induces overexpression of the procoagulant tissue factor in primate monocytes and macrophages, suggesting that

inhibition of the tissue-factor pathway could ameliorate the effects of EBOV HF (Geisbert et al., 2003c). In further studies macaques were administered recombinant nematode anticoagulant protein c2 (rNAPc2), a potent inhibitor of tissue factor-initiated blood coagulation, and post-exposure protection was conferred and provided a new foundation for therapeutic regimens that target the disease process rather than viral replication (Geisbert et al., 2003a). Treated animals had increased survival times with 33% survival rates and attenuation of the coagulation and proinflammatory responses.

1.7.5 Vaccine developments

The first attempts to develop a vaccine for EBOV began soon after the first outbreak in 1976 and used formalin-fixed or heat-inactivated virus in an attempt to confer protection to guinea pigs and non-human primates (Feldmann et al., 2003; Lupton et al., 1980; Mikhailov et al., 1994). Despite initial optimism, the protection achieved in both studies was inconsistent and it was later demonstrated that inactivated virus did not induce sufficient immunity to reliably protect baboons against a lethal dose of virus (Chupurnov et al., 1995).

Since the late 1990's there has been a greater effort on vaccine development particularly for EBOV. The majority of these attempts have focused on subunit vaccines that are based on one or more of the viral structural proteins. A variety of approaches including naked DNA, adenovirus, vaccinia virus, vesicular stomatitis virus (VSV), Venezuelan equine encephalitis virus (VEEV) replicons and virus-like particles (VLPs) have been used as mechanisms to deliver GP_{1,2}, NP, VP24, VP30, VP35 and/or VP40 (Garbutt et al., 2004; Geisbert et al., 2002; Pushko et al., 2000; Sullivan et al., 2003;

Sullivan et al., 2000; Vanderzanden et al., 1998; Warfield et al., 2003; Wilson et al., 2001; Xu et al., 1998). A summary of these vaccine attempts can be seen in Table 3.

(Table 3)

Delivery System	Viral Protein	Animal Model	Survivors/ challenged	References
Vaccinia virus	GP	Guinea pig	3/5	(Gilligan et al., 1997)
Vaccinia virus	GP	Cynomolgus macaque	0/3	(Geisbert et al., 2002)
VEEV replicon	VP24	Mouse	37/60*	(Wilson et al., 2001)
VEEV replicon	VP30	Mouse	30/60*	(Wilson et al., 2001)
VEEV replicon	VP35	Mouse	23/59*	(Wilson et al., 2001)
VEEV replicon	VP40	Mouse	32/60*	(Pushko et al., 2000; Wilson et al., 2001)
VEEV replicon	NP	Mouse	20/20	(Wilson et al., 2001)
VEEV replicon	GP	Guinea pig	8/10	(Pushko et al., 2000)
VEEV replicon	GP	Mouse	18/20	(Pushko et al., 2000)
VEEV replicon	GP	Cynomolgus macaque	0/3	(Geisbert et al., 2002)
VEEV replicon	NP	Cynomolgus macaque	0/3	(Geisbert et al., 2002)
VEEV replicon	GP+NP	Cynomolgus macaque	0/3	(Geisbert et al., 2002)
DNA	NP	Guinea pig	5/8	(Xu et al., 1998)
DNA	NP	Mouse	70-80% [†]	(Vanderzanden et al., 1998)
DNA	GP	Guinea pig	13/15	(Sullivan et al., 2000; Xu et al., 1998)
DNA	GP	Mouse	50-100% [†]	(Vanderzanden et al., 1998)
DNA	sGP	Guinea pig	8/11	(Xu et al., 1998)
DNA	GP+NP	Guinea pig	8/8	(Sullivan et al., 2000)
DNA + adenovirus	GP+NP	Cynomolgus macaque	4/4	(Sullivan et al., 2000)
Adenovirus	GP+NP	Cynomolgus macaque	100%	(Sullivan et al., 2003)
VLP	GP+ VP40	Mouse	100%	(Warfield et al., 2003)
VSV	GP	Mouse	100%	(Garbutt et al., 2004)

Table 3. Summary of EBOV vaccine candidates. * represents the combined data for 2 mouse strains although 1 strain was protected better than the other. † Survival was dependent on the dose of DNA administered. GP, surface glycoprotein; NP, nucleoprotein; sGP, secreted glycoprotein; VEEV, Venezuelan equine encephalitis virus; VP, virion protein; VSV, vesicular stomatitis virus; VLP, virus-like particles. Table modified from Feldmann et al, 2003 with permission.

The efficacy and specific details of these vaccine strategies have been recently reviewed in great detail (Feldmann et al., 2003; Geisbert and Jahrling, 2003; Hart, 2003). One point that is important to note in all these studies is that results using small animal models are not always predictive of outcome in non-human primates. Whilst they are useful and necessary screening tools, results should be confirmed in a non-human primate model that is more representative of human infection.

In the past the necessity for an EBOV vaccine was questioned since the number of outbreaks were limited and occurred in isolated areas. With the appearance of REBOV in North America, increased international travel and the escalating threat of bioterrorism this view has changed. Additionally, in the past few years the number of EBOV outbreaks has been increasing. It seems likely that if a vaccine became available all at-risk medical personnel would be vaccinated including first-responders, hospital workers, laboratory workers and military personnel (Feldmann et al., 2003).

1.8 Pathogenesis

The pathology of EBOV infections has been examined extensively from tissues obtained during human outbreaks in addition to studies using susceptible animal models (mice, guinea pigs and non-human primates). The high containment setting necessary to study filoviruses, along with certain inconsistencies between animal models and human infection have proven to be challenges in the push to gain further understanding of filovirus pathogenesis. One aspect concerning animal models that should be kept in mind is that they do not always adequately reproduce EHF, specifically, there are differences in hemorrhagic manifestations, coagulopathy, and bystander apoptosis. Despite these

challenges, recent studies have added significant light on the current model of pathogenesis.

1.8.1 Projected sequence of infection

As described earlier, the primary mechanism for human filoviral infection is close contact with skin and secretory products from infected individuals. Virus is believed to enter via small skin lesions and mucus membranes from which it can acquire direct access to the vascular system or indirect access through the lymphatic system (Schnittler and Feldmann, 1999).

Primary sites of viral replication occur in monocytes/macrophages and dendritic cells (DC) (Geisbert et al., 2003b; Geisbert et al., 1992; Ryabchikova and Price, 2004; Zaki and Peters, 1997). Cells of the mononuclear phagocytic system (MPS) located in multiple organs including the liver (Kupffer cells), spleen, lymph nodes, lung (alveolar macrophages), serous cavities (pleural and peritoneal macrophages) and nervous system (microglia) are infected, however, the lymph nodes, liver and spleen are the three organs consistently preferred for filovirus replication (Feldmann and Klenk, 1996). Schnittler and Feldmann have suggested that this organ tropism is largely due to direct access of particles to sessile cells of the MPS without penetration of cellular or tissue barriers (Schnittler and Feldmann, 1998). Subsequent to infection and replication in macrophages, viral particles gain access to secondary lymph nodes and then ultimately the vascular system which marks a state of viremia (Schnittler and Feldmann, 1999). In addition to tissues from fatal human cases and *in vitro* studies, a serial sacrifice experiment of EHF in cynomolgus monkeys has given a tremendous amount of data regarding the progression of disease in an animal model that most closely resembles

human infection (Geisbert et al., 2003b; Geisbert et al., 2003d). Virus was shown to spread from initial infection sites by monocytes and DC to regional lymph nodes, most probably via lymphatics, and to liver and spleen via blood. Virus was then shown to infect tissue macrophages, DC and fibroblastic reticular cells (FRC) (Geisbert et al., 2003b). Monocytes/macrophages have been shown experimentally to be early and sustained targets of EBOV in both guinea pigs and moribund monkeys (Connolly et al., 1999; Davis et al., 1997; Geisbert et al., 1992; Jaax et al., 1996). The recent study in cynomolgus monkeys confirmed these observations with viral RNA detected in lymphoid monocytes/macrophages as early as two days postinfection (Geisbert et al., 2003b). Unlike monocytes/macrophages, until the current study by Geisbert et al. the relative significance of DC in EBOV pathogenesis was not well documented. DC are professional antigen-presenting cells, derived from bone marrow, that possess the ability to initiate and modulate cell-mediated immune responses by capturing and processing exogenous antigens in peripheral tissues and then migrating to regional lymph nodes where they undergo maturation characterized by up-regulation of MHC and costimulatory molecules and then are able to present antigen leading to T-cell activation (Geisbert et al., 2003b). The ability of a virus to attack and manipulate cells that play critical roles for initiating the antiviral immune response is not novel. In fact, several well-characterized viruses including measles, Dengue and HIV, have evolved mechanisms to specifically impair the function of DC, thereby increasing their likelihood of survival (Fugier-Vivier et al., 1997; Grosjean et al., 1997; Ho et al., 2001). Human cytomegalovirus has been shown to partially down-regulate MHC molecules and up-regulate the apoptosis-inducing ligands CD95L and TNF-related apoptosis-inducing

ligand (TRAIL) to remove activated T-lymphocytes (Raftery et al., 2001). Geisbert et al. have speculated that the interaction between filoviruses and DC is critical for the outcomes of EBOV infections based on the observations that TRAIL expression is increased and MHC II partially suppressed during EBOV infection of immature DC *in vitro* (Hensley et al., 2002); bystander apoptosis of lymphocytes observed in tissues of moribund monkeys (Geisbert et al., 2000); and the existence of an immunosuppressive motif in the C-terminal region of GP_{1,2} (Bukreyev et al., 1993a; Sanchez et al., 1993; Sanchez et al., 1996). In tandem to T-lymphocyte depletion, infected monocytes/macrophages release a host of soluble mediators including proinflammatory cytokines including MIP-1 α and MCP-1 that function in the recruitment of additional macrophages to infected areas thereby increasing the number of target cells available for viral infection and further amplifying an already dysregulated host response (Geisbert et al., 2003b). Cultured primary human monocytes/macrophages are also activated upon infection resulting in an increase of TNF- α , interleukins (IL)-1 β , IL-6, and IL-8 (Feldmann et al., 1996; Stroher et al., 2001). Infection by MARV led to a significant increase in release of TNF- α with peak values of 3ng/mL by 12-24 hours post-infection. Stroher et al were able to demonstrate that UV-inactivation of whole virus did not impair the activation and production of cytokines on either the transcriptional nor protein level (Stroher et al., 2001). Since these studies used inactivated virus stocks (ie: non-purified virus) it remained unknown whether this activation was due to an interaction of the inactivated virus with monocytes/macrophages or by soluble factors (ie: secreted glycoproteins). EBOV infected patients also exhibit increased serum levels of various cytokines and studies have correlated increased levels of IL-10, neopterin and IL-1

receptor A (IL-1RA) with fatal outcome, whilst presence of IL-1 β and elevated concentrations of IL-6 in the plasma during the symptomatic phase have been indicated as markers of non-fatal infections (Baize et al., 2002; Baize et al., 1999; Leroy et al., 2000; Villinger et al., 1999).

1.8.2 Viral spreading and role of the endothelium

Infected macrophages discovered in various tissues are thought to originate from infected circulating monocytes/macrophages that extravasate following infection (Feldmann et al., 1996; Geisbert et al., 1992; Ryabchikova and Price, 2004). Virus-induced cytokine release activates the endothelium and is proposed to be the trigger for extravasation. Specifically, various inflammatory mediators including TNF- α , IL-1 β and H₂O₂, have been shown to increase expression of various cell adhesion molecules on endothelial cells including intravascular adhesion molecule-1 (ICAM-1), vascular cell adhesion molecule-1 (VCAM-1) and E- and P-selectin (Schnittler and Feldmann, 1999). E- and P-selectin, Ca²⁺-dependent lectins, mediate the binding of leukocytes to the surface of the endothelium and initiate extravasation (Lenter et al., 1994; Vestweber, 1992; Vestweber, 1993). This first step in extravasation consists of leukocyte “rolling” on the endothelium and involves the selectins that permit loose binding and therefore facilitate the rolling. Selectins allow leukocytes to roll in the direction of flow to the proximity of activating signals exhibited by the endothelial cells (Vallet, 2003). The second stage of extravasation involves the integrin family and immunoglobulin-like receptors that allow for leukocyte arrest and strengthening of adhesion. In the case of endothelial cells these adhesion molecules include ICAMs and VCAMs. In a third step, the leukocytes migrate to the borders of the endothelial cells to interact with the adhesion

molecules. Diapedesis into the tissue by leukocytes is believed to be mediated by the interaction of lymphocyte function-associated antigen (LFA-1) and ICAM-1, and the movement is directed by a chemotactic gradient (Hogg, 1993). Another challenge leukocytes encounter when crossing the endothelium is that interendothelial junctions must be opened. The cadherin/catenin complex and platelet endothelial cell adhesion molecule (PECAM)-1 are localized at these junctions (Schnittler and Feldmann, 1999).

(Figure 6)

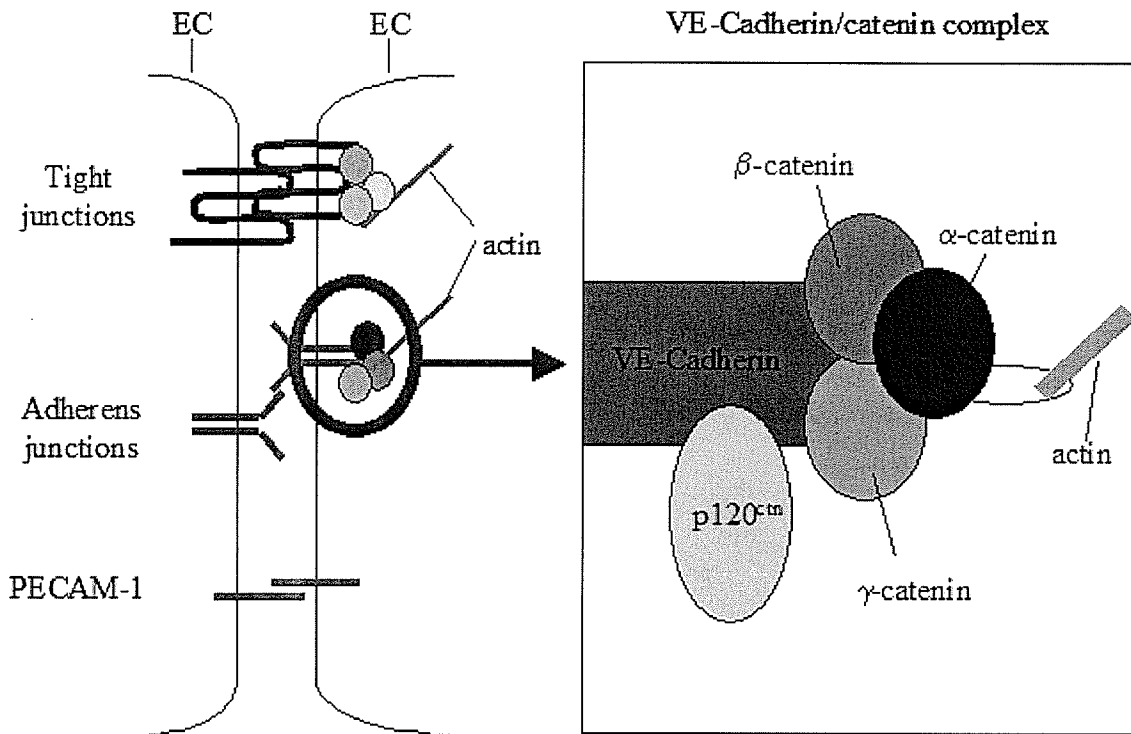


Figure 6. Organization of endothelial junctions. The endothelium displays an extended adherens junctional zone in which gap (not shown) and tight junctions are morphologically inserted. Adherens junctions are shown in greater detail. Ca^{2+} -dependent VE-cadherin occurs as homodimers and are associated with the catenins (alpha, beta, and gamma) and p120. The cadherin/catenin complex is also associated with the actin cytoskeleton. EC, endothelial cell; PECAM-1, platelet endothelial cell adhesion molecule, VE-cadherin, vascular endothelial-cadherin.

PECAM-1 has been associated with leukocyte recruitment into sites of inflammation and the distribution of the protein in situ was altered following systemic

application of histamine (Liao et al., 1995). The cadherin/catenin complex also becomes disorganized following leukocyte adhesion allowing monocytes to enter sites of inflammation (Del Maschio et al., 1996). Interestingly, during filovirus infection there is a lack of leukocyte infiltrates in areas of focal necrosis thereby suggesting a deficient immunoreaction of unknown etiology (Ryabchikova and Price, 2004).

Endothelial dysfunction can lead to a multitude of vascular effects that may cause disturbances in vascular permeability or hemorrhage. During filovirus infection the endothelium appears to be affected in two ways: directly by infection with filoviruses, leading to activation and eventual cytopathogenic replication, and indirectly by a mediator-induced inflammatory response (Feldmann et al., 2003). *In vitro* data has shown that virus-induced cytokine release leads to activation of the endothelium that can be defined as increased expression and/or release of adhesion molecules as well as a breakdown of the endothelial barrier function (Schnittler and Feldmann, 2003; Vallet, 2003). While the molecular mechanisms for the breakdown of endothelial barrier function are not completely understood, there is evidence for changes in the protein organization of the adherens junction, specifically the VE-cadherin/catenin complex (Schnittler and Feldmann, 1999). Additionally, supernatants from MARV-infected macrophages are able to increase permeability in endothelial monolayers and this can be partially blocked by antibodies which neutralize TNF- α , indicating a critical role for this protein in virus-induced shock (Feldmann et al., 1996). A recent serial sacrifice experiment of EHF in monkeys revealed ultrastructural evidence of endothelial cell activation and disruption but attributes it to indirect mechanisms since they were unable to associate the changes with the presence of intracytoplasmic EBOV antigens. Overall,

this study concluded that EBOV infection primarily affects the function rather than the structure of endothelial cells and that EBOV-induced coagulopathy results primarily from vascular disruption induced by factors secreted from infected monocytes/macrophages and dendritic cells (including cytokines and tissue factor, TF), whereas direct virus-induced cytolysis of endothelial cells plays a minimal, secondary role in hemorrhagic diathesis (Geisbert et al., 2003d). The fact that antigen-positive endothelial cells are a hallmark of human infection and filoviruses readily replicate in human umbilical cord endothelial cells (HUVEC) *in vitro* cannot be dismissed. Whether their infection plays a major role in EBOV pathogenesis as compared to indirect effects of mediators remains to be determined. The role of EBOV soluble glycoproteins in endothelial activation and dysfunction has never been tested. EBOV sGP was suggested to play a role in immune suppression by inactivation of neutrophils but this data has been disputed (Maruyama et al., 1999b; Sui and Marasco, 2002; Yang et al., 1998). The ability of sGP to function in endothelial activation has been suggested in a model by Schnittler et al. as a third mechanism by which the endothelium is altered during filovirus infection (Schnittler and Feldmann, 2003).

1.9 Objectives and hypothesis

The mechanisms by which EBOV mediates severe disease remain largely unknown. Major breakthroughs in pathogenesis studies have provided interesting data regarding potential cellular receptor co-factors, role of DC during infection, and release of tissue factor by infected macrophages contributing to coagulopathy among others (Alvarez et al., 2002; Empig and Goldsmith, 2002; Geisbert et al., 2003b; Geisbert et al., 2003c; Simmons et al., 2003a). One of the major enigmas of EBOV pathogenesis is the

role of the secreted glycoproteins. The secreted glycoprotein, sGP, and its smaller cleavage product, Δ peptide are the major products from the glycoprotein gene and sGP has been detected in patient serum (Feldmann et al., 1999; Sanchez et al., 1999). A multitude of papers have speculated that a protein as abundant as sGP surely plays a role in pathogenesis, however, the only data to date suggests a role in down-regulating cytotoxicity of GP_{1,2} (on the transcriptional level by producing sGP preferentially to GP_{1,2}) and possibly an interaction with neutrophils, although the later point has been disputed. The identification of truncated forms of the transmembrane glycoprotein has also spiked interest in a potential decoy role or perhaps an ability of these proteins to activate target cells.

I hypothesize that the soluble glycoproteins of filoviruses function as target cell activators and therefore serve as pathogenic determinants. Previous studies have established that viral replication is not necessary for activation of macrophages, however, the activating factor was not determined (Stroher et al., 2001). It is reasonable to assume that activation may be due to either direct binding of inactivated virus to macrophages or by an interaction with soluble glycoproteins also present in the inoculum. It is unknown whether the soluble glycoproteins contribute to activation of secondary target cells, specifically, endothelial cells. Studies with MARV, which lacks sGP and Δ peptide, demonstrated an important role of TNF- α but antibodies to this cytokine were not sufficient to completely abolish the permeability enhancing effects of macrophage supernatants on endothelial cells (Feldmann et al., 1996). The soluble forms of the transmembrane glycoprotein may play a role in the activation and dysfunction of the endothelium. It has been speculated that sGP may account for more severe clinical

disease in EBOV infection by interacting with the endothelium, although this was never tested (Feldmann et al., 2003; Schnittler and Feldmann, 1999; Schnittler and Feldmann, 2003).

The goal of this study was to synthesize authentic soluble glycoproteins in amounts sufficient for analysis and functional testing. The extensive glycosylation of the proteins, however, presents a unique challenge since most standard methods are not appropriate (bacterial, yeast and baculovirus expression systems). In this study I sought to biosynthesize the soluble glycoproteins in a mammalian system, scale-up the production to larger amounts, purify the proteins and analyze their authenticity based on characterization described in previous studies. Following protein production, I used the proteins in functional studies to analyze their roles in activation of target cells (macrophages and endothelial cells).

1.10 Significance of the study

This is the first report of the biosynthesis and purification of EBOV secreted glycoproteins authentic to those produced during wildtype EBOV infection. Studies regarding the function of the soluble glycoproteins were previously hampered by lack of purified proteins for testing. Once these proteins are produced numerous studies finally investigating their role in pathogenesis can be initiated. They can also serve as extremely useful tools in future work to establish antibodies, determine protein levels in serum by ELISA and attempt protection in animal models.

2.0 Materials and Methods

2.1 Cells

2.1.2 Eukaryotic continuous cell lines

The human embryonic kidney cell line (293T) were the generous gift of Dirk Lindemann (Technical University, Dresden, Germany). Cells were maintained in Dulbecco's Modified Eagle Medium (DMEM, Sigma) supplemented with 10% heat-inactivated (1h @ 56°C) fetal bovine serum (FBS), L-glutamine (2mM), penicillin (100U/mL) and streptomycin (100µg/mL) antibiotic solution. The 293T cell line contains the gene for the temperature-sensitive simian virus 40 large T antigen and is a derivative of the 293 cell line (DuBridge et al., 1987). Tissue culture dishes were coated with poly-D-lysine (1mg/mL, Sigma) for 30 minutes at 37°C to minimize cell detachment prior to seeding of cells. Following incubation, poly-D-lysine was removed and the tissue culture dishes were washed one time with sterile water before cells were seeded. Cells were maintained at 37°C in a humidified (95%), 5% CO₂ environment.

Baby hamster kidney cells which stably express the bacteriophage T7 promoter are designated "BHK-T7". Cells were the generous gift of Klaus Conzelmann (Max-von-Pettenkofer Institute, University of Munich, Germany). BHK-T7 cells were maintained in Glasgow Minimal Essential Medium (G-MEM, Invitrogen) supplemented with L-glutamine and without tryptose-phosphate. Media was supplemented with 1mg/mL geneticin, 10% heat-inactivated newborn calf serum, tryptose-phosphate (1X), MEM amino acid solution without glutamine (2X), L-glutamine (2mM), penicillin (100U/mL) and streptomycin (100µg/mL) antibiotic solution. A stock bottle of medium was prepared with all ingredients except for heat-inactivated newborn calf serum and

geneticin, which were added fresh. All medium and supplements for BHK-T7 cells were purchased from Gibco-BRL. Cells were maintained at 37°C in a humidified (95%), 5% CO₂ environment.

The epithelial cell line Vero E6 (*Cercopithecus aethiops* kidney, ATCC CRL-1586) as well as baby hamster (*Mesocricetus auratus*) kidney-21 (BHK-21, ATCC CCL-10) cells were maintained in DMEM supplemented with 10% heat-inactivated FBS, L-glutamine (2mM), and penicillin (100U/mL) and streptomycin (100µg/mL) antibiotic solution. Cells were maintained at 37°C in a humidified (95%), 5% CO₂ environment.

2.1.3 Isolation and culture of primary human monocytes/macrophages

Human peripheral blood mononuclear cells (PBMC) consisting of monocytes and lymphocytes were separated from healthy whole blood using Ficoll-Paque Plus density gradient centrifugation (Amersham Biosciences). Donor blood was non-pooled. PBMCs were seeded into *Primaria* 24-well culture plates (Becton Dickenson) and allowed to adhere for 1 h. Following the 1 h incubation monolayers were washed extensively to remove non-adherent cells. Cells were incubated at 37°C in a humidified (95%), 5% CO₂ environment for 7 days to allow differentiation into mature macrophages. The cells were cultured in RPMI 1640 (Invitrogen) containing 20% heat-inactivated (1 h @ 56°C) human AB serum, penicillin (100U/mL), streptomycin (100µg/mL), L-glutamine (2mM), nonessential amino acids (2mM), and sodium pyruvate (2mM).

2.1.4 Isolation and culture of primary human umbilical cord endothelial cells

Endothelial cells were isolated from human umbilical veins (HUVEC). Cords were cut at both ends with sterile surgical scissors and blood allowed to drain from the umbilical vein. A sterile blunt-end needle was inserted into the umbilical vein and

stabilized with a sterile hemostat to clamp that end of the umbilical cord. A 20mL syringe was attached to the needle and the vein washed three times with sterile PBS that was pre-warmed to 37°C. After the final wash air only was pumped through the umbilical vein using the 20mL syringe with no PBS. The other end of the umbilical cord was then clamped using a second sterile hemostat. 10-20mL of pre-warmed (37°C) collagenase A from *Clostridium histolyticum* (Boehringer Mannheim) was added to the cord using a new 20mL syringe attached to the blunt-end needle. The entire umbilical cord was then submerged in a beaker containing sterile, pre-warmed (37°C) PBS for a total of 8 minutes. Every 2 minutes the cord was briefly removed and gently massaged to ensure contact with collagenase. 10mL of Medium 199 (Invitrogen) was added to a 15mL centrifuge tube and pre-warmed to 37°C. Following the 8 minute incubation with collagenase, the cord was inverted such that collagenase plus endothelial cells drained into the 15mL tube with M199. Cells were centrifuged at 200g for 10 minutes at 23°C. The cell pellet was resuspended in 10mL of M199 + 20% FBS. Cells plus medium were transferred to a T-25cm² tissue culture flask that was pre-treated with 0.5% porcine gelatin for 1 h at 37°C and then washed one time with sterile PBS. Cells were confirmed to be of endothelial origin by routine staining with antibodies for the endothelial marker PECAM-1. Furthermore, cells were subjected to low density lipoprotein (LDL) uptake assay. LDL uptake assay was performed precisely as described by the manufacturer (BIOTREND Chemikalien GmbH, Germany).

Cells were passaged one time only and grown to confluence in Endothelial Growth Medium (Promocell). At this point, all culture dishes were treated by adding 0.5% porcine gelatin (heated to 37°C) to dishes for 1 h at room temperature. Gelatin was

removed and 2% glutaraldehyde in phosphate buffered saline (PBS) was added to dishes for 30 minutes at room temperature. Dishes were then disinfected by removing glutaraldehyde and incubating with 70% ethanol for 30 minutes at room temperature. Dishes were then extensively washed three times with sterile PBS (5 minutes per wash), washed one time with sterile PBS + 2mM glutamate, and washed three times at 5 minutes per wash with sterile PBS. Following the final wash, PBS was removed and replaced with Endothelial Growth Medium to ensure more equal distribution of cells across the surface area of the vessel before cells were seeded.

2.1.5 *Escherichia coli* (*E.coli*)

The XL-1 Blue strain of *E.coli* was purchased from Stratagene with the genotype: *recA1 endA1 gyrA96 thi-1 hsdR17 supE44 relA1 lac* [F'*proAB lacI^qZAM15 Tn10* (Tet^r)]. Cells were made competent by adding 0.5mL of an overnight culture, grown in Lauria/Lenox (0.5% NaCl) broth (LB), to 50mL of fresh LB. Cells were grown at 37°C with shaking until an optical density of 0.5-0.8 at 600nm was achieved. Cells were then incubated on ice for 20 minutes and centrifuged at 2,500g for 10 minutes at 4°C. Supernatants were discarded and the pellet resuspended in transformation storage solution (TSS) buffer. TSS buffer consists of a filter-sterilized solution of 85% LB broth, 10% polyethylene glycol, 5% dimethyl sulfoxide (DMSO) and 50mM MgCl₂. Cells were stored as 100μL aliquots at -80°C.

2.2 Antibodies and Primers

A comprehensive description of antibodies used in these studies is seen in Table 4. All primers are listed in Appendix A. Primers are based on the published sequences

for ZEBOV strain Mayinga (Genbank # AF272001) and MARV Musoke (Genbank # Z12132).

2.3 Molecular Techniques

2.3.1 RNA extraction

RNA extraction was performed on glycoprotein treated human macrophages and subsequently used in reverse-transcriptase polymerase chain reactions (RT-PCR). Supernatants were removed and stored for enzyme linked immunosorbent assays (ELISA) as described in section 2.9.1. Macrophages were then disrupted using the guanidinium isothiocyanate-based RLT buffer of an RNeasy® Mini Kit (QIAGEN). RNA was isolated according to the protocol for animal cells provided by the manufacturer (pages 31- 35 of RNeasy Mini Handbook 06/2001). RNA was eluted in RNase-free water (provided with kit) and the concentration was determined using a NanoDrop® ND-1000 UV-Vis spectrophotometer (NanoDrop Technologies). Working stocks of 10ng/μL RNA in RNase-free water were prepared and used for all RT-PCR reaction. RNA was stored at -80°C.

(Table 4)

<i>Antibody</i>	<i>Company</i>	<i>Source</i>	<i>Method</i>	<i>Working Dilution</i>
<i>Primary Antibodies</i>				
α -HA	Sigma	rabbit	Western Blot	1:2000
α -HA High Affinity; FITC	Roche	rat IgG ₁	IFA	1 μ g/mL
α -human Cadherin 5	Transduction Laboratories	mouse	IFA	1:100
α -polymeric F actin (Phalloidin); TRITC	Sigma	Phalloidin from <i>Amanita phalloides</i>	IFA	1:400
α -human PECAM-1 (CD31)	R&D Systems	mouse	IFA	1:100
α -human VCAM-1 (CD106)	R&D Systems	goat	IFA	1:100
α -human ICAM-1 (CD54)	R&D Systems	goat	IFA	1:100
α -human E-selectin (CD62E)	R&D Systems	mouse	IFA	1:100
α -VSV G	Sigma	mouse	Western Blot	1:1000
α -MARV GP17.1.91 GPII	University of Marburg, Germany	guinea pig	Western Blot	1:4000
α -ZGP12/1.1	Ayato Takada (Univ. of Tokyo)	mouse	Western Blot; IFA	1:4000 1:400
<i>Secondary Antibodies</i>				
α -mouse IgG (H+L); Alexa 488	Molecular Probes	goat	IFA	1:400
α -goat IgG (H+L); Cy3	Jackson ImmunoResearch Laboratories	donkey	IFA	1:50
α -guinea pig IgG; peroxidase	KPL Labs	goat	Western Blot	1:30,000
α -mouse IgG; peroxidase	KPL Labs	goat	Western Blot	1:50,000
α -rabbit IgG; peroxidase	Sigma	goat	Western Blot	1:30,000

Table 4. Summary of antibodies used in studies. IFA, immunofluorescent assay.

2.3.2 Polymerase Chain Reaction (PCR)

PCR reactions were performed using the Pwo DNA polymerase (isolated from *Pyrococcus woesei*) kit (Roche). Pwo DNA polymerase is a highly processive 5'-3' DNA polymerase and possesses 3'-5' exonuclease (proofreading) activity. The proofreading activity of Pwo results in 10-fold increased fidelity of DNA synthesis compared to Taq DNA polymerase (Roche, 2003). PCR was performed on template DNA containing either the 7A or 8A variants of ZEBOV Mayinga GP gene in the vector pTM1, template DNA of ZEBOV VP40 gene in pTM1, or on MARV Musoke GP gene in the vector pDisplay.

A typical 100 μ L PCR reaction was setup as 2 master mixes as seen in Tables 5 and 6. Template DNA was prepared as 10-fold dilutions from template cDNA and 1 μ L added to PCR tubes.

(Table 5)

<i>Components of PCR Master Mixes</i>	
<u>Master Mix 1</u>	<u>Amount Needed</u>
sterile distilled water	up to 50 μ L
dATP	200 μ M final concentration
dCTP	200 μ M final concentration
dGTP	200 μ M final concentration
dTTP	300 μ M final concentration
forward primer	600nM final concentration
reverse primer	600nM final concentration
<u>Master Mix 2</u>	<u>Amount Needed</u>
sterile distilled water	up to 50 μ L
10X PCR buffer with 20mM MgSO ₄	10 μ L
Pwo DNA polymerase	2.5U final concentration

Table 5. PCR master mix setup.

Master mixes 1 and 2 were then mixed and 99 μ L was added to each PCR tube containing template cDNA. All reactions were set up on ice. PCR reactions were performed in a Biometra T1 Thermocycler (Montreal Biotech Inc.). A typical thermocycling protocol is seen below in Table 6.

(Table 6)

<i>Number of Cycles</i>	<i>Conditions</i>
1X	94°C for 2 minutes (denaturation)
30-50X	94°C for 30 seconds (denaturation) 45-65°C for 30 seconds (annealing) - temperature depends on melting temperature of primers used) 72°C (elongation) - elongation time depends on fragment length - up to 1.0 kilobases 45 seconds - up to 1.5 kilobases 1 minute - up to 3.0 kilobases 2 minutes
1X	72°C for 7 minutes (prolonged elongation)
∞ (pause)	4°C

Table 6. PCR cycling parameters.

2.3.3 Reverse Transcriptase PCR (RT-PCR)

RT-PCR was performed using the OneStep RT-PCR kit purchased from QIAGEN. This kit contains Omniscript™ and Sensiscript™ reverse transcriptases which together provide a highly efficient and sensitive reverse transcription of RNA quantities in the range of 1pg to 2 μ g. HotStartTaq™ DNA polymerase is also included in the enzyme mix, however, this enzyme is not active during the RT reaction and must be heated to 95°C for 15 minutes to become activated. This temperature will simultaneously inactivate the reverse transcriptases. The reaction components for a single reaction of the one-step RT-PCR are seen in the table below. The master mix was setup on ice.

Component	Amount Needed
RNase-free water	up to 50 μ L
5X QIAGEN OneStep RT-PCR Buffer	10.0 μ L
dNTP Mix (10mM each dNTP)	2.0 μ L
forward primer	275ng
reverse primer	275ng
QIAGEN OneStep RT-PCR Enzyme Mix	2.0 μ L

1 μ L of 10ng/ μ L RNA stock was added to a PCR tube on ice and 49 μ L of RT-PCR mix was added. The PCR tubes were kept on ice until the thermocycler reached 50°C and then tubes were quickly added and the cycling initiated. A typical thermocycling setup is seen below.

Number of Cycles	Conditions
1X	50°C for 30 minutes (reverse transcription)
1X	95°C for 15 minutes (activate HotStart polymerase)
20-33X	94°C for 30 seconds (denaturation) 50-68°C for 30 seconds (annealing) - temperature depends on melting temperature of primers used) 72°C for 1 minute (elongation)
1X	72°C for 7 minutes (prolonged elongation)
∞ (pause)	4°C

2.3.4 Real Time PCR- Relative quantification of transcript levels

The concentration of the total RNA was determined by measuring the absorbance at 260nm. The reverse transcriptase reaction for the generation of cDNA was performed using approximately 1 μ g RNA in a reaction volume of 100 μ l and TaqMan Reverse Transcriptase reagents (Applied Biosystems) following the manufacturers protocol. The relative quantification of levels of specific transcripts in the RNA samples was performed by real-time PCRs using the ABI Prism 5700 Detection System. All reactions were performed in triplicates in a 25- μ l reaction volume containing 12.5 μ l Sybr Green

mastermix (Applied Biosystems), 40nM of each HPLC-purified primer, 25ng yeast tRNA (Sigma) and the sample cDNA translated from approximately 40ng of total RNA. The amplification specificity was monitored by dissociation curves. Relative quantification was performed using the comparative CT method (Applied Biosystems User Bulletin #2, Dec. 11. 1997) after verification of equal amplification efficiencies between the genes tested as specified in the User Bulletin #2. The mRNA level of the housekeeping gene GAPDH served as an endogenous reference for normalization.

2.3.5 Amplicon Analysis

All amplicons were analyzed for proper size and quality by 1.0% agarose gel electrophoresis. Analytical gels were stained with ethidium bromide added to melted agarose at the time the gel was cast. Preparative gels used for DNA extraction were stained in 1X TAE (Tris/acetate/EDTA) buffer with ethidium bromide after the gel was run. All gels were run at 120 volts for 30 minutes and DNA was visualized using a MacroVue UV-25 Hoefer transilluminator.

2.4 Cloning

Sequence specific primers were used to amplify relevant regions from template DNA using PCR techniques. Amplicons were assessed by analytical gels as described above. Preparative gels were run and amplicons gel purified using the QIAquick gel extraction kit (QIAGEN) and subsequently digested in parallel with vector using the restriction enzyme as indicated by the forward primer. All restriction enzymes were purchased from Roche. Following the first digest, the DNA was purified using the QIAquick PCR purification kit (QIAGEN). The second digest (as indicated by the reverse primer) was performed. Following the second digest the digested insert and

vector were again gel extracted (QIAquick gel extraction kit, QIAGEN) and DNA was quantitated using a NanoDrop[®] ND-1000 UV-Vis spectrophotometer (NanoDrop Technologies). Insert and vector were ligated using 1 unit/ μ L of T4 DNA ligase (Roche), 1.0 μ L of 10X T4 DNA ligase buffer (Roche), 0.5 μ L vector, x μ L of water to bring total reaction up to 10 μ L and appropriate amounts of insert to give ratios of insert:vector of 3:1, 6:1 and 10:1. Water controls with no insert were also included to control for the ability of vector to re-ligate. Ligation mixtures were incubated overnight at 12-16°C. *E.coli* XL-1 Blue cells (TSS competent) were transformed by thawing cells on ice and adding the 10 μ L ligation mixture to the cells. The cells were incubated on ice for 20 minutes and then heat shocked for 90 seconds at 42°C. Cells were then incubated on ice for an additional 3 minutes after which time 800 μ L of LB broth was added. Cells were then allowed to recover for 1 hour at 37°C to develop antibiotic resistance. Following incubation cells were plated on LB + ampicillin (100 μ g/mL) plates and incubated overnight at 37°C. Colonies were screened by miniprep analysis (QIAprep Spin Miniprep kit, QIAGEN) and restriction enzyme digest or PCR Screen (see below). All positive plasmids were fully sequenced using the dideoxy technique based on Sanger *et al* (Sanger, Nicklen, and Coulson, 1977). Analysis was performed using an ABI 3100 Genetic Analyzer.

2.4.1 PCR Screen

PCR screening is used when large numbers of bacterial colonies must be analyzed for positive clones following transformation. Any positive clones observed using PCR screens must be further confirmed using standard miniprep and restriction digest methods

as described above. A PCR master mix (shown below as 30 μ L/reaction) is prepared by adding the following to a PCR tube:

3 μ L of 10X PCR buffer (500mM KCl; 100mM Tris-HCl pH 8.3; 0.001% Triton X-100;
15mM MgCl₂; sterile distilled water)
2.5 μ L dNTP mix (10mM stock)
0.3 μ L forward primer of insert
0.3 μ L reverse primer of insert
0.2 μ L *Taq* polymerase (1.25U/reaction final concentration)
23.7 μ L sterile distilled water

LB + ampicillin (100 μ g/mL) plates are prepared by drawing a grid on the bottom of the plate and numbering the squares. For each bacterial colony to be tested a sterile 200 μ L eppendorff tip was used to touch the sample colony and then a numbered grid square on the LB + ampicillin plate. The tip was then placed in a correspondingly numbered PCR tube containing 30 μ L of PCR master mix. This is continued until all bacterial colonies have been transferred and PCR tubes set up. The LB + ampicillin plate is incubated at 37° for 16 hours. All eppendorff tips are then carefully removed from PCR tubes and tubes are transferred to a Biometra T1 thermocycler (Montreal Biotech Inc.). Following PCR, samples are assessed by analytical gel electrophoresis for the band of interest. If positive samples are observed then they are selected from the appropriate grid of the LB + ampicillin plate and further analyzed by miniprep and restriction enzyme digest.

2.4.2 Recombinant Vesicular Stomatitis Virus plasmid

Marburg virus (MARV) strain Musoke GP DNA was used as template for PCR using sequence specific primers for the region of the gene encoding the soluble GP₁. This region includes the signal peptide through the furin cleavage site of pre-GP. Primers were designed with the restriction sites *Xho*I and *Nhe*I to allow for direct cloning into the

full-length vector encoding the complete genome of Vesicular Stomatitis Virus (VSV). This plasmid (VSVXN2) contains the five VSV genes (nucleoprotein N, phosphoprotein P, matrix protein M, glycoprotein G, and polymerase L) in order flanked by the bacteriophage T7 promoter, the VSV leader, and the hepatitis delta virus (HDV) ribozyme, and the T7 terminator sequence. Between the G and L genes a unique linker site (XhoI, NheI) is present, flanked by a transcriptional start and stop signal for the additional gene to be expressed. This plasmid, when co-transfected with transcriptional support plasmids for VSV P, N, and L, will yield a recombinant virus that expresses VSV G on its surface but also expresses the additional protein (Lawson et al., 1995; Whelan et al., 1995) (secreted MARV GP₁ in this case).

2.4.3 Soluble glycoprotein plasmids

The cloning strategy for generation of the soluble glycoproteins is shown diagrammatically in Figure 7. A table listing all plasmids generated is shown in Appendix A. The template cDNA for GP_{1,2}, GP₁ and GP_{1,2}ΔTM originated from the prototype ZEBOV (Mayinga strain) GP gene containing 8 adenosines (8A) at the RNA editing site (Volchkov et al., 1995). Template cDNA for sGP and Δ peptide contained 7 adenosines (7A). The regions amplified include nucleotide positions 238-1629 for GP₁; 238-2052 for GP_{1,2}ΔTM; 238-1101 for sGP; and 1114-1236 for Δ peptide. ZEBOV GP₁ was amplified using the primers EBOVGPBgl2f and EBOVGP1SacIIr. The shed GP_{1,2}ΔTM was generated using the primers EBOVGPBgl2f and EBOVGP1,2shedSac2r. The full length GP_{1,2} was generated using the primers EBOVGPBgl2f and EBOVGP2Sac2r. ZEBOV sGP was amplified using EBOVGPBgl2f and the reverse primer EBOVsGPPstIr that amplified the region between the signal peptide and furin

cleavage site of pre-sGP. Delta peptide was amplified from a region of the pre-sGP ORF between the furin cleavage site and the end of the ORF using the primers EBOVdPBgl2f and EBOVdPSac2r. All PCR products of soluble glycoproteins were cloned into the expression vector pDisplay (Invitrogen) such that recombinant proteins contain the amino-terminal influenza hemagglutinin (HA) epitope tag. All reverse primers were designed with sequences for two consecutive stop codons that would terminate translation prior to the carboxy-terminal *myc* tag and transmembrane domain. pDisplay incorporates an N-terminal signal peptide and in doing so, all proteins would then be targeted to the secretory pathway.

(Figure 7)

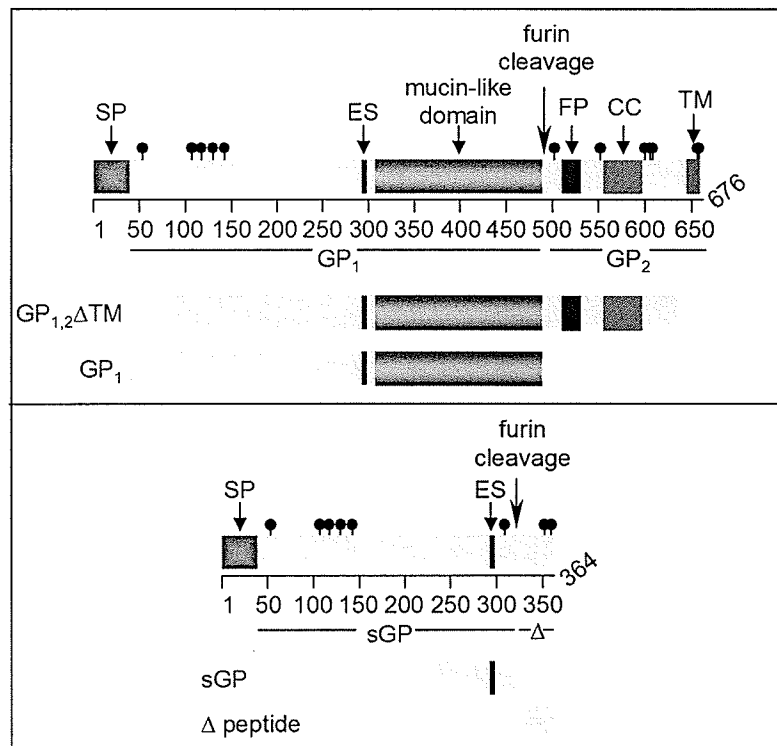


Figure 7. Schematic representation of cloning strategy for recombinant proteins. GP1,2 delta TM and GP1 were cloned using template DNA with 8 adenosines in the editing site (ES). sGP and delta peptide were cloned using template DNA with 7 adenosines in the ES. Known significant domains are shown with respect to their amino acid positions including the signal peptide (SP); editing site (ES); mucin-like domain; furin cleavage site; fusion peptide (FP); coiled-coil (CC); and transmembrane domain (TD). Cysteine residues are represented by black lines with dots

2.4.4 ZEBOV plasmids for virus-like particle production

Plasmid DNA of ZEBOV VP40 and full-length GP_{1,2}, both in the vector pTM1, were used to amplify the inserts with sequence specific primers designed with *EcoRI* and *XhoI* restriction sites for cloning (Appendix A). VP40 and GP_{1,2} inserts were cloned into the eukaryotic expression vector pCAGGS (Niwa, Yamamura, and Miyazaki, 1991). This vector contains a derivative of the chicken beta-actin promoter and yields high levels of expression in eukaryotic cells.

2.5 Site-Directed Mutagenesis of ZEBOV glycoproteins

Cysteine mutants for ZEBOV GP₁ (amino acid positions 53, 108, 121, 135 and 147) and ZEBOV GP₂ (amino acid positions 511, 556, 601, 608 and 609) were generated using PCR and the QuikChange™ Site-Directed Mutagenesis Kit (Stratagene). All cysteines were changed to glycines by mutation of the first nucleotide in the codon. Primers used for introduction of mutations are listed in Appendix A. All plasmids were confirmed by sequence determination.

2.6 Transfections

2.6.1 Optimization of transfection protocol

293T, Vero E6 and BHK-T7 cells were plated 24 hours prior to transfection in 24-well plates so that they were 70% confluent the day of the transfection. Six eppendorff tubes were used to dilute Lipofectamine 2000 cationic lipid reagent (Invitrogen) and DMEM without serum as seen below for one 24-well plate:

Materials and Methods

<u>Tube/Column on 24-well plate</u>	<u>Volume OptiMEM (μL)</u>	<u>Volume Lipofectamine 2000 (μL)</u>
1	120	5
2	117.5	7.5
3	115	10
4	112.5	12.5
5	110	15
6	107.5	17.5

Diluted Lipofectamine 2000 was then added to each of 4 wells of the appropriate column of a sterile 24-well plate ($25\mu\text{L}/\text{well}$). DNA was then prepared by diluting a green fluorescent protein-expressing plasmid (under control of either a CMV or T7 promoter) in $140\mu\text{L}$ of DMEM as show below for one 24-well plate:

<u>Tube/Row on 24-well plate</u>	<u>DNA (μg)</u>
A	1.4
B	2.8
C	5.6
D	8.4

$20\mu\text{L}$ of diluted DNA from tube A was then added to each of 6 wells of the sterile 24-well plate containing diluted Lipofectamine 2000. This process was continued for tubes B, C and D and the plate was incubated at room temperature for 15 minutes. During this incubation period cells were washed one time in fresh DMEM. Following the wash step, $160\mu\text{L}$ of fresh DMEM was added to each well of the 24-well plate containing DNA-cationic lipid reagent complexes and they were briefly mixed by gentle pipetting and then added to 24-well plates of cells. Cells were incubated at 37°C for 4 hours and then media was removed and replaced with DMEM plus 10% FBS and re-incubated for up to 48 hours. Cells were monitored for expression of GFP by UV illumination on a Zeiss Axiovert 100 microscope. Pictures were taken using Northern Eclipse software and the number of GFP-expressing cells was estimated as a percentage of the total cell

population. In this manner the efficiency of transfection was compared for three cell types and varying amounts of DNA and cationic lipid reagent.

In addition to Lipofectamine 2000 the efficacy of the transfection reagent FuGENE6 (Roche) was tested in combination with 293T cells plated in a 6-well plate, 24 hours prior to transfection. A CMV-driven GFP plasmid was used to test the efficiency of transfection. DMEM was added to each of 3 sterile 1.5mL tubes such that the total volume in the tube would be 100 μ L after addition of FuGENE6 and DNA. FuGENE6 was then added to DMEM as shown below, followed by addition of DNA.

<u>FuGENE 6:DNA Ratio</u>	<u>FuGENE6 Volume (μL)</u>	<u>DNA Mass (μg)</u>
3:2	3	2
3:1	3	1
6:1	6	1

Tubes containing the transfection complex were incubated at room temperature for 30 minutes. Cells were washed once with DMEM and 900 μ L of fresh DMEM added to wells. The transfection complex was then added dropwise to wells and the plate incubated at 37°C for 4 hours. After 4 hours medium was removed and replaced with fresh DMEM containing 10% FBS. Transfection efficiency was monitored as described above for Lipofectamine 2000 protocols.

2.6.2 Expression and purification of recombinant proteins

293T cells were seeded into poly-D-lysine (Sigma) coated triple layer (500cm²) flasks (NUNC, VWR) 24 hours prior to transfection in DMEM + 10% FBS without antibiotics. Plasmids (sGP, GP₁, GP_{1,2} Δ TM, Δ peptide, and control pDisplay vector) were individually transfected using FuGene6 (Roche) and incubated for 4 hours at 37°C

in a humidified (95%) 5% CO₂ environment. After 4 hours, media was removed from flasks and replaced with DMEM supplemented with 10% FBS. Flasks were re-incubated for a total of 72 hours. The purification procedure is shown diagrammatically in Appendix B. Supernatants were removed after 72 hours and clarified by centrifugation at 200g, for 10 minutes at 4°C. Clarified supernatants were concentrated using Centricon Plus-80 filters (Millipore) with molecular weight cut-offs (MWCOs) of 10kDa (sGP, GP1, GP_{1,2}ΔTM, control pDisplay) or 5kDa (Δ peptide). Following concentration, supernatants were immuno-affinity purified using an anti-HA matrix (Roche). The column consisted of 1mL total bed volume of matrix. The column was equilibrated using 10 bed-volumes of 20mM Tris (pH 7.5); 0.1M NaCl; 0.1mM EDTA buffer referred to as “equilibration buffer” (Appendix B). The column was then plugged and concentrated supernatant added to resuspend the matrix. The matrix + supernatant was then transferred to a sterile 50mL centrifuge tube (Falcon) and this mixture was incubated for 1.5 hours at room temperature with constant end-over-end rotation. While the manufacturer recommends simply adding supernatants to the column and allowing it to flow through it was found through these studies to be insufficient time for binding of the proteins to the matrix. A prolonged binding time (1.5 hours) greatly enhanced the end recovery of protein. After 1.5 hours the matrix + supernatant mixture was added back to the plugged column. A 22-gauge syringe tip was added to the end of the column and the supernatant allowed to flow through. The flow-through was saved at 4°C for analysis. The column was then washed with 30 bed-volumes of wash buffer (equilibration buffer + 0.05% Tween 20) or until an OD_{280nm} of 0.0 was achieved. This indicates that the only proteins present in the column are those bound to the matrix. The column was then

plugged and 1 bed-volume of elution buffer was added. The elution buffer consists of 1mg/mL HA peptide (Roche) resuspended in equilibration buffer. The column was then incubated for 45 minutes at 37°C. Following the incubation a sterile 22-gauge needle was re-applied to the column and the eluate collected and stored at 4°C. This method of protein elution was repeated for a total of 3 times and eluates pooled. The matrix was regenerated using 20 bed-volumes of 0.1M glycine (in water) at pH 2.0. The matrix was then equilibrated using 20 bed-volumes of equilibration buffer and stored in 2 bed-volumes equilibration buffer with 0.09% sodium azide at 4°C. HA peptide was removed from final eluates and proteins further concentrated using Centricon YM filters with MWCOs of 3kDa (Δ peptide), 10kDa (sGP) or 100kDa (GP₁, GP_{1,2} Δ TM). The proteins were washed 4 times with 2mL of elution buffer. Filter flow-throughs were saved and the final concentration of proteins and flow-throughs were determined using the DC Protein Assay (Bio-Rad). The fourth flow-through of the washes always showed a zero value (ie: equal to the blank of equilibration buffer only). All proteins were aliquoted and stored at -20°C.

2.7 Protein analysis

2.7.1 Harvesting of Cell Lysates

Infected or transfected cells were collected by diluting 4X SDS-gel loading buffer (0.312M Tris-HCl; 0.346M SDS; 50% (v/v) glycerol; 0.1% (w/v) bromophenol blue pH 6.8) with water to a working concentration of 1X. In cases where proteins would be analyzed under reducing conditions 4X SDS-gel loading buffer was prepared with 20% (v/v) 2-mercaptoethanol and this was then diluted to 1X. Tissue culture plates were incubated on ice and 40 μ L of 1X SDS-gel loading buffer was added per 1cm² of well

surface area. Plates were incubated on ice for 5 minutes and lysates collected using a pipette tip. Cell lysates were boiled at 99°C for 5 minutes and then stored at -20°C.

2.7.2 SDS-PAGE and Semi-dry Transfer

Protein samples for SDS-PAGE were electrophoresed using the Protean 3 mini-gel system (Bio-Rad). Samples were resolved using either 7.5%, 10% or 15% (0.75mm thick) or 4-20% gradient gels run at 100V for 1.5 hours. Reagents for casting gels (40% bis-acrylamide, stacking buffer and resolving buffer) were purchased from Invitrogen. Following electrophoresis, proteins were transferred to PVDF membranes (Amersham Pharmacia Biotech) using a Trans-blot SD semi-dry transfer apparatus (Bio-Rad).

PVDF membranes were pre-soaked in methanol for 5 minutes then extensively washed in anode buffer (75mL 0.67M boric acid; 200mL MeOH; 725mL sterile distilled H₂O). The trans-blot apparatus was wet with distilled water and an extra-thick filter pad (Bio-Rad) pre-soaked in anode buffer was placed on the wet apparatus surface. The PVDF membrane was then applied to the top of the filter pad. The stacking gel of the SDS-gel was then removed and the resolving portion of the gel briefly washed in anode buffer. The gel was then placed on the PVDF membrane and the edges of the gel outlined on the PVDF using a ball-point pen. Another extra-thick filter pad was prepared by soaking it in cathode buffer (75mL 0.67M Boric acid; 50mL MeOH; 875mL sdH₂O) and applying it to the top of the SDS-gel. As each layer was added air bubbles were removed by rolling a serological pipette across the surface. The top of the semi-dry apparatus was wet with distilled water and applied. Once assembled the transfer was run at 60mA per mini-gel for a total of 90 minutes.

2.7.3 Immunoblot

Following transfer of proteins PVDF membranes were blocked for 1 hour at room temperature in PBS with 0.1% Tween 20 (PBS-T) containing 5.0% skim milk. Following the blocking step the membrane was washed three times in PBS-T (5 minutes per wash) at room temperature. Primary antibody was added in PBS-T containing 5.0% skim milk and membranes incubated overnight at 4°C with gentle rocking. The next morning the membranes were extensively washed three times in PBS-T (5 minutes per wash). Secondary antibody was added in PBS-T containing 5.0% skim milk and membranes incubated for 1 hour at room temperature with gentle rocking. Membranes were then extensively washed three times in PBS-T (5 minutes/wash) and two times in PBS. Proteins were visualized using the ECL Plus (chemiluminescence) western blotting detection system (Amersham Biosciences) as described by the manufacturer. In cases where several antibodies were tested membranes were stripped of antibodies following detection of proteins. Membranes were submerged in stripping buffer (62.5mM Tris-HCl pH 6.7; 2% (w/v); 100mM 2-mercaptoethanol) for 30 minutes at 50°C. Membranes were then washed extensively three times in PBS-T (10 minutes/wash) and immunoblot performed again as described above.

2.8 Production of Recombinant Vesicular Stomatitis Virus

BHK-T7 cells were grown to approximately 80% confluence in 6cm dishes. The cells were then transfected in a biosafety level 2 laboratory (BSL2) with the support plasmids for transcription/replication encoding the viral ribonucleoprotein (RNP) constituents (0.5µg N; 1.25µg P; 0.25µg L) and 2µg of the recombinant VSV-MARV GP₁ (Figure 8). Transfections were performed using Lipofectamine 2000 (Invitrogen) as

per manufacturer instructions. Due to the fact that work with recombinant viruses of this nature had not been classified in terms of biosafety level required, transfected cells were immediately transferred to the biosafety level 4 laboratory (BSL4). After 48 hours incubation at 37°C, supernatants were blind passaged onto Vero E6 cells (90% confluent). Recovery of infectious virus was confirmed by scanning Vero E6 monolayers for cytopathic effect (CPE). Rescued rVSVs were passaged 1 time on Vero E6 cells to obtain virus stocks. The virus stock was titrated on Vero E6 cells.

(Figure 8)

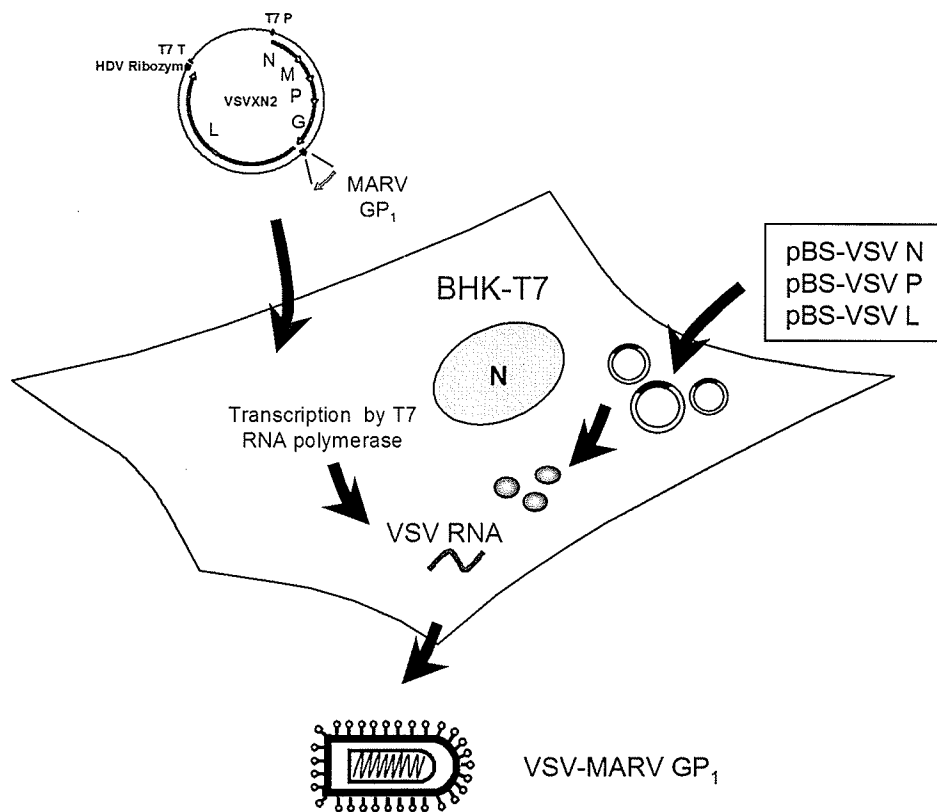


Figure 8. Schematic drawing of the infectious clone system for vesicular stomatitis virus (VSV), Indiana serotype. BHK-T7 cells were co-transfected with a plasmid containing the VSV genome (VSVXN2) and the plasmids expressing the VSV nucleoprotein (pBS-VSV N), phosphoprotein (pBS-VSV P), and polymerase (pBS-VSV L). Transcription of all plasmids is under the control of the bacteriophage T7 RNA promoter. MARV GP₁ was inserted as an additional gene into the vector VSVXN2.

2.8.1 Recombinant VSV MARV GP₁ expression and growth characteristics

Vero E6 cells were cultured to a cell density of 10^6 per well of a 12-well tissue culture dish and infected with rVSV-MARV GP₁ at an MOI of 10 for 1 hour at 37°C. Cells were washed three times in DMEM and 1mL of fresh media containing 2% heat-inactivated (1 hour at 56°C) FBS. Supernatants were harvested at 2, 4, 8, 12, 16, 20 and 24 h post infection and centrifuged at 3000g for 5 minutes at 4°C. Samples were inactivated by gamma irradiation (5 mega rads) and transferred to BSL2 for SDS-PAGE and immunoblot analysis. Supernatants were stored at -20°C until analysis.

Virus titration was performed by defining the 'tissue culture infectious dose 50' (TCID₅₀). For this, infectious supernatants were harvested as described above. Supernatants were then diluted 10-fold and the dilutions were used to infect Vero E6 cells in 96-wells (five wells per dilution). The cultures were scored periodically for CPE over a period of 7 days. The end point virus titer for culture supernatants were calculated using the method of Reed and Muench (Reed, 1938). Viral titers are expressed as log 10 of the 50 percent titration endpoint for infectivity as calculated by the method of Spearman-Karber (Karber, 1931; Spearman, 1908).

2.9 Characterization of recombinant proteins

2.9.1 Glycosylation

All secreted glycoproteins were tested for carbohydrate processing (glycosylation) by digestion with the enzymes Endoglycosidase H (Roche), N-glycanase[®] PNGase F (PROzyme), Sialidase A[™] (PROzyme) and O-glycanase (PROzyme). Endoglycosidase H removes high mannose N-glycans while N-glycanase[®] PNGase F cleaves all types of asparagine bound N-linked oligosaccharides. O-Glycanase (endo- α -N-

acetylgalactosaminidase) removes O-linked oligosaccharides until only the Gal β (1-3)GalNAc core remains attached to the serine or threonine residue. The most common modification of the core Gal β (1-3)GalNAc is mono-, di-, or tri-sialylation. To suitably remove these structures Sialidase A (*Arthrobacter ureafaciens* sialidase) is used to cleave the NeuAc α (2-8)NeuAc bond. Complete removal of O-linked structures is achieved by combining the Sialidase A, and O-Glycanase. Purified proteins were incubated with enzymes at 37°C for 3 hours (as per manufacturer instructions) and results analyzed by assessing the extent of deglycosylation by mobility shifts on sodium dodecyl-sulfate polyacrylamide electrophoresis (SDS-PAGE). In addition to the soluble ZEBOV glycoproteins, a positive control protein (bovine fetuin) was included. This protein will demonstrate increased mobility in SDS-PAGE following sequential addition of each of the three enzymes N-Glycanase, Sialidase A and O-Glycanase. Following SDS-PAGE proteins were transferred to PVDF membranes and detected using anti-HA antibodies.

2.9.2 Oligomerization of proteins

To test whether proteins were properly processed and in the correct conformation samples were run in SDS-PAGE under both reducing and non-reducing conditions. Proteins were transferred to PVDF membranes and detected using anti-HA antibodies or the GP specific monoclonal antibody α ZGP12/1.1 kindly provided by Ayato Takata (University of Tokyo).

2.9.3 Characterization of GP₁ cysteine mutants

All GP₁ cysteine mutant plasmids were expressed in 293T cells using Fugene6 (Roche). Cell lysates were collected in 1X SDS gel loading buffer without 2-mercaptoethanol. Samples were then run under both reducing and non-reducing SDS-

PAGE conditions to assess expression and oligomerization. Proteins were detected using anti-HA antibodies or the GP specific monoclonal antibody α ZGP12/1.1.

2.10 Treatment of macrophages with secreted glycoproteins and VLPs

At 6 d post-seeding media was removed from macrophages and replaced with fresh RPMI 1640 (Invitrogen) containing 2% donor (human AB) serum, penicillin (100U/mL), streptomycin (100 μ g/mL), L-glutamine (2mM). Cells were incubated for 24h in a humidified (95%), 5% CO₂ environment. After 24 h cells were treated with either 10 μ g/mL or 50 μ g/mL of each secreted glycoprotein, HA peptide, control vector, *E.coli* 0111:B4 LPS (10ng/mL), VLPs (10 particles/cell), VP40 particles (10 particles/cell), or mock treated (untreated) by adding samples directly to wells. Cells were incubated with samples for 1, 6, 12 and 24 h.

2.10.1 Enzyme Linked Immunosorbent Assay

Following incubation supernatants were removed from macrophage cell cultures and clarified from cell debris by centrifugation (8,000g, 4°C, 10 min), and stored at minus 80°C. Supernatants were thawed only once (at the time of the assays). ELISA for the cytokines TNF- α , IL-1 β and IL-6 and EIA for the chemokines IL-8 were all performed using kits purchased from Promocell using methods provided by the manufacturer.

2.11 Treatment of HUVECs with proteins and VLPs

HUVECs were used in passage number one. Recombinant proteins or VLPs were added to culture medium of confluent HUVECs at 10 μ g/mL or 50 μ g/mL quantities for proteins or 10 particles/cell for VLPs. Cells were incubated for 6, 12 or 24 hours post treatment in a 95% humidified, 5% CO₂ environment. TNF- α (100ng/mL) served as a

positive control while HA peptide and purified control vector-transfected cells served as negative controls.

2.12 Immunofluorescence Assays (IFA)

2.12.1 Activation of HUVECs

Upregulation of cell adhesion molecules (ICAM-1, VCAM-1, E-selectin and PECAM-1) on HUVECs was determined at 6, 12 and 24 hours post-treatment with proteins or VLPs. Cells were fixed at the respective time points in 2% paraformaldehyde for 15 min at room temperature (RT) and subsequently washed 3 times with PBS and then permeabilized with 0.1% Triton X-100 for 10 min at RT. Cells were washed 3 times with PBS and primary antibodies (α ICAM-1, α VCAM-1, α E-selectin, or α PECAM-1, R&D Systems) were applied at a dilution of 1:100 and incubated overnight at 4°C. Following overnight incubation cells were washed 3 times with PBS and appropriate secondary antibodies conjugated to Alexa Fluor 488 (Molecular Probes) or CY3 (Jackson Labs) were applied for 1 h at 1:400 or 1:50, respectively. Cells were washed 3 times with PBS then post-fixed with 2% paraformaldehyde for 15 min and washed 1 additional time with PBS. Cells were examined with a Zeiss microscope.

2.12.2 Junction proteins

Rearrangement of the junctional protein VE-cadherin and distribution of cellular actin was assessed at 24h post-treatment with secreted glycoproteins and VLPs. Cells were fixed and permeabilized as described above and stained overnight with an antibody to Cadherin-5 (1:100, Transduction Labs). Cells were washed 3 times with PBS and an anti-mouse Alexa 488 antibody was applied for 1h at RT. Cells were then washed 3

times and stained for 30 minutes at RT with Phalloidin conjugated with TRITZ (1:400, Sigma). After this final staining, cells were washed and post-fixed as described above.

2.12.3 Interaction of VLPs with macrophages and HUVECs

Macrophages and HUVECs were incubated with VLPs (10 particles/cell) for 1h at 37°C or 4° in a humidified, 5% CO₂ environment. Following incubation, cells were fixed and surface stained or the sample permeabilized. Cells were incubated for 1h with a 1:200 dilution of the ZEBOV GP-specific monoclonal antibody α ZGP12/1.1, kindly provided by Ayato Takata (University of Tokyo, Japan). The secondary antibody anti-mouse Alexa 488 was applied at a dilution of 1:400 and cells post-fixed as described above. Binding and internalization of VLPs was assessed by fluorescence microscopy using a Zeiss microscope.

2.13 Impedance Spectroscopy

Chambered slides for impedance spectroscopy were prepared by applying indium tin oxide (ITO)-coated polyester film (75mm x 25mm x 2mm) (Delta Technologies Ltd, Stillwater, Minnesota) with photo-sensitive lacquer (CRC Industries, Germany). Electrode areas were generated by exposing masked ITO slides to UV light for 3 minutes. Electrode areas were cleared of lacquer by treatment with sodium hydroxide solution (0.7% w/v) and then rinsed with distilled water. Chambers removed from LabTek slides (VWR) were fixed to the ITO with silicon and baked overnight at 60°C. A photo of the chamber slide is shown in Figure 9. Slides were treated with 0.5% porcine gelatin for 1h at RT. The entire slide was then submerged in 2% glutaraldehyde solution for 10 minutes. The slide was then extensively washed with sterile phosphate buffered saline (PBS) and then sterile PBS + 2mM glycine (overnight). The slide was then washed 3

additional times with sterile PBS prior to seeding of HUVECs. Cells were incubated at 37°C in a humidified, CO₂ environment until confluence. The transendothelial electrical resistance (TER) was determined as previously described (Seebach et al., 2000). Briefly, an alternating voltage was applied and the impedance magnitude was measured at frequencies between 10Hz and 1MHz between the electrode area of the ITO slide and a counter electrode. A relay connecting the electrodes to an impedance spectrophotometer (SI-1260A, Solartron Instruments, Farnborough, UK) made it possible to acquire impedance spectra from several wells of a chambered slide. The TER was calculated from the resultant spectra (Seebach et al., 2000). For all impedance experiments the cells were allowed to equilibrate for approximately 1h or until a constant TER spectra was observed prior to addition of secreted glycoproteins or VLPs. Impedance spectra was monitored for up to 36 hours post-treatment. At the termination of all experiments, a 3mM solution of ethylene glycol-bis(β -aminoethyl ether)-N,N,N',N'-tetraacetic acid (EGTA) (Sigma) was added to wells as a positive control that the TER could be decreased.

(Figure 9)

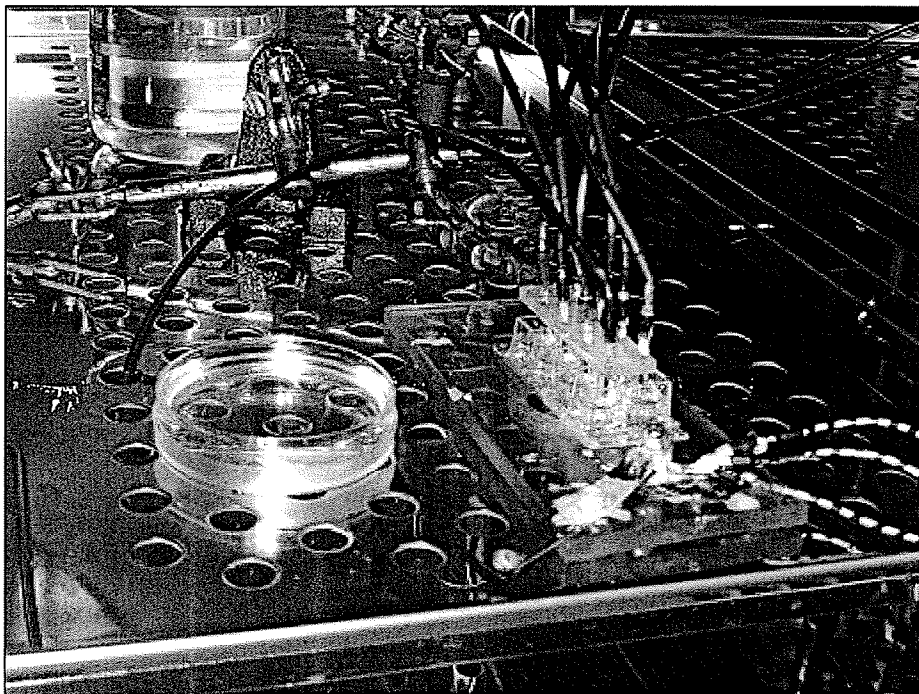


Figure 9. Impedance spectroscopy electrode chambers. A single slide containing 8 chambers is shown. Notice electrodes above the slide used for making measurements. The entire slide is kept in a 5% carbon dioxide, 95% humidified tissue culture incubator for the duration of the experiment.

2.14 Negative stain and immunoelectron microscopy of VLPs

Purified VLPs were prepared for negative stain and immuno EM examination essentially as previously described (Hazelton and Coombs, 1999). Briefly, purified VLPs were diluted in 50 μ l 0.1% glutaraldehyde in PBS, pH 7.2, allowed to fix for 10 min at 4°C, and centrifuged directly onto Formvar-coated, carbon-stabilized 400 mesh copper or nickel electron microscopy grids (Beckman Airfuge EM-90 rotor (Beckman, Palo Alto, USA), 26psi, 30 min). For indirect immunolabelling, VLPs pelleted to nickel grids were reacted against anti-ZGP12/1.1 for 60 min at 20°C. The primary antibody was detected with polyclonal anti-mouse IgG:gold conjugates (18nm) (Jackson ImmunoResearch, West Grove, USA) and fixed with 0.1% glutaraldehyde to stabilize the reactions.

Samples were negatively stained with 1.2 mM phosphotungstic acid (PTA), pH 7.0, and examined in a Phillips model 201 electron microscope. Images were recorded at machine magnifications of 30,000 and 70,000 on Kodak Direct Positive film 5302 (Kodak, Rochester, USA), and printed on Kodak Polycontrast III paper.

2.15 Atomic Force Microscopy (AFM)

AFM was performed in contact mode using a Nanoscope III Multimode-AFM (Digital Instruments, Santa Barbara, California, USA) with an J-type scanner (maximal scan area: 100x100 μ m). For sample preparation, mica surfaces were attached to stainless steel punches and purified VLPs were immobilized on the surfaces using poly-L-lysine. Prior to imaging, samples were washed with ultra pure water to remove excessive salt crystals and gently dried under a stream of air. V-shaped oxide sharpened cantilevers with spring constants of 0.06 N/m (Digital Instruments) were used for scanning in air. Images (512 x 512 pixels) were captured with scan sizes between 2 and 4 μ m² at a scan rate of 6 Hz (6 scan lines/s). Images were processed using the SPIP (Image Metrology, Lyngby, Denmark) and Nanoscope III software (Digital Instruments). A three-dimensional rendering was used for processing, to allow better visualization.

3.0 Results

3.1 Cloning of MARV GP₁ into VSVXN2

Vesicular stomatitis virus (VSV) has previously been described as a useful expression system for foreign genes due to its ability to tolerate additional transcription units (Haglund et al., 2000; Kretzschmar et al., 1997). The soluble MARV GP₁ was cloned into the full-length vesicular stomatitis virus genome plasmid, VSVXN2. MARV GP₁ was used rather than ZEBOV soluble glycoproteins because more molecular and immunological tools were available for analysis. VSVXN2 contains the five VSV genes (N, P, M, G, and L) in order flanked by the bacteriophage T7 promoter, the VSV leader, and the hepatitis delta virus (HDV) ribozyme, and the T7 terminator sequence. There is a unique linker site (XhoI, NheI) located after the VSV G where I inserted the sequence for MARV GP₁. The complete vector map of VSVXN2 and agarose gel demonstrating the excised MARV GP₁ from the vector backbone following restriction enzyme digest are seen in Figure 10. It is interesting to note that large-scale production of the full-length VSV construct (in 100mL of bacterial culture medium for Maxiprep) could not be accomplished directly from a smaller (3mL) overnight starter bacterial culture. To overcome this obstacle, miniprep DNA was used to transform competent *E.coli* XL-1 Blue cells. The 1mL of competent cells was then used as a starter culture for a 100mL overnight LB + ampicillin culture used for Maxiprep.

Infectious virus was generated by cotransfection of BHK-T7 cells with a plasmid containing the VSV genome with MARV GP₁ inserted as an additional gene (VSVXN2-MARV GP₁) and plasmids expressing the VSV nucleoprotein, phosphoprotein and polymerase. Transcription of all plasmids is under the control of the bacteriophage T7

Results

RNA promoter. Supernatants from transfected cells were blind passaged onto VeroE6 cells and rescued virus was passaged on VeroE6 cells to obtain a viral stock.

(Figure 10)

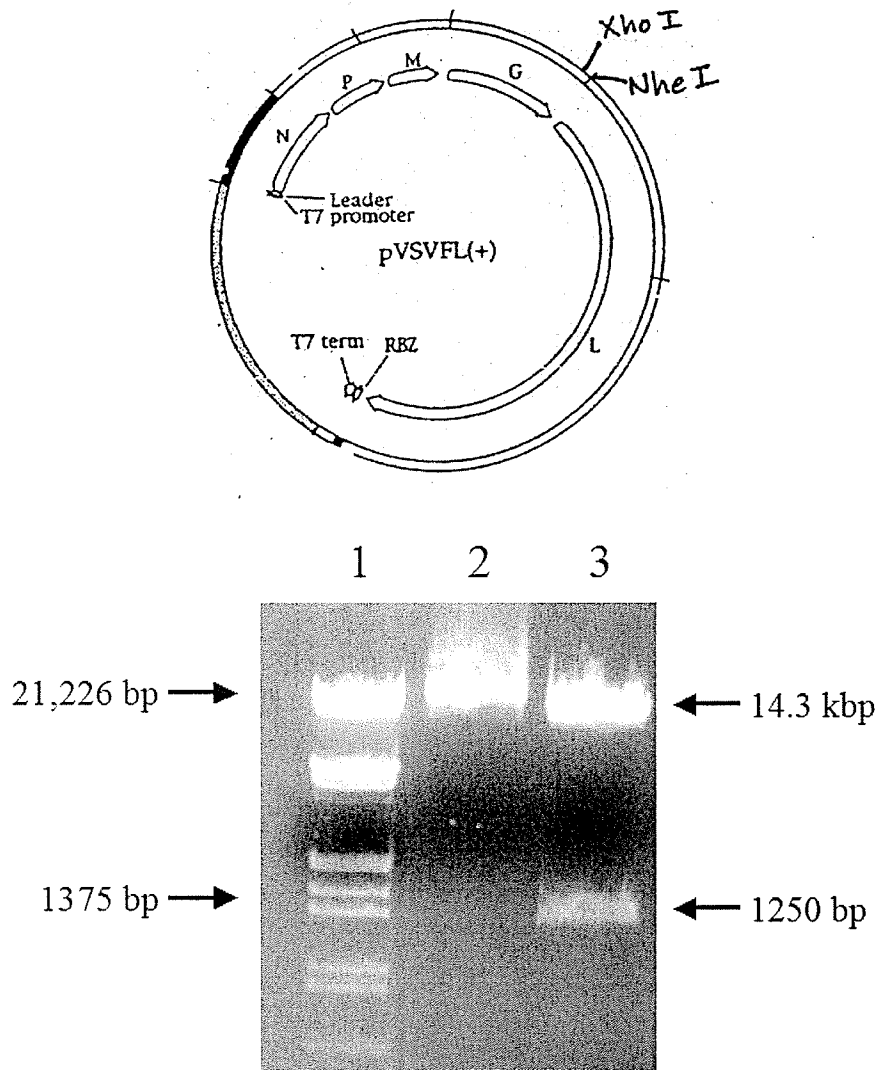


Figure 10. Cloning of MARV GP1 into the pVSVXN2 (full-length VSV genome). The vector, pVSVXN2, contains the VSV G protein with restriction sites Xho I and Nhe I for insertion of an additional transcriptional unit. GP1 was cloned into Xho I and Nhe I restriction enzyme sites. Lane 1, DNA ladder; Lane 2, undigested maxi prep DNA; Lane 3, maxi prep DNA digested with Xho I and Nhe I with vector and 1250 bp GP1 shown.

3.1.2 Expression and characterization of rVSV-MARV GP₁

Expression of MARV GP₁ by recombinant VSV infection was tested as a method for generating high quantities of soluble filovirus glycoproteins. Vero E6 cells were infected with recombinant VSV MARV GP₁ (rVSV-MARV GP₁) and supernatants collected over time. Expression of MARV GP₁ was observed as early as 16 hours post-infection in un-concentrated supernatants as seen in Figure 11. Expression increased through 24 hours post-infection. Vero E6 cell cultures were also visually inspected. Despite good expression levels of MARV GP₁, cells were heavily damaged from replication of the recombinant virus. There was a great deal of cellular debris in cultures by 12 hours post-infection. For this reason, the recombinant VSV system was deemed suboptimal for expression of soluble glycoproteins. Despite this conclusion, the virus was further characterized as part of a larger project on which I am co-author, to use recombinant VSVs as vaccine candidates for filoviruses (Garbutt et al., 2004).

(Figure 11)

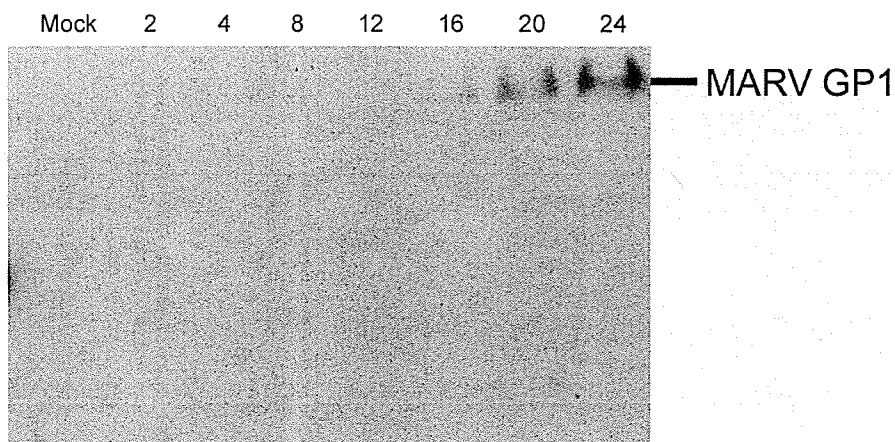


Figure 11. Timecourse of MARV GP₁ expression. Vero E6 cells were infected with rVSV-MARV GP₁ and supernatants harvested over time. Supernatants were subjected to reducing SDS-PAGE and immunoblotting using a GP-specific antibody, anti-GP17.1.91 GP_{II} (1:4000).

Results

To confirm expression and secretion of MARV GP₁ cell lysates and/or supernatants were harvested at 24 hours and subjected to reducing SDS-PAGE and western blotting. VSV wildtype and a recombinant VSV expressing EBOV sGP were included as controls. All viruses are positive for expression of VSV G (Figure 12). Only those recombinant viruses expressing soluble glycoproteins were positive for the respective proteins; rVSV-EBOV sGP and rVSV-MARV GP₁. Note that the MARV GP-specific antibody is slightly cross-reactive with a 60kDa protein (likely albumin).

(Figure 12)

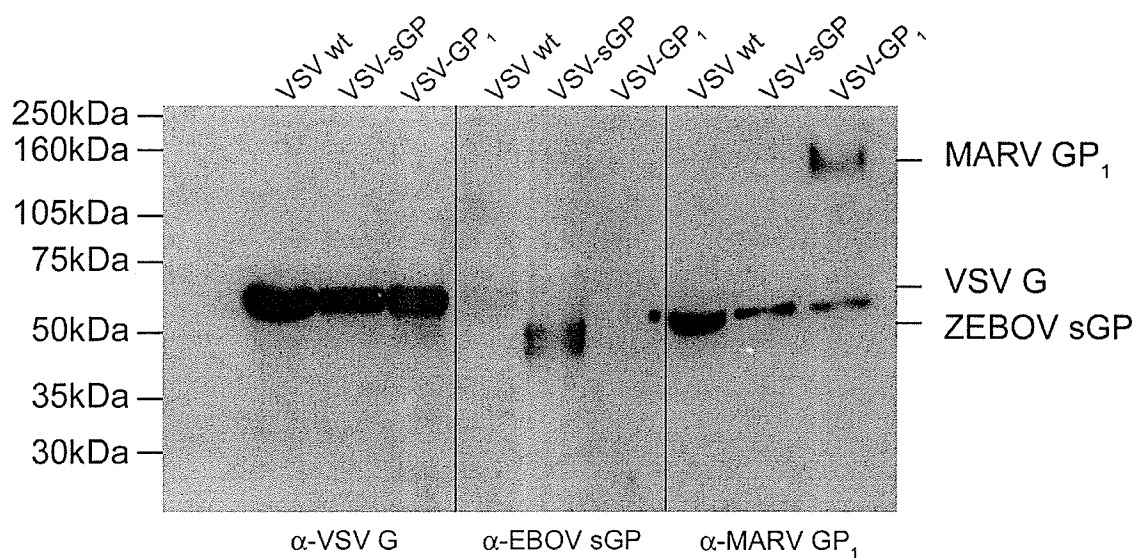


Figure 12. Expression of rVSV proteins. Vero E6 cells were infected with VSV wt, rVSV-MARV GP₁ or rVSV-EBOV sGP (MOI 10). Cell lysates were collected for detection of VSV G and supernatants for EBOV sGP or MARV GP₁. All samples were subjected to reducing SDS-PAGE and immunoblotted using anti-VSV G (1:1000), anti-EBOV GP (1:4000) or anti-MARV GP (1:4000). MW marker was loaded in lane 1 and virus samples as indicated above blot.

Results

To determine the morphology of the recombinant VSV-MARV GP₁ supernatants of infected Vero E6 cells were collected and particles negative stained for transmission electron microscopy (TEM). As seen in Figure 13, particles maintain the characteristic bullet-shaped morphology of a rhabdovirus. Spikes are seen studded on the surface of the particle (Figure 13, arrow).

(Figure 13)



Figure 13. Electron micrograph of rVSV MARV GP₁. Supernatants from rVSV-MARV GP₁ infected cells were clarified by centrifugation, fixed with 2% paraformaldehyde and 0.1% glutaraldehyde. Samples were negative stained and visualized by TEM at a final magnification of 80,000X.

Growth of rVSV-MARV GP₁ was compared to VSV wildtype by determining the 50% tissue culture infective dose (TCID₅₀). The recombinant virus containing an additional transcription unit was not attenuated in its growth kinetics, with maximum

titers occurring between approximately 8 and 12 hours postinfection, as observed for wild-type VSV. Results for all time points are shown in Figure 14.

(Figure 14)

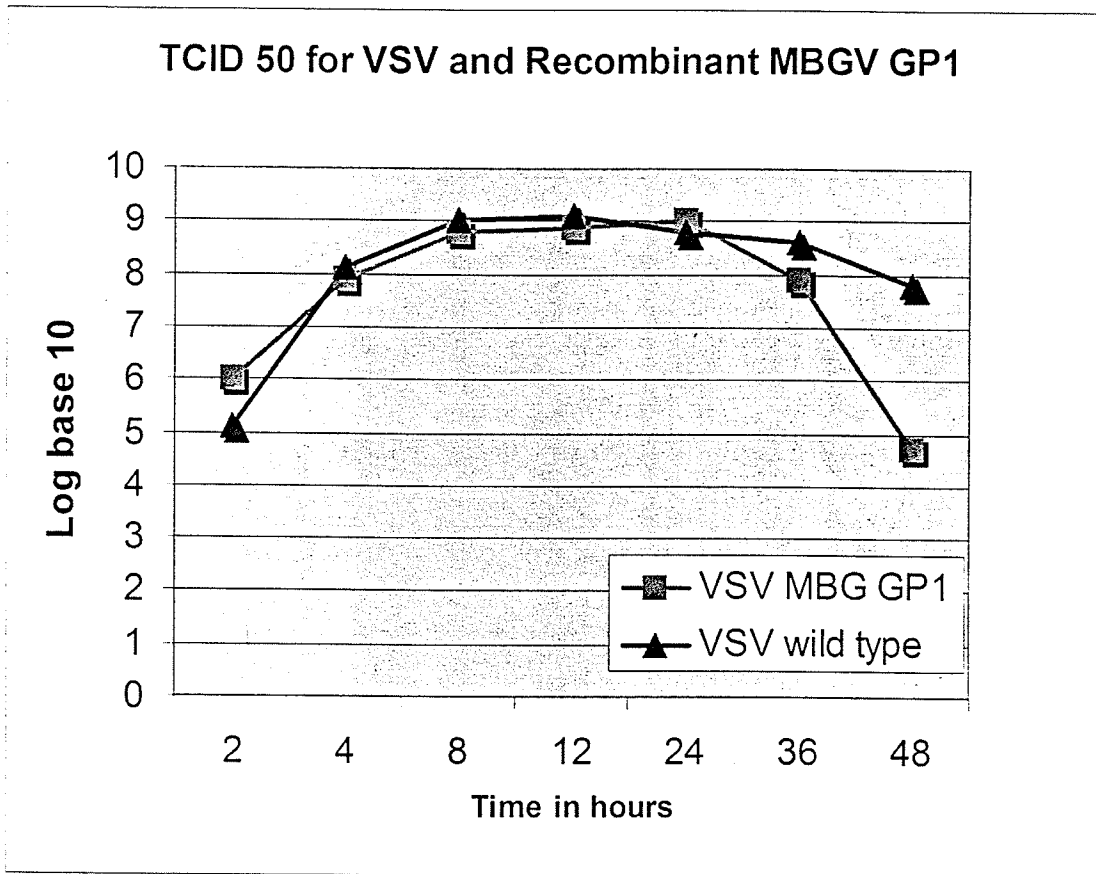


Figure 14. rVSV growth kinetics. The TCID₅₀ of rVSV-MARV GP1 and VSV wild-type in VeroE6 cells was determined over time. The kinetics for both viruses are comparable.

3.2 Cloning of glycoproteins into a mammalian expression vector

A mammalian transient transfection expression system was explored as an alternate approach to recombinant VSV expression of secreted filovirus glycoproteins. The soluble glycoproteins of ZEBOV were cloned into the eukaryotic expression vector, pDisplay. This vector contains several critical elements with respect to expression of the

ZEBOV constructs including both T7 and CMV promoters, a signal peptide, followed by an influenza hemagglutinin epitope tag and the multiple cloning site. Due to the fact that this vector also contains a carboxy-terminal *myc* tag and transmembrane domain, two elements I did not want to incorporate into expressed proteins, all reverse primers had to be designed with two consecutive stop codons to terminate translation prior to these regions. In doing so, all expressed proteins would then be expressed in a secreted form as desired and the two proteins in membrane-anchored forms (GP₂ constructs) were indeed anchored due to their internal, EBOV-specific transmembrane domain. In order to generate expression plasmids for VLP production, GP_{1,2} and VP40 were each cloned into pCAGGS. This vector contains the strong chicken beta-actin promoter but no epitope tags. Vector maps indicating restriction enzymes utilized for cloning and agarose gels demonstrating excised ZEBOV DNA from these vectors (following MaxiPrep DNA preparation) are shown in Figures 15 and 16.

(Figure 15)

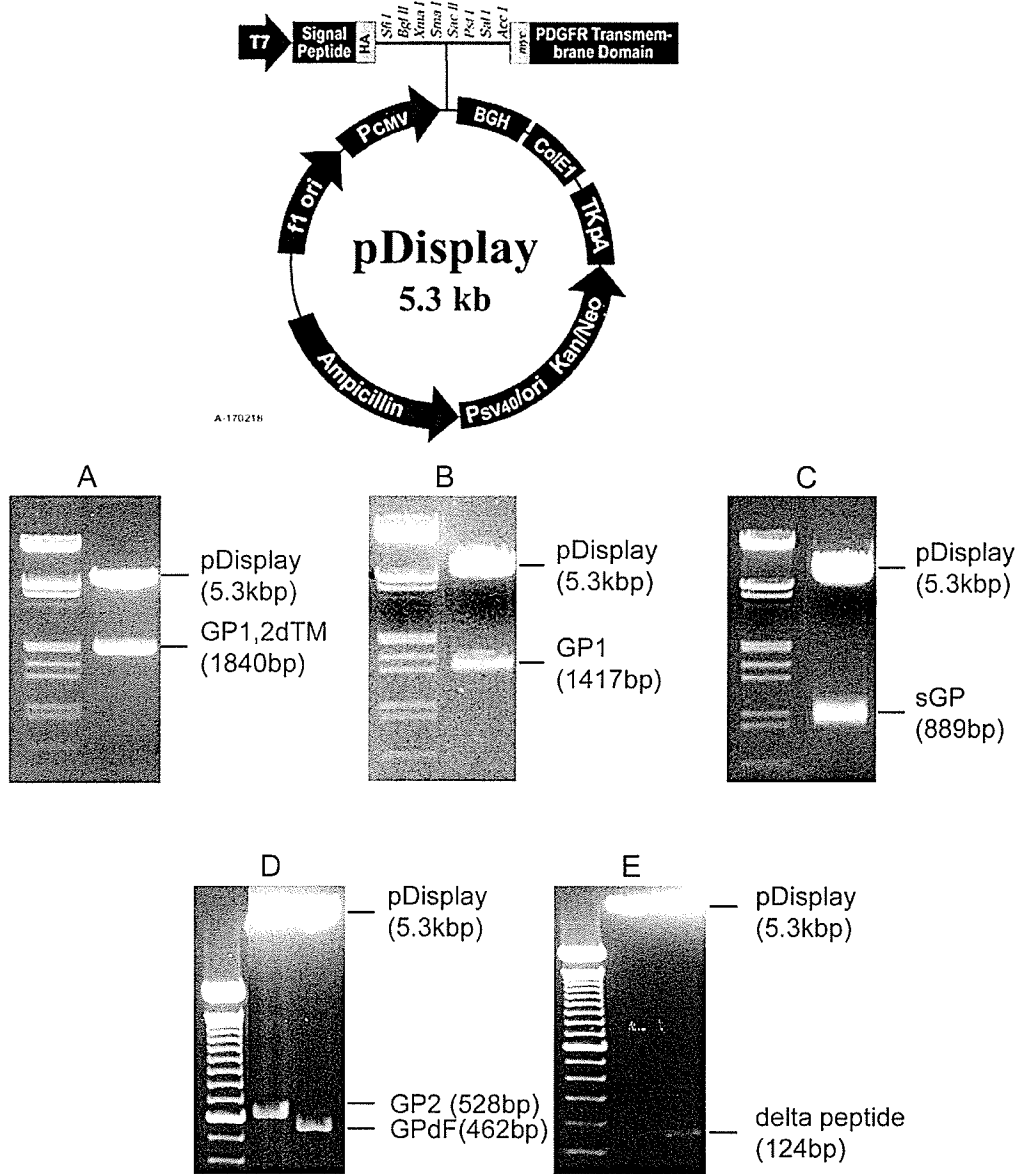


Figure 15. Cloning of pDisplay constructs. A map of pDisplay is shown and agarose gels demonstrating restriction enzyme (BglII/SacII) digested plasmid DNA for GP1,2dTM (A), GP1 (B), sGP (C), GP2/GP2dF (D) and delta peptide (E). Note that all reverse primers used for cloning contained the sequences for 2 stop codons thereby preventing expression of the myc tag and transmembrane domain normally encoded by the vector.

(Figure 16)

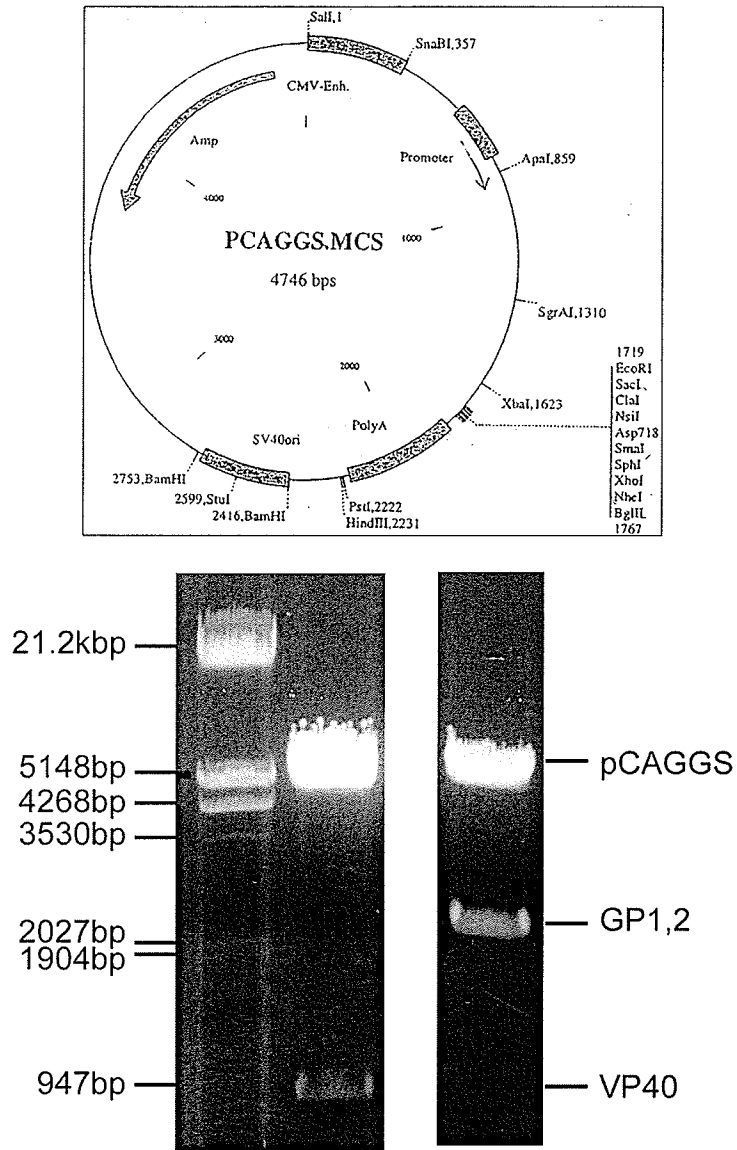


Figure 16. Cloning of VP40 and GP1,2 into pCAGGS. ZEBOV VP40 and GP1,2 were cloned into the vector pCAGGS which possesses the strong chicken beta-actin promoter. Plasmid DNA was digested with restriction enzymes used for cloning (EcoRI/XhoI).

3.3 Optimization of transfection procedures

In order to successfully test my hypothesis regarding the role of soluble glycoproteins the obvious and necessary tools are in fact the glycoproteins themselves. A fairly significant amount of protein was necessary to perform all the experiments in several trials and replicates per sample, therefore it would be a worthwhile investment of time to first optimize the transfection protocols. I tested two mammalian cell lines, 293T and BHK-T7 cells. 293T cells are known for high transfection efficiency, however, the BHK-T7 cells constitutively express the bacteriophage T7 polymerase. Since the pDisplay constructs contain both CMV (ubiquitous) and T7 promoters it seemed reasonable to assume that a cell expressing both promoters may better facilitate expression. In addition to testing both cell lines, three different transfection reagents were compared. The transfection efficiency was monitored by expression of plasmids expressing green-fluorescent protein from either CMV or T7-driven plasmids. The 293T cells exhibited higher transfection efficiencies than the BHK-T7 cells with either Lipofectamine 2000 or Lipofectamine Plus used as transfection reagents (Figure 17). The best results were obtained using 1.0 μ L of Lipofectamine 2000 and 0.8 μ g of DNA for transfection of a 2cm² well. I also confirmed that these ratios could be scaled up to surface areas as high as 500cm², however, it is critical to prepare the cationic lipid complexes in no more than 20% of the total volume used for incubation of the cells since this increases the interaction of DNA to cationic reagent. Shortly after these initial optimizations were performed another transfection reagent, FuGENE6, was recommended and tested. Results comparing the optimized Lipofectamine 2000 protocol and FuGENE6 are seen in Figure 18. The FuGENE6 performed better under similar

Results

conditions and was therefore adopted for all experiments requiring large-scale protein production.

(Figure 17)

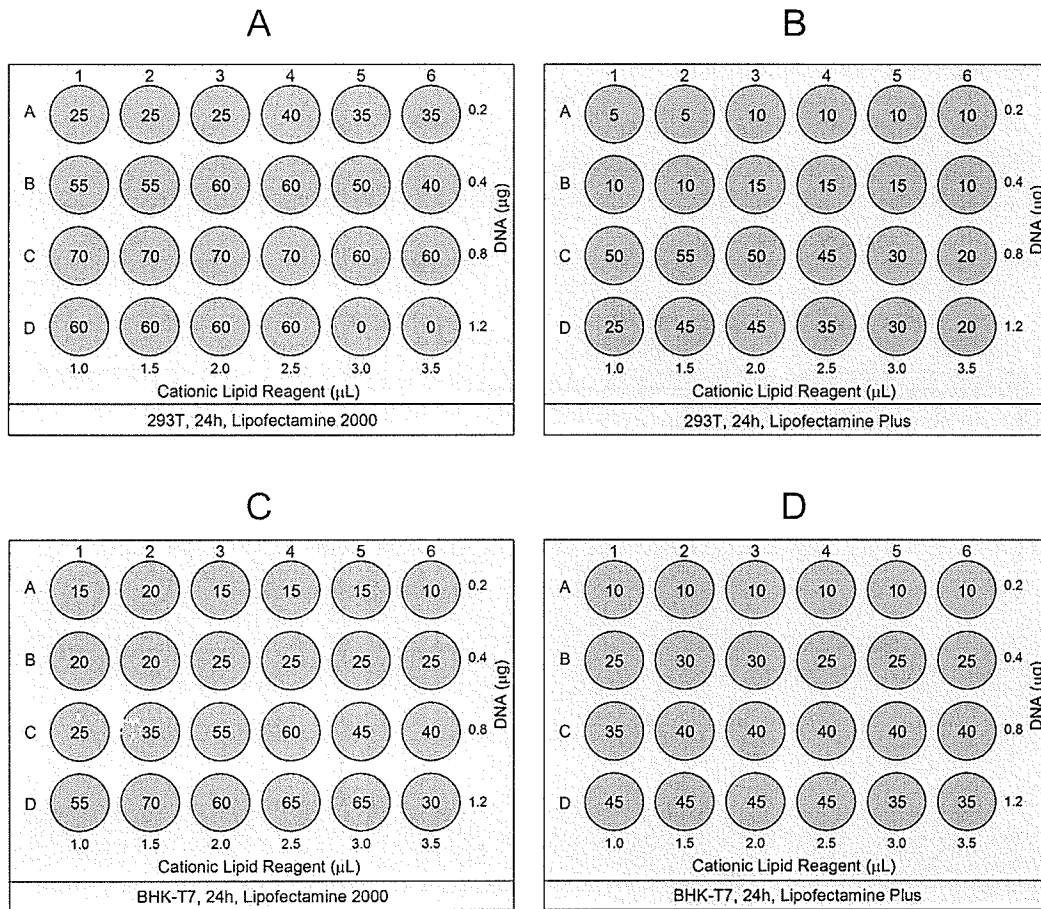


Figure 17. Transfection Optimization. Transfection efficiency was compared between 293T cells (A & B) and BHK-T7 cells (C & D). Two transfection reagents were compared for each cell line: Lipofectamine 2000 (A & C) and Lipofectamine Plus (B & D). Transfection efficiency was monitored by expression of green fluorescent protein from either CMV (A & B) or T7 (C & D) driven plasmids. Values in circles represent the percentage of cells expressing GFP after 24 hours of incubation.

(Figure 18)

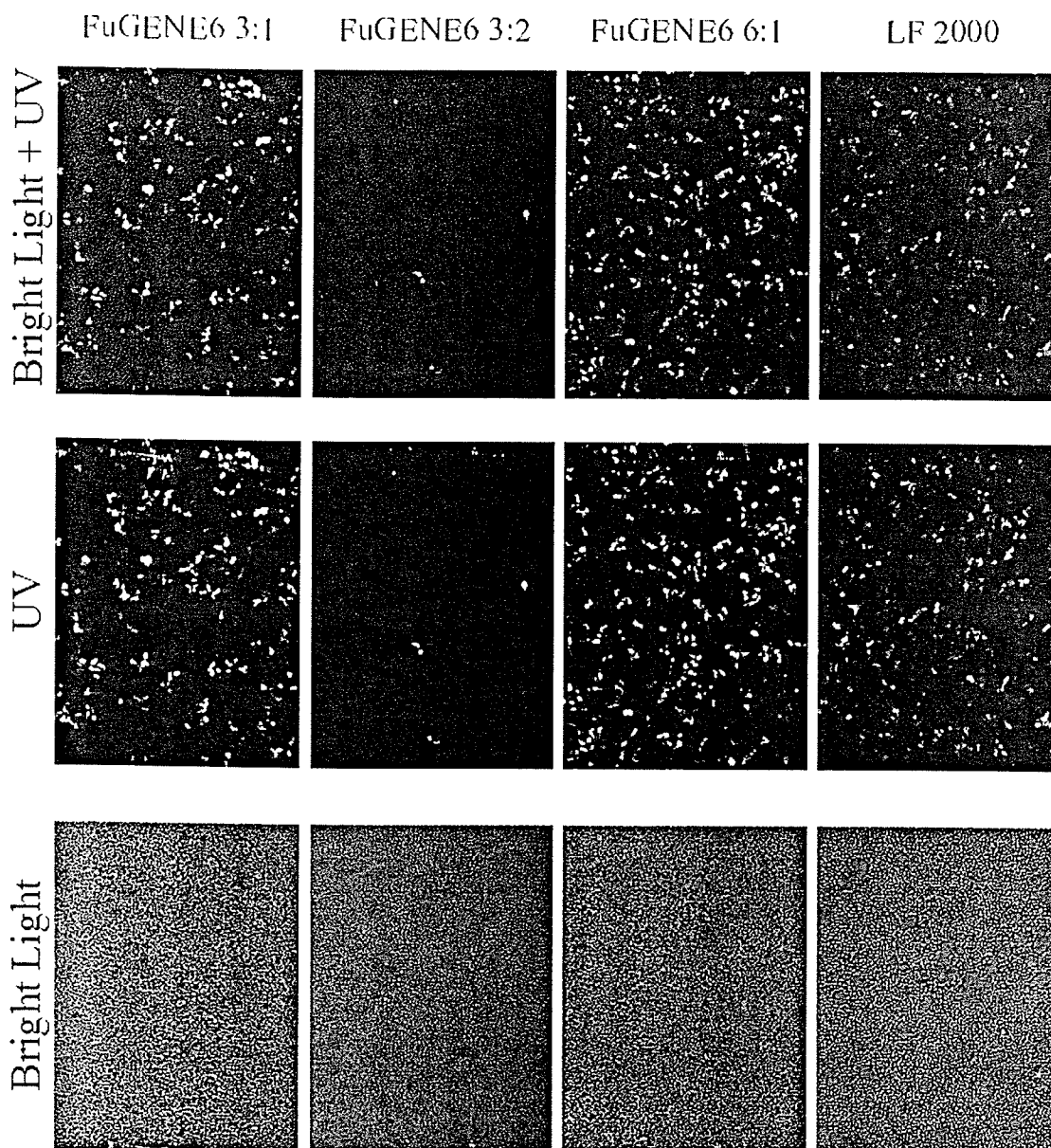


Figure 18. Optimization of FuGENE6 transfections and comparison to Lipofectamine 2000. 293T cells were transfected with either Lipofectamine 2000 or FuGENE6 and a CMV-driven green-fluorescent protein plasmid. Results shown are following 36 hours of incubation and acquired at 100X magnification. FuGENE6 used at a 6:1 ratio was determined to be superior to previously optimized transfections using Lipofectamine 2000.

3.4 Generation of recombinant proteins

3.4.1 Expression and purification from pDisplay constructs

All soluble glycoproteins were expressed by transient transfection of expression plasmids in 293T cells using the optimized FuGENE6 protocol. For each protein three Nunclon triple flasks (500cm² each) were coated with poly-D-lysine and seeded with 293T the day prior to transfection. Following transfection, cells were incubated for 3-5 hrs after which time the medium was replaced with DMEM containing 10% heat-inactivated FBS. The transfection was then incubated for a total of 72 hours after which time supernatants were harvested and purified. The purification was performed using size-exclusion centrifugation and immuno-affinity chromatography, as described in the materials and methods (chapter 2.6.2) and shown in Appendix B. During the initial attempts at immuno-affinity purification I determined that increasing the time for proteins to bind the matrix using batch purification greatly increased the final yield of protein. Rather than simply passing supernatants through the column, I removed the matrix by resuspending it in supernatant and transferred them to sterile 50mL tubes. I then incubated the tubes for 1.5 hours at room temperature with end-over-end rotation. After this incubation, the supernatants and matrix were transferred back to the column. The protein of interest was then bound to the column while other proteins and supernatant passed through. The procedure was then continued as per manufacturers instructions until the elution step, which I also modified. Rather than eluting at 37°C for 15 minutes I increased the time to 45 minutes. Three elutions were used to liberate the recombinant protein from the matrix. As seen in the Figure 19, the majority of the protein is released in the first elution (lane 1) and continues to be removed through the second and third

elutions (lanes 2 and 3, respectively). In combination with the modified batch purification I was then able to achieve significantly higher final protein yields.

(Figure 19)

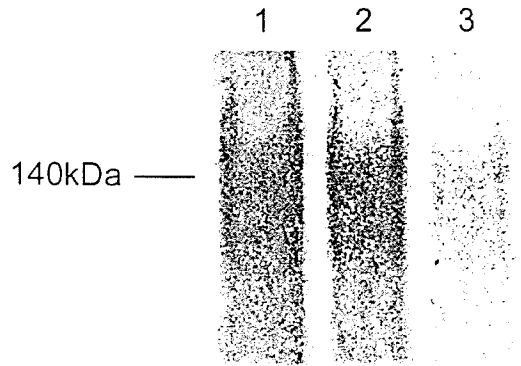


Figure 19. Silver stained SDS-PAGE gel of ZEBOV GP1. Fractions 1 through 3 were subjected to reducing SDS-PAGE. The majority of the protein is removed from the matrix in the first elution. The second elution also removes a significant amount of protein while the 3rd elution removes the remaining protein. GP1 is shown as a 140kDa protein under reducing conditions.

Following the immuno-affinity purification I added a polishing step involving size-exclusion centrifugation to remove the HA-peptide used in the elution step. The size-exclusion centrifugation columns used were dependent on the size of the protein to be purified as mentioned before (chapter 2.6.2). Following this last step the protein of interest was aliquoted and stored at -20°C . One aliquot was used to determine protein concentration using a commercial protein assay kit. Average concentrations attained for various proteins can be seen in Table 7.

Results

(Table 7)

Protein	Concentration Range ($\mu\text{g}/\mu\text{l}$)
sGP	2.0 – 6.0
Δ peptide	0.3 – 0.6
GP ₁	0.5 – 3.0
GP _{1,2} Δ TM	0.4 – 2.0
GP ₁ C53G	1.5 – 3.08

Table 7. Concentrations of purified recombinant proteins. The concentration range for recombinant soluble glycoproteins is shown as $\mu\text{g}/\mu\text{l}$ amounts. Purified proteins were typically resuspended in 200-250 μl of equilibration buffer.

Throughout the purification the samples were monitored in flow-through fractions to detect any potential loss of protein. Representative results are shown in Figure 20 for sGP where the protein can be detected in the initial, clarified supernatant and the final purified product but at no other point along the purification procedure.

All proteins were successfully expressed as demonstrated by Western blot (Figure 21) and IFA (Figure 22). For Western blot, the gel was run under reducing conditions therefore the size of GP₁ and GP_{1,2} Δ TM are the same. Unfortunately, there is no GP₂-specific antibody for detecting that portion of GP_{1,2} Δ TM and the size difference is only distinguished when the proteins are run under non-reducing conditions as will be shown in section 3.5.

(Figure 20)

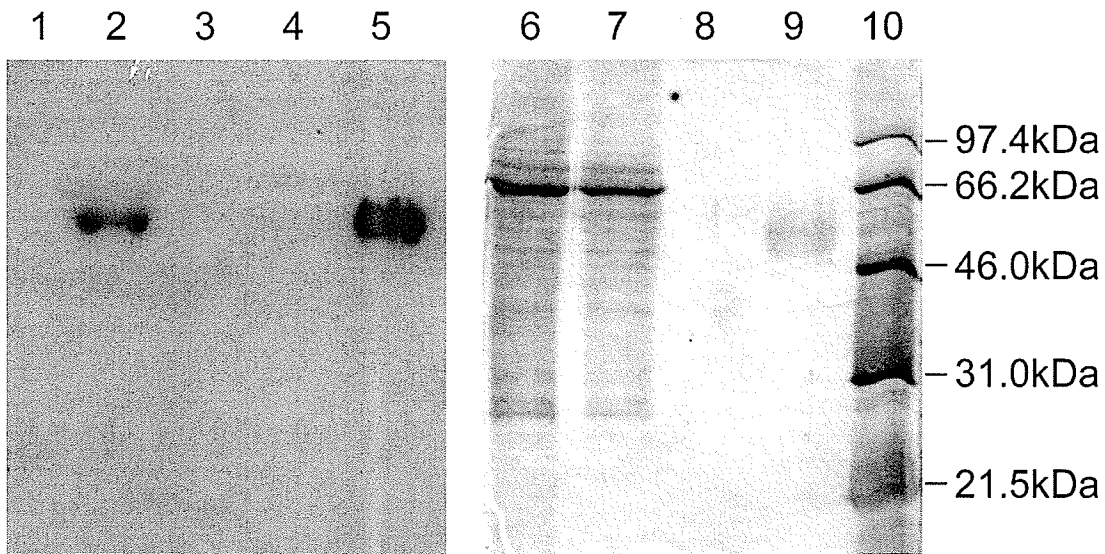


Figure 20. Purification steps for sGP. A 12.5% SDS gel was run under reducing conditions. Following electrophoresis, the gel was cut in half with lanes 1 through 5 used for Western blotting and lanes 6 through 10 used for Silver staining. Anti-HA antibody was used for western blotting. Samples were loaded as follows: For Western blotting: RPN 800 rainbow marker (lane 1); 15uL clarified supernatant following transfection (lane 2); 15uL column flow-through following batch purification (lane 3); 15uL YM-10 MWCO filter flow-through (lane 4); 15uL purified and concentrated sGP (lane 5). For Silver staining: 15uL clarified supernatant following transfection (lane 6); 15uL column flow-through following batch purification (lane 7); 15uL YM-10 MWCO filter flow-through (lane 8); 15uL purified and concentrated sGP (lane 9); Low range silver stain standard (lane 10). Note that sGP is detected only in initial supernatant and final protein product. No detectable levels of sGP were lost during the purification procedure and no contaminating proteins are seen in the final product by silver staining.

(Figure 21)

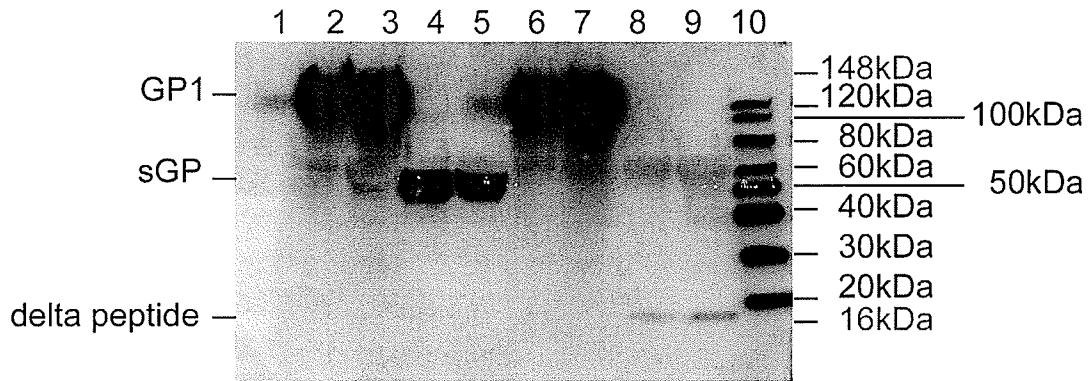


Figure 21. Expression of all secreted glycoproteins. A 4-20% gradient SDS gel was run under reducing conditions and Western blotted using anti-HA antibodies (1:2000). Supernatants were harvested from transfected cells 72h post-transfection and analyzed for expression. Samples loaded were as follows: RPN 800 protein marker (lane 1); 3uL GP1 (lane 2); 6uL GP1 (lane 3); 3uL sGP (lane 4); 6uL sGP (lane 5); 3uL GP1,2deltaTM (lane 6); 6uL GP1,2deltaTM (lane 7); 3uL delta peptide (lane 8); 6uL delta peptide (lane 9); Magic Mark ladder (lane 10). Molecular weights are shown to the right; note that sizes seen in red were determined using MW ladder RPN 800. All others were based on Magic Mark ladder. Proteins are shown to the left. Note that anti-HA antibody cross-reacts with albumin, also present in supernatants, at approximately 60kDa.

(Figure 22)

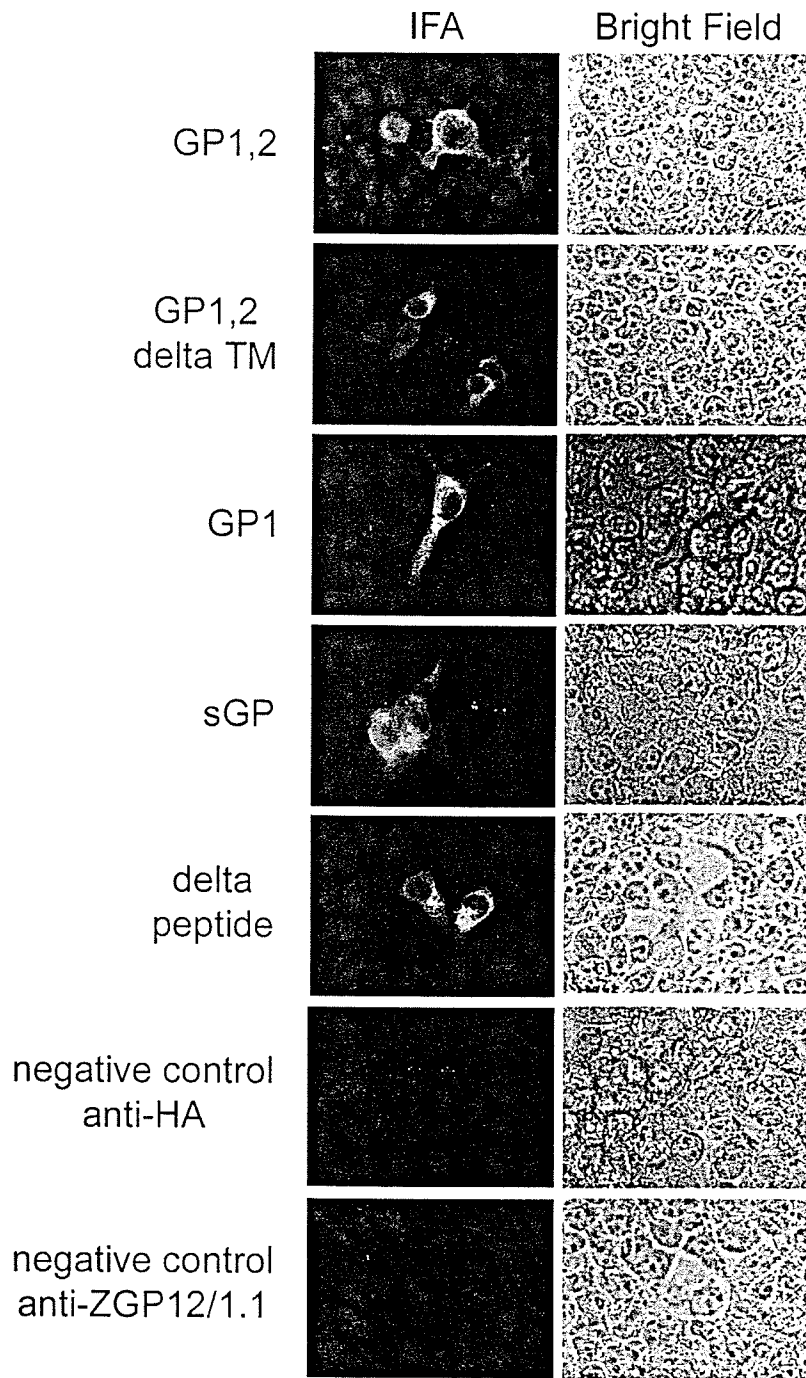


Figure 22. Expression of proteins by IFA. Transfected 293T cells were permeabilized and stained for expression of proteins with anti-HA antibody (1:200; delta peptide) or anti-ZGP12/1.1 antibody (1:200; remaining proteins). Magnification is 400X.

3.5 Characterization of proteins: oligomerization and glycosylation

Following expression and purification by transient transfection, soluble glycoproteins were subjected to extensive characterization to ensure their authenticity. The first aspect of characterization was analysis of oligomeric structures. In particular, sGP is secreted as a dimer and delta peptide as a monomer (Volchkova et al., 1998; Volchkova, Klenk, and Volchkov, 1999). Purified sGP was tested first and run in reducing and non-reducing SDS-PAGE. Following electrophoresis the gel was subjected to either Coomassie brilliant blue staining (Figure 23A), silver staining (Figure 23B) or Western blotting using anti-HA antibodies (1:2000; Figure 23C). sGP was determined to be expressed as a dimer, while monomers were observed under reducing conditions. Delta peptide was also analyzed by immunoblotting with anti-HA antibody (1:2000). This protein, which is believed to be expressed during viral infection as a monomer, displayed no shift in molecular weight when run under non-reducing conditions. This result confirms that the recombinant delta peptide expressed in this study is authentic and in monomeric conformation only as seen in Figure 23D.

(Figure 23)

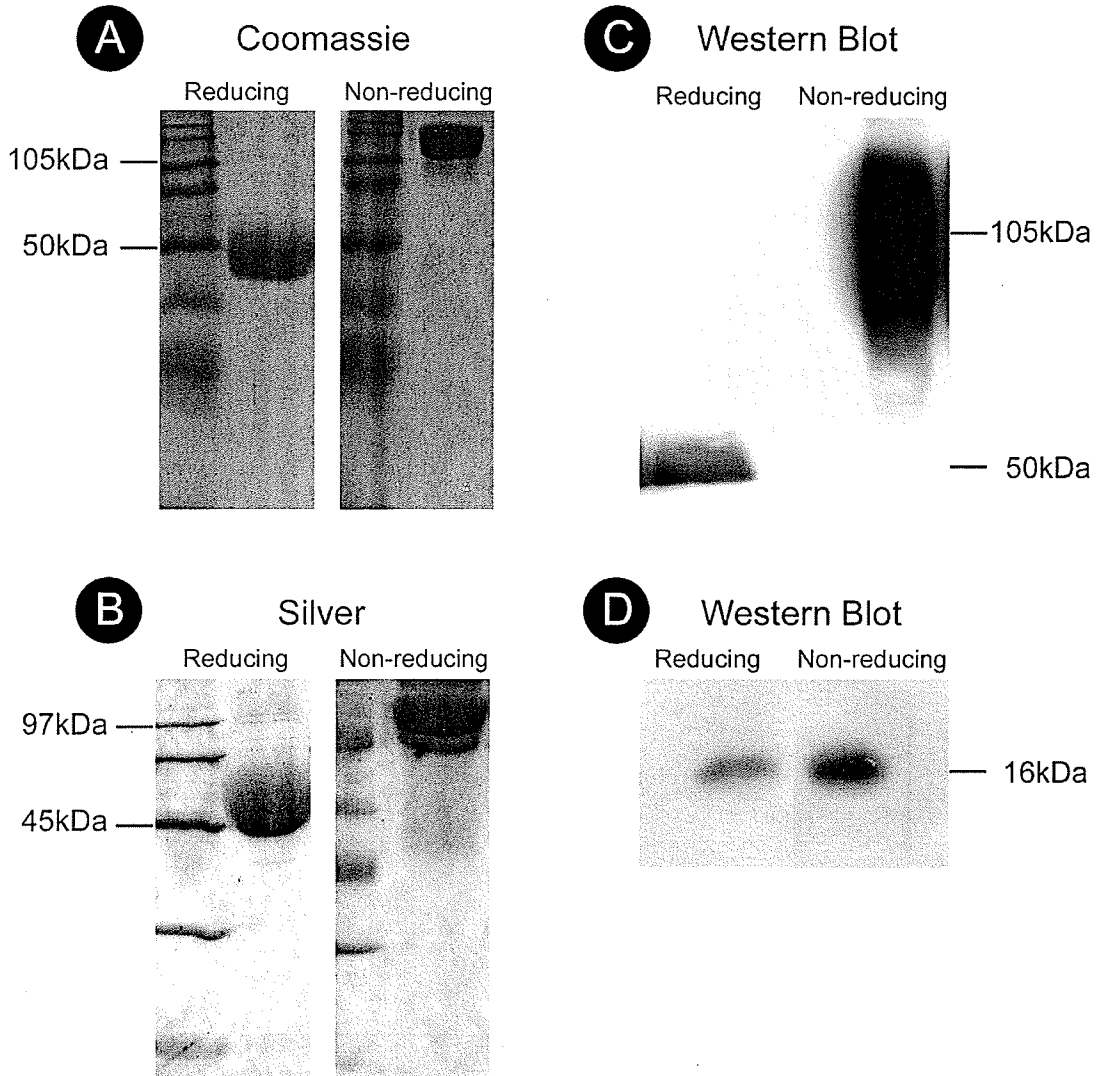


Figure 23. Oligomerization of sGP and delta peptide. Purified sGP was analyzed under reducing and non-reducing SDS-PAGE and gels stained with Coomassie brilliant blue (A), silver stain (B) or immunoblotted and probed with anti-HA antibody (1:2000; C). Monomers of sGP are observed at 50kDa and dimers at approximately 100kDa (A,B,C). Purified delta peptide was immunoblotted with anti-HA antibody (1:2000; D). Delta peptide is observed at 16kDa under both reducing and non-reducing conditions (D).

Full-length GP_{1,2} expressed on the surface of virions maintains a trimeric conformation (Sanchez, 2001). Full-length GP_{1,2} (in the vector pDisplay) was expressed as a control and analyzed by SDS-PAGE. As expected, full-length GP_{1,2} assembles into oligomeric structures consistent with monomers, dimers and trimers (Figure 24A). Interestingly, sGP is also detected (as a monomer and dimer) indicating that RNA editing must occur in this system (Volchkov et al., 1995). All three conformations of GP_{1,2} are clearly visible by Western blot using an anti-HA antibody at a dilution of 1:2000 (Figure 24A). Recombinant GP₁ was expected to form monomers in the absence of GP₂, although this has never been shown experimentally. Unexpectedly, this protein was able to form oligomers (most likely trimers) in the absence of GP₂, similar to that of full-length GP_{1,2} (Figure 24B). Although GP_{1,2}ΔTM lacks the transmembrane domain, it does contain cysteine residues thought to play a role in trimer formation. Thus, it was both expected and observed to form multimers when analyzed under non-reducing conditions. GP₁ and GP_{1,2}ΔTM were analyzed together in the same gel for comparative purposes (Figure 24C).

(Figure 24)

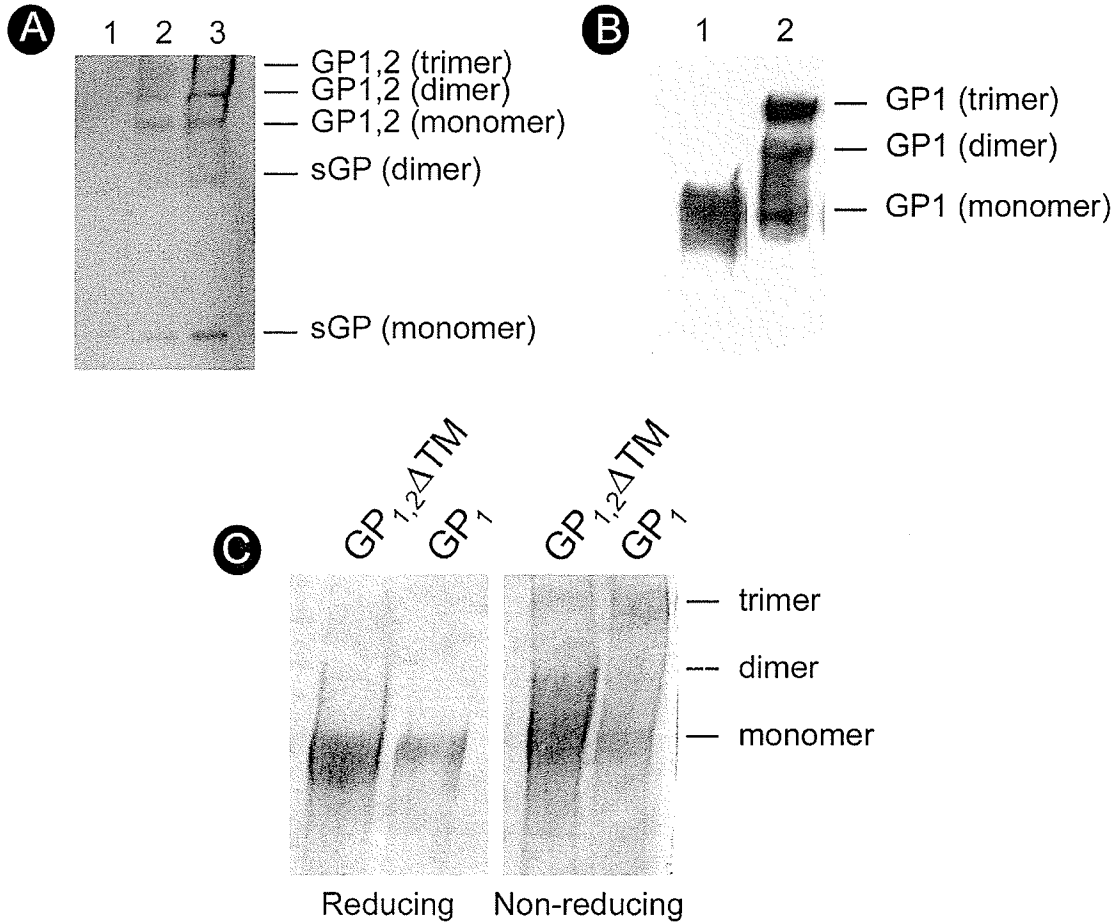


Figure 24. Expression of GP oligomers. Full-length GP1,2 in the vector pDisplay was expressed in 293T cells. Cell lysates were harvested and run under non-reducing SDS-PAGE conditions and immunoblotted (A). Mock transfected cells (A, lane 1), 10uL lysate (A, lane 2) and 20uL lysate (A, lane 3) are shown. Oligomers of GP1,2 and sGP are demonstrated. Purified GP1 was run under reducing (B, lane 1) or non-reducing (B, lane 2) conditions. Oligomers of GP1 are seen (B, lane 2). Purified GP1,2dTM and GP1 (C) were run under reducing and non-reducing conditions as indicated (C) and gels stained with Coomassie brilliant blue. Oligomers are labelled. Immunoblots (A & B) were probed with anti-HA antibody at a 1:2000 dilution.

Cysteine bridging is thought to be involved in multimer formation in full-length GP_{1,2}. To further elucidate the mechanism for GP₁ trimer formation each of the individual cysteine residues in GP₁ were mutated to glycines by site-directed mutagenesis. As seen by Western blot (Figure 25), cysteine 53 is critical in multimer formation, as its mutation abolishes these structures with only monomers detected. Mutation of cysteines 108, 121, 135 and 147 dramatically reduced expression of GP₁ and I suspect, based on similar studies performed on sGP (Volchkova et al., 1998), that these mutations resulted in misfolding of proteins and directed them to the degradation pathway.

(Figure 25)

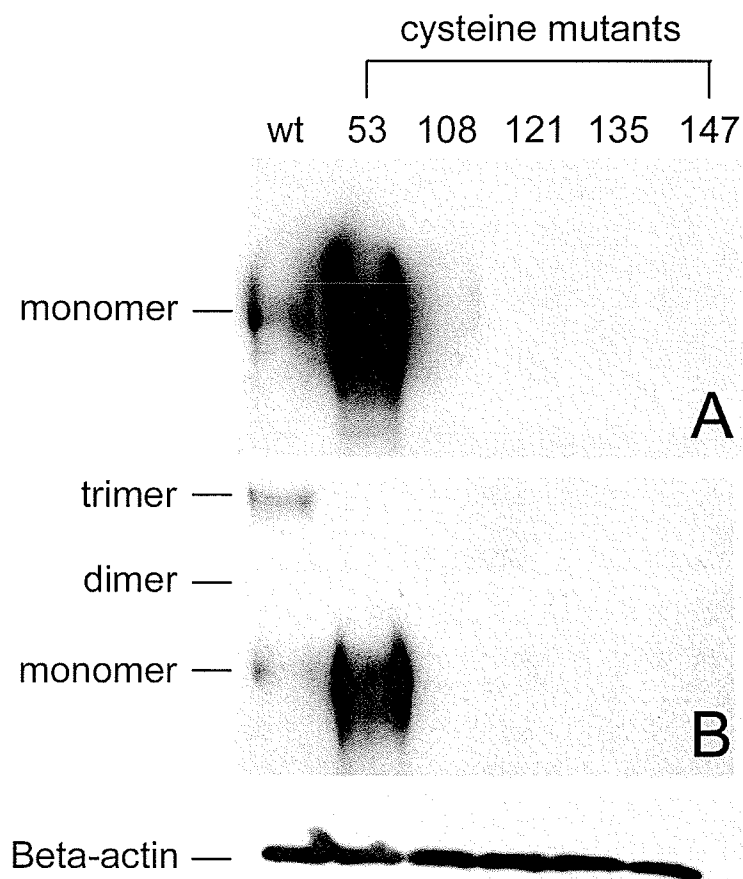


Figure 25. Expression of GP1 mutants. GP1 was mutated at each of the 5 cysteines present in the protein. Plasmids encoding mutated DNA was expressed in 293T cells and supernatants harvested at 48 hours post-transfection. Proteins were subjected to SDS-PAGE analysis under reducing (upper panel, A) or non-reducing (lower panel, B) conditions and Western blot was performed using an anti-GP specific antibody (anti-ZGP12/1.1; 1:2000). Beta-actin is shown as a loading control (anti-beta actin; 1:2000). Wildtype GP1 produces oligomers (most likely trimers) under non-reducing conditions while mutant C53G produces only monomers. All other mutants failed to produce detectable levels of GP1 in the supernatants.

During the course of this study GP₂ constructs, in pDisplay, were constructed as part of a collaborative project. Previous studies, particularly with respect to structural data, suggested that trimerization of GP_{1,2} was mediated by GP₂ (Malashkevich et al., 1999; Watanabe et al., 2000; Weissenhorn et al., 1998). Both GP₂ constructs were

analyzed under reducing conditions: GP₂, which encodes the entire sequence of GP₂, and GP₂Δfusion, which lacks the putative fusion domain. As expected, GP₂ was able to oligomerize into trimers, independent of the presence of the fusion domain (Figure 26).

(Figure 26)

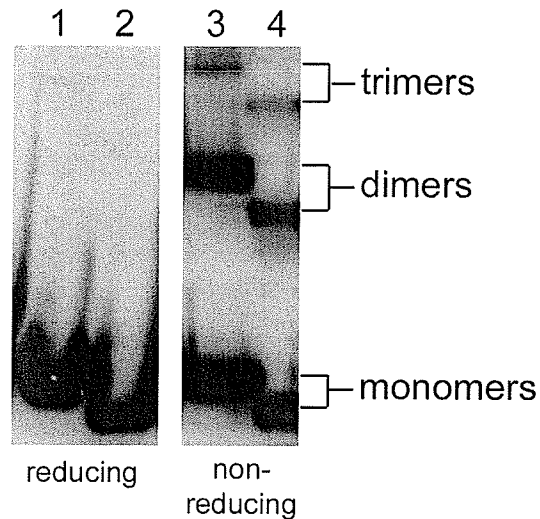


Figure 26. Expression of GP₂ constructs. Cell lysates from transfected cells were subjected to SDS-PAGE under reducing or non-reducing conditions and immunoblotted using anti-HA antibodies (1:2000). Expression of full-length GP₂ is seen in lanes 1 and 3, while the delta fusion domain construct is seen in lanes 2 and 4. Oligomers of GP₂ are visualized under non-reducing conditions.

The ability of GP₂ to form dimers and trimers was further analyzed by performing site-directed mutagenesis on each of the 5 cysteines in full-length GP₂ to glycines. Interestingly, no single cysteine could be identified as integral for multimerization (Figure 27). While some mutants appear to produce differing amounts of each oligomer it was not found to be significant. These results are consistent with those recently reported for full-length GP_{1,2} when GP₂ cysteines were mutated and will be discussed in detail in Chapter 4 (Jeffers, Sanders, and Sanchez, 2002).

(Figure 27)

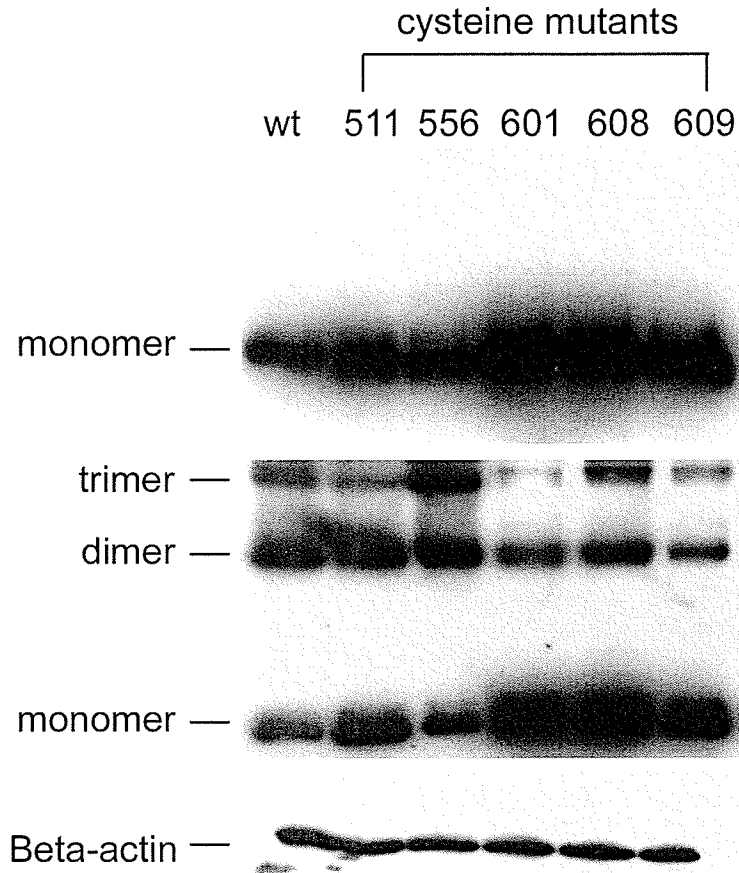


Figure 27. Expression of GP2 mutants. GP2 was mutated at each of the 5 cysteines present in the protein. Plasmids encoding mutated DNA was expressed in 293T cells and supernatants harvested at 48 hours post-transfection. Proteins were subjected to SDS-PAGE analysis under reducing (upper panel) or non-reducing (lower panel) conditions and Western blot was performed using anti-HA antibody (1:2000). Beta-actin is shown as a loading control (anti-beta actin; 1:2000). Wild-type GP2, as well as all mutants, were able to produce monomers, dimers and trimers.

The final characterization of the secreted glycoproteins involved analysis of glycosylation as demonstrated in Figure 28. N-linked glycosylation was assessed by digesting proteins with N-glycosidase F to demonstrate a shift in the molecular weight (MW) corresponding to the known glycosylation patterns. A shift of 15kDa was observed for sGP, while a shift of 40kDa was seen for GP₁ and GP_{1,2}ΔTM. All three

Results

proteins also experienced decreases in their MW following digestion with Sialidase A and O-glycosidase. Delta peptide does not contain complex N-linked sugars and these results confirm this as no shift in MW was observed, however a shift of approximately 10kDa was observed following treatment with Sialidase A and O-glycosidase.

(Figure 28)

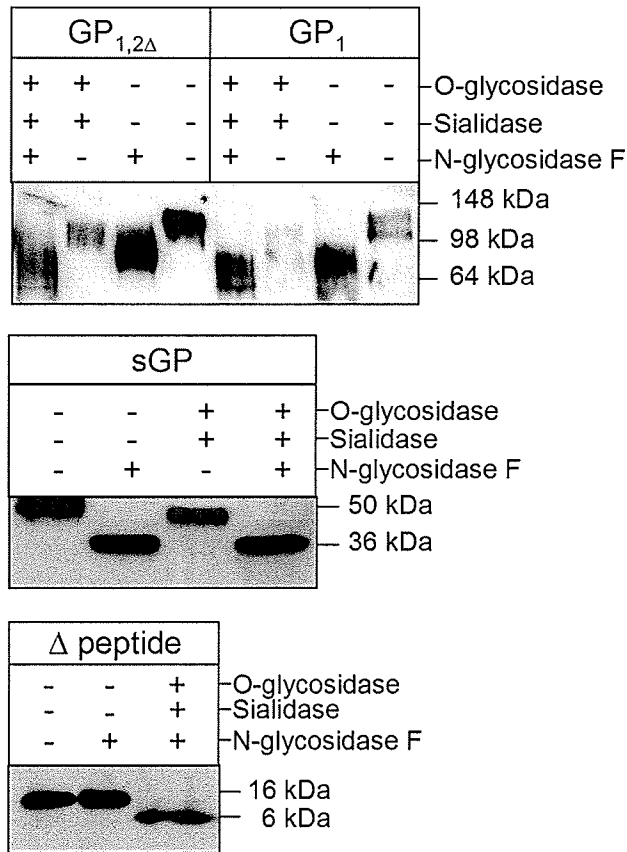


Figure 28. Deglycosylation of secreted glycoproteins. Proteins were enzymatically treated with N-glycosidase F, Sialidase and/or O-glycosidase and subjected to SDS-PAGE and immunoblot using anti-HA antibodies (1:2000). Removal of sugars is visualized by a shift in MW. (+) = enzyme added; (-) = enzyme omitted.

3.6 Generation of Virus-Like Particles (VLPs)

Virus-like particles (VLPs) were produced as a tool to study initial interactions of particles with target cells. VLPs were cloned into the vector pCAGGS as described above and transfected into 293T cells using FuGENE6. After 48 h supernatants were collected and clarified by centrifugation. Clarified supernatants were then subjected to SDS-PAGE under reducing conditions and immunoblotted using antibodies to the glycoprotein and VP40. GP₁ was loaded as a positive control for the glycoprotein present on the surface of particles. The presence of both the glycoprotein and VP40 in the supernatant provided the first evidence that VLPs may have been successfully produced (see Figure 29A). The two bands present for VP40 are expected because VP40 contains a second, in-frame start codon (Jasenosky et al., 2001).

Once expression was confirmed I tested optimal times for harvesting following transfection. 293T cells were transfected and supernatants harvested at 24, 48, or 72 hours later. Clarified supernatants were then subjected to SDS-PAGE and immunoblotting using anti-ZGP12/1.1 antibody (1:2000). Expression was seen to increase over time, reaching maximal expression by 72 hours (Figure 29B). Cells were visualized by microscopy at 96 hours post-transfection as well, however, they were heavily damaged with almost no cells attached to tissue culture flasks. For this reason, the 96 h post-transfection timepoint was not considered.

(Figure 29)

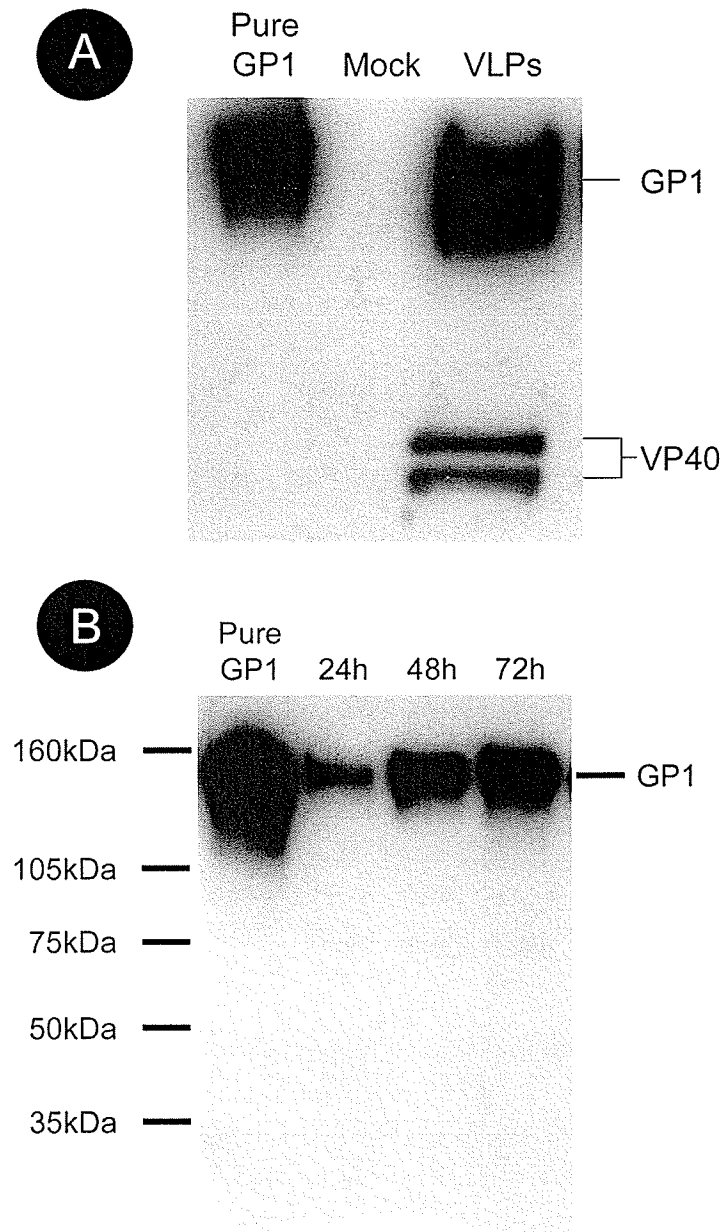


Figure 29. Expression of VLP proteins. Supernatants of GP1,2 and VP40 co-transfected cells were analyzed by reducing SDS-PAGE and immunoblotting using anti-ZGP12/1.1 (1:4000) and anti-VP40 (1:2000) antibodies (A). Supernatants were harvested at 24, 48, and 72 hours post-transfection and expression of GP1 determined using anti-ZGP12/1.1 (1:2000). Expression is greatest at 72 hours.

While expression of GP_{1,2} and VP40 in the supernatant was a good indication that VLPs were being produced, it remained to be seen whether they were assembling into particles representative of wildtype virus. In order to ascertain the morphology of VLPs both immunofluorescence staining of transfected cells and transmission electron microscopy of supernatants were performed. For electron microscopy, supernatants were collected at 48 hours post-transfected and clarified from cellular debris. The clarified supernatants were then fixed with 0.1% gluteraldehyde and Airfuged (ie: centrifuged) onto copper electron microscopy grids. By concentrating the sample onto the grid all particles in the supernatant should be forced onto the grid, as opposed to a standard “drop method” approach. Electron microscopy studies revealed high quantities of filamentous particles that were studded with an ordered surface projection (at this point, presumably the glycoprotein, GP_{1,2}). Particles appeared identical to those published for wildtype ZEBOV (Ryabchikova and Price, 2004). VLPs exhibited branched structures as well as intertwined particles resembling “end-to-end” figure 8’s. The particles varied in length with some particles measuring up to 5-10µm in length. Representative transmission electron micrographs are displayed below in Figures 30.

For the purposes of activation studies, VLPs would have to be purified. It was unknown whether purification would alter the morphology of particles. VLPs were purified by layering clarified supernatants on a 20% sucrose cushion, and centrifuging the sample to pellet the VLPs (26,000 rpm in an SW41Ti rotor). VLPs were washed once in equilibration buffer and resuspended in the same buffer. Particles retained their filamentous morphology and surface projections were still visible, indicating that purification had no adverse effects on particle structure (Figure 30D).

(Figure 30)

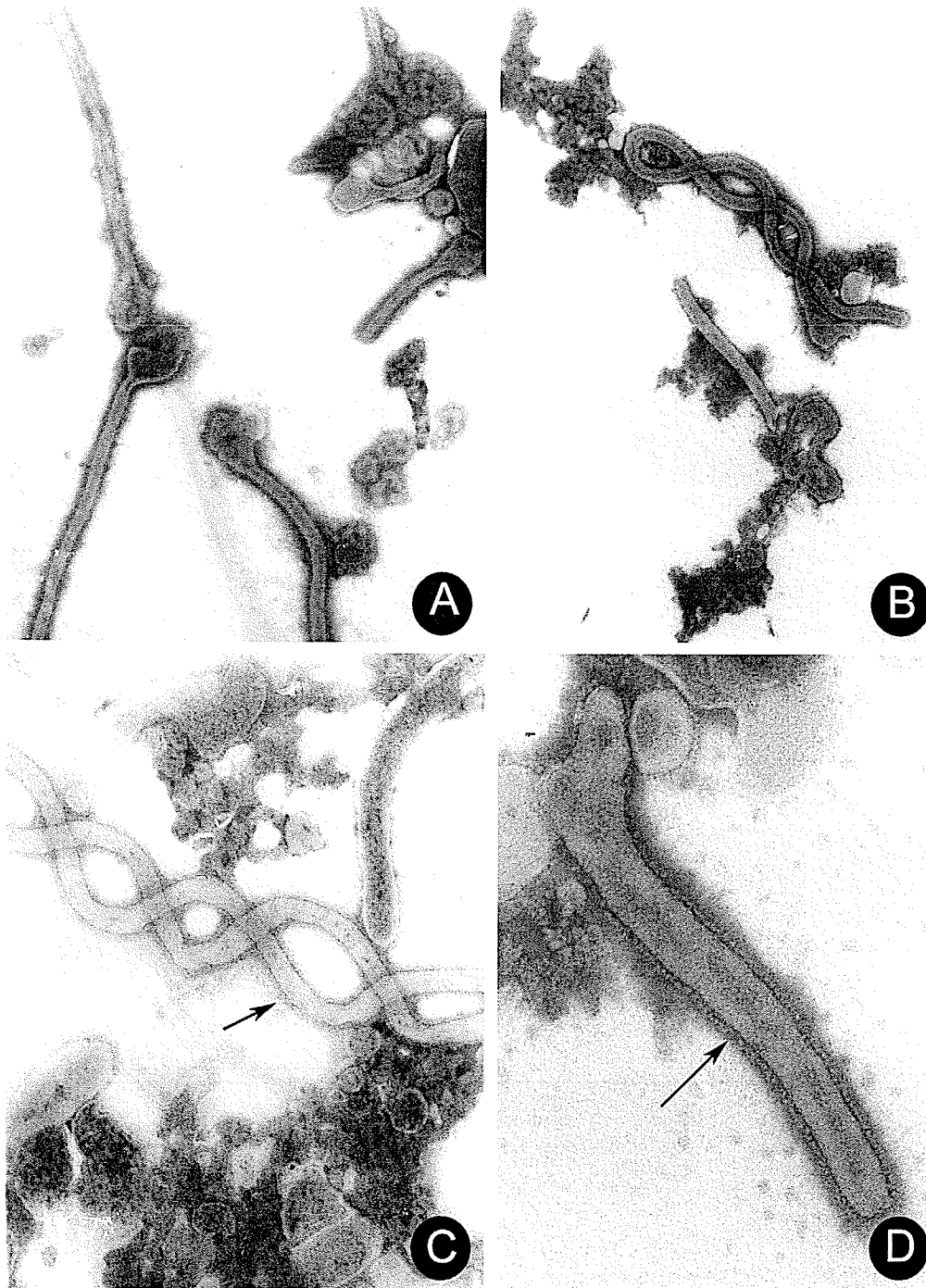


Figure 30. Transmission electron micrographs of VLPs. Clarified supernatants from GPI,2 and VP40 transfected cells or purified VLPs were fixed with 0.1% glutaraldehyde, Airfuged onto copper grids, negative stained and viewed. Images of clarified supernatants are 80,000x (A&B) and 200,000x (C). Clarified supernatants were purified through a 20% sucrose cushion and VLP morphology analyzed by diluting purified VLPs 1:100. Purified VLPs maintained their morphology (D). Glycoprotein spikes are highlighted by arrows (C&D).

Storage conditions of VLPs were tested by aliquoting purified VLPs and storing them for 4 months at +4°C, -20°C or -80°C. After 4 months, VLPs were analyzed by electron microscopy (Figure 31). The optimal storage condition was determined to be -20°C since particle morphology and glycoprotein distribution was most well maintained.

Electron micrograph studies indicated that VLPs were quite long. Due to this observation, I speculated that VLPs may actually be observed by UV-microscopy using a GP-specific antibody. 293T cells were transfected and fixed at 24 hours post-transfection. Cells were stained with anti-ZGP12/1.1 at a dilution of 1:200 and anti-mouse Alexa 488 used at 1:400 as secondary antibody. A network of particles are clearly visible on the surface of the cells (Figure 32). Size bars are included and the limit of detection with this method is approximately particles 2nm or longer. These results were used as the basis for attempting binding studies of VLPs with both macrophages and endothelial cells.

To conclusively demonstrate expression of GP_{1,2} on the surface of VLPs, immunogold labelling of particles was performed. Purified particles were fixed and diluted 1:100 and Airfuged onto nickel grids. Immuno-gold labelling was performed as described in Chapter 2 using anti-ZGP12/1.1 as primary antibody. Filamentous particles were visualized and associated with gold-antibodies that reacted with the primary antibody. Representative images are shown in Figure 33.

(Figure 31)

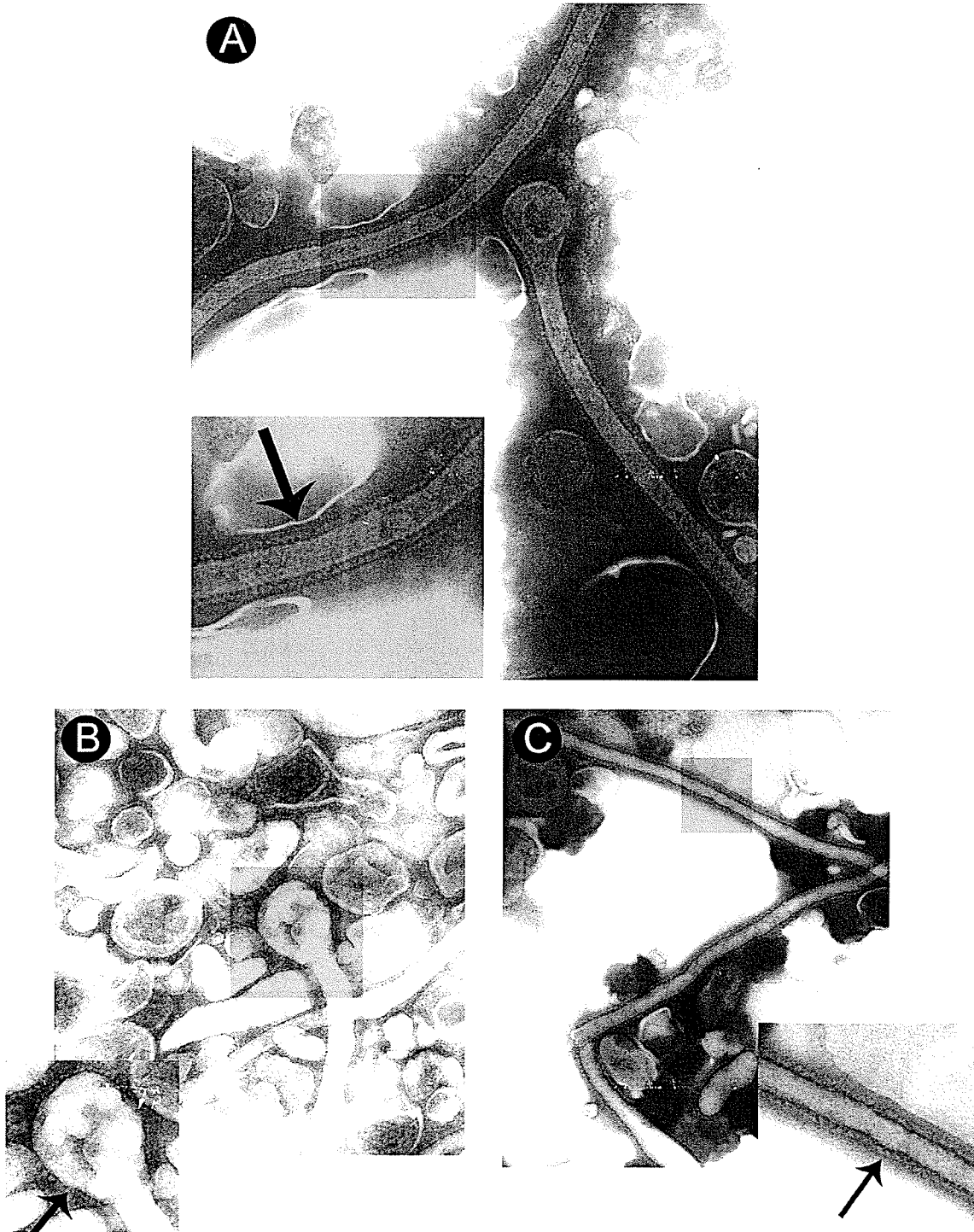


Figure 31. Morphological comparison of VLPs following 4 months of storage at different temperatures. Purified VLPs were stored for 4 months at +4C, -20C, or -80C. After 4 months VLPs were thawed and analyzed by transmission electron microscopy. Particles stored at -20C (A) maintained the best structure as compared to samples stored at -80C (B) or +4C (C). Arrows highlight the surface glycoprotein GP1,2. Magnifications are 80,000x (C) and 200,000x (A&B). Highlighted boxes indicate areas further enlarged.

(Figure 32)

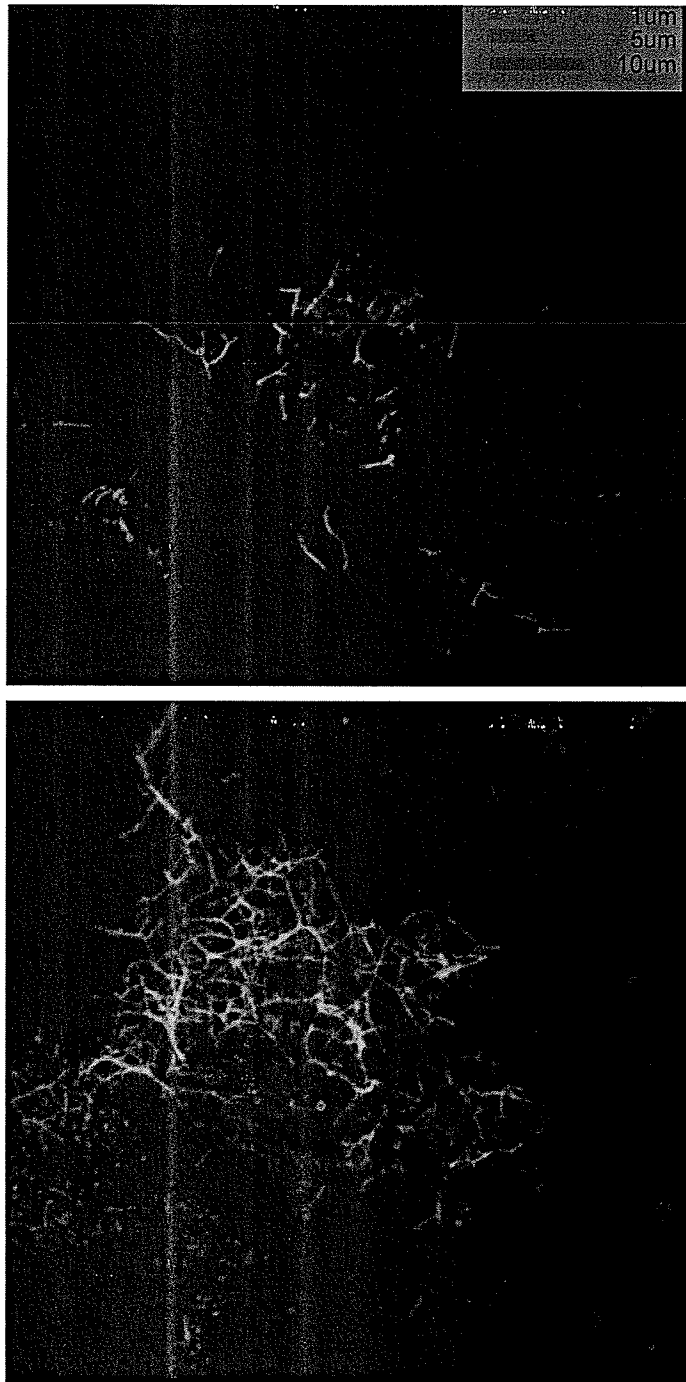


Figure 32. 293T cells transfected with plasmids to generate VLPs. 293T cells were fixed at 24 h post-transfection and stained with anti-ZGP12/1.1 antibody (1:200). VLPs are seen budding from the surface of cells. Size bars are 1, 5 and 10µm in length and representative for both images.

(Figure 33)

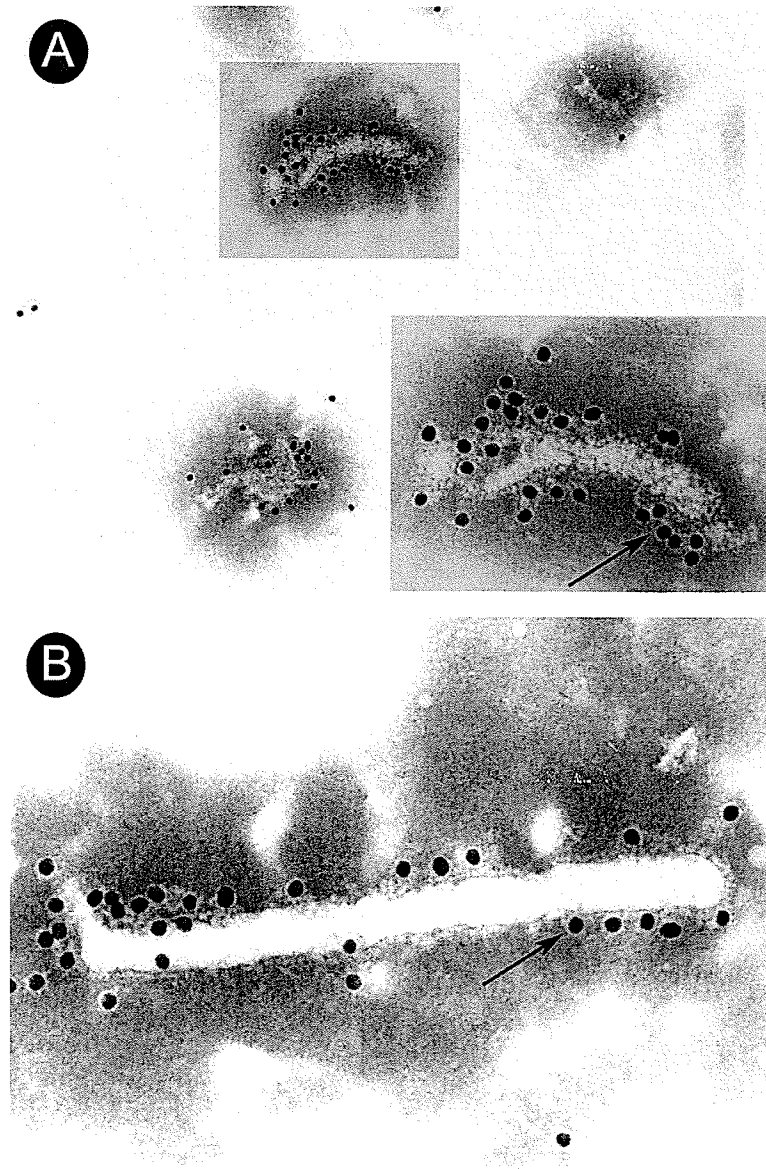


Figure 33. Immunogold labelling of VLPs. Purified VLPs were labelled with anti-ZGP12/1.1 (1:100) and anti-mouse conjugated to gold (1:50). Gold particles are seen in association with the surface of particles as highlighted by arrows. Images are 80,000x (A; with enlarged image in shadowbox) and 200,000x (B) magnification.

VLPs and VP40-only particles were morphologically compared by TEM and atomic force microscopy (AFM). VP40-only particles possess a smoother surface when observed by AFM, whereas, particles which also express GP_{1,2} tended to have a rougher surface as seen in Figure 34. The lack of surface glycoprotein was also observed in negative stained TEM images where the surface protein created a more ordered surface to the particles (data not shown). Despite differences in the surface of particles they remained otherwise identical in the types of sizes and shapes. Similar to results previously reported by Noda *et al* (Noda et al., 2002), expression of particles was greatly enhanced when both proteins were co-expressed. Typical yields of VLPs were 4×10^7 particles/mL for VLPs but only $1-2 \times 10^7$ /mL for VP40-only particles. The diameter of VLPs was 75nm as measured by AFM.

(Figure 34)

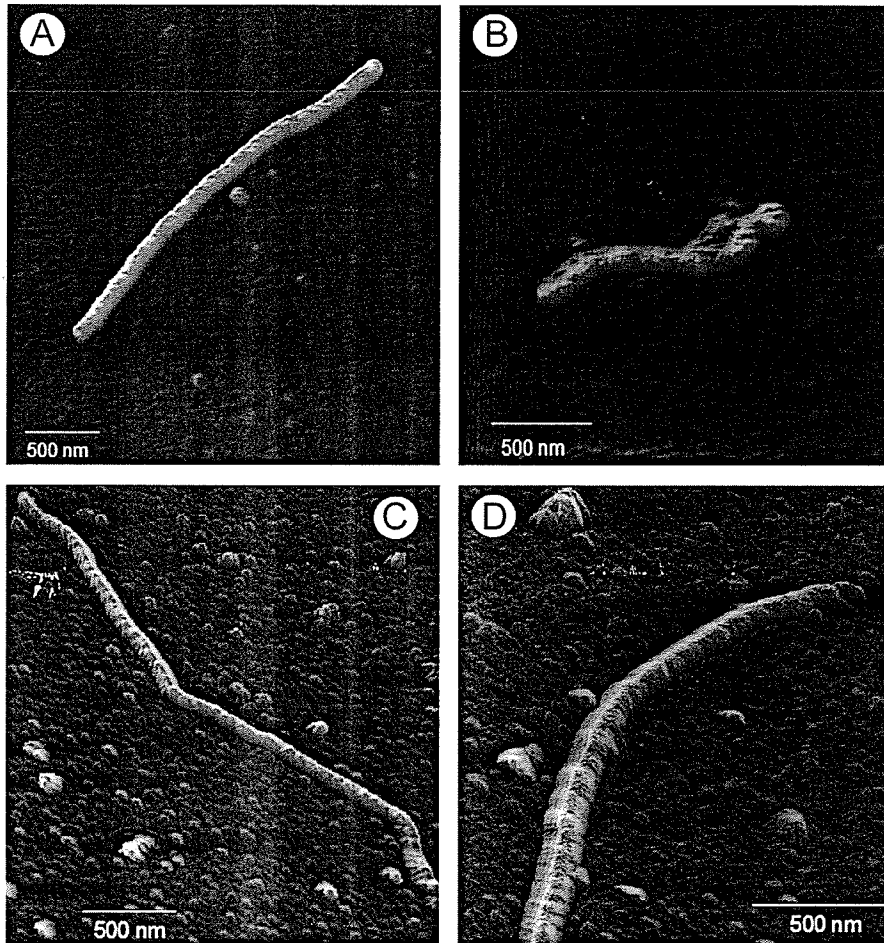


Figure 34. Atomic force microscopy of VLPs. Purified VP40-only particles (A&B) or VLPs (C&D) were prepared on mica and scanned by atomic force microscopy in air mode. VP40-only particles (A&B) appear to have a smoother surface than VLPs (C&D) which contain the spike protein GP1,2. Images were scanned by Dr. Hermann Schillers, Department of Nanophysiology, University of Muenster, Germany.

3.7 Activation of macrophages by secreted glycoproteins and VLPs

3.7.1 Binding of VLPs to macrophages

Binding of purified VLPs to macrophages was assessed by immunofluorescence assay (IFA). VLPs were bound to cells for 1 hour at either 4°C or 37°C. Cells were either surface stained or permeabilized with Triton X-100 then stained, in both cases with anti-ZGP12/1.1 GP monoclonal antibody at a 1:200 dilution. Secondary staining was performed using anti-mouse Alexa 488 and analyzed by UV-light microscopy. No specific staining was observed at 4°C, however, VLPs were observed in association with cells at physiological temperature. Specific staining is observed only for VLP treated and not mock treated cells (Figure 35). VLPs appear most frequently at the cell periphery and when macrophages were not permeabilized, VLPs can also be observed associated with the cell surface. The staining pattern for VLPs appears as aggregates, most likely because purified particles were used. In comparison, single particles can be distinguished when supernatants are used (see Figure 43). The ability of the soluble glycoproteins to bind macrophages was also investigated, however, results were negative. The inability to detect binding may be a function of the sensitivity of IFA or proteins may have been rapidly internalized and degraded.

(Figure 35)

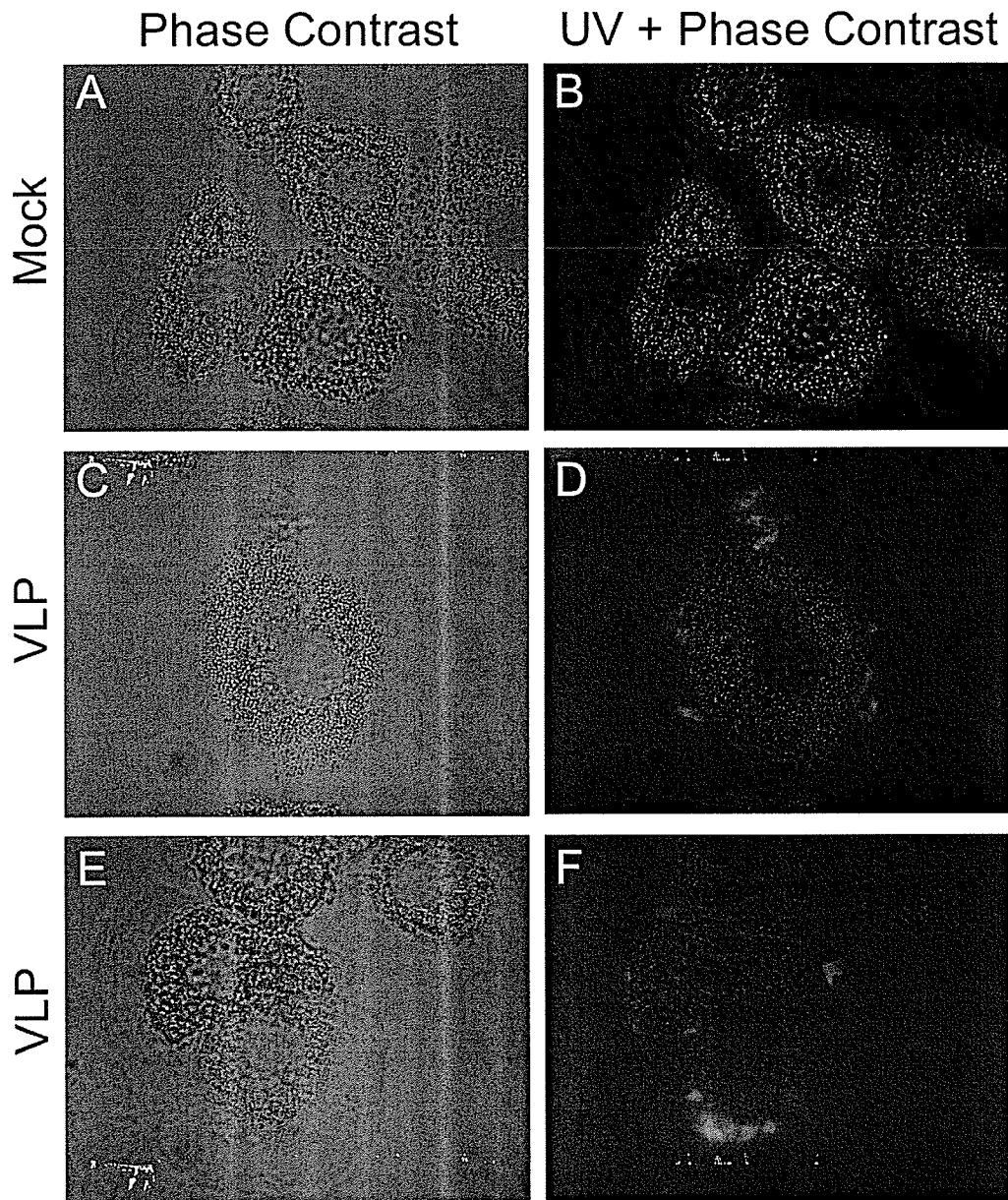


Figure 35. Binding of VLPs to macrophages. Mock supernatants (A&B) or VLPs (C-F) were incubated for 1h at 37C with human macrophages. Cells were extensively washed and permeabilized (A,B,E,F) or non-permeabilized (C&D) and stained with anti-ZGP12/1.1 (1:200) to detect GP1,2 on VLPs. VLPs were associated with VLPs as seen in D & F. Images are 1000x magnification.

3.7.2 Transcriptional activation

While previous studies have shown that Ebola virus infection leads to activation of human macrophages, the role of the soluble glycoproteins in this process is unknown (Stroher et al., 2001). In order to elucidate the role of exogenous soluble glycoproteins and replication deficient particles (VLPs) on macrophage activation, human macrophages were cultured for 7 days and subsequently treated with VLPs at 10 particles per cell (PPC) or with secreted glycoproteins at concentrations of either 10 μ g/mL or 50 μ g/mL. Several controls were also used including lipopolysaccharide (LPS), purified supernatants from empty pDisplay-transfected cells, HA peptide, untreated cells, VP-40 only particles and purified empty pCAGGS-transfected supernatants. RNA was extracted from cells to analyze transcriptional activation of specific cytokines/chemokines, whereas supernatants were harvested for the detection of cytokines/chemokines by ELISA, at 1, 6, 12 and 24 hours post-transfection. RNA was analyzed by real-time PCR and results shown in Figures 36-39. Interestingly, soluble glycoproteins, even at high concentrations, did not induce increased transcription levels of TNF-alpha, IL-6, IL-8 or IL-1 beta. Alternatively, VLPs induced a robust response with transcription levels equal to or exceeding that of the positive control, LPS. Transcriptional activation was observed for IL-6, IL-8 and TNF-alpha as early as 1 hour post-treatment and at 6 hours for IL-1 beta. VP40-only particles, which were used as control particles, did cause increases in gene transcription levels for the investigated cytokines/chemokines, however, the effect was markedly increased with addition of GP_{1,2} into particles as demonstrated by VLPs.

(Figure 36)

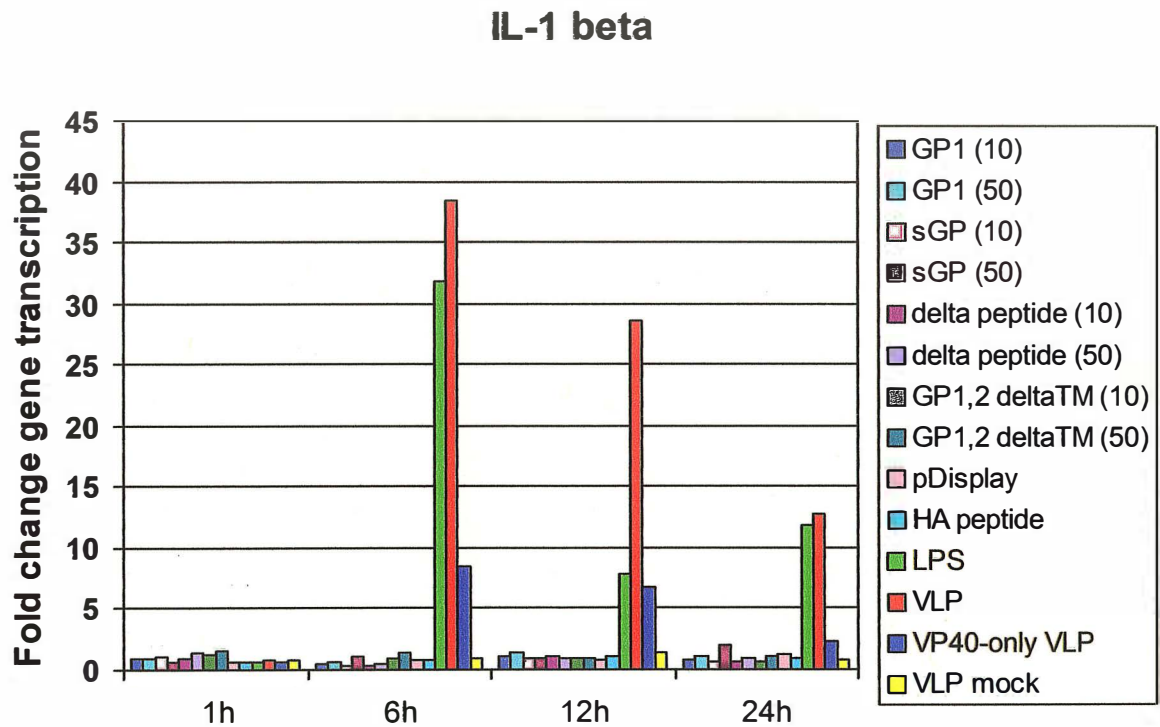


Figure 36. Real time PCR analysis of IL-1 beta gene transcription. Macrophages were incubated for 1, 6, 12 and 24 hours with secreted glycoproteins, VLPs or controls (pDisplay, HA peptide, LPS, VLP mock). Secreted glycoproteins were used at 50ug/mL (50) or 10ug/mL (10). Data is reported as fold change in gene transcription for IL-1 beta. Increases in expression of IL-1 beta are observed for VLPs, VP40-only particles and LPS.

(Figure 37)

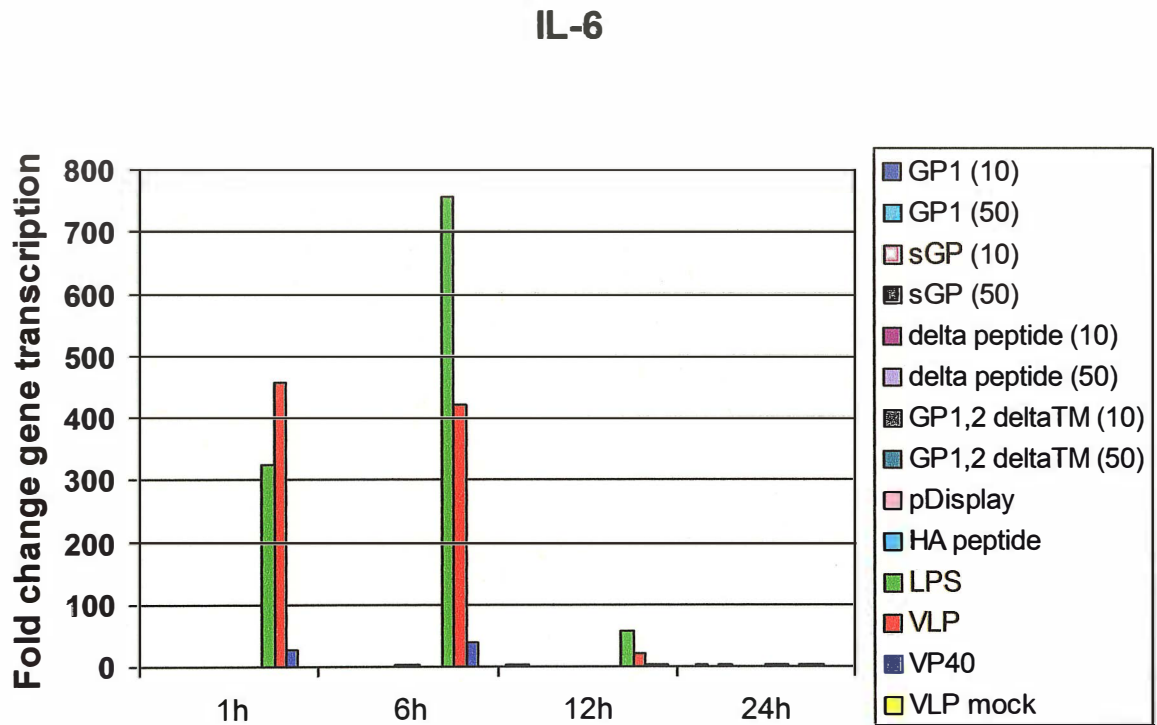


Figure 37. Real time PCR analysis of IL-6 gene transcription. Macrophages were incubated for 1, 6, 12 and 24 hours with secreted glycoproteins, VLPs or controls (pDisplay, HA peptide, LPS, VLP mock). Secreted glycoproteins were used at 50ug/mL (50) or 10ug/mL (10). Data is reported as fold change in gene transcription for IL-6. Increases in expression of IL-6 are seen for VLPs, VP40-only particles and LPS at 1 and 6h post-treatment.

(Figure 38)

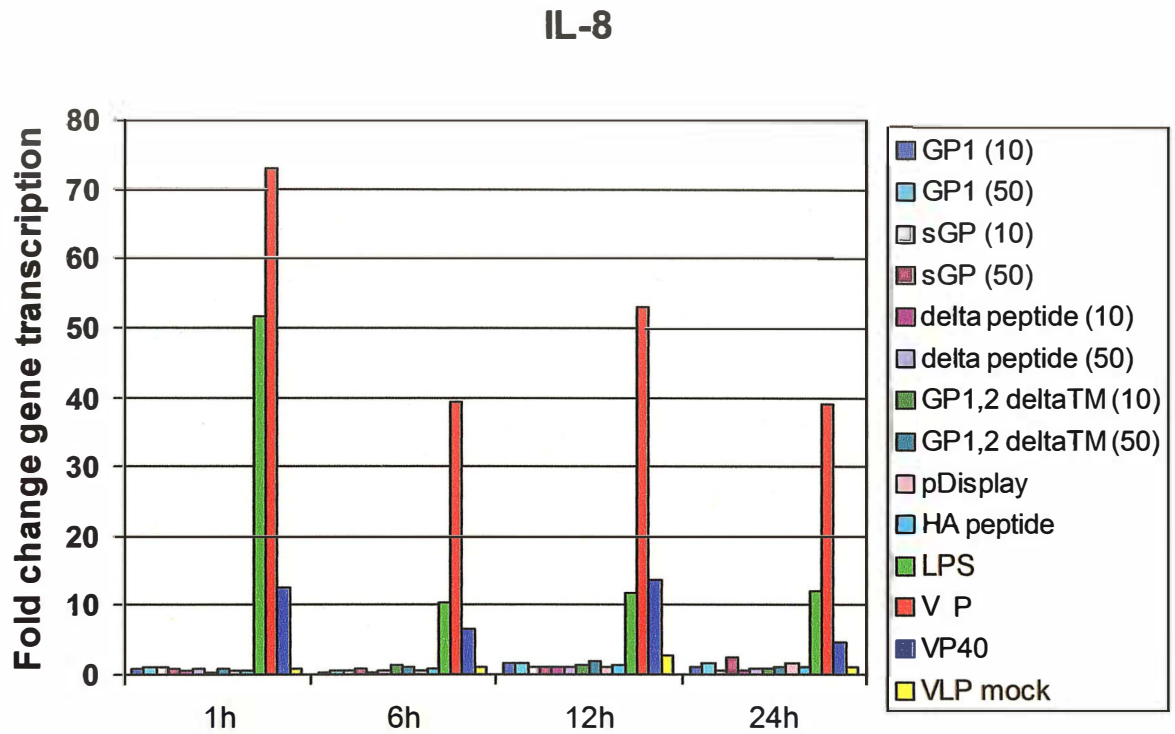


Figure 38. Real time PCR analysis of IL-8 gene transcription. Macrophages were incubated for 1, 6, 12 and 24 hours with secreted glycoproteins, VLPs or controls (pDisplay, HA peptide, LPS, VLP mock). Secreted glycoproteins were used at 50ug/mL (50) or 10ug/mL (10). Increases in expression of IL-8 are seen for VLPs, VP40-only particles and LPS at all time points.

(Figure 39)

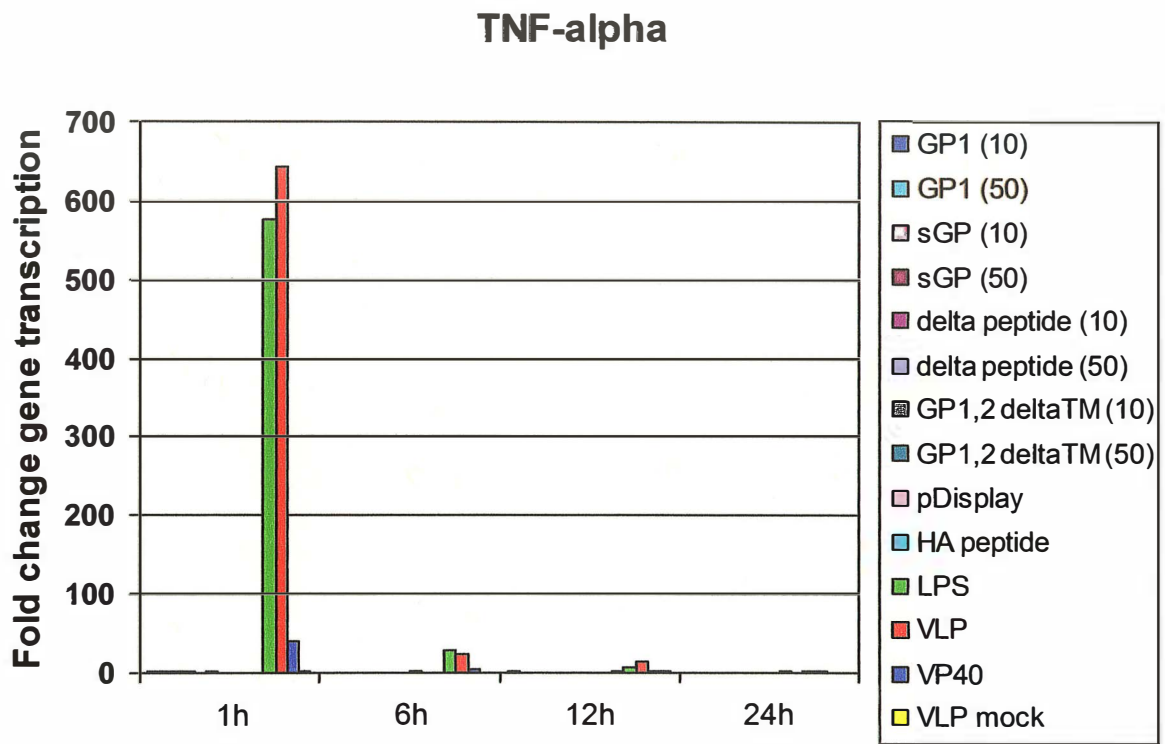


Figure 39. Real time PCR analysis of TNF-alpha gene transcription. Macrophages were incubated for 1, 6, 12 and 24 hours with secreted glycoproteins, VLPs or controls (pDisplay, HA peptide, LPS, VLP mock). Secreted glycoproteins were used at 50ug/mL (50) or 10ug/mL (10). Increases in expression of TNF-alpha are seen for VLPs, VP40-only particles and LPS at 1h post-treatment but already begin to dramatically decrease by 6 h.

3.7.3 Secretion of cytokines/chemokines into tissue culture supernatants

The ability of secreted glycoproteins and VLPs to induce expression and release of cytokines into tissue culture supernatants was analyzed by commercial ELISA (IL-6, TNF- α and IL-1 β) and EIA (IL-8) kits. All samples were tested in duplicate. Results are shown for IL-6, TNF- α and IL-8. IL-1 β was not detected at appreciable levels in the supernatant most likely because of the long time period required for its processing.

IL-6 is seen in supernatants from LPS, VLP and to a lesser extent from VP40-only particle treated cells as early as 6 hours post treatment (Figure 40). Expression begins to decline for VLP and VP40-only particle treated cells over time while LPS treated samples continue to rise through the remaining time points. Maximal expression of VLP treated cells is reached at 6 hours with 693pg/mL released.

TNF- α is observed in supernatants of VLP and LPS treated cells as early as 1 hour post-treatment (Figure 41). Unfortunately, VP40-only particles could not be tested at this time for comparison and were not tested later due to cost of the ELISA kits. The kinetics of expression are similar for VLPs and LPS with both reaching maximal concentrations of approximately 2060pg/mL by 6-12 hours post-treatment. This concentration is at the upper limits of detection for the assay.

Finally, IL-8 secretion was detected using a commercial EIA kit. As seen in Figure 42, LPS, VLPs and VP40-only particles induce significant expression of this chemokine. The highest concentration released was approximately 20ng/mL for all three stimulants and occurred at 12 hours post-treatment. Additionally, sGP and GP_{1,2} Δ TM both increased expression of IL-8 albeit at very low levels.

(Figure 40)

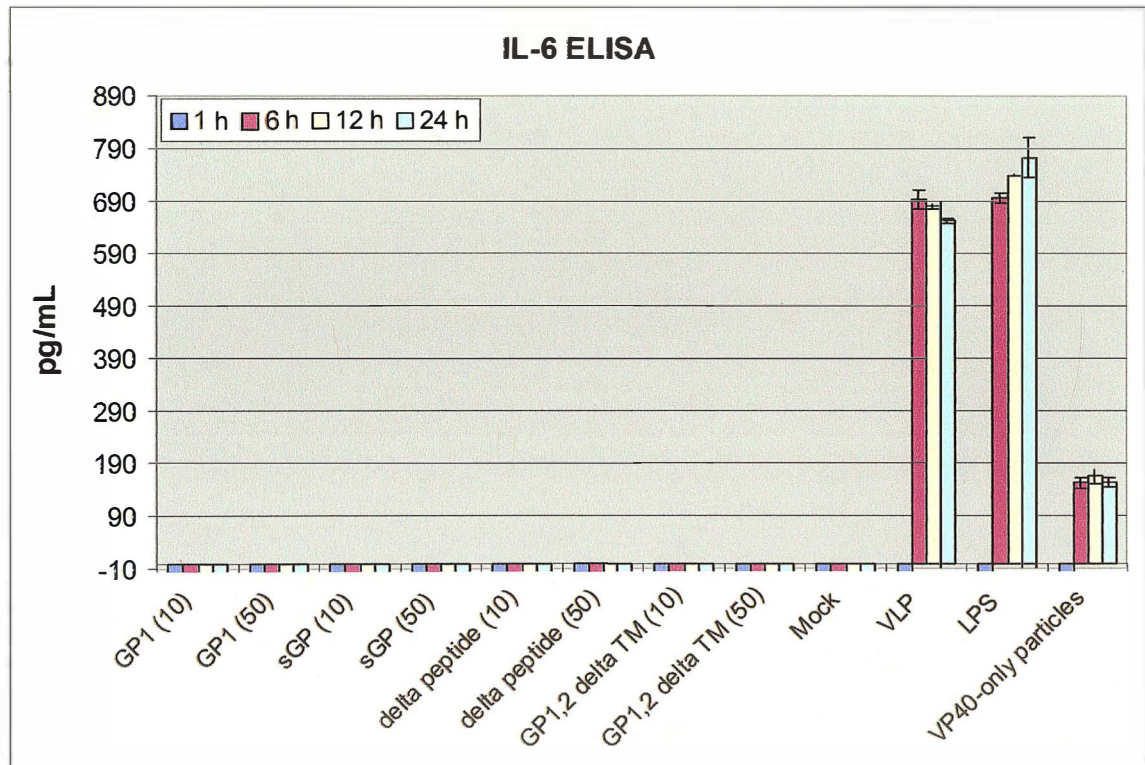
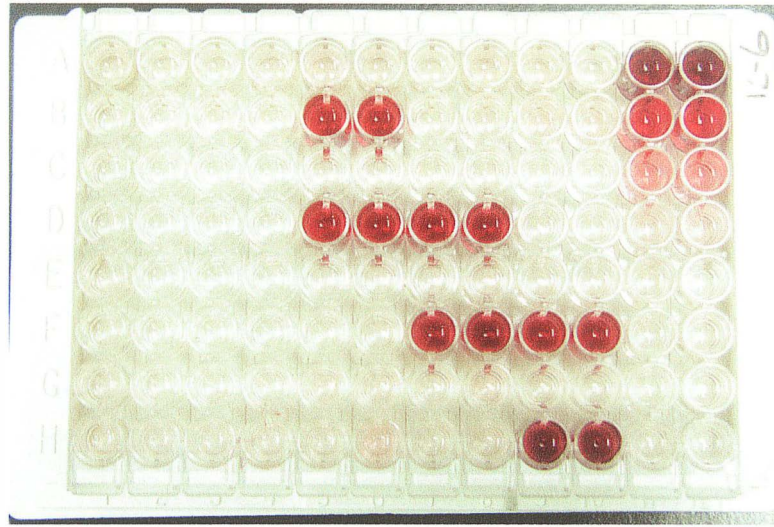


Figure 40. IL-6 ELISA. Supernatants were analyzed for presence of IL-6. The ELISA plate is seen in the upper panel and analyzed data shown in the graph below. Secreted glycoproteins were added at 10ug/mL (10) or 50ug/mL (50). Only LPS, VLPs and to a small extent, VP40-only particles, induce release of IL-6. For all positive samples, IL-6 is detected in supernatants as early as 6 hours post-treatment. All samples were run in duplicate and standard deviations shown by error bars.

(Figure 41)

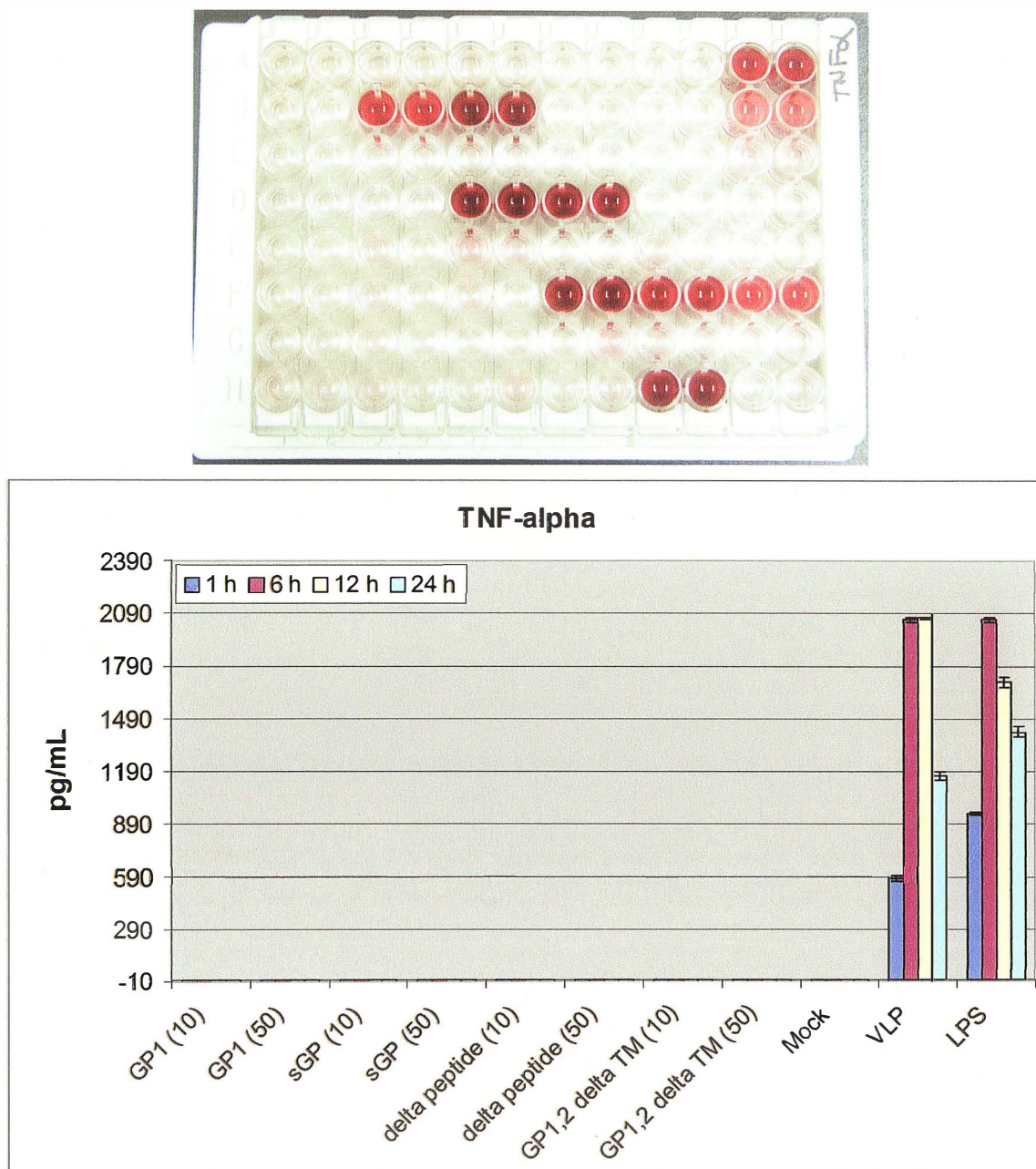


Figure 41. TNF-alpha ELISA. Supernatants were analyzed for presence of TNF-alpha. The ELISA plate is seen in the upper panel and analyzed data shown in the graph below. Secreted glycoproteins were added at 10ug/mL (10) or 50ug/mL (50). Only LPS and VLPs induce release of TNF-alpha. For all positive samples, TNF-alpha is detected in supernatants as early as 6 hours post-treatment. All samples were run in duplicate and standard deviations shown by error bars.

(Figure 42)

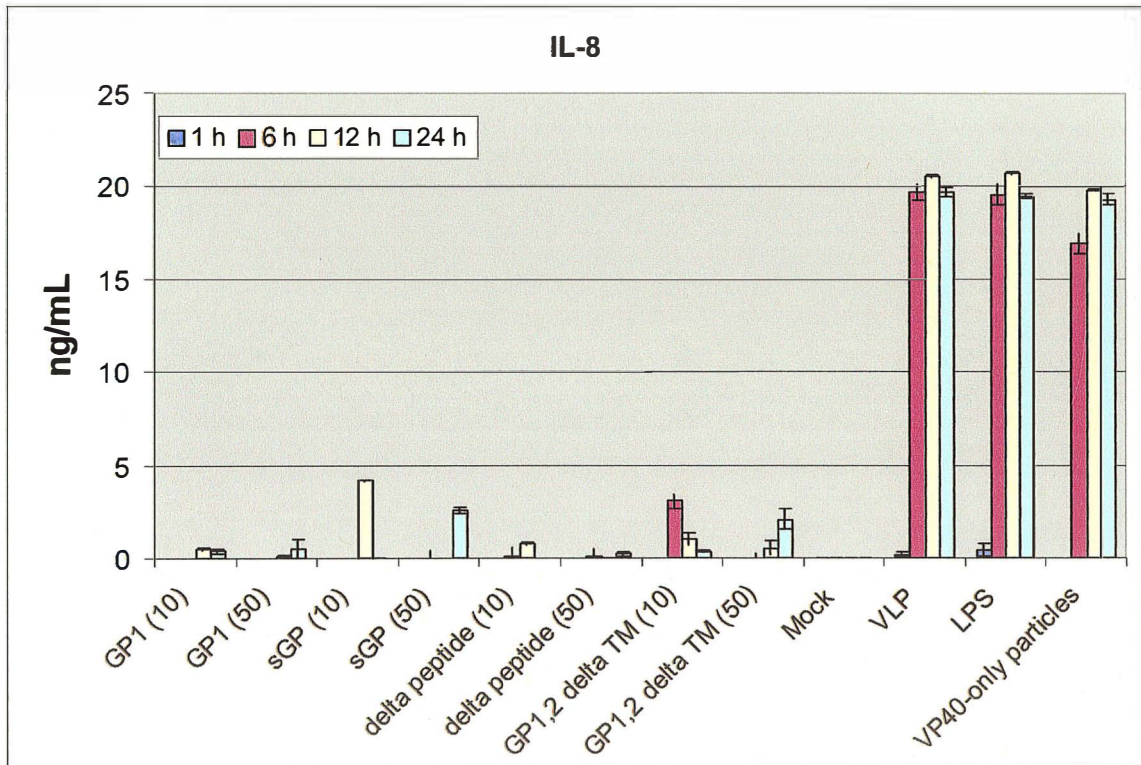
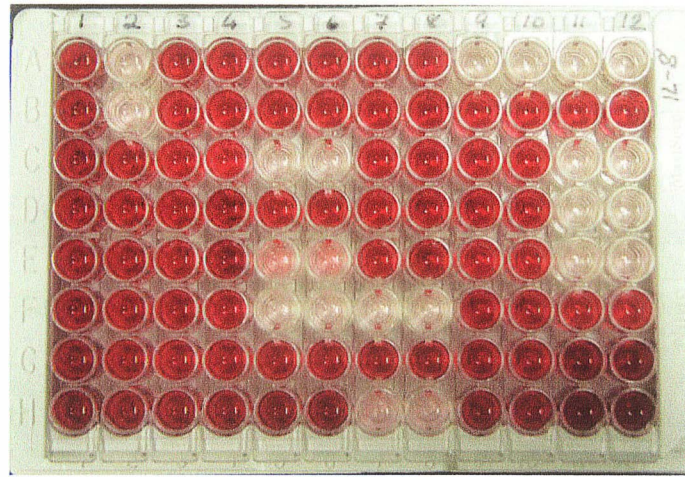


Figure 42. IL-8 EIA. Supernatants were analyzed for presence of IL-8. The EIA plate is seen in the upper panel and analyzed data shown in the graph below. Secreted glycoproteins were added at 10ug/mL (10) or 50ug/mL (50). LPS, VLPs and VP40-only particles induce significant release of IL-8. For all positive samples, IL-8 is detected in supernatants as early as 6 hours post-treatment. All samples were run in duplicate and standard deviations shown by error bars.

3.8 Activation of the endothelium

A prerequisite of leukocyte recruitment into inflamed tissue is the expression of cell adhesion molecules including the selectins, ICAM-1 and VCAM-1 on the surface of endothelial cells. These adhesion molecules function as counter receptors that interact with leukocytes in rolling, firm adhesion and transmigration and have all been shown to be upregulated following filovirus infection in a primate model and *in vitro* (Geisbert et al., 2003d; Schnittler et al., 2004). It has been suggested that the soluble glycoproteins may be involved in the activation of endothelial cell adhesion molecules after their release from infected primary cells (macrophages) (Feldmann et al., 2003; Schnittler et al., 2004; Schnittler and Feldmann, 1999; Schnittler and Feldmann, 2003).

3.8.1 Binding of soluble glycoproteins and VLPs to endothelial cells

The ability of soluble glycoproteins and VLPs to activate the endothelium may be dependent on their ability to bind these cells. Therefore, association of soluble glycoproteins and VLPs to human umbilical vein endothelial cells (HUVEC) was assessed by IFA. Firstly, supernatants of VP40/GP_{1,2} or mock transfected cells were incubated with cells as described in 3.7.1 and cells permeabilized. No specific staining was observed at 4°C, however, VLPs were observed in association with HUVECs at physiological temperature. Specific staining is observed only for VLP treated and not mock treated cells (Figure 43). VLPs appear as filamentous structures in association with HUVECs. Because cells were permeabilized, it is not known whether the particles are simply bound to the surface of HUVECs or internalized. Several attempts were made to demonstrate binding of soluble glycoproteins to HUVECs and binding was not detected.

However, this could potentially be a function of the sensitivity of the IFA or rapid degradation of any internalized protein.

(Figure 43)

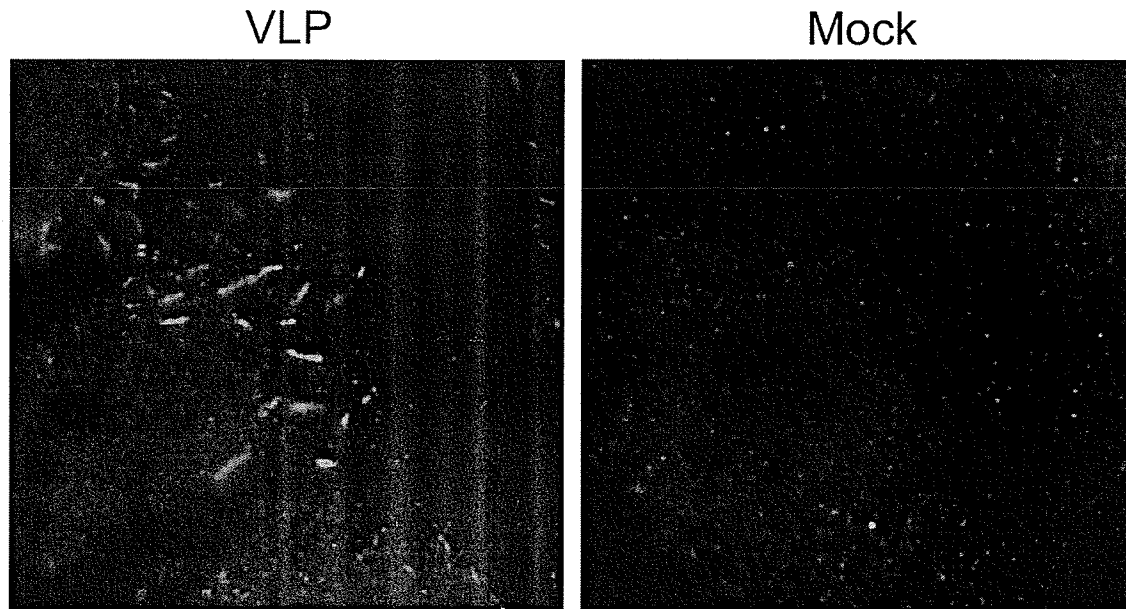


Figure 43. Binding of VLPs to HUVECs. Clarified supernatants of GP1,2 & VP40 transfected cells (A) or mock transfected cell supernatants (B) were applied to human umbilical cord endothelial cells (HUVEC) for 1h at 37C. Cells were permeabilized and stained with anti-ZGP12/1.1 (1:200). Filamentous particles are seen associated with VLP treated cells. Images are 1000x magnification.

3.8.2 Upregulation of endothelial cell adhesion molecules

The role of soluble glycoproteins and purified VLPs on endothelial cell activation was determined by applying samples to human umbilical cord endothelial cells (HUVECs) at concentrations of 10 μ g/mL, 50 μ g/mL and 10 particles per cell, respectively. Activation was monitored on the protein level for all samples at 6, 12 and 24 hours post-treatment. Recombinant human TNF- α (rhTNF- α) was used as a positive control at a concentration of 100ng/mL. Recombinant HA peptide, purified empty pDisplay vector transfected supernatants, and untreated cells were also included as controls. Data for this experiment is summarized in Figures 45-47, however, the reader is

referred to the Appendix for the complete data set. While the soluble glycoproteins failed to activate HUVECs, VLPs demonstrated strong activation as seen in Figures 44-46. VLPs induced E-selectin, ICAM-1 and VCAM-1 upregulation by 6 hours post-treatment (Figure 44) and their expression declined to normal levels over time.

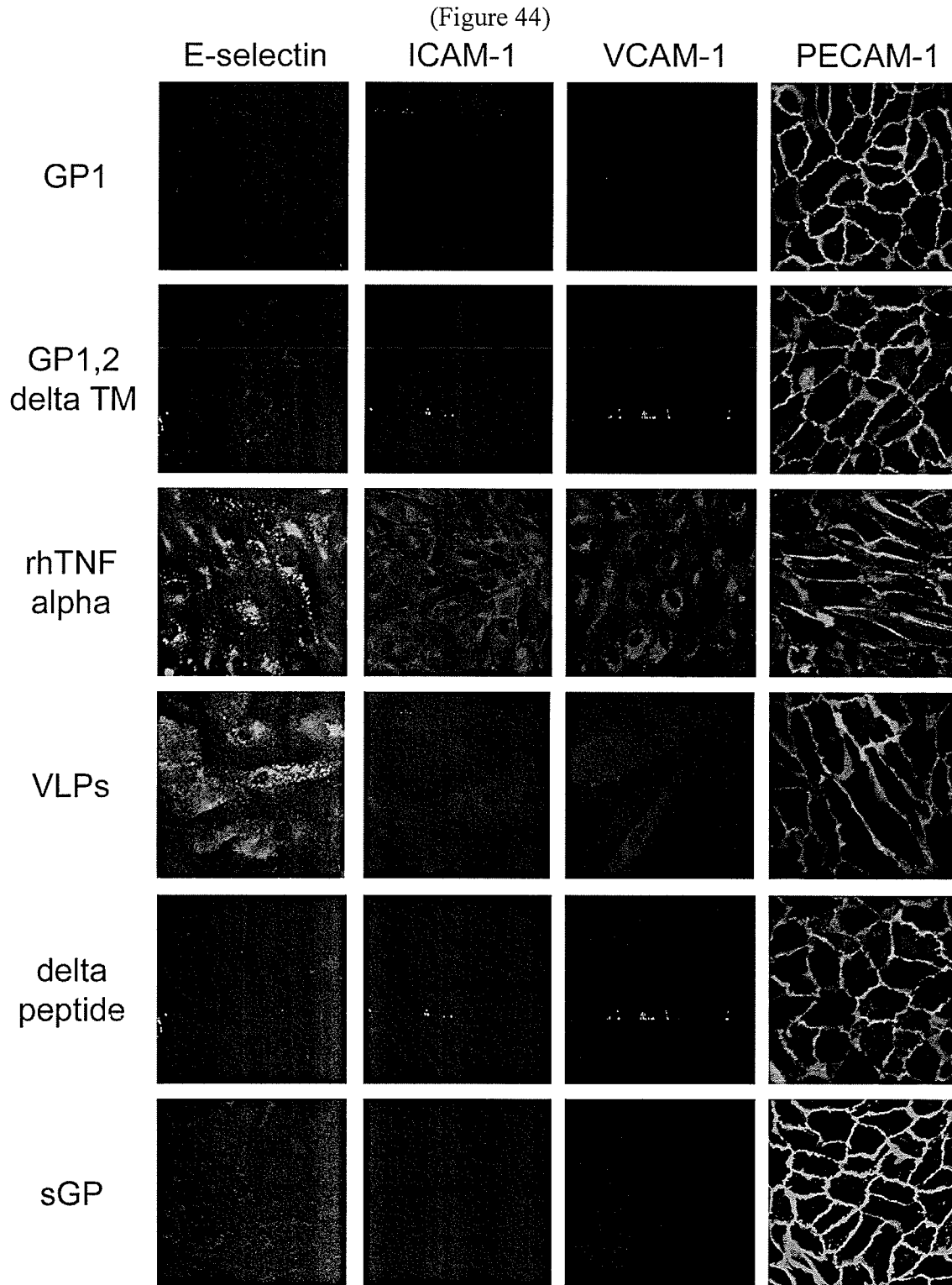


Figure 44. HUVEC activation at 6 h post treatment with soluble glycoproteins and VLPs. HUVECs were treated with 10ug/mL soluble glycoproteins, (100ng/mL) rhTNF-alpha or VLPs (10 particles per cell) at 37C. Cells were fixed at 6 h post treatment and stained with antibodies against E-selectin, ICAM-1, VCAM-1 and PECAM-1 (1:100 for all antibodies). Images are 400x and 1000x (VLPs only) magnification.

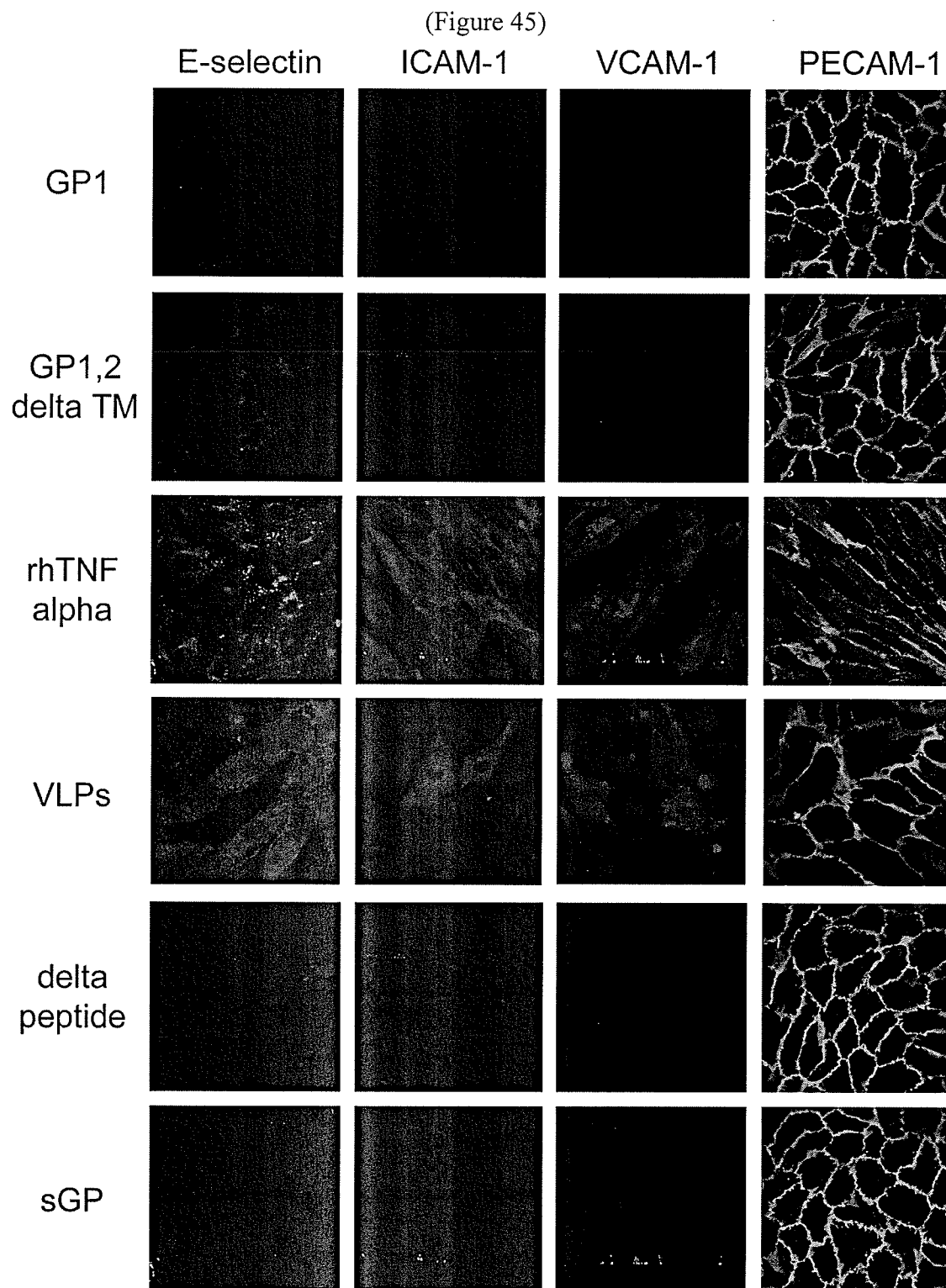


Figure 45. HUVEC activation at 12 h post treatment with soluble glycoproteins and VLPs. HUVECs were treated with 10ug/mL soluble glycoproteins, (100ng/mL) rhTNF-alpha or VLPs (10 particles per cell) at 37C. Cells were fixed at 12 h post treatment and stained with antibodies against E-selectin, ICAM-1, VCAM-1 and PECAM-1 (1:100 for all antibodies). Images are 400x and 1000x (VLPs only) magnification.

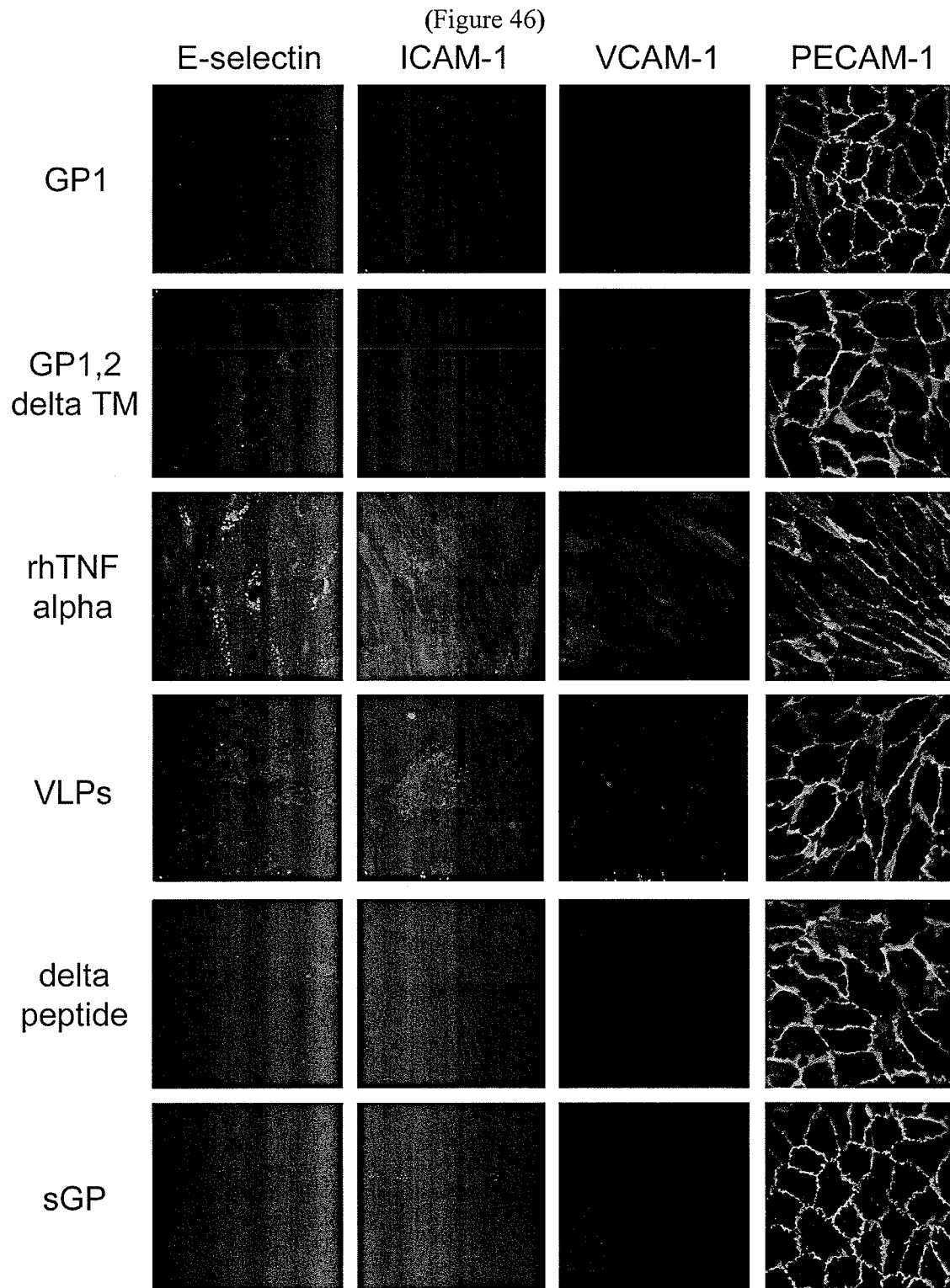


Figure 46. HUVEC activation at 24 h post treatment with soluble glycoproteins and VLPs. HUVECs were treated with 10ug/mL soluble glycoproteins, (100ng/mL) rhTNF-alpha or VLPs (10 particles per cell) at 37C. Cells were fixed at 24 h post treatment and stained with antibodies against E-selectin, ICAM-1, VCAM-1 and PECAM-1 (1:100 for all antibodies). Images are 400x and 1000x (VLPs only) magnification.

3.8.2 Analysis of VE-cadherin and actin distribution following treatment with soluble glycoproteins and VLPs

Previous studies have shown that the adherens junction protein, VE-cadherin, is rearranged following treatment with supernatants of filovirus-infected monocytes/macrophages and that this rearrangement may contribute towards enhanced endothelial cell permeability since adherens junctions normally restrict uncontrolled solute exchange in a paracellular manner (Feldmann et al., 1996; Schnittler et al., 2004). Similarly, activation of the actin filament system was also associated with filovirus infection and may further contribute to increased permeability (Schnittler et al., 2004). In order to assess the role of soluble and particle-associated glycoproteins in these events, HUVECs were treated with soluble glycoproteins at concentrations of 10µg/mL and 50µg/mL or with VLPs (10 particles/cell). All samples were analyzed at 24 hours post-treatment by immunofluorescence for redistribution of the adherens junction protein, VE-cadherin, using a monoclonal antibody to VE-cadherin. Rhodamine labelled phalloidin was used to stain cellular actin. The soluble glycoproteins did not alter the distribution of neither VE-cadherin, nor actin. VE-cadherin superstructures, characteristic continuous and netlike structures found in non-permeabilized adherens junctions (Geyer et al., 1999), are evident in all soluble glycoprotein-treated samples. Interestingly, VLPs induced formation of actin stress fibers, however, distribution of VE-cadherin remained unchanged. Figure 47 demonstrates data with GP₁ shown as representative data acquired for all soluble glycoproteins. A comprehensive collection of supporting data is shown in Appendix section E.

(Figure 47)

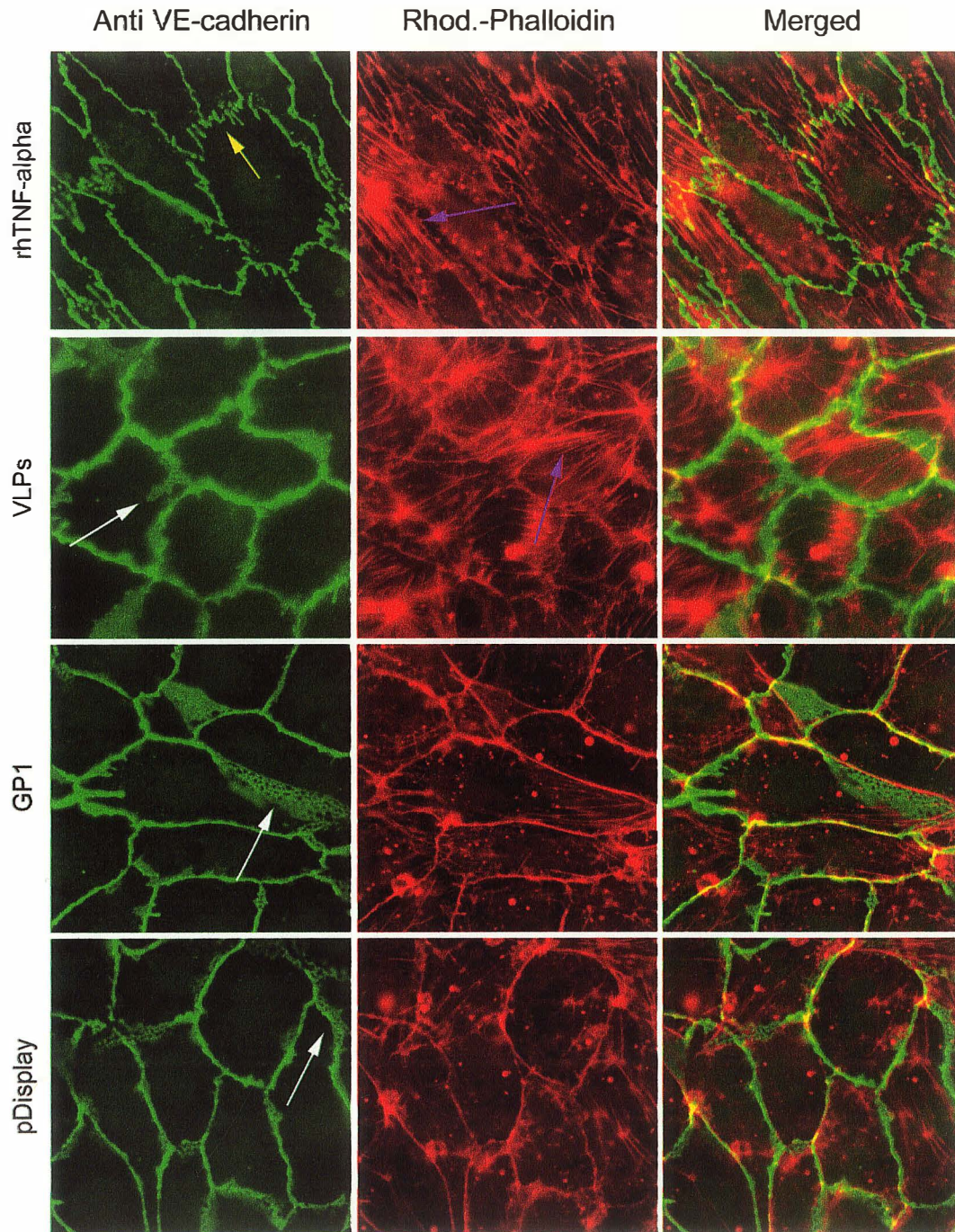


Figure 47. VE-cadherin and actin IFAs. HUVECs were treated with rhTNF-alpha (100ng/mL), VLPs ('moi' 10), GP1 (50ug/mL) or pDisplay negative control for 24 h. Cells were fixed, permeabilized and stained with anti VE-cadherin (1:100) or Rhodamine labelled phalloidin (Rhod.-Phalloidin; 1:400). Arrows highlight VE-cadherin superstructures (white), rearrangement of VE-cadherin (yellow) and actin stress fiber formation (purple). Images were acquired at 400x magnification. Merged images are shown to highlight distribution of actin within individual cells.

3.8.3 Analysis of transendothelial electrical resistance (TER)

Previous studies by Feldmann *et al* demonstrated increased permeability of HUVEC monolayers following treatment with supernatants of MARV-infected monocytes/macrophages (Feldmann *et al.*, 1996). While TNF- α was implicated as a major mediator of this permeability change, the role of soluble glycoproteins could not be excluded. Additionally, the soluble glycoproteins of ZEBOV have received considerable attention as potential mediators of endothelial cell activation and permeability change. Since the initial studies of Feldmann *et al* a more sophisticated method of measuring endothelial cell permeability has been described and has the distinct advantage of measuring changes as small as 2% and in real time (Seebach *et al.*, 2000). Impedance spectroscopy was therefore utilized to test the role of the various glycoproteins in endothelial cell permeability changes. HUVECs were seeded into impedance spectroscopy slides as described in materials and methods and treated with soluble glycoproteins or VLPs. Impedance spectra were monitored in real time and data normalized (TER/TER₀). At the termination of all experiments EDTA was added to wells to control for the ability of cells to experience a drop in TER. In all cases, a drop in TER was observed. All experiments were performed a minimum of 3 times or as otherwise noted in graphs.

Barrier function was not affected by controls (pDisplay, HA peptide or mock supernatants for VLPs) as seen in Figures 48 through 53. When administered at 10 μ g/mL, none of the secreted glycoproteins had long-term deleterious effects on TER as seen in a compiled graph in Figure 48. However, both GP₁ and sGP demonstrated a transient decrease in TER during the first 2 hours of the experiment, after which time the

barrier function was restored (Figures 49 and 51). No decrease was observed for delta peptide or GP_{1,2}ΔTM at any time (Figures 50 and 52). Interestingly, high concentrations of GP₁ (50μg/mL) led to a long-term decrease in TER with a total decrease of approximately 35% (Figure 51). To ascertain whether the ability of GP₁ to decrease barrier function was dependent on trimerization of the protein the mutant GP₁-C53G, which is expressed predominantly in monomeric form, was analyzed. Indeed, this mutant did not alter the barrier function thereby suggesting that conformation of GP₁ is important for its effect on TER (Figure 51). Finally, HUVECs were treated with VLPs and as seen in Figure 53, these purified particles decreased TER by 17% over the course of the experiment.

While sGP did not alter the barrier function of HUVECs, I speculated that it might have a cumulative effect when used in conjunction with TNF-α. The rationale for this hypothesis is that both TNF-α and sGP are produced during viral infection and are therefore available to interact with each other and with the endothelium. In order to determine if sGP may enhance or even reduce the effect on rhTNF-α treated HUVECs, cells were first treated with increasing doses of rhTNF-α (Figure 54) to determine baseline effects of this cytokine. Amounts as low as 100pg/mL caused decreases in TER. Once the baseline effects of rhTNF-α were established, cells were treated with 10μg/mL of sGP and either 1ng/mL, 100pg/mL or 10pg/mL of rhTNF-α. Interestingly, sGP had no additive effects on rhTNF-α decreases in barrier function, however, this protein either partially (100pg/mL rhTNF-α) or completely (1ng/mL rhTNF-α) restored HUVEC barrier function (Figure 55).

(Figure 48)

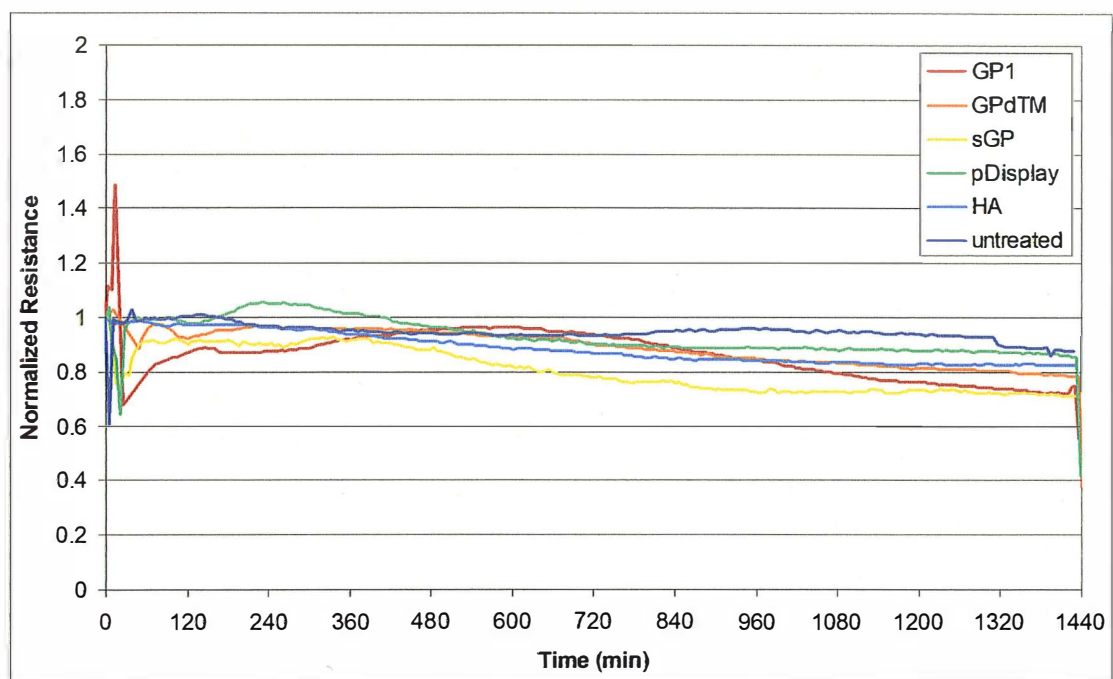


Figure 48. TER results of HUVECs treated with 10ug/mL of soluble glycoproteins. HUVECs were treated with 10ug/mL soluble glycoproteins and impedance spectra monitored over time. Control wells were treated with an equimolar amount of HA peptide as control. No significant long-term changes in TER are observed.

(Figure 49)

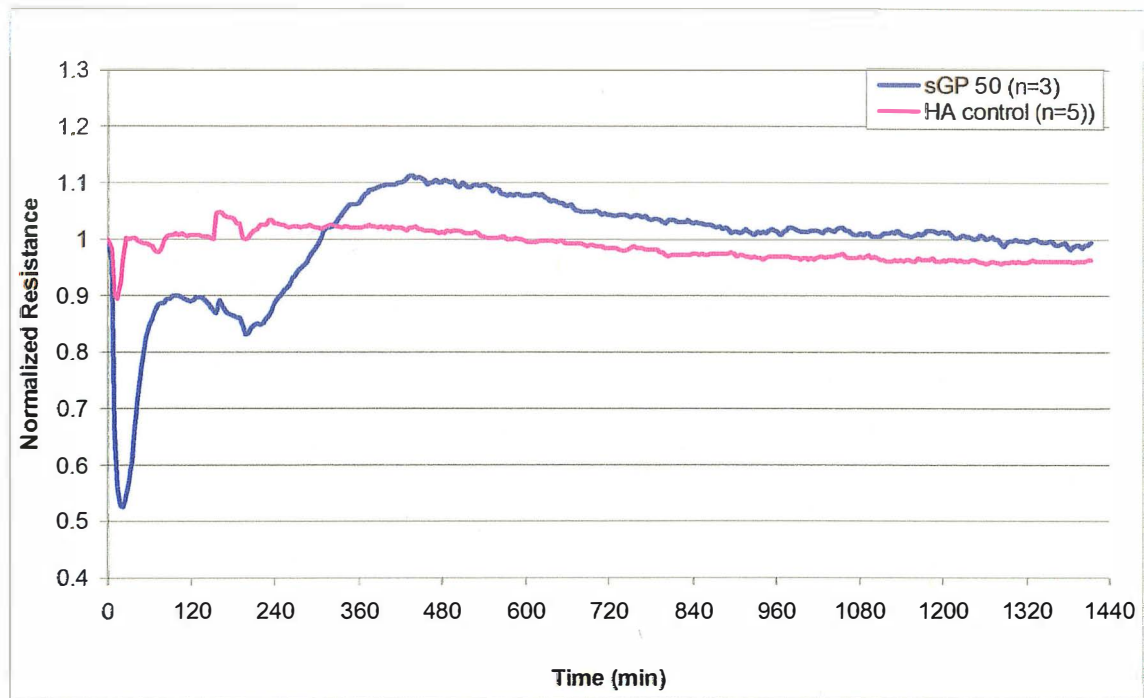


Figure 49. Impedance spectroscopy. HUVECs were treated with 50ug/mL sGP and impedance spectra monitored over time. Control wells were treated with an equimolar amount of HA peptide. An initial drop is observed for sGP in the first 2 h then recovers.

(Figure 50)

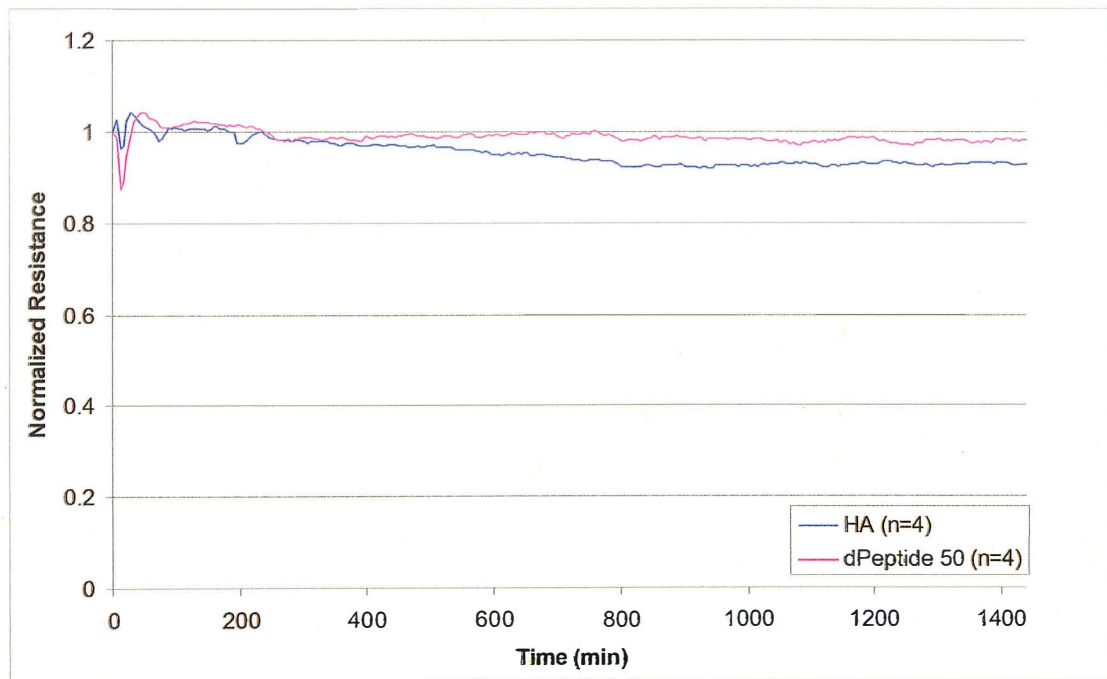


Figure 50. Impedance spectroscopy. HUVECs were treated with 50ug/mL delta peptide and impedance spectra monitored over time. Control wells were treated with an equimolar amount of HA peptide. No significant change in TER is seen over time.

(Figure 51)

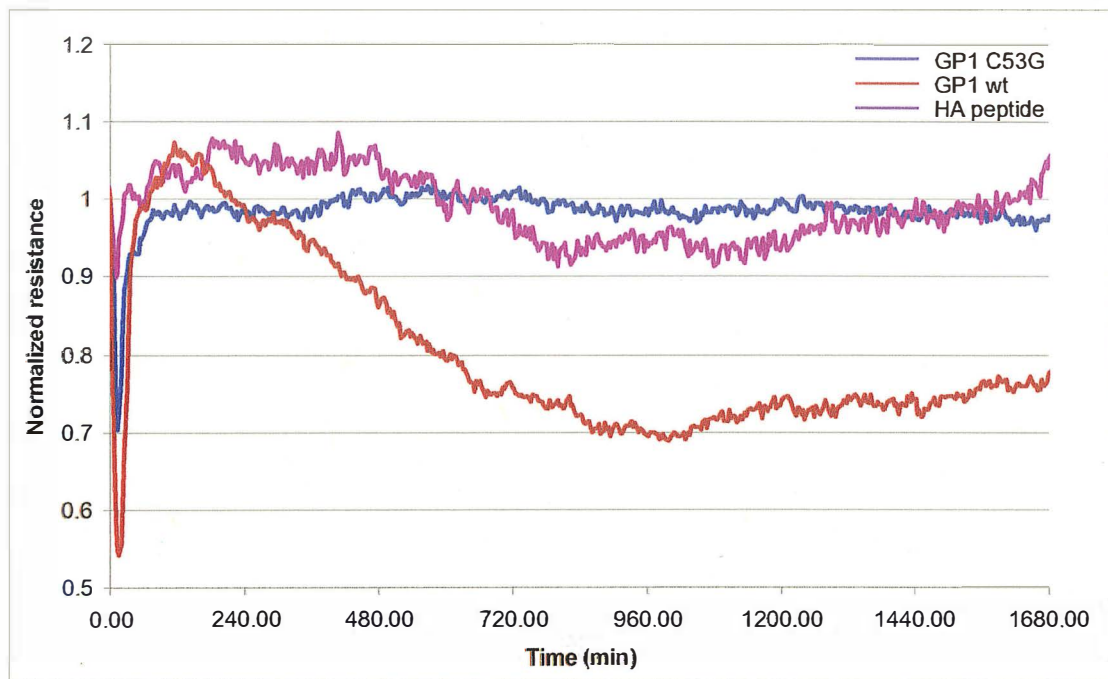


Figure 51. Impedance spectroscopy. HUVECs were treated with 50ug/mL GP1 wt or GP1-C53G mutant and impedance spectra monitored over time. Control wells were treated with an equimolar amount of HA peptide. An initial drop is observed for GP1 wt and C53G in the first 2 h then recovers. GP1 exhibits a significant long-term decrease in TER as compared to C53G mutant and HA peptide control.

(Figure 52)

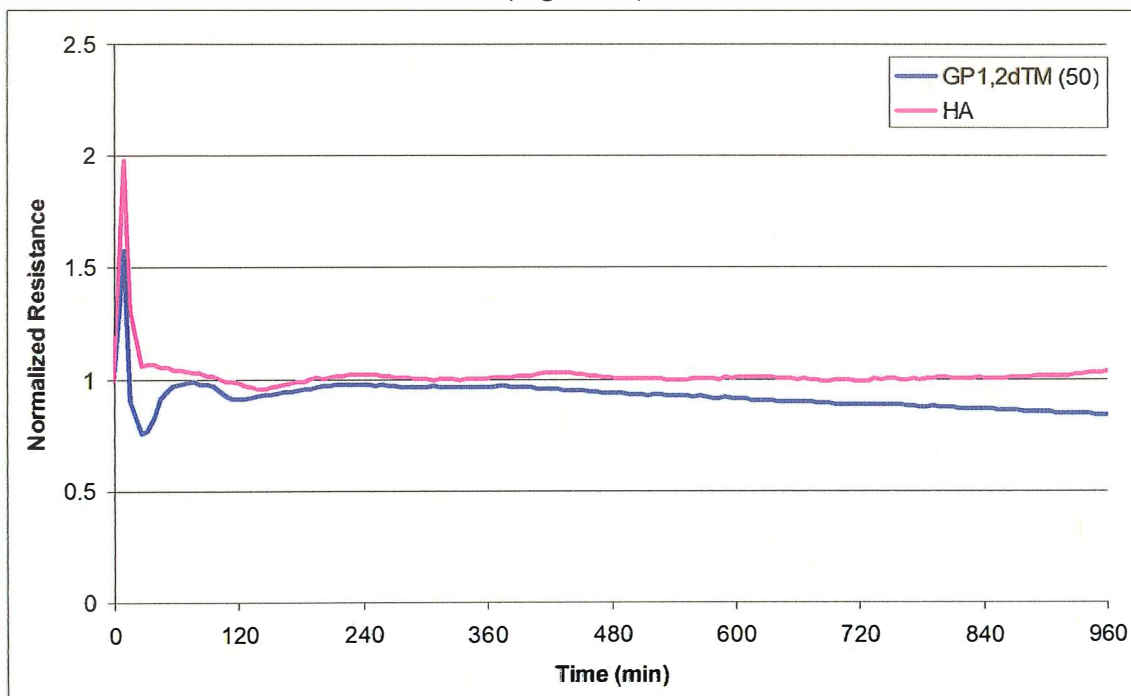


Figure 52. Impedance spectroscopy. HUVECs were treated with 50ug/mL GP1,2deltaTM and impedance spectra monitored over time. Control wells were treated with an equimolar amount of HA peptide. No significant changes are observed.

(Figure 53)

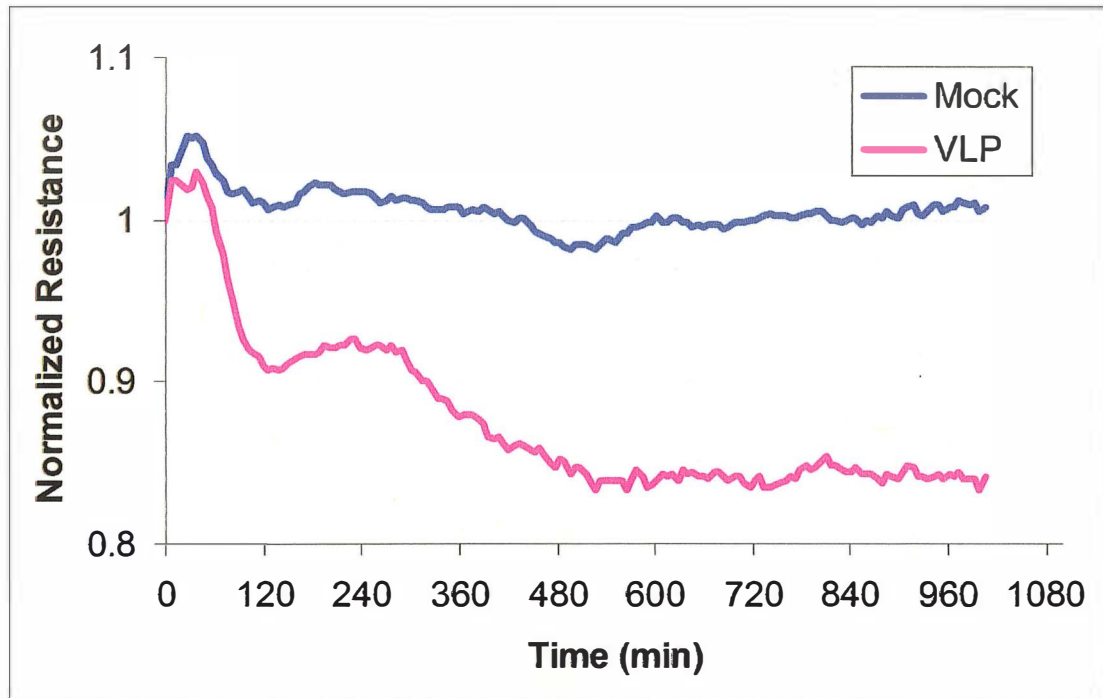


Figure 53. Impedance spectroscopy. HUVECs were treated with VLPs (10 particles/cell) and impedance spectra monitored over time. An equal volume of purified supernatants from mock transfected cells is included as a negative control. A drop of 17% in TER is seen for VLP treated HUVECs.

(Figure 54)

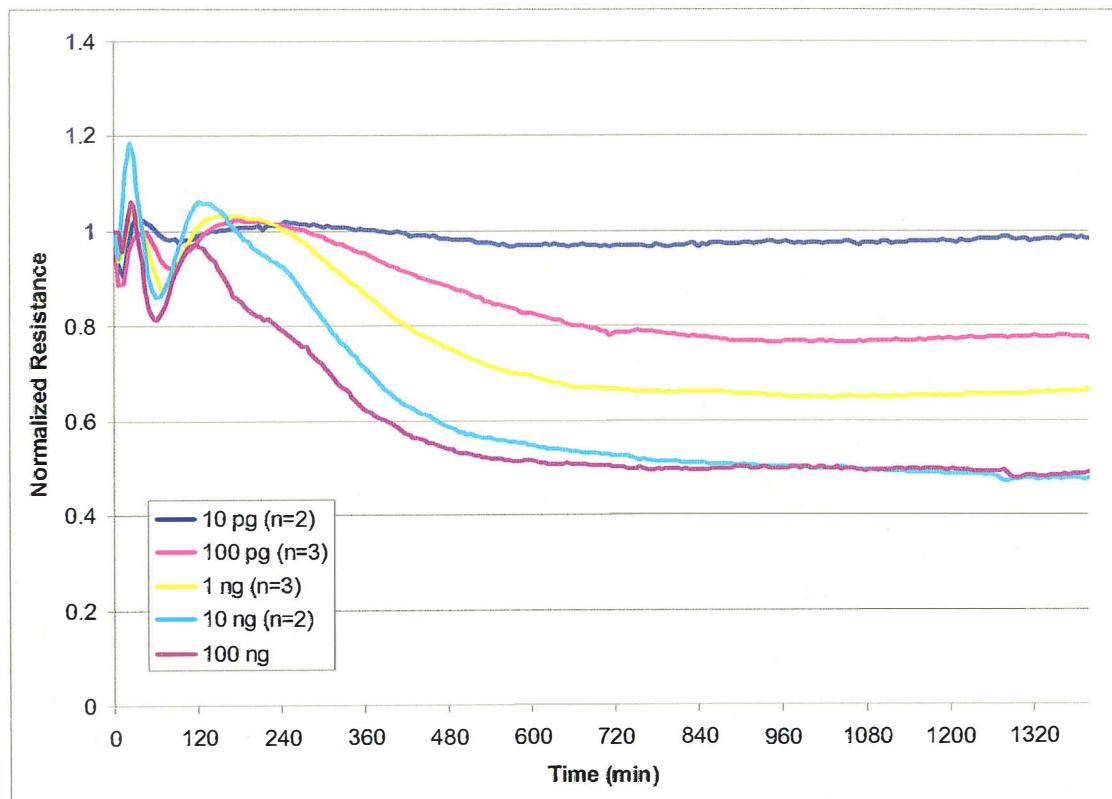


Figure 54. Impedance spectroscopy. HUVECs were treated with increasing amounts of rhTNF-alpha. A dose-dependent decrease in barrier function is observed.

(Figure 55)

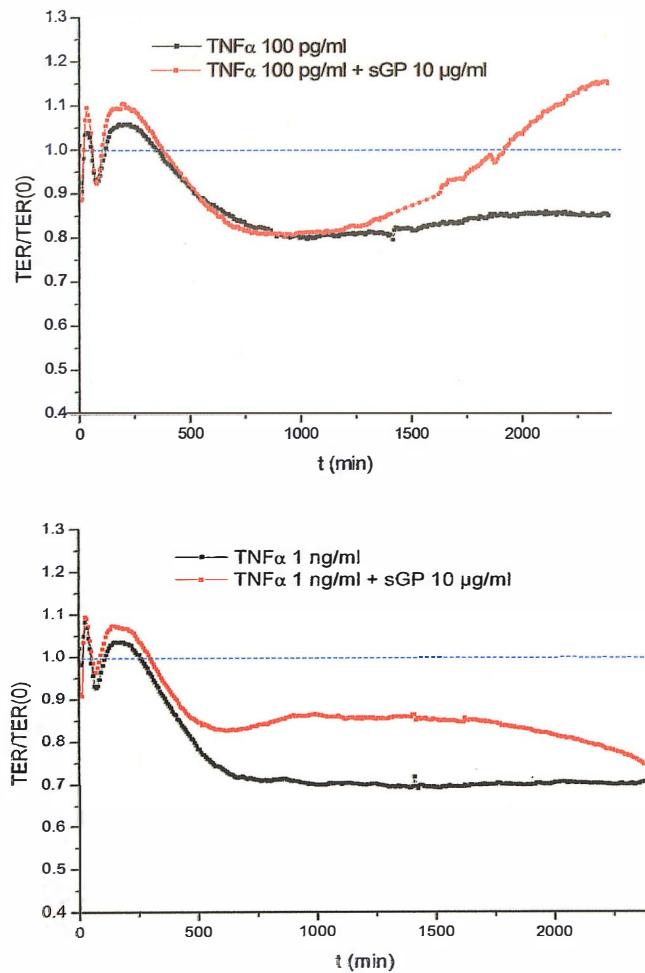


Figure 55. Protective effect of sGP. HUVECs were treated with sGP (10 μ g/mL) and/or rhTNF-alpha (100 μ g/mL, upper panel; 1ng/mL, lower panel) and impedance spectra recorded. sGP restores barrier function completely (upper panel) or partially (lower panel).

4.0 Discussion

4.1 Project Background

Ebola virus is a member of the order *Mononegavirales* that includes other non-segmented, RNA viruses of negative polarity. The filovirus genome contains seven genes which encode seven structural proteins (Feldmann, 2004; Kiley, Regnery, and Johnson, 1980). The reader is referred to Chapter 1.5 for a more detailed description regarding the structure and proposed functions of these proteins. Whilst all viral proteins may play a role in pathogenesis, during the past 5-10 years a great deal of attention has been given to the viral glycoprotein products. Much of the work has focused on GP_{1,2}, however, those studies involving the soluble glycoproteins focused largely on their identification, mechanism of production (transcription) and finally, their oligomerization and glycosylation (summarized in Volchkov *et al.*, 2004). The only studies to date that specifically investigated the role of soluble glycoproteins in pathogenesis reported that sGP may bind to neutrophils through CD16b, the neutrophil-specific form of the Fc gamma receptor III (Yang *et al.*, 1998), although this point has been challenged (Maruyama *et al.*, 1998; Sui and Marasco, 2002). Chan *et al* reported that expression of ZEBOV GP_{1,2} in 293T cells caused significant levels of cellular detachment in the absence of cell death or virus replication while sGP did not have this effect (Chan, Ma, and Goldsmith, 2000). In many of these studies sGP was produced either by a pseudotype system or in the case of the study by Yang *et al*, a mammalian system, although protein was not purified nor the concentration determined. Finally, an antibody decoy role of sGP has been hypothesized but not yet determined experimentally (Feldmann *et al.*, 2003).

The role of EBOV secreted glycoproteins in the pathogenesis of EBOV hemorrhagic fever (EHF) has been a point of speculation and controversy since their discovery. Virus-infected cells produce these proteins abundantly in tissue culture and sGP has also been detected in the blood of infected patients (Sanchez et al., 1999; Sanchez et al., 1996; Sanchez et al., 1998b; Volchkov et al., 1998b). Once released, these proteins are free to interact with host cells including cells of the mononuclear phagocytic system and the endothelium. Studies regarding the interaction of these proteins with host cells and their role in pathogenesis have largely been hampered due to an inability to biosynthesize large quantities of protein that remain authentic to those seen during a natural virus infection. Heavy glycosylation and post-translational modifications limit the use of less expensive and more conventional methods of synthesis such as bacterial or yeast systems. While viral vectors such as VSV are efficient (as shown in this study), the inherent cytotoxicity of VSV makes it suboptimal. An additional obstacle for recombinant secreted glycoprotein detection and purification is the lack of antibodies specific for these proteins, particularly for Δ peptide.

The hypothesis of this project was that the soluble and particle-associated glycoproteins of EBOV will act as pathogenic determinants during infection and will contribute towards disease development. In order to study the effects of the glycoproteins on target cells, the first goal of this project was to biosynthesize the secreted glycoproteins and virus-like particles using a mammalian expression system. Specific aspects of macrophage and endothelial cell activation would then be tested. While previous studies were suggestive of a potential role of glycoproteins in activation of both macrophages and endothelial cells (Feldmann et al., 1996; Stroher et al., 2001),

this study was the first to directly address the role of exogenous soluble and membrane-associated glycoproteins on target cell activation.

4.2 Biosynthesis of soluble glycoproteins and VLPs

The commercial vector, pDisplay, was chosen as the expression vector for all the soluble glycoproteins and the cloning strategy is shown in Figures 7 and 15. This vector was optimal since it already contained an N-terminal signal peptide. All the soluble glycoproteins must be properly processed, however, in some cases such as Δ peptide, the coding sequence of the protein was not adjacent to the signal peptide since it is a product of proteolytic cleavage (Volchkov et al., 1998a). Therefore, a signal peptide had to be engineered into the vector or primer so the protein would be shuttled through the secretory pathway. Since pDisplay has its own signal peptide, it was used for all the soluble glycoproteins. Immediately downstream of the signal peptide, this vector encodes a nonapeptide sequence of influenza HA that is expressed on the N-terminal portion of all the secreted glycoproteins. This epitope tag was used both for detection of the glycoproteins as well as subsequent immuno-affinity purification. Following the multiple cloning site, pDisplay also possesses a *myc* tag and a transmembrane domain. To avoid expression of these domains, the reverse primers for all soluble glycoproteins were engineered with sequences encoding two consecutive stop codons. Therefore, all proteins would be shuttled through the secretory pathway, have an N-terminal HA epitope tag incorporated and finally, be secreted from transfected cells.

An alternative method of protein production was also explored. Recombinant vesicular stomatitis virus (VSV) encoding GP₁ of MARV between VSV G and M was generated (Figures 10-13). MARV GP₁ was chosen preferentially to EBOV because at

the time of construction better molecular and immunological tools existed for MARV within our lab. Despite high levels of protein production (Figures 11-12) this system was not further pursued because of the inherent cytotoxicity of VSV M (Kopecky and Lyles, 2003). Specifically, infected cells may produce VSV-mediated cytokines or other soluble factors which would interfere with downstream functional studies. The recombinant virus was, however, useful in a collaborative study that investigated the utility of recombinant VSVs as potential vaccine candidates (Garbutt et al., 2004).

The strategy for expressing full-length GP_{1,2} and VP40 for VLP production was slightly different. In a publication by Noda *et al* the authors expressed these proteins using the eukaryotic expression vector pCAGGS (Noda et al., 2002). This vector contains a chicken beta-actin promoter which typically yields higher levels of expression than CMV or T7 promoters (Niwa, Yamamura, and Miyazaki, 1991). Because the vector contains the SV40 origin of replication and the 293T cells express the large T antigen, episomal replication of the plasmid is possible and facilitates high expression rates. Unlike the soluble glycoproteins, an epitope tag was not necessary since antibodies to GP_{1,2} and VP40 were available. Additionally, purification of VLPs could easily be performed using simple ultracentrifugation methods.

The first major challenge in this study was to produce the soluble glycoproteins in relatively high quantities. Based on results with rVSV and transient transfection the later was chosen as the method of biosynthesis, however, the exact method of transfection and cell line had to be determined experimentally. Using FuGENE6 and 293T cells, transfection efficiencies of approximately 80-85% could be achieved. Because a large amount of recombinant protein would be required for functional studies these initial

transfection optimization studies were critical to maximized protein output. Transfections were then scaled-up from 2cm² wells to 500cm² flasks. One critical point for maintaining high efficiency was that the DNA-FuGENE6 complexes must not be prepared in more than 20% of the total volume of medium that the cells would be incubated in. The remaining 80% of medium is added to the cells and after the transfection complexes formed they were added to the rest of the medium on the cells. The smaller volume contributes to increased interaction between the DNA and transfection reagent. Using optimized transfection and purification methods (as described in Materials and Methods) large quantities of all proteins and VLPs were produced (Table 7 and Figure 21)

4.3 Characterization of soluble glycoproteins

The soluble glycoproteins used in these studies were analyzed for proper glycosylation and oligomerization and the results compared to previously published data (Feldmann, 2004; Sanchez et al., 1998b; Volchkov, 1999; Volchkova et al., 1998; Volchkova, Klenk, and Volchkov, 1999). Of all the soluble glycoproteins sGP is the most well characterized in terms of its oligomeric structure (Sanchez et al., 1998b; Volchkova et al., 1998). The mature protein is secreted as a homodimer in anti-parallel orientation. Often the conformation of a protein will be critical for its proper biological function. Examples of this include necessity of trimers for fusogenic potential of membrane glycoproteins such as HIV gp160, retroviral Env proteins and influenza virus hemagglutinin (Dutch, Jardetzky, and Lamb, 2000). It is critical to analyze the protein following purification to ensure that manipulation did not induce alterations in conformation. Indeed, sGP maintained its dimeric conformation as seen in Figure 23.

The protein was easily visualized by western blot as well as less sensitive methods such as silver staining and finally coomassie staining.

Following cleavage of pre-sGP a smaller cleavage product designated Δ peptide is released. Volchkova *et al* (Volchkova, Klenk, and Volchkov, 1999) have previously reported that secretion of Δ peptide appears to be less efficient than for sGP. This study confirmed that result, as total yields of Δ peptide were consistently lower than sGP. The conformation of Δ peptide was also in agreement with previous results by Volchkova *et al* as seen in Figure 23.

The two soluble forms of the full-length glycoprotein, GP_{1,2} Δ TM and GP₁, were analyzed for their oligomerization. Soluble GP₁ was first described by Volchkov *et al* when GP₁ was found released into culture medium of HeLa cells (Volchkov *et al.*, 1998b). The critical linkage between GP₁ and GP₂ has been hypothesized to occur between cysteines 53 in GP₁ and 609 in GP₂ (Sanchez, 2001). Recently, Jeffers *et al* demonstrated the role of cysteine 53 in this disulfide bridging, however, the binding partner could not be completely elucidated although the authors speculate that it must be cysteine 609 based on similarities to avian retroviruses (Jeffers, Sanders, and Sanchez, 2002). Based on these data, I expected that expression of GP_{1,2} Δ TM would result in formation of trimers as reported by Dolnik *et al* (Dolnik *et al.*, 2004) and GP₁ would most likely be expressed as monomers in the absence of GP₂, although no one had previously shown if GP₁ occurred as monomers or multimers. Using my established expression system, GP_{1,2} Δ TM and GP₁ were consistently produced as oligomers similar to full-length GP_{1,2}, thereby suggesting formation of trimers (Figure 24). Interestingly, GP₁

appeared to preferentially form trimers and monomers with dimers most likely occurring as a transient intermediate form.

The ability of GP₁ to form oligomeric structures in the absence of GP₂ was an interesting finding worthy of further investigation. Cysteine 53 is critical for multimer formation since its mutation resulted in exclusive expression of monomers (Figure 25). Therefore, cysteine 53 plays a critical role in disulfide bonding of sGP (Volchkova et al., 1998), full-length GP_{1,2} (Jeffers, Sanders, and Sanchez, 2002), and finally, GP₁ as demonstrated in these studies. It was also interesting to note that mutation of cysteines 108, 121, 135 and 147 all resulted in dramatic decrease in secretion of GP₁. Similar results were reported with mutation of these cysteines in sGP and the authors speculated that those mutations most likely cause improper folding of the protein, thereby targeting it to the degradative pathway (Volchkova et al., 1998).

The popular conception regarding GP_{1,2} trimer formation is that GP₂ mediates trimerization (Sanchez, 2001). The results of this study are somewhat contradictory to this hypothesis, therefore, I investigated if GP₂ would form trimers independently of GP₁. GP₂ can clearly form oligomers in the absence of GP₁ (Figure 26), however, no single cysteine was critical for multimer formation (Figure 27). Taken together with data obtained from GP₁ cysteine 53 is critical, however, cysteines in GP₂ may somehow compensate for each other, particularly cysteines 601, 608 and 609. Alternatively, non-covalent bonding through ionic, hydrogen or hydrophobic bonding may contribute substantially to the multimer formation observed for these proteins, an idea that needs further investigation.

Filovirus glycoproteins mature during their export through the exocytotic transport route where co- and post-translational modifications, including removal of the signal peptide, oligomerization and N-linked glycosylation, occurs in the endoplasmic reticulum (ER) (Becker, Klenk, and Muhlberger, 1996; Feldmann et al., 1994; Feldmann et al., 1991; Sanchez et al., 1998b; Volchkov et al., 1995; Will et al., 1993). N-glycans are trimmed back and matured in the Golgi apparatus where O-glycosylation also occurs (Becker, Klenk, and Muhlberger, 1996; Feldmann et al., 1994; Feldmann et al., 1991; Geyer et al., 1992; Volchkov et al., 1995; Will et al., 1993). O-linked glycosylation is believed to be a rate-limiting step in glycoprotein transport (Jeffers, Sanders, and Sanchez, 2002). Glycosylation of full-length GP_{1,2}, particularly with respect to the mucin-like domain in GP₁, is thought to play a significant role in the function of this protein. Indeed, other groups have reported that when O-linked sugars were removed there was a reduction in cytopathic effects resulting from GP_{1,2} expression (Volchkov et al., 2001; Yang et al., 2000). Additionally, a reduction in the loss of adherence of GP-expressing cells (Chan, Ma, and Goldsmith, 2000; Simmons et al., 2002) was also observed. All the purified soluble glycoproteins produced in these studies were analyzed for their glycosylation and results were consistent with current data in the literature (Figure 28) (Volchkov, 1999).

4.4 Characterization of VLPs

Expression of VLPs was first confirmed by Western blot analysis (Figure 29). Clarified supernatants of GP_{1,2} and VP40 transfected cells were positive for both proteins. While this result was promising, the formation of virus-like particles was important for future studies. Previous groups have reported that expression of VP40 alone will result in

filamentous particles (Noda et al., 2002), while GP_{1,2} expressed on its own will form membranous blebs that are studded with glycoprotein (Bavari et al., 2002; Noda et al., 2002; Volchkov et al., 1998b). To confirm whether these two membrane proteins assembled into VLPs transmission electron microscopy was utilized to scan supernatants for filamentous particles with GP_{1,2}. As expected, VLPs were visualized (Figure 30). VLPs were also confirmed by immunofluorescence assay (IFA) microscopy of transfected cells (Figure 32). A unique staining pattern reminiscent of filamentous structures were observed over the surface of 293T cells. The ability to detect VLPs by IFA was later applied to binding studies to determine if VLPs bound to human macrophages and/or endothelial cells. Following incubations under physiological conditions, VLPs were detected in close association with these cells (Figures 35 and 43).

For the purposes of comparison in functional studies using soluble glycoproteins, it was desirable for VLPs to be purified and resuspended in the same buffer as soluble glycoproteins (“equilibration buffer”). Bavari *et al* described a method of purification relying on gradient sucrose cushions to purify VLPs. Based on methods already in place in our group, I decided to purify the VLPs in these studies using a single 20% sucrose cushion (VLPs will pellet), followed by a washing step after which VLPs are again pelleted. To ensure that the structure of VLPs remained intact the particles were viewed by TEM under high magnification (200,000X) and the morphology was identical to VLPs pre-purification (Figure 30D). Purified particles were also used in immunogold TEM studies to confirm expression of GP_{1,2} on the surface of particles (Figure 33) and for atomic force microscopy studies (Figure 34). In all cases, VLPs appear virtually identical to previously published images of wildtype ZEBOV (Geisbert and Jahrling, 1995). This

observation suggests that VLPs are a useful tool for studying initial interactions of ZEBOV with target cells. The ability of VLPs to bind macrophages and endothelial cells provides the first evidence that VLPs have the same binding specificity as live ZEBOV. The benefit of using VLPs over inactivated virus for studying events independent of virus replication is that less manipulation (freeze-thawing, side effects of inactivation, etc.) of the particles is performed. Any effects induced by VLPs can be attributed to GP_{1,2} and/or VP40. Additionally, certain methods such as impedance spectroscopy are not possible to perform under high bio-containment. The use of VLPs circumvents this obstacle. Finally, while previous studies have used pseudotyped systems such as retroviruses, adenoviruses or VSV (Medina et al., 2003; Takada et al., 1997; Wool-Lewis and Bates, 1998; Yang et al., 2000), if the unique morphology of filovirus particles contributes to potent immune stimulation, these systems may not accurately represent a natural scenario.

4.5 Activation of human macrophages

In contrast to another report which did not find macrophage activation with gamma-irradiated, inactivated ZEBOV (Hensley et al., 2002), previous studies by our group have reported that UV-inactivated viral stocks could induce expression of several key cytokines when applied to human monocytes and macrophages (Stroher et al., 2001). This observation led to the hypothesis that viral replication was not a prerequisite for activation and that secreted glycoproteins, also present in viral stocks, may contribute to the activation (Feldmann et al., 2001). Surprisingly, none of the secreted glycoproteins, even at high concentrations, were able to activate macrophages as demonstrated in this study (Figures 36-42). However, this is the first report of purified VLPs, in the absence

of other soluble factors (including viral secreted glycoproteins) to be sufficient for activation. Additionally, these data suggest that only GP_{1,2} and VP40 are necessary for activation. Interestingly, “VP40-only” particles are able to induce low level of macrophage activation but that addition of GP_{1,2} in VLPs greatly enhances the effect. This may be due to introduction of foreign membranes to macrophages which triggers a non-specific activation, although the exact mechanism for the activation with GP_{1,2}-deficient VLPs has not been tested in this study and requires further investigation.

In terms of cytokine protein expression, levels of soluble cytokines expressed by UV-inactivated virus (Stroher et al., 2001) were slightly higher than values observed in this study with VLPs. These differences may be attributed to differences between donors or may suggest that additional viral proteins not present in VLPs, or other soluble factors (e.g., cytokines) produced during viral infection and present in viral stocks may further enhance activation. Studies to directly compare effects of purified, inactivated virus and VLPs on macrophage activation would help elucidate this question. It is extremely interesting to note, however, that although recombinant GP₁ and GP_{1,2}ΔTM are essentially secreted forms of the spike glycoprotein, they are not sufficient to induce macrophage activation. Therefore, I propose that the EBOV glycoprotein activation may occur in a manner similar to that of vesicular stomatitis virus (VSV) induction of B cells (Bachmann, Hengartner, and Zinkernagel, 1995). Specifically, I hypothesize that the rigid form of the glycoprotein, spaced 5nm apart on VLPs and virions (Sanchez, 2001), presents a repetitive antigenic stimulus to macrophages and may function by cross-linking receptors resulting in strong activation (Figure 56). The presentation of the antigen in a specific organization may be more important than simply supplying the

protein in solution. In the absence of this rigid presentation of antigen, as in the case with soluble GP₁ and GP_{1,2}ΔTM, a potent signal may not be induced. Previous studies, which have shown that VLPs were immunogenic and sufficient to activate dendritic cells was demonstrated by their ability to confer complete protection from a lethal challenge of mouse-adapted ZEBOV (Warfield et al., 2003), support this concept. If binding to target cells is a prerequisite for activation then perhaps the ability of VLPs to bind macrophages is critical. Other groups have reported an inability of sGP to bind endothelial cells and macrophages (Kindzelskii et al., 2000; Yang et al., 2000). I performed experiments to bind the soluble glycoproteins to leukocytes and endothelial cells and analyze binding by FACS or IFA. In all cases, no binding was detected and this might explain the inability of the soluble glycoproteins to activate macrophages.

(Figure 56)

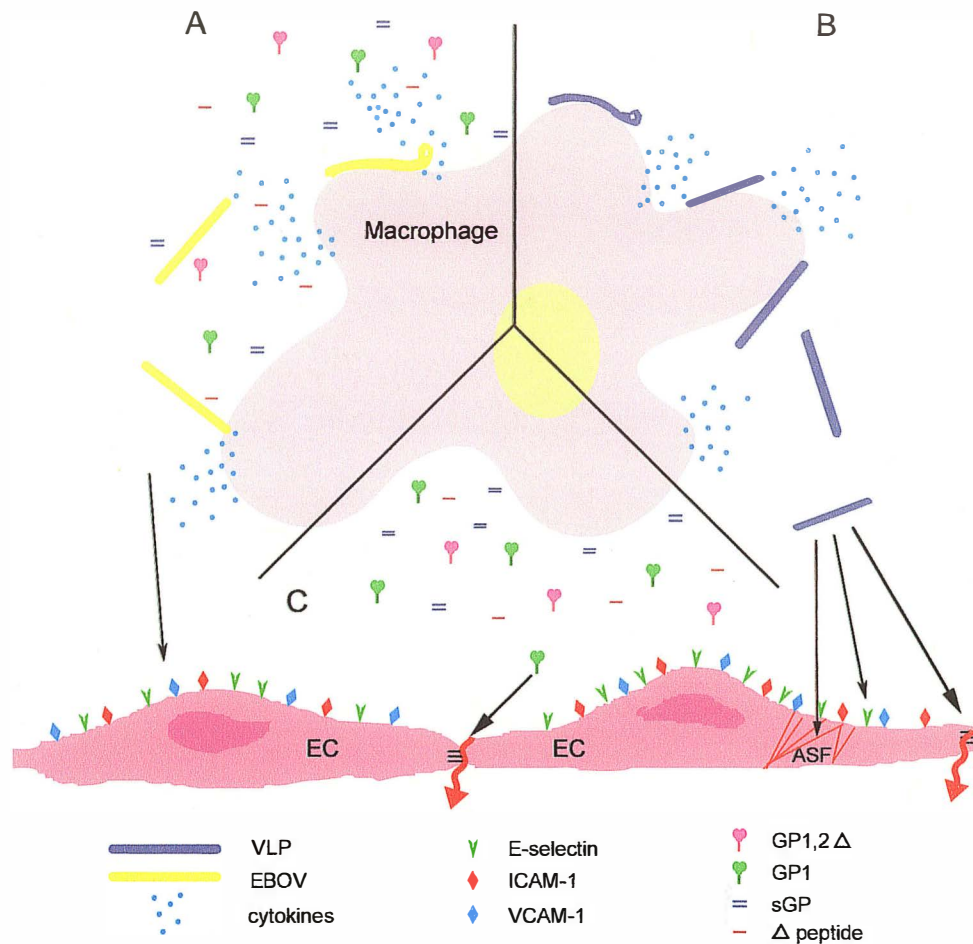


Figure 56. Pathogenesis model. Macrophages are primary target cells of EBOV. Once infected cells produce progeny virus, proinflammatory cyto/chemokines and soluble glycoproteins (A). Supernatants from these cells activate endothelial cells (EC) and cause increases in permeability and reorganization of VE-cadherin/actin. The ability of VLPs to induce activation of macrophages and EC, increase EC permeability (red arrows) and actin stress fiber (ASF) formation, provides evidence that virus replication is not necessary (B). GP1 increases permeability without causing activation or changes in VE-cadherin/actin organization (red arrow,C).

4.6 Activation of the endothelium

Of all the viral hemorrhagic fevers, those caused by EBOV are the most severe and display high case-fatality rates (Schnittler and Feldmann, 1999). The dramatic clinical presentation of disease as well as extensive laboratory data generated in the past has led to the idea that filovirus-induced disease is as much an immune syndrome as a

virus-induced disease (Feldmann et al., 2003; Feldmann et al., 1999). While the clinical picture of disease has become more clear through non-human primate studies, the molecular mechanisms, particularly with respect to vascular dysregulation, remain largely elusive. It has been hypothesized that the secreted glycoproteins of EBOV may function as mediators in the activation of endothelial cells and loss of barrier function (Feldmann et al., 1996; Feldmann et al., 2003; Feldmann et al., 1999; Schnittler and Feldmann, 2003). Endothelial cells are largely considered secondary target cells during EBOV infection while primary replication occurs within monocytes/macrophages and dendritic cells (Geisbert et al., 2003b; Stroher et al., 2001). It seems logical to presume that as EBOV replicates in these primary target cells there will be release of soluble glycoproteins that may affect secondary target cells, vis-à-vis endothelial cells. Many studies that have investigated the involvement of the endothelium during infection were not able to distinguish the role of sGP in pathogenesis and the need to test secreted glycoproteins generated through a mammalian expression system has been raised. In this study purified glycoproteins were used to treat cultured endothelial cells. Despite the fact that the soluble glycoproteins are produced at high amounts *in vitro*, they do not cause an activation of the endothelium (Figures 44-46). Previous studies using MARV have shown that when antibodies to tumor necrosis factor alpha (TNF-alpha) were added to supernatants of MARV-infected macrophages those supernatants displayed a reduced ability to increase permeability of endothelial cells thereby suggesting a crucial role of TNF-alpha in permeability changes during filovirus infection (Feldmann et al., 1996). It is also worth noting that MARV, which causes disease similar to EBOV, does not produce sGP due to different organization of its glycoprotein gene. While this might

suggest a role of sGP in reducing the transcription of GP_{1,2} (to prevent extensive cytotoxicity), a biological role for sGP must not be excluded (Feldmann et al., 2003).

In contrast to the soluble glycoproteins, VLPs were able to bind and activate HUVECs (Figures 43-46). Recently, similar studies investigated the role of EBOV on activation of HUVECs (Geisbert et al., 2003d). Geisbert *et al* demonstrated an increase in mRNA transcripts of several genes associated with activation of endothelial cells including cyclooxygenase (COX)-2, inducible nitric oxide synthase (iNOS), ICAM-1, and VCAM-1 (among others) following ZEBOV infection of HUVECs. When the authors tested gamma-irradiated ZEBOV the only significant changes observed were an increase in COX-2 mRNA transcripts. This led the authors to conclude that in the majority of cases ZEBOV replication was necessary to induce changes in levels of mRNA transcripts. In this study VLPs were able to induce ICAM-1, VCAM-1 and E-selectin thereby contradicting previous results (at least for the genes/proteins tested). This raises an interesting question as to whether or not VLPs and gamma-irradiated virus can be used interchangeably to represent replication-deficient EBOV. Chemical attack by free radicals and reactive oxygen species typically generated by the interaction of radiation with water molecules and oxygen has been recognized as a damaging secondary effects of gamma-irradiation (Grieb et al., 2002) and in combination with excess heat generated during the procedure the biological function of proteins may be negatively effected. Perhaps detailed structural analysis of EBOV following gamma-irradiation should be performed and compared to both live virus and VLPs to determine if discrepancies are attributed largely to structural differences. In summary, these results support the notion that activation of the endothelium occurs directly through binding of

viral particles (VLPs used as a model in this study) or indirectly through mediators from activated macrophages (activated by viral particles).

4.7 Alterations of VE-cadherin, actin and barrier function

Endothelial cells provide a barrier between the vascular bed and interstitial tissue space. Junctions between endothelial cells are comprised of adherens junctions in which gap junctions and strands of tight junctions are morphologically inserted. Whilst gap and tight junctions are heterogeneously disseminated within different organs and within the vascular bed, adherens junctions are universally found throughout the vascular bed (Schnittler et al., 2004). The common distribution of adherens junctions and the fact that endothelial changes are most frequently observed in post-capillary venules during inflammation, suggest that adherens junctions may be a critical factor in EBOV pathogenesis (Schnittler et al., 2004). HUVECs are an appropriate model to study barrier function since they lack tight junction strands both *in vivo* and *in vitro* (Franke WW, 1988). Previous studies have shown that the structural components of the adherens junctions (VE-cadherin and associated catenins) are reorganized following treatment with tissue culture supernatants derived from filovirus infected monocytes/macrophages, thereby causing intercellular gaps (Schnittler and Feldmann, 1999). In addition to loss of junctional integrity, actin-myosin interactions are pivotal in endothelial permeability. Specifically, actin cytoskeletal remodeling occurs during cell migration and is intimately linked with endothelial cell barrier regulation (Garcia, Davis, and Patterson, 1995). In this study both soluble glycoproteins and VLPs were tested for their abilities to alter the arrangement of VE-cadherin and cellular actin. In conjunction with these analyses,

barrier function was directly assessed by impedance spectroscopy in real-time as described by others (Seebach et al., 2000).

The soluble glycoproteins and VLPs did not alter VE-cadherin, nor actin organization. Of all the glycoproteins tested, only GP₁ and VLPs changed the barrier function of the endothelium, interestingly, without changing arrangement of VE-cadherin. Unlike GP₁, VLPs did induce changes in actin resulting in increased stress fiber formation (Figure 47). While it has been shown that cytokine-containing supernatants from Marburg virus infected macrophages can efficiently increase permeability and alter the cadherin–catenin complex of proteins, the direct infection of endothelium with EBOV is believed to affect the function more than the structure of cells (Feldmann et al., 1996; Geisbert et al., 2003d). These findings support this notion, however, I cannot exclude that other junction proteins may also play a role in gap formation between adjacent cells.

It was particularly interesting that while VLPs and GP₁ increased endothelial cell permeability, GP_{1,2}ΔTM did not. Additionally, GP₁ decreased barrier function to a higher degree than VLPs. It has been previously shown that certain proteins require proteolytic cleavage or covalent modifications (ie: phosphorylation) to be functionally activated (Berg, Tymoczko, and Stryer, 2002). The mechanisms whereby GP₁ and VLPs induce changes in barrier function requires further investigation, however, it could be that it occurs by two distinct mechanisms. The first may involve receptor cross-linking and activation (VLPs) whereas the second may require a functionally active protein to interact with cells, thereby explaining why GP₁ and not GP_{1,2}ΔTM functions this manner. One aspect that became clear from this study, however, was that the oligomerization of GP₁

was important for its biological function as a mutant that only forms monomers does not change the barrier function (Figure 51). Finally, mechanisms by which VLPs and GP₁ are able to change the barrier function of cells appears not likely to occur by gross destruction of the cells as VE-cadherin arrangement and general morphology was not altered.

As mentioned previously, increased cytokine and chemokine release following filovirus infection of macrophages contributes to decreased barrier function of endothelial cells (Feldmann et al., 1996). This *in vitro* observation fits the *in vivo* scenario of fluid distribution problems and terminal shock development, however, the lack of leukocyte infiltration into virus induced areas of tissue necrosis in guinea pigs, humans and non-human primates (Ryabchikova and Price, 2004; Zaki and Goldsmith, 1999) is contradictory to the generally accepted idea that endothelial activation promotes leukocyte transmigration/extravasation. This led to the hypothesis that one or several steps of leukocyte recruitment/migration are negatively affected during filovirus infection (Schnittler et al., 2004). Since sGP is the major glycoprotein product and secreted in high amounts, I hypothesized that this soluble product would potentially inhibit cytokine-induced changes in barrier function. The fact that sGP did not activate the endothelium, induce changes in VE-cadherin or actin arrangements, and did not reduce barrier function further strengthens this hypothesis. Indeed, sGP was able to either completely or partially restore endothelial cell barrier function following TNF- α induced changes (Figure 55). The idea that sGP could interfere with TNF- α induced endothelial cell alterations fits with the observation that leukocytes are not observed in areas of focal tissue necrosis. Specifically, infected primary target cells may activate the endothelium

and extravasate, however, presence of sGP released from these and other macrophages may downregulate activation induced by directly binding TNF- α , interfering with its receptor or by binding an as yet unidentified receptor resulting in the inhibition of downstream signal transduction events. A proposed model is shown in Figure 57.

(Figure 57)

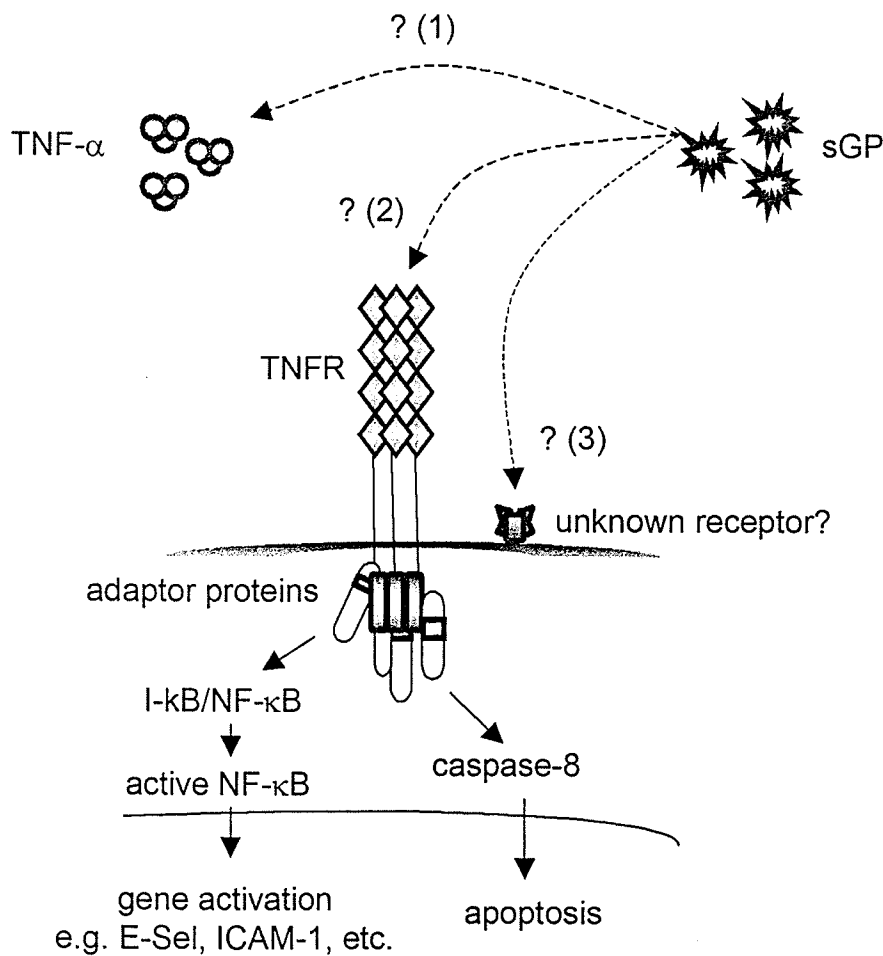


Figure 57. Model of sGP protection. sGP restores barrier function of TNF-alpha treated endothelial cells. Potential mechanisms for this observation are presented: interaction of sGP with TNF-alpha (1), interaction with the TNF-alpha receptor (TNFR) (2), or interaction with an unknown receptor (3). Interference by one of more of these mechanisms may interfere with downstream signal transduction, thereby preventing leukocyte recruitment.

The ability of viruses to interfere with cytokines or their receptors has been well described for other viruses, such as poxviruses (Johnston and McFadden, 2003). Interestingly, sGP is similar in size and conformation to the virus-encoded immunomodulator M-T2, a tumor necrosis factor receptor (TNF-R) homologue of Myxoma virus (Xu, Nash, and McFadden, 2000). M-T2 is secreted as monomeric and dimeric species that bind and inhibit rabbit TNF. While poxviruses have large genomes, the ability of a small RNA virus such as EBOV to encode such an immunomodulatory protein would indeed be novel. Regardless, elucidation of the exact mechanism of sGP protection would greatly increase the general understanding of filovirus-induced vascular dysregulation.

4.8 Summary

The high pathogenic potential of filoviruses, possible use as a bio-terrorist threat weapon and more frequent outbreaks have hastened the need to increase understanding of basic mechanisms of filovirus induced hemorrhagic fever. A great deal of research in the past decade has contributed to the knowledge base, however, the need for high bio-containment facilities to conduct such research had previously limited work to only those individuals with access to such laboratories. With the advent of protein expression systems, pseudotype viruses, and other molecular techniques, the field has greatly expanded and now includes experts from a wider scientific field. In combination with research at high containment labs, including animal studies, the picture of filovirus pathogenesis is coming into clearer focus.

This study answers longstanding questions regarding the role of soluble and membrane-associated glycoproteins in macrophage activation and vascular dysregulation,

associated with EBOV infection. Purified soluble glycoproteins and VLPs were produced and are authentic to those expressed in EBOV infection. Presentation of antigen is critical for macrophage activation, with only the membrane-associated form of the glycoprotein (VLPs) able to induce expression of several cytokines and chemokines that were previously identified as important in EBOV infection. In this respect, replication of virus is not necessary for activation.

Endothelial cells are important secondary target cells and are activated by VLPs but not soluble glycoproteins. VLPs were also able to increase permeability of endothelial cells, possibly through activation, however, activation does not necessarily correlate with the ability to induce changes in barrier function as GP₁, which does not activate HUVECs, does increase endothelial cell permeability. The mechanism for GP₁-induced changes in barrier function is dependent on its oligomeric structure since monomers of GP₁ do not change permeability. The mechanisms for VLP and GP₁ induced changes in barrier function are not known, however, actin reorganization may contribute to VLP-induced changes. Finally, sGP was shown to restore TNF- α induced changes in barrier function. It is possible that sGP may interact with TNF- α , its receptor, or an as yet identified receptor. Based on these results a new model of EBOV pathogenesis is suggested (Figure 56). The ability of sGP to restore barrier function is omitted from this figure but shown in detail in Figure 57.

4.9 Future studies

Like many studies, these experiments have answered a number of questions while opening doors for future research. One of the most interesting and potentially significant findings from these studies is the observation that sGP restores TNF- α induced changes in barrier function. In these studies sGP was added simultaneously with TNF- α . It would be interesting to see if pretreatment of HUVECs or TNF- α would completely abolish the deleterious effects of this cytokine on barrier function. It also remains to be seen if the sGP effect is specific to TNF- α or if it is a more general mechanism. Determining if sGP can protect against interferon-gamma or other cytokine-induced changes in barrier function could answer this question. Alternatively, specific binding of sGP to TNF- α or its receptor can be directly assessed by a number of methods currently available. Another aspect that should be investigated is whether sGP changes efficiency of leukocyte transmigration. Methods described by Allport *et al* (Allport et al., 2002) would allow for measurement of leukocyte migration through endothelial cells, even under flow conditions.

The importance of dimer formation in sGP's ability to restore barrier function should also be investigated. Since oligomers were found to be critical in GP_I induced decreases in barrier function, one could hypothesize that dimers may be an important conformation for sGP, particularly if this protein is found to bind TNF- α or its receptor. Single mutations of cysteines 53 and 306 (Volchkova et al., 1998), resulting in parallel dimers and monomers, respectively, would be useful to test this hypothesis.

The ability of viruses to activate innate immune responses is gaining more interest with the discovery of toll-like receptors (TLRs). It would be interesting to determine if

VLP-induced activation of macrophages was mediated by TLRs. The ability of measles virus to activate TLR2 through its hemagglutinin (HA) protein was recently described (Bieback et al., 2002). Signaling through TLR2 by measles virus HA induced expression of the cellular receptor (SLAM) and induced expression of IL-6 in macrophages. If common mechanism of recognition exists for members of the order *Mononegavirales*, perhaps EBOV will also signal through this TLR. Additionally, TLRs 3 and 7 may be important since TLR3 recognizes dsRNA and TLR7 has very recently been associated with recognition of ssRNA, particularly for VSV and influenza virus (Diebold et al., 2004; Lund et al., 2004; Matsumoto et al., 2004). A major obstacle for this work in the past was that stable cell lines expressing various TLRs were required. Recently, these cell lines have become commercially available and in combination with known ligands and reporter assay kits, signaling can be more easily assessed. If EBOV interacts with one or more of these TLRs, studies can be expanded to include primary macrophages or dendritic cells. The benefits of such studies include increased understanding of pathogenesis and determination of potential points for therapeutic interventions.

Bibliography

- Allport, J. R., Lim, Y. C., Shipley, J. M., Senior, R. M., Shapiro, S. D., Matsuyoshi, N., Vestweber, D., and Luscinskas, F. W. (2002). Neutrophils from MMP-9- or neutrophil elastase-deficient mice show no defect in transendothelial migration under flow in vitro. *J Leukoc Biol* **71**(5), 821-8.
- Alvarez, C. P., Lasala, F., Carrillo, J., Muniz, O., Corbi, A. L., and Delgado, R. (2002). C-type lectins DC-SIGN and L-SIGN mediate cellular entry by Ebola virus in cis and in trans. *J Virol* **76**(13), 6841-4.
- Anderson, R. G. (1998). The caveolae membrane system. *Annu Rev Biochem* **67**, 199-225.
- Antony, A. C. (1996). Folate receptors. *Annu Rev Nutr* **16**, 501-21.
- Artsob, H., Conlan, W., Dunn, P., Fry, S., Groves, D., Langevin, P., Leitner, R., Linarez, L., Orzechowski, J., Peat, B., Sander, M. and L. Thompson (2001). "The Laboratory Biosafety Guidelines." 3rd ed. (M. B. a. M. HEISZ, Ed.), Ottawa.
- Bachmann, M. F., Hengartner, H., and Zinkernagel, R. M. (1995). T helper cell-independent neutralizing B cell response against vesicular stomatitis virus: role of antigen patterns in B cell induction? *Eur J Immunol* **25**(12), 3445-51.
- Baize, S., Leroy, E. M., Georges, A. J., Georges-Courbot, M. C., Capron, M., Bedjabaga, I., Lansoud-Soukate, J., and Mavoungou, E. (2002). Inflammatory responses in Ebola virus-infected patients. *Clin Exp Immunol* **128**(1), 163-8.
- Baize, S., Leroy, E. M., Georges-Courbot, M. C., Capron, M., Lansoud-Soukate, J., Debre, P., Fisher-Hoch, S. P., McCormick, J. B., and Georges, A. J. (1999). Defective humoral responses and extensive intravascular apoptosis are associated with fatal outcome in Ebola virus-infected patients. *Nat Med* **5**(4), 423-6.
- Baron, R. C., McCormick, J. B., and Zubeir, O. A. (1983). Ebola virus disease in southern Sudan: hospital dissemination and intrafamilial spread. *Bull World Health Organ* **61**(6), 997-1003.
- Basler, C. F., Mikulasova, A., Martinez-Sobrido, L., Paragas, J., Muhlberger, E., Bray, M., Klenk, H. D., Palese, P., and Garcia-Sastre, A. (2003). The Ebola virus VP35 protein inhibits activation of interferon regulatory factor 3. *J Virol* **77**(14), 7945-56.
- Basler, C. F., Wang, X., Muhlberger, E., Volchkov, V., Paragas, J., Klenk, H. D., Garcia-Sastre, A., and Palese, P. (2000). The Ebola virus VP35 protein functions as a type I IFN antagonist. *Proc Natl Acad Sci U S A* **97**(22), 12289-94.
- Bavari, S., Bosio, C. M., Wiegand, E., Ruthel, G., Will, A. B., Geisbert, T. W., Hevey, M., Schmaljohn, C., Schmaljohn, A., and Aman, M. J. (2002). Lipid raft microdomains: a gateway for compartmentalized trafficking of Ebola and Marburg viruses. *J Exp Med* **195**(5), 593-602.
- Becker, S., Huppertz, S., Klenk, H. D., and Feldmann, H. (1994). The nucleoprotein of Marburg virus is phosphorylated. *J Gen Virol* **75** (Pt 4), 809-18.
- Becker, S., Klenk, H. D., and Muhlberger, E. (1996). Intracellular transport and processing of the Marburg virus surface protein in vertebrate and insect cells. *Virology* **225**(1), 145-55.
- Becker, S., and Muhlberger, E. (1999). Co- and posttranslational modifications and functions of Marburg virus proteins. *Curr Top Microbiol Immunol* **235**, 23-34.

- Becker, S., Rinne, C., Hofsass, U., Klenk, H. D., and Muhlberger, E. (1998). Interactions of Marburg virus nucleocapsid proteins. *Virology* **249**(2), 406-17.
- Becker, S., Spiess, M., and Klenk, H. D. (1995). The asialoglycoprotein receptor is a potential liver-specific receptor for Marburg virus. *J Gen Virol* **76** (Pt 2), 393-9.
- Bender, F. C., Whitbeck, J. C., Ponce de Leon, M., Lou, H., Eisenberg, R. J., and Cohen, G. H. (2003). Specific association of glycoprotein B with lipid rafts during herpes simplex virus entry. *J Virol* **77**(17), 9542-52.
- Berg, J. M., Tymoczko, J. L., and Stryer, L. (2002). "Biochemistry." 5th ed., 1. 1 vols. W.H. Freeman.
- Bieback, K., Lien, E., Klagge, I. M., Avota, E., Schneider-Schaulies, J., Duprex, W. P., Wagner, H., Kirschning, C. J., Ter Meulen, V., and Schneider-Schaulies, S. (2002). Hemagglutinin protein of wild-type measles virus activates toll-like receptor 2 signaling. *J Virol* **76**(17), 8729-36.
- Bowen, M. D., Thurman, K., Minor, E., Ibrahim, M.S., Meyer, R.F., Malfatti, S.A., Do, L.H., Smith, K.L., McCready, P.M. and Chain, P.S.G. (2003). Marburg virus strain M/S.Africa/Johannesburg/1975/Ozolin, complete sequence.
- Bukreyev, A., Volchkov, V. E., Blinov, V. M., and Netesov, S. V. (1993a). The GP-protein of Marburg virus contains the region similar to the 'immunosuppressive domain' of oncogenic retrovirus P15E proteins. *FEBS Lett* **323**(1-2), 183-7.
- Bukreyev, A. A., Belanov, E. F., Blinov, V. M., and Netesov, S. V. (1995a). Complete nucleotide sequences of Marburg virus genes 5 and 6 encoding VP30 and VP24 proteins. *Biochem Mol Biol Int* **35**(3), 605-13.
- Bukreyev, A. A., Volchkov, V. E., Blinov, V. M., Dryga, S. A., and Netesov, S. V. (1995b). The complete nucleotide sequence of the Popp (1967) strain of Marburg virus: a comparison with the Musoke (1980) strain. *Arch Virol* **140**(9), 1589-600.
- Bukreyev, A. A., Volchkov, V. E., Blinov, V. M., and Netesov, S. V. (1993b). The VP35 and VP40 proteins of filoviruses. Homology between Marburg and Ebola viruses. *FEBS Lett* **322**(1), 41-6.
- Calvo, M., Tebar, F., Lopez-Iglesias, C., and Enrich, C. (2001). Morphologic and functional characterization of caveolae in rat liver hepatocytes. *Hepatology* **33**(5), 1259-69.
- CDC (1995). Outbreak of Ebola viral hemorrhagic fever--Zaire, 1995. *MMWR Morb Mortal Wkly Rep* **44**(19), 381-2.
- CDC (2001). Outbreak of Ebola hemorrhagic fever Uganda, August 2000-January 2001. *MMWR Morb Mortal Wkly Rep* **50**(5), 73-7.
- Chain, P. S. G., Ichou, M.A., Malfatti, S.A., Hajjaj, A., Vergez, L.M., Paragas, J., Do, L.H., Jahrling, P.B., Smith, K.L., McCready, P.M. and Ibrahim, M.S. (2003). Zaire Ebola virus, complete genome (Zaire 1995 strain).
- Chan, S. Y., Empig, C. J., Welte, F. J., Speck, R. F., Schmaljohn, A., Kreisberg, J. F., and Goldsmith, M. A. (2001). Folate receptor-alpha is a cofactor for cellular entry by Marburg and Ebola viruses. *Cell* **106**(1), 117-26.
- Chan, S. Y., Ma, M. C., and Goldsmith, M. A. (2000). Differential induction of cellular detachment by envelope glycoproteins of Marburg and Ebola (Zaire) viruses. *J Gen Virol* **81**(Pt 9), 2155-9.

- Chan, S. Y., Speck, R. F., Ma, M. C., and Goldsmith, M. A. (2000). Distinct mechanisms of entry by envelope glycoproteins of Marburg and Ebola (Zaire) viruses. *J Virol* **74**(10), 4933-7.
- Chupurnov, A. A., Chernukhin, I. V., Ternovoi, V. A., Kudoiarova, N. M., Makhova, N. M., Azaev, M., and Smolina, M. P. (1995). [Attempts to develop a vaccine against Ebola fever]. *Vopr Virusol* **40**(6), 257-60.
- Connolly, B. M., Steele, K. E., Davis, K. J., Geisbert, T. W., Kell, W. M., Jaax, N. K., and Jahrling, P. B. (1999). Pathogenesis of experimental Ebola virus infection in guinea pigs. *J Infect Dis* **179 Suppl 1**, S203-17.
- Davis, K. J., Anderson, A. O., Geisbert, T. W., Steele, K. E., Geisbert, J. B., Vogel, P., Connolly, B. M., Huggins, J. W., Jahrling, P. B., and Jaax, N. K. (1997). Pathology of experimental Ebola virus infection in African green monkeys. Involvement of fibroblastic reticular cells. *Arch Pathol Lab Med* **121**(8), 805-19.
- Del Maschio, A., Zanetti, A., Corada, M., Rival, Y., Ruco, L., Lampugnani, M. G., and Dejana, E. (1996). Polymorphonuclear leukocyte adhesion triggers the disorganization of endothelial cell-to-cell adherens junctions. *J Cell Biol* **135**(2), 497-510.
- Dessen, A., Volchkov, V., Dolnik, O., Klenk, H. D., and Weissenhorn, W. (2000). Crystal structure of the matrix protein VP40 from Ebola virus. *Embo J* **19**(16), 4228-36.
- Diebold, S. S., Kaisho, T., Hemmi, H., Akira, S., and Reis, E. S. C. (2004). Innate antiviral responses by means of TLR7-mediated recognition of single-stranded RNA. *Science* **303**(5663), 1529-31.
- Dolnik, O., H-D. Klenk, W. Garten, V.A. Volchkova, and V.E. Volchkov (2003). *XII International Conference on Negative Strand Viruses, Pisa, Italy*.
- Dolnik, O., Volchkova, V., Garten, W., Becker, S., Kahnt, J., Ströher, U., Klenk, H.-D., and Volchkov, V. (2004). Ectodomain Shedding of the Glycoprotein of Ebola Virus. *Embo J* **in press**.
- DuBridge, R. B., Tang, P., Hsia, H. C., Leong, P. M., Miller, J. H., and Calos, M. P. (1987). Analysis of mutation in human cells by using an Epstein-Barr virus shuttle system. *Mol Cell Biol* **7**(1), 379-87.
- Dutch, R. E., Jardetzky, T. S., and Lamb, R. A. (2000). Virus membrane fusion proteins: biological machines that undergo a metamorphosis. *Biosci Rep* **20**(6), 597-612.
- Elliott, L. H., Kiley, M. P., and McCormick, J. B. (1985). Descriptive analysis of Ebola virus proteins. *Virology* **147**(1), 169-76.
- Elliott, L. H., Sanchez, A., Holloway, B. P., Kiley, M. P., and McCormick, J. B. (1993). Ebola protein analyses for the determination of genetic organization. *Arch Virol* **133**(3-4), 423-36.
- Empig, C. J., and Goldsmith, M. A. (2002). Association of the caveola vesicular system with cellular entry by filoviruses. *J Virol* **76**(10), 5266-70.
- Feldmann, H., Bugany, H., Mahner, F., Klenk, H. D., Drenckhahn, D., and Schnittler, H. J. (1996). Filovirus-induced endothelial leakage triggered by infected monocytes/macrophages. *J Virol* **70**(4), 2208-14.
- Feldmann, H., Geisbert, T., Jahrling, P.B., Klenk, H-D., Netesov, S.V., Peters C.J., Sanchez, A., Swanepoel, R., and V. Volchkov (2004). Filoviridae.

- Feldmann, H., Jones, S., Klenk, H. D., and Schnittler, H. J. (2003). Ebola virus: from discovery to vaccine. *Nat Rev Immunol* **3**(8), 677-85.
- Feldmann, H., and Kiley, M. P. (1999). Classification, structure, and replication of filoviruses. *Curr Top Microbiol Immunol* **235**, 1-21.
- Feldmann, H., and Klenk, H. D. (1996). Marburg and Ebola viruses. *Adv Virus Res* **47**, 1-52.
- Feldmann, H., Muhlberger, E., Randolph, A., Will, C., Kiley, M. P., Sanchez, A., and Klenk, H. D. (1992). Marburg virus, a filovirus: messenger RNAs, gene order, and regulatory elements of the replication cycle. *Virus Res* **24**(1), 1-19.
- Feldmann, H., Nichol, S. T., Klenk, H. D., Peters, C. J., and Sanchez, A. (1994). Characterization of filoviruses based on differences in structure and antigenicity of the virion glycoprotein. *Virology* **199**(2), 469-73.
- Feldmann, H., Volchkov, V. E., Volchkova, V. A., and Klenk, H. D. (1999). The glycoproteins of Marburg and Ebola virus and their potential roles in pathogenesis. *Arch Virol Suppl* **15**, 159-69.
- Feldmann, H., Volchkov, V. E., Volchkova, V. A., Stroher, U., and Klenk, H. D. (2001). Biosynthesis and role of filoviral glycoproteins. *J Gen Virol* **82**(Pt 12), 2839-48.
- Feldmann, H., Will, C., Schikore, M., Slenczka, W., and Klenk, H. D. (1991). Glycosylation and oligomerization of the spike protein of Marburg virus. *Virology* **182**(1), 353-6.
- Franke WW, C. P., Grund C, Kuhn C, and Kapprell HP (1988). The endothelial junction: The plaque and its components, pp. 147-166. Plenum Publishing Corp, New York.
- Fugier-Vivier, I., Servet-Delprat, C., Rivailier, P., Rissoan, M. C., Liu, Y. J., and Roubourdin-Combe, C. (1997). Measles virus suppresses cell-mediated immunity by interfering with the survival and functions of dendritic and T cells. *J Exp Med* **186**(6), 813-23.
- Gallaher, W. R. (1996). Similar structural models of the transmembrane proteins of Ebola and avian sarcoma viruses. *Cell* **85**(4), 477-8.
- Garbutt, M., Liebscher, R., Wahl-Jensen, V., Jones, S., Moeller, P., Wagner, R., Volchkov, V., Klenk, H.-D., Feldmann, H., and Stroher, U. (2004). Properties of replication-competent vesicular stomatitis virus vectors expressing glycoproteins of filoviruses and arenaviruses. *J Virol* **in press**.
- Garcia, J. G., Davis, H. W., and Patterson, C. E. (1995). Regulation of endothelial cell gap formation and barrier dysfunction: role of myosin light chain phosphorylation. *J Cell Physiol* **163**(3), 510-22.
- Gear, J. S., Cassel, G. A., Gear, A. J., Trappler, B., Clausen, L., Meyers, A. M., Kew, M. C., Bothwell, T. H., Sher, R., Miller, G. B., Schneider, J., Koornhof, H. J., Gomperts, E. D., Isaacson, M., and Gear, J. H. (1975). Outbreak of Marburg virus disease in Johannesburg. *Br Med J* **4**(5995), 489-93.
- Geisbert, T. W., Hensley, L. E., Gibb, T. R., Steele, K. E., Jaax, N. K., and Jahrling, P. B. (2000). Apoptosis induced in vitro and in vivo during infection by Ebola and Marburg viruses. *Lab Invest* **80**(2), 171-86.
- Geisbert, T. W., Hensley, L. E., Jahrling, P. B., Larsen, T., Geisbert, J. B., Paragas, J., Young, H. A., Fredeking, T. M., Rote, W. E., and Vlasuk, G. P. (2003a). Treatment of Ebola virus infection with a recombinant inhibitor of factor VIIa/tissue factor: a study in rhesus monkeys. *Lancet* **362**(9400), 1953-8.

- Geisbert, T. W., Hensley, L. E., Larsen, T., Young, H. A., Reed, D. S., Geisbert, J. B., Scott, D. P., Kagan, E., Jahrling, P. B., and Davis, K. J. (2003b). Pathogenesis of Ebola hemorrhagic fever in cynomolgus macaques: evidence that dendritic cells are early and sustained targets of infection. *Am J Pathol* **163**(6), 2347-70.
- Geisbert, T. W., and Jahrling, P. B. (1995). Differentiation of filoviruses by electron microscopy. *Virus Res* **39**(2-3), 129-50.
- Geisbert, T. W., and Jahrling, P. B. (2003). Towards a vaccine against Ebola virus. *Expert Rev Vaccines* **2**(6), 777-89.
- Geisbert, T. W., Jahrling, P. B., Hanes, M. A., and Zack, P. M. (1992). Association of Ebola-related Reston virus particles and antigen with tissue lesions of monkeys imported to the United States. *J Comp Pathol* **106**(2), 137-52.
- Geisbert, T. W., Pushko, P., Anderson, K., Smith, J., Davis, K. J., and Jahrling, P. B. (2002). Evaluation in nonhuman primates of vaccines against Ebola virus. *Emerg Infect Dis* **8**(5), 503-7.
- Geisbert, T. W., Young, H. A., Jahrling, P. B., Davis, K. J., Kagan, E., and Hensley, L. E. (2003c). Mechanisms underlying coagulation abnormalities in ebola hemorrhagic fever: overexpression of tissue factor in primate monocytes/macrophages is a key event. *J Infect Dis* **188**(11), 1618-29.
- Geisbert, T. W., Young, H. A., Jahrling, P. B., Davis, K. J., Larsen, T., Kagan, E., and Hensley, L. E. (2003d). Pathogenesis of Ebola hemorrhagic fever in primate models: evidence that hemorrhage is not a direct effect of virus-induced cytolysis of endothelial cells. *Am J Pathol* **163**(6), 2371-82.
- Georges-Courbot, M. C., Sanchez, A., Lu, C. Y., Baize, S., Leroy, E., Lansout-Soukate, J., Tevi-Benissan, C., Georges, A. J., Trappier, S. G., Zaki, S. R., Swanepoel, R., Leman, P. A., Rollin, P. E., Peters, C. J., Nichol, S. T., and Ksiazek, T. G. (1997). Isolation and phylogenetic characterization of Ebola viruses causing different outbreaks in Gabon. *Emerg Infect Dis* **3**(1), 59-62.
- Geyer, H., Geyer, R., Odenthal-Schnittler, M., and Schnittler, H. J. (1999). Characterization of human vascular endothelial cadherin glycans. *Glycobiology* **9**(9), 915-25.
- Geyer, H., Will, C., Feldmann, H., Klenk, H. D., and Geyer, R. (1992). Carbohydrate structure of Marburg virus glycoprotein. *Glycobiology* **2**(4), 299-312.
- Grieb, T., Forng, R. Y., Brown, R., Owolabi, T., Maddox, E., McBain, A., Drohan, W. N., Mann, D. M., and Burgess, W. H. (2002). Effective use of gamma irradiation for pathogen inactivation of monoclonal antibody preparations. *Biologicals* **30**(3), 207-16.
- Groseth, A., Stroher, U., Theriault, S., and Feldmann, H. (2002). Molecular characterization of an isolate from the 1989/90 epizootic of Ebola virus Reston among macaques imported into the United States. *Virus Res* **87**(2), 155-63.
- Grosjean, I., Caux, C., Bella, C., Berger, I., Wild, F., Banchereau, J., and Kaiserlian, D. (1997). Measles virus infects human dendritic cells and blocks their allostimulatory properties for CD4+ T cells. *J Exp Med* **186**(6), 801-12.
- Haglund, K., Forman, J., Krausslich, H. G., and Rose, J. K. (2000). Expression of human immunodeficiency virus type 1 Gag protein precursor and envelope proteins from a vesicular stomatitis virus recombinant: high-level production of virus-like particles containing HIV envelope. *Virology* **268**(1), 112-21.

- Han, Z., Boshra, H., Sunyer, J. O., Zwiars, S. H., Paragas, J., and Harty, R. N. (2003). Biochemical and functional characterization of the Ebola virus VP24 protein: implications for a role in virus assembly and budding. *J Virol* **77**(3), 1793-800.
- Hart, M. K. (2003). Vaccine research efforts for filoviruses. *Int J Parasitol* **33**(5-6), 583-95.
- Hartlieb, B., Modrof, J., Muhlberger, E., Klenk, H. D., and Becker, S. (2003). Oligomerization of Ebola virus VP30 is essential for viral transcription and can be inhibited by a synthetic peptide. *J Biol Chem*.
- Hazelton, P. R., and Coombs, K. M. (1999). The reovirus mutant tsA279 L2 gene is associated with generation of a spikeless core particle: implications for capsid assembly. *J Virol* **73**(3), 2298-308.
- Hensley, L. E., Young, H. A., Jahrling, P. B., and Geisbert, T. W. (2002). Proinflammatory response during Ebola virus infection of primate models: possible involvement of the tumor necrosis factor receptor superfamily. *Immunol Lett* **80**(3), 169-79.
- Heymann, D. L., Barakamfitye, D., Szczeniowski, M., Muyembe-Tamfum, J. J., Bele, O., and Rodier, G. (1999). Ebola hemorrhagic fever: lessons from Kikwit, Democratic Republic of the Congo. *J Infect Dis* **179 Suppl 1**, S283-6.
- Ho, L. J., Wang, J. J., Shaio, M. F., Kao, C. L., Chang, D. M., Han, S. W., and Lai, J. H. (2001). Infection of human dendritic cells by dengue virus causes cell maturation and cytokine production. *J Immunol* **166**(3), 1499-506.
- Hogg, N. (1993). A model of leukocyte adhesion to vascular endothelium. *Curr Top Microbiol Immunol* **184**, 79-86.
- Huang, Y., Xu, L., Sun, Y., and Nabel, G. J. (2002). The assembly of Ebola virus nucleocapsid requires virion-associated proteins 35 and 24 and posttranslational modification of nucleoprotein. *Mol Cell* **10**(2), 307-16.
- Ikegami, T., Calaor, A. B., Miranda, M. E., Niikura, M., Saijo, M., Kurane, I., Yoshikawa, Y., and Morikawa, S. (2001). Genome structure of Ebola virus subtype Reston: differences among Ebola subtypes. Brief report. *Arch Virol* **146**(10), 2021-7.
- Ito, H., Watanabe, S., Sanchez, A., Whitt, M. A., and Kawaoka, Y. (1999). Mutational analysis of the putative fusion domain of Ebola virus glycoprotein. *J Virol* **73**(10), 8907-12.
- Jaax, N. K., Davis, K. J., Geisbert, T. J., Vogel, P., Jaax, G. P., Topper, M., and Jahrling, P. B. (1996). Lethal experimental infection of rhesus monkeys with Ebola-Zaire (Mayinga) virus by the oral and conjunctival route of exposure. *Arch Pathol Lab Med* **120**(2), 140-55.
- Jahrling, P. B., Geisbert, T. W., Dalgard, D. W., Johnson, E. D., Ksiazek, T. G., Hall, W. C., and Peters, C. J. (1990). Preliminary report: isolation of Ebola virus from monkeys imported to USA. *Lancet* **335**(8688), 502-5.
- Jasenosky, L. D., Neumann, G., Lukashevich, I., and Kawaoka, Y. (2001). Ebola virus VP40-induced particle formation and association with the lipid bilayer. *J Virol* **75**(11), 5205-14.
- Jeffers, S. A., Sanders, D. A., and Sanchez, A. (2002). Covalent modifications of the ebola virus glycoprotein. *J Virol* **76**(24), 12463-72.
- Johnson, E., Jaax, N., White, J., and Jahrling, P. (1995). Lethal experimental infections of rhesus monkeys by aerosolized Ebola virus. *Int J Exp Pathol* **76**(4), 227-36.

- Johnson, E. D., Johnson, B. K., Silverstein, D., Tukei, P., Geisbert, T. W., Sanchez, A. N., and Jahrling, P. B. (1996). Characterization of a new Marburg virus isolated from a 1987 fatal case in Kenya. *Arch Virol Suppl* **11**, 101-14.
- Johnston, J. B., and McFadden, G. (2003). Poxvirus immunomodulatory strategies: current perspectives. *J Virol* **77**(11), 6093-100.
- Karber, G. (1931). Beitrag zur kollektiven Behandlung pharmakologischer Reihenversuche. *Arch Exp Pathol Pharmacol* **162**, 480-487.
- Kerstiens, B., and Matthys, F. (1999). Interventions to control virus transmission during an outbreak of Ebola hemorrhagic fever: experience from Kikwit, Democratic Republic of the Congo, 1995. *J Infect Dis* **179 Suppl 1**, S263-7.
- Kiley, M. P., Bowen, E. T., Eddy, G. A., Isaacson, M., Johnson, K. M., McCormick, J. B., Murphy, F. A., Pattyn, S. R., Peters, D., Prozesky, O. W., Regnery, R. L., Simpson, D. I., Slenczka, W., Sureau, P., van der Groen, G., Webb, P. A., and Wulff, H. (1982). Filoviridae: a taxonomic home for Marburg and Ebola viruses? *Intervirology* **18**(1-2), 24-32.
- Kiley, M. P., Cox, N. J., Elliott, L. H., Sanchez, A., DeFries, R., Buchmeier, M. J., Richman, D. D., and McCormick, J. B. (1988). Physicochemical properties of Marburg virus: evidence for three distinct virus strains and their relationship to Ebola virus. *J Gen Virol* **69 (Pt 8)**, 1957-67.
- Kiley, M. P., Regnery, R. L., and Johnson, K. M. (1980). Ebola virus: identification of virion structural proteins. *J Gen Virol* **49**(2), 333-41.
- Kindzelskii, A. L., Yang, Z., Nabel, G. J., Todd, R. F., 3rd, and Petty, H. R. (2000). Ebola virus secretory glycoprotein (sGP) diminishes Fc gamma RIIIB-to-CR3 proximity on neutrophils. *J Immunol* **164**(2), 953-8.
- Kiss, A. L., Turi, A., Muller, N., Kantor, O., and Botos, E. (2002). Caveolae and caveolin isoforms in rat peritoneal macrophages. *Micron* **33**(1), 75-93.
- Kiss, A. L., Turi, A., Mullner, N., and Timar, J. (2000). Caveolin isoforms in resident and elicited rat peritoneal macrophages. *Eur J Cell Biol* **79**(5), 343-9.
- Kopecky, S. A., and Lyles, D. S. (2003). The cell-rounding activity of the vesicular stomatitis virus matrix protein is due to the induction of cell death. *J Virol* **77**(9), 5524-8.
- Krasnianskii, B. P., Mikhailov, V. V., Borisevich, I. V., Gradoboev, V. N., Evseev, A. A., and Pshenichnov, V. A. (1995). [Preparation of hyperimmune horse serum against Ebola virus]. *Vopr Virusol* **40**(3), 138-40.
- Kretzschmar, E., Buonocore, L., Schnell, M. J., and Rose, J. K. (1997). High-efficiency incorporation of functional influenza virus glycoproteins into recombinant vesicular stomatitis viruses. *J Virol* **71**(8), 5982-9.
- Ksiazek, T. G., Rollin, P. E., Williams, A. J., Bressler, D. S., Martin, M. L., Swanepoel, R., Burt, F. J., Leman, P. A., Khan, A. S., Rowe, A. K., Mukunu, R., Sanchez, A., and Peters, C. J. (1999). Clinical virology of Ebola hemorrhagic fever (EHF): virus, virus antigen, and IgG and IgM antibody findings among EHF patients in Kikwit, Democratic Republic of the Congo, 1995. *J Infect Dis* **179 Suppl 1**, S177-87.
- Kurzchalia, T. V., and Parton, R. G. (1999). Membrane microdomains and caveolae. *Curr Opin Cell Biol* **11**(4), 424-31.

- Lawson, N. D., Stillman, E. A., Whitt, M. A., and Rose, J. K. (1995). Recombinant vesicular stomatitis viruses from DNA. *Proc Natl Acad Sci U S A* **92**(10), 4477-81.
- Le Guenno, B., Formenty, P., and Boesch, C. (1999). Ebola virus outbreaks in the Ivory Coast and Liberia, 1994-1995. *Curr Top Microbiol Immunol* **235**, 77-84.
- Leibovitz, A., McCombs, W. M., 3rd, Johnston, D., McCoy, C. E., and Stinson, J. C. (1973). New human cancer cell culture lines. I. SW-13, small-cell carcinoma of the adrenal cortex. *J Natl Cancer Inst* **51**(2), 691-7.
- Lenter, M., Levinovitz, A., Isenmann, S., and Vestweber, D. (1994). Monospecific and common glycoprotein ligands for E- and P-selectin on myeloid cells. *J Cell Biol* **125**(2), 471-81.
- Leroy, E. M., Baize, S., Mavoungou, E., and Apetrei, C. (2002a). Sequence analysis of the GP, NP, VP40 and VP24 genes of Ebola virus isolated from deceased, surviving and asymptotically infected individuals during the 1996 outbreak in Gabon: comparative studies and phylogenetic characterization. *J Gen Virol* **83**(Pt 1), 67-73.
- Leroy, E. M., Baize, S., Volchkov, V. E., Fisher-Hoch, S. P., Georges-Courbot, M. C., Lansoud-Soukate, J., Capron, M., Debre, P., McCormick, J. B., and Georges, A. J. (2000). Human asymptomatic Ebola infection and strong inflammatory response. *Lancet* **355**(9222), 2210-5.
- Leroy, E. M., Souquiere, S., Rouquet, P., and Drevet, D. (2002b). Re-emergence of ebola haemorrhagic fever in Gabon. *Lancet* **359**(9307), 712.
- Liao, F., Huynh, H. K., Eiroa, A., Greene, T., Polizzi, E., and Muller, W. A. (1995). Migration of monocytes across endothelium and passage through extracellular matrix involve separate molecular domains of PECAM-1. *J Exp Med* **182**(5), 1337-43.
- Licata, J. M., Simpson-Holley, M., Wright, N. T., Han, Z., Paragas, J., and Harty, R. N. (2003). Overlapping motifs (PTAP and PPEY) within the Ebola virus VP40 protein function independently as late budding domains: involvement of host proteins TSG101 and VPS-4. *J Virol* **77**(3), 1812-9.
- Lund, J. M., Alexopoulou, L., Sato, A., Karow, M., Adams, N. C., Gale, N. W., Iwasaki, A., and Flavell, R. A. (2004). Recognition of single-stranded RNA viruses by Toll-like receptor 7. *Proc Natl Acad Sci U S A*.
- Lupton, H. W., Lambert, R. D., Bumgardner, D. L., Moe, J. B., and Eddy, G. A. (1980). Inactivated vaccine for Ebola virus efficacious in guineapig model. *Lancet* **2**(8207), 1294-5.
- Malashkevich, V. N., Schneider, B. J., McNally, M. L., Milhollen, M. A., Pang, J. X., and Kim, P. S. (1999). Core structure of the envelope glycoprotein GP2 from Ebola virus at 1.9-A resolution. *Proc Natl Acad Sci U S A* **96**(6), 2662-7.
- Manes, S., del Real, G., and Martinez, A. C. (2003). Pathogens: raft hijackers. *Nat Rev Immunol* **3**(7), 557-68.
- Martini, G. A., Knauff, H. G., Schmidt, H. A., Mayer, G., and Baltzer, G. (1968). A hitherto unknown infectious disease contracted from monkeys. "Marburg-virus" disease. *Ger Med Mon* **13**(10), 457-70.
- Martin-Serrano, J., Zang, T., and Bieniasz, P. D. (2001). HIV-1 and Ebola virus encode small peptide motifs that recruit Tsg101 to sites of particle assembly to facilitate egress. *Nat Med* **7**(12), 1313-9.

- Maruyama, T., Buchmeier, M. J., Parren, P. W., Burton, D. R., Yang, Z., Delgado, R., Xu, L., Todd, R. F., Nabel, E. G., Sanchez, A., and Nabel, G. J. (1998). Ebola Virus, Neutrophils, and Antibody Specificity. *Science* **282**, 843.
- Maruyama, T., Parren, P. W., Sanchez, A., Rensink, I., Rodriguez, L. L., Khan, A. S., Peters, C. J., and Burton, D. R. (1999a). Recombinant human monoclonal antibodies to Ebola virus. *J Infect Dis* **179 Suppl 1**, S235-9.
- Maruyama, T., Rodriguez, L. L., Jahrling, P. B., Sanchez, A., Khan, A. S., Nichol, S. T., Peters, C. J., Parren, P. W., and Burton, D. R. (1999b). Ebola virus can be effectively neutralized by antibody produced in natural human infection. *J Virol* **73**(7), 6024-30.
- Matsumoto, M., Funami, K., Oshiumi, H., and Seya, T. (2004). Toll-Like Receptor 3: A Link between Toll-Like Receptor, Interferon and Viruses. *Microbiol Immunol* **48**(3), 147-54.
- McCormick, J. B., Bauer, S. P., Elliott, L. H., Webb, P. A., and Johnson, K. M. (1983). Biologic differences between strains of Ebola virus from Zaire and Sudan. *J Infect Dis* **147**(2), 264-7.
- Medina, M. F., Kobinger, G. P., Rux, J., Gasmi, M., Looney, D. J., Bates, P., and Wilson, J. M. (2003). Lentiviral vectors pseudotyped with minimal filovirus envelopes increased gene transfer in murine lung. *Mol Ther* **8**(5), 777-89.
- Mikhailov, V. V., Borisevich, I. V., Chernikova, N. K., Potryvaeva, N. V., and Krasnianskii, V. P. (1994). [The evaluation in hamadryas baboons of the possibility for the specific prevention of Ebola fever]. *Vopr Virusol* **39**(2), 82-4.
- Modrof, J., Moritz, C., Kolesnikova, L., Konakova, T., Hartlieb, B., Randolph, A., Muhlberger, E., and Becker, S. (2001). Phosphorylation of Marburg virus VP30 at serines 40 and 42 is critical for its interaction with NP inclusions. *Virology* **287**(1), 171-82.
- Muhlberger, E., Lotfering, B., Klenk, H. D., and Becker, S. (1998). Three of the four nucleocapsid proteins of Marburg virus, NP, VP35, and L, are sufficient to mediate replication and transcription of Marburg virus-specific monocistronic minigenomes. *J Virol* **72**(11), 8756-64.
- Muhlberger, E., Sanchez, A., Randolph, A., Will, C., Kiley, M. P., Klenk, H. D., and Feldmann, H. (1992). The nucleotide sequence of the L gene of Marburg virus, a filovirus: homologies with paramyxoviruses and rhabdoviruses. *Virology* **187**(2), 534-47.
- Muhlberger, E., Weik, M., Volchkov, V. E., Klenk, H. D., and Becker, S. (1999). Comparison of the transcription and replication strategies of marburg virus and Ebola virus by using artificial replication systems. *J Virol* **73**(3), 2333-42.
- Mupapa, K., Massamba, M., Kibadi, K., Kuvula, K., Bwaka, A., Kipasa, M., Colebunders, R., and Muyembe-Tamfum, J. J. (1999). Treatment of Ebola hemorrhagic fever with blood transfusions from convalescent patients. International Scientific and Technical Committee. *J Infect Dis* **179 Suppl 1**, S18-23.
- Neumann, G., Feldmann, H., Watanabe, S., Lukashevich, I., and Kawaoka, Y. (2002). Reverse genetics demonstrates that proteolytic processing of the Ebola virus glycoprotein is not essential for replication in cell culture. *J Virol* **76**(1), 406-10.
- Niwa, H., Yamamura, K., and Miyazaki, J. (1991). Efficient selection for high-expression transfectants with a novel eukaryotic vector. *Gene* **108**(2), 193-9.

- Noda, T., Sagara, H., Suzuki, E., Takada, A., Kida, H., and Kawaoka, Y. (2002). Ebola virus VP40 drives the formation of virus-like filamentous particles along with GP. *J Virol* **76**(10), 4855-65.
- Parren, P. W., Geisbert, T. W., Maruyama, T., Jahrling, P. B., and Burton, D. R. (2002). Pre- and postexposure prophylaxis of Ebola virus infection in an animal model by passive transfer of a neutralizing human antibody. *J Virol* **76**(12), 6408-12.
- Peters, C. J. (1996). Emerging infections--Ebola and other filoviruses. *West J Med* **164**(1), 36-8.
- Peters, C. J., and Khan, A. S. (1999). Filovirus diseases. *Curr Top Microbiol Immunol* **235**, 85-95.
- Prevention, C. f. D. C. a. (1995). Outbreak of Ebola viral hemorrhagic fever--Zaire, 1995. *MMWR Morb Mortal Wkly Rep* **44**(19), 381-2.
- Pushko, P., Bray, M., Ludwig, G. V., Parker, M., Schmaljohn, A., Sanchez, A., Jahrling, P. B., and Smith, J. F. (2000). Recombinant RNA replicons derived from attenuated Venezuelan equine encephalitis virus protect guinea pigs and mice from Ebola hemorrhagic fever virus. *Vaccine* **19**(1), 142-53.
- Raftery, M. J., Schwab, M., Eibert, S. M., Samstag, Y., Walczak, H., and Schonrich, G. (2001). Targeting the function of mature dendritic cells by human cytomegalovirus: a multilayered viral defense strategy. *Immunity* **15**(6), 997-1009.
- Reed, L. J., and H. A. Muench (1938). A simple method of determining fifty percent endpoints. *Am J Hyg* **27**, 493-497.
- Regnery, R. L., Johnson, K. M., and Kiley, M. P. (1980). Virion nucleic acid of Ebola virus. *J Virol* **36**(2), 465-9.
- Rizzo, V., Sung, A., Oh, P., and Schnitzer, J. E. (1998). Rapid mechanotransduction in situ at the luminal cell surface of vascular endothelium and its caveolae. *J Biol Chem* **273**(41), 26323-9.
- Roche (2003). Pwo DNA Polymerase. Roche.
- Rowe, A. K., Bertolli, J., Khan, A. S., Mukunu, R., Muyembe-Tamfum, J. J., Bressler, D., Williams, A. J., Peters, C. J., Rodriguez, L., Feldmann, H., Nichol, S. T., Rollin, P. E., and Ksiazek, T. G. (1999). Clinical, virologic, and immunologic follow-up of convalescent Ebola hemorrhagic fever patients and their household contacts, Kikwit, Democratic Republic of the Congo. Commission de Lutte contre les Epidemies a Kikwit. *J Infect Dis* **179** Suppl 1, S28-35.
- Ruiz-Arguello, M. B., Goni, F. M., Pereira, F. B., and Nieva, J. L. (1998). Phosphatidylinositol-dependent membrane fusion induced by a putative fusogenic sequence of Ebola virus. *J Virol* **72**(3), 1775-81.
- Ryabchikova, E., and Price, B. B. S. (2004). "Ebola and Marburg Viruses: A View of Infection Using Electron Microscopy." Battelle Press, Columbus, OH.
- Saijo, M., Niikura, M., Morikawa, S., Ksiazek, T. G., Meyer, R. F., Peters, C. J., and Kurane, I. (2001). Enzyme-linked immunosorbent assays for detection of antibodies to Ebola and Marburg viruses using recombinant nucleoproteins. *J Clin Microbiol* **39**(1), 1-7.
- Sanchez, A., A.S. Khan, S.R. Zaki, G.J. Nabel, T.G. Ksiazek, C.J. Peters (2001). Filoviridae: Marburg and Ebola viruses. 4th ed. In "Fields' Virology" (R. A. L. D.M. Knipe and P.M. Howley with D.E. Griffin, M.A. Martin, B. Roizman, S.E. Strauss, Ed.), pp. 1279-1304. Lippincott, Williams, and Wilkins, Philadelphia.

- Sanchez, A., and Kiley, M. P. (1987). Identification and analysis of Ebola virus messenger RNA. *Virology* **157**(2), 414-20.
- Sanchez, A., Kiley, M. P., Holloway, B. P., and Auperin, D. D. (1993). Sequence analysis of the Ebola virus genome: organization, genetic elements, and comparison with the genome of Marburg virus. *Virus Res* **29**(3), 215-40.
- Sanchez, A., Kiley, M. P., Holloway, B. P., McCormick, J. B., and Auperin, D. D. (1989). The nucleoprotein gene of Ebola virus: cloning, sequencing, and in vitro expression. *Virology* **170**(1), 81-91.
- Sanchez, A., Kiley, M. P., Klenk, H. D., and Feldmann, H. (1992). Sequence analysis of the Marburg virus nucleoprotein gene: comparison to Ebola virus and other non-segmented negative-strand RNA viruses. *J Gen Virol* **73** (Pt 2), 347-57.
- Sanchez, A., Ksiazek, T. G., Rollin, P. E., Miranda, M. E., Trappier, S. G., Khan, A. S., Peters, C. J., and Nichol, S. T. (1999). Detection and molecular characterization of Ebola viruses causing disease in human and nonhuman primates. *J Infect Dis* **179** Suppl 1, S164-9.
- Sanchez, A., Trappier, S. G., Mahy, B. W., Peters, C. J., and Nichol, S. T. (1996). The virion glycoproteins of Ebola viruses are encoded in two reading frames and are expressed through transcriptional editing. *Proc Natl Acad Sci U S A* **93**(8), 3602-7.
- Sanchez, A., Trappier, S. G., Stroher, U., Nichol, S. T., Bowen, M. D., and Feldmann, H. (1998a). Variation in the glycoprotein and VP35 genes of Marburg virus strains. *Virology* **240**(1), 138-46.
- Sanchez, A., Yang, Z. Y., Xu, L., Nabel, G. J., Crews, T., and Peters, C. J. (1998b). Biochemical analysis of the secreted and virion glycoproteins of Ebola virus. *J Virol* **72**(8), 6442-7.
- Sanger, F., Nicklen, S., and Coulson, A. R. (1977). DNA sequencing with chain-terminating inhibitors. *Proc Natl Acad Sci U S A* **74**(12), 5463-7.
- Schnittler, H., Stroher, U., Afanasieva, T., and Feldmann, H. (2004). The role of endothelial cells in filovirus hemorrhagic fever. In "Ebola and Marburg Viruses: Molecular and Cellular Biology" (H.-D. Klenk, and H. Feldmann, Eds.), pp. 279-304. Horizon Biosciences, Norfolk.
- Schnittler, H. J., and Feldmann, H. (1998). Marburg and Ebola hemorrhagic fevers: does the primary course of infection depend on the accessibility of organ-specific macrophages? *Clin Infect Dis* **27**(2), 404-6.
- Schnittler, H. J., and Feldmann, H. (1999). Molecular pathogenesis of filovirus infections: role of macrophages and endothelial cells. *Curr Top Microbiol Immunol* **235**, 175-204.
- Schnittler, H. J., and Feldmann, H. (2003). Viral hemorrhagic fever--a vascular disease? *Thromb Haemost* **89**(6), 967-72.
- Schnittler, H. J., Mahner, F., Drenckhahn, D., Klenk, H. D., and Feldmann, H. (1993). Replication of Marburg virus in human endothelial cells. A possible mechanism for the development of viral hemorrhagic disease. *J Clin Invest* **91**(4), 1301-9.
- Seebach, J., Dieterich, P., Luo, F., Schillers, H., Vestweber, D., Oberleithner, H., Galla, H. J., and Schnittler, H. J. (2000). Endothelial barrier function under laminar fluid shear stress. *Lab Invest* **80**(12), 1819-31.
- Simmons, G., Reeves, J. D., Grogan, C. C., Vandenberghe, L. H., Baribaud, F., Whitbeck, J. C., Burke, E., Buchmeier, M. J., Soilleux, E. J., Riley, J. L., Doms, R. W., Bates, P., and

- Pohlmann, S. (2003a). DC-SIGN and DC-SIGNR bind ebola glycoproteins and enhance infection of macrophages and endothelial cells. *Virology* **305**(1), 115-23.
- Simmons, G., Rennekamp, A. J., Chai, N., Vandenberghe, L. H., Riley, J. L., and Bates, P. (2003b). Folate receptor alpha and caveolae are not required for Ebola virus glycoprotein-mediated viral infection. *J Virol* **77**(24), 13433-8.
- Simmons, G., Wool-Lewis, R. J., Baribaud, F., Netter, R. C., and Bates, P. (2002). Ebola virus glycoproteins induce global surface protein down-modulation and loss of cell adherence. *J Virol* **76**(5), 2518-28.
- Sinn, P. L., Hickey, M. A., Staber, P. D., Dylla, D. E., Jeffers, S. A., Davidson, B. L., Sanders, D. A., and McCray, P. B., Jr. (2003). Lentivirus vectors pseudotyped with filoviral envelope glycoproteins transduce airway epithelia from the apical surface independently of folate receptor alpha. *J Virol* **77**(10), 5902-10.
- Slenczka, W. G. (1999). The Marburg virus outbreak of 1967 and subsequent episodes. *Curr Top Microbiol Immunol* **235**, 49-75.
- Smith, D. H., Johnson, B. K., Isaacson, M., Swanapoel, R., Johnson, K. M., Killey, M., Bagshawe, A., Siongok, T., and Keruga, W. K. (1982). Marburg-virus disease in Kenya. *Lancet* **1**(8276), 816-20.
- Spearman, C. (1908). The method of right and wrong cases (constant stimuli) with Gauss formulae. *Brit J Psychol* **2**, 227-242.
- Stille, W., Bohle, E., Helm, E., van Rey, W., and Siede, W. (1968). An infectious disease transmitted by Cercopithecus aethiops. ("Green monkey disease"). *Ger Med Mon* **13**(10), 470-8.
- Stroehrer, U. (2002). Immunoplaque assay for EBOV (V. Jensen, Ed.), Winnipeg.
- Stroher, U., West, E., Bugany, H., Klenk, H. D., Schnittler, H. J., and Feldmann, H. (2001). Infection and activation of monocytes by marburg and ebola viruses. *J Virol* **75**(22), 11025-33.
- Sui, J., and Marasco, W. A. (2002). Evidence against Ebola virus sGP binding to human neutrophils by a specific receptor. *Virology* **303**(1), 9-14.
- Sullivan, N. J., Geisbert, T. W., Geisbert, J. B., Xu, L., Yang, Z. Y., Roederer, M., Koup, R. A., Jahrling, P. B., and Nabel, G. J. (2003). Accelerated vaccination for Ebola virus haemorrhagic fever in non-human primates. *Nature* **424**(6949), 681-4.
- Sullivan, N. J., Sanchez, A., Rollin, P. E., Yang, Z. Y., and Nabel, G. J. (2000). Development of a preventive vaccine for Ebola virus infection in primates. *Nature* **408**(6812), 605-9.
- Takada, A., Robison, C., Goto, H., Sanchez, A., Murti, K. G., Whitt, M. A., and Kawaoka, Y. (1997). A system for functional analysis of Ebola virus glycoprotein. *Proc Natl Acad Sci USA* **94**(26), 14764-9.
- Timmins, J., Schoehn, G., Ricard-Blum, S., Scianimanico, S., Vernet, T., Ruigrok, R. W., and Weissenhorn, W. (2003). Ebola virus matrix protein VP40 interaction with human cellular factors Tsg101 and Nedd4. *J Mol Biol* **326**(2), 493-502.
- Turville, S., Wilkinson, J., Cameron, P., Dable, J., and Cunningham, A. L. (2003). The role of dendritic cell C-type lectin receptors in HIV pathogenesis. *J Leukoc Biol* **74**(5), 710-8.
- Vallet, B. (2003). Bench-to bedside review: endothelial cell dysfunction in severe sepsis: a role in organ dysfunction? *Crit Care* **7**(2), 130-8.

- Vanderzanden, L., Bray, M., Fuller, D., Roberts, T., Custer, D., Spik, K., Jahrling, P., Huggins, J., Schmaljohn, A., and Schmaljohn, C. (1998). DNA vaccines expressing either the GP or NP genes of Ebola virus protect mice from lethal challenge. *Virology* **246**(1), 134-44.
- Vestweber, D. (1992). Selectins: cell surface lectins which mediate the binding of leukocytes to endothelial cells. *Semin Cell Biol* **3**(3), 211-20.
- Vestweber, D. (1993). The selectins and their ligands. *Curr Top Microbiol Immunol* **184**, 65-75.
- Villinger, F., Rollin, P. E., Brar, S. S., Chikkala, N. F., Winter, J., Sundstrom, J. B., Zaki, S. R., Swanepoel, R., Ansari, A. A., and Peters, C. J. (1999). Markedly elevated levels of interferon (IFN)-gamma, IFN-alpha, interleukin (IL)-2, IL-10, and tumor necrosis factor-alpha associated with fatal Ebola virus infection. *J Infect Dis* **179 Suppl 1**, S188-91.
- Volchkov, V., Blinov, V., Kotov, A., Chepurnov A., and S. Netesov (1993). *LXth International Congress of Virology, Glasgow, Scotland*.
- Volchkov, V. E. (1999). Processing of the Ebola virus glycoprotein. *Curr Top Microbiol Immunol* **235**, 35-47.
- Volchkov, V. E., Becker, S., Volchkova, V. A., Ternovoj, V. A., Kotov, A. N., Netesov, S. V., and Klenk, H. D. (1995). GP mRNA of Ebola virus is edited by the Ebola virus polymerase and by T7 and vaccinia virus polymerases. *Virology* **214**(2), 421-30.
- Volchkov, V. E., Blinov, V. M., and Netesov, S. V. (1992). The envelope glycoprotein of Ebola virus contains an immunosuppressive-like domain similar to oncogenic retroviruses. *FEBS Lett* **305**(3), 181-4.
- Volchkov, V. E., Chepurnov, A. A., Volchkova, V. A., Ternovoj, V. A., and Klenk, H. D. (2000). Molecular characterization of guinea pig-adapted variants of Ebola virus. *Virology* **277**(1), 147-55.
- Volchkov, V. E., Feldmann, H., Volchkova, V. A., and Klenk, H. D. (1998a). Processing of the Ebola virus glycoprotein by the proprotein convertase furin. *Proc Natl Acad Sci U S A* **95**(10), 5762-7.
- Volchkov, V. E., Volchkova, V. A., Chepurnov, A. A., Blinov, V. M., Dolnik, O., Netesov, S. V., and Feldmann, H. (1999). Characterization of the L gene and 5' trailer region of Ebola virus. *J Gen Virol* **80 (Pt 2)**, 355-62.
- Volchkov, V. E., Volchkova, V. A., Muhlberger, E., Kolesnikova, L. V., Weik, M., Dolnik, O., and Klenk, H. D. (2001). Recovery of infectious Ebola virus from complementary DNA: RNA editing of the GP gene and viral cytotoxicity. *Science* **291**(5510), 1965-9.
- Volchkov, V. E., Volchkova, V. A., Slenczka, W., Klenk, H. D., and Feldmann, H. (1998b). Release of viral glycoproteins during Ebola virus infection. *Virology* **245**(1), 110-9.
- Volchkova, V. A., Feldmann, H., Klenk, H. D., and Volchkov, V. E. (1998). The nonstructural small glycoprotein sGP of Ebola virus is secreted as an antiparallel-orientated homodimer. *Virology* **250**(2), 408-14.
- Volchkova, V. A., Klenk, H. D., and Volchkov, V. E. (1999). Delta-peptide is the carboxy-terminal cleavage fragment of the nonstructural small glycoprotein sGP of Ebola virus. *Virology* **265**(1), 164-71.
- Warfield, K. L., Bosio, C. M., Welcher, B. C., Deal, E. M., Mohamadzadeh, M., Schmaljohn, A., Aman, M. J., and Bavari, S. (2003). Ebola virus-like particles protect from lethal Ebola virus infection. *Proc Natl Acad Sci U S A* **100**(26), 15889-94.

- Watanabe, S., Takada, A., Watanabe, T., Ito, H., Kida, H., and Kawaoka, Y. (2000). Functional importance of the coiled-coil of the Ebola virus glycoprotein. *J Virol* **74**(21), 10194-201.
- Watanabe, S., Watanabe, T., Noda, T., Takada, A., Feldmann, H., Jasenosky, L. D., and Kawaoka, Y. (2004). Production of Novel Ebola Virus-Like Particles from cDNAs: an Alternative to Ebola Virus Generation by Reverse Genetics. *J Virol* **78**(2), 999-1005.
- Weissenhorn, W., Carfi, A., Lee, K. H., Skehel, J. J., and Wiley, D. C. (1998). Crystal structure of the Ebola virus membrane fusion subunit, GP2, from the envelope glycoprotein ectodomain. *Mol Cell* **2**(5), 605-16.
- Whelan, S. P., Ball, L. A., Barr, J. N., and Wertz, G. T. (1995). Efficient recovery of infectious vesicular stomatitis virus entirely from cDNA clones. *Proc Natl Acad Sci USA* **92**(18), 8388-92.
- Whitaker, A. M., and Hayward, C. J. (1985). The characterization of three monkey kidney cell lines. *Dev Biol Stand* **60**, 125-31.
- Bull World Health Organ (1976). Ebola haemorrhagic fever in Sudan, 1976. WHO.
- Bull World Health Organ (1978). Ebola haemorrhagic fever in Zaire, 1976. Report of an international commission. WHO.
- WHO (1992). Viral haemorrhagic fever in imported monkeys. *Wkly Epidemiol Rec* **67**, 142-143.
- WHO (1997). Ebola haemorrhagic fever. A summary of the outbreak in Gabon. *Wkly Epidemiol Rec* **72**(1-2), 7-8.
- WHO (1999). Weekly Epidemiological Record. WHO. 20. May 21, 2003.
- WHO (2002). Ebola haemorrhagic fever in Gabon - Update 23. WHO. May 9, 2002.
- WHO (2003a). Ebola haemorrhagic fever in the Republic of the Congo - Update 2. WHO. November 21, 2003.
- WHO (2003b). Ebola haemorrhagic fever in the Republic of the Congo - Update 12. WHO. May 7, 2003.
- Will, C., Muhlberger, E., Linder, D., Slenczka, W., Klenk, H. D., and Feldmann, H. (1993). Marburg virus gene 4 encodes the virion membrane protein, a type I transmembrane glycoprotein. *J Virol* **67**(3), 1203-10.
- Wilson, J. A., Bray, M., Bakken, R., and Hart, M. K. (2001). Vaccine potential of Ebola virus VP24, VP30, VP35, and VP40 proteins. *Virology* **286**(2), 384-90.
- Wilson, J. A., and Hart, M. K. (2001). Protection from Ebola virus mediated by cytotoxic T lymphocytes specific for the viral nucleoprotein. *J Virol* **75**(6), 2660-4.
- Wilson, J. A., Hevey, M., Bakken, R., Guest, S., Bray, M., Schmaljohn, A. L., and Hart, M. K. (2000). Epitopes involved in antibody-mediated protection from Ebola virus. *Science* **287**(5458), 1664-6.
- Wool-Lewis, R. J., and Bates, P. (1998). Characterization of Ebola virus entry by using pseudotyped viruses: identification of receptor-deficient cell lines. *J Virol* **72**(4), 3155-60.
- Xu, L., Sanchez, A., Yang, Z., Zaki, S. R., Nabel, E. G., Nichol, S. T., and Nabel, G. J. (1998). Immunization for Ebola virus infection. *Nat Med* **4**(1), 37-42.
- Xu, X., Nash, P., and McFadden, G. (2000). Myxoma virus expresses a TNF receptor homolog with two distinct functions. *Virus Genes* **21**(1-2), 97-109.

- Yang, Z., Delgado, R., Xu, L., Todd, R. F., Nabel, E. G., Sanchez, A., and Nabel, G. J. (1998). Distinct cellular interactions of secreted and transmembrane Ebola virus glycoproteins. *Science* **279**(5353), 1034-7.
- Yang, Z. Y., Duckers, H. J., Sullivan, N. J., Sanchez, A., Nabel, E. G., and Nabel, G. J. (2000). Identification of the Ebola virus glycoprotein as the main viral determinant of vascular cell cytotoxicity and injury. *Nat Med* **6**(8), 886-9.
- Yasuda, J., Nakao, M., Kawaoka, Y., and Shida, H. (2003). Nedd4 Regulates Egress of Ebola Virus-Like Particles from Host Cells. *J Virol* **77**(18), 9987-9992.
- Zaki, S. R., and Goldsmith, C. S. (1999). Pathologic features of filovirus infections in humans. *Curr Top Microbiol Immunol* **235**, 97-116.
- Zaki, S. R., and Peters, C. J. (1997). Viral hemorrhagic fevers. In "The pathology of infectious diseases" (D. H. Connor, F. W. Chandler, D. A. Schwartz, H. J. Manz, and E. E. Lack, Eds.), pp. 347-364. Appleton and Lange, Norwalk, CT.

A Primer List

Primer #	Name	Sequence (5'-3')	RE sites	Insert/Vector (plasmid generated)
49	MARVgp1 Sallr	GCGCGGTCGACTTACTATCGCTTCTTCTGAAATATACAAG	Sall	MARV Musoke GP1/pDisplay (5.2)
73	MARVgp1 Bgl2f	GCGCGCAGATCTCTCCCATTTAGAGATAGCTAG	BglII	
67	MARVgp1XhoIf	GCGCGCTCGAGAACAATGAAGACCACATGTTTCC	XhoI	
68	MARVgpNheIr	GCGCGGCTAGCTTACTATCGCTTCTTCTGAAATATACAAG	NheI	MARV Musoke GP1/VSVXN2 (3)
85	EBOVGPBgl2f	GACAGATCTATCCCACTGGAGTCAATCC	BglII	ZEBOV Mayinga GP1/pDisplay (4)
87	EBOVGP1SacIIr	GACCCGGGTTACTATCTTCGAGTCTTCTCTCCCG	SacII	
85	EBOVGPBgl2f	GACAGATCTATCCCACTGGAGTCAATCC	BglII	ZEBOV Mayinga sGP/pDisplay (5)
86	EBOVsGPPstIr	GACCTGCAGTTACTAGCGCCGGACTCTGACC	PstI	
173	EBOVdPBgl2f	GACAGATCTGAACTTCTTCCGACCCAG	BglII	ZEBOV Mayinga Δ peptide/pDisplay (36)
174	EBOVdPSac2r	GACCCGGGTTATTAGATGCGGACACTGCAG	SacII	
175	EBOVGP2Bgl2f	GACAGATCTGAAAGCAAATTGTCAATGCT	BglII	ZEBOV Mayinga GP2/pDisplay (37)
176	EBOVGP2Sac2r	GACCCGGGTTACTAAAAGACAAATTTGC	SacII	
177	EBOVGP2fus Bgl2f	GACAGATCTGGTGCTGCAATCGGACTG	BglII	ZEBOV Mayinga GP2 fusion domain/pDisplay (38)
178	EBOVdPEcoRIIf	GACGAAATTCACCATGGAACCTTCTTCCGACCCAG	EcoRI	
179	EBOVdPXhoIr	GACCTCGAGTTATTAGATGCGGACACTGCAG	XhoI	ZEBOV Mayinga Δ peptide/pTM1 (8A)

Primer #	Name	Sequence (5'-3')	RE sites	Insert/Vector (plasmid generated)
178	EBOVdPEcoRif	GACCGAATTCACCATGGAACCTTCTTCCGACCCAG	EcoRI	ZEBOV Mayinga Δ peptide/pCAGGS (35)
179	EBOVdPXhoI	GACCTCGAGTTATTAGATGCCACTGCAG	XhoI	
85	EBOVGPBgl2f	GACAGATCTATCCCACCTGGAGTCATCC	BglII	ZEBOV Mayinga GP1,2/pDisplay (72)
176	EBOVGP2Sac2r	GACCCGCGGTTACTAAAGACAAAATTTGC	SacII	
600	EBOVGP1,2EcoRif	GACCGAATTCATGGGCGTTACAGGAATATTG	EcoRI	ZEBOV Mayinga GP1,2/pCAGGS (162)
601	EBOVGP1,2XhoI	GACCTCGAGCTAAAGACAAAATTTGC	XhoI	
602	EBOVVP40EcoRif	GACCGAATTCATGAGGCGGGTTATATTGCCTAC	EcoRI	ZEBOV Mayinga VP40/pCAGGS (161)
603	EBOVVP40XhoI	GACCTCGAGTTACTTCTCAATCACAGCTGG	XhoI	
85	EBOVGPBgl2f	GACAGATCTATCCCACCTGGAGTCATCC	BglII	ZEBOV Mayinga GP1,2ΔTM /pDisplay (164)
631	EBOVGP1,2shed Sac2r	GACCCGCGGTTACTAGTCCGGGAAGGGTTTATCAAC	SacI	
356	b-actin1f	GTGGGGCGCCCCAGGCACCA	--	
357	b-actin2r	CTCCTTAATGTACGCACGATTC	--	
358	TNF1f	AGCATGATCCGGGACGTGGAG	--	
359	TNF2r	CCCAGACTCGGCAAAAGTCGAG	--	
360	IL-1b1f	TGGCAGAAGTACCTGAGCTCG	--	
361	IL-1b2r	TTAGGAAGACACAAAATTGCATGGTG	--	
362	IL-61f	CTCCTTCTCCACAAGCGCCTCG	--	
363	IL-62r	GAGCCCTCAGGCTGGACTGCAGG	--	
364	IL8-1f	TTCTGCAGCTCTGTGTGAAGGTAAG	--	
365	IL-8-2r	GGATCCTGGCTAGCAGACTAG	--	
366	gro-1f	CAGTGTTCAGACCCTG	--	

Primer #	Name	Sequence (5'-3')	RE sites	Insert/Vector (plasmid generated)
367	gro-2r	CATGTTGCAGGCTCCTCAG	--	
377	TissueFf	AGTGTGACCTCACCGACGAGA	--	
378	TissueFr	AGCCAGGATGATGACAAAGGATG	--	
380	GAPDHf	GGTTTTCTAGACGGCAGGTCA	--	
381	GAPDHr	TGGCAAATTCATGGCACCCGTCA	--	
382	ICAM-1f	CAGTGACTGTCACCTCGAGATCT	--	
383	ICAM-1r	CCTCTTGGCTTAGTCATGTGAC	--	
384	VCAM-1f	CTGGAGGATGCAGACAGGAAG	--	
385	VCAM1-r	CCAATCTGAGCAGCAATCCGG	--	
386	E-selectinf	AGTGCCACCGTGAATGTGTA	--	
387	E-selectinr	CCCAGATGAGGTACACTGAAG	--	
532	C53G fwd	GTCGACAAACTAGTTGGTCGTGACAAACTGTCAATCC	--	ZEBOV Mayinga GP1 mutant; C53G (111)
533	C53G rev	GGATGACAGTTTGTACACGACCAACTAGTTTGTCCGAC	--	
534	C108G fwd	GGTGAATGGGCTGAAAACGGCTACAACTTTGAAATC	--	ZEBOV Mayinga GP1 mutant; C108G (112)
535	C108G rev	GATTTCAAAGATTGTAGCCGTTTTCAGCCCAATTCACC	--	
536	C121G fwd	CCTGACGGGAGTGAGGGTCTACCAGCAGCGCCAGACGG G	--	ZEBOV Mayinga GP1 mutant; C121G (120)
537	C121G rev	CCGTCTGGCCGCTGCTGGTAGACCCCTCACTCCCCTCAGG	--	
538	C135G fwd	CGGGGCTTCCCCCGGGCCGGTATGTGCACAAAAG	--	ZEBOV Mayinga GP1 mutant; C135G (113)
539	C135G rev	CTTTGTGCACATACCCGGCCCCGGGAAAGCCCCCG	--	
540	C147G fwd	CAGGAACGGACCGGGTGCCTCGGAGACTTTTGCC	--	ZEBOV Mayinga GP1 mutant; C147G (114)
541	C147G fwd	GGCAAAGTCTCCGGCACCCCGTCCCCTCCCTG	--	
592	C511G fwd	CAATGCTCAACCCCAAAGGCAACCCTAATTTACATTACT GG	--	ZEBOV Mayinga GP2 mutant; C511G (121)
593	C511G rev	CCAGTAATGTAAATTAGGGTTGCCCTTTGGGTTGAGCAT TG	--	
594	C556G fwd	CAATCAAGATGGTTTAAATCCGGTGGGTTGAGACAGCTG GCC	--	ZEBOV Mayinga GP2 mutant; C556G

Primer #	Name	Sequence (5'-3')	RE sites	Insert/Vector (plasmid generated)
595	C556G rev	GGCCAGCTGTCTCAACCCACCAGATTAAACCACTTTGAT TG	--	(122)
596	C601G fwd	GCAAGCGATGGGGCGGCACAGGCCACATTCTGGGACCG G	--	ZEBOV Mayinga GP2 mutant; C601G (123)
597	C601G rev	CCGGTCCCAGAAATGTGGCCTGTGCCGCCCCCATCGCTGC	--	
598	C608G fwd	GCCACATTCTGGGACCGGACGGCTGTATCGAACCCACA TGATTGG	--	ZEBOV Mayinga GP2 mutant; C608G (124)
599	C608G rev	CCAATCATGTGGTTCGATACAGCCCGTCCCGGTCCCAG ATGTGGC	--	
600	C609G fwd	GCCACATTCTGGGACCGGACTGCGGTATCGAACCCACA TGATTGG	--	ZEBOV Mayinga GP2 mutant; C609G (126)
601	C609G rev	CCAATCATGTGGTTCGATACCGCAGTCCCGGTCCCAG ATGTGGC	--	

B Protein Purification Scheme

(Figure 58)

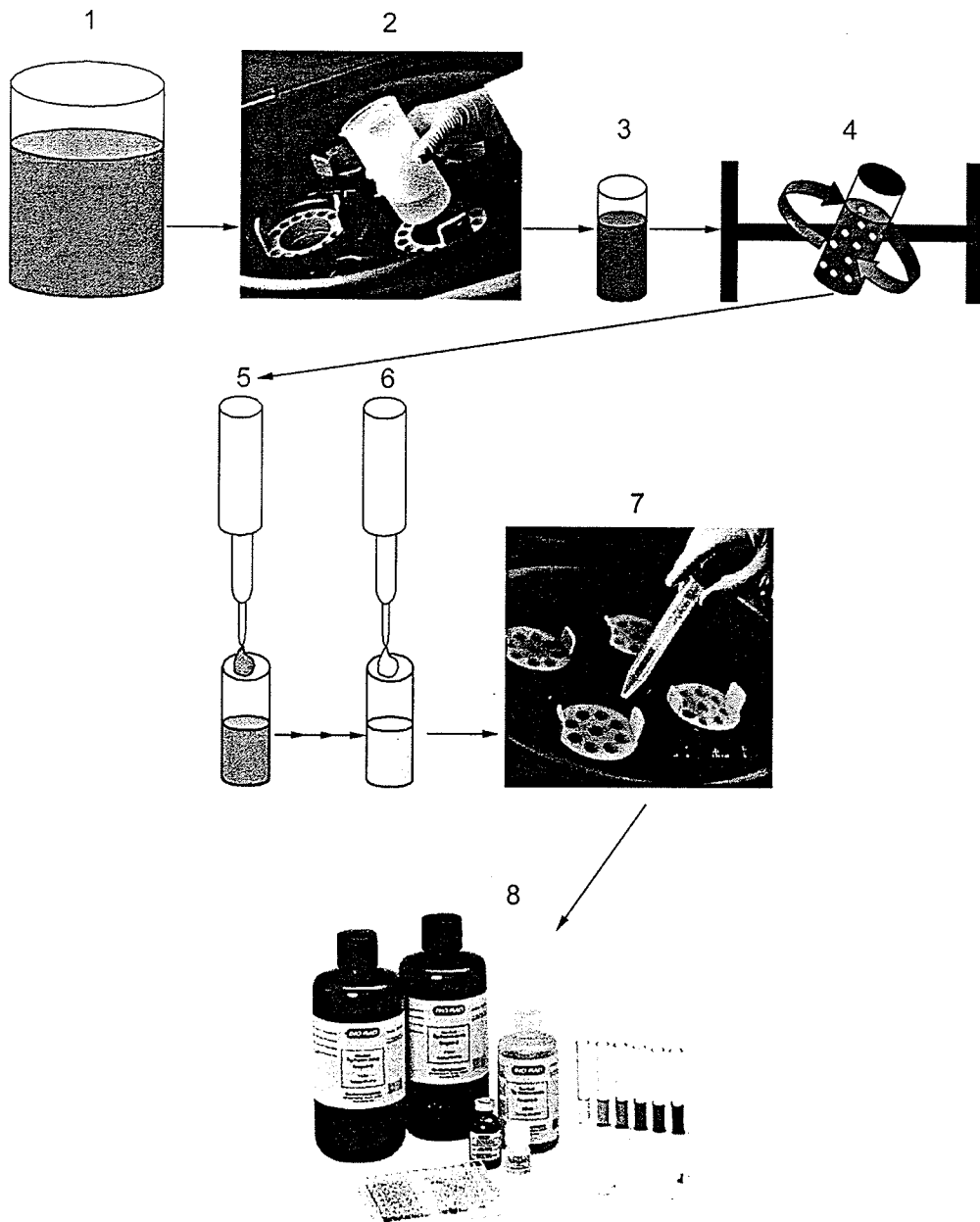


Figure 58. Protein purification scheme. 150mL of media is collected from 3 (triple layer) flasks (1) and concentrated using Centricon Plus 80 size exclusion centrifugation (2). Concentrated media (3) is added to anti-HA matrix and batch purified for 1.5h at room temperature with end-over-end rotation (4). Media + matrix is added back to the chromatography column and media flows through while matrix + protein remains (5). The column is washed 3X and protein competitively eluted with HA peptide (3 elutions) (6). The combined eluate is concentrated and HA peptide removed by Amicon Ultra size exclusion centrifugation (7). Total protein concentration is determined using a commercial protein assay kit (8). Purified protein is aliquoted and stored at -20C.

C Buffers for protein purification

EQUILIBRATION BUFFER

20mM Tris (pH 7.5); 0.1M NaCl; 0.1mM EDTA (TNE)

Tris: 1.0M stock, pH 7.5
(1.0M)x = (0.02M)(400mL)
x = 8mL of 1.0M stock Tris-HCl

NaCl: 5.0M stock
(5.0M)x = (0.1M)(400mL)
x = 8mL of 5.0M stock NaCl

EDTA: 0.5M stock (Gibco)
(0.5M)x = (0.0001M)(400mL)
x = 0.08mL or 80μL EDTA

Add all above components to a flask. Add 375.92mL sdH₂O. Filter sterilize.

WASH BUFFER

Equilibration buffer + 0.05% Tween-20
Tween-20 = 100% stock

(100%) x = (0.05%)(60mL)
x = 0.30mL or 30μL

Add 30μL Tween-20 to 60mL equilibration buffer

COLUMN STORAGE BUFFER

Equilibration buffer + 0.09% sodium azide
Sodium azide = 2.0% stock solution

(2.0%)x = (0.09%)(5mL)
x = 225μL of 2.0% sodium azide + 4.775mL equilibration buffer

REGENERATION BUFFER

0.1M glycine, pH 2.0

- Add 0.375g glycine to 50mL sdH₂O
- pH to 2.0 with 10N HCl (approx. 6 drops)
- Filter sterilize with syringe tip filter

D Supporting data for HUVEC activation studies

(Figure 59)

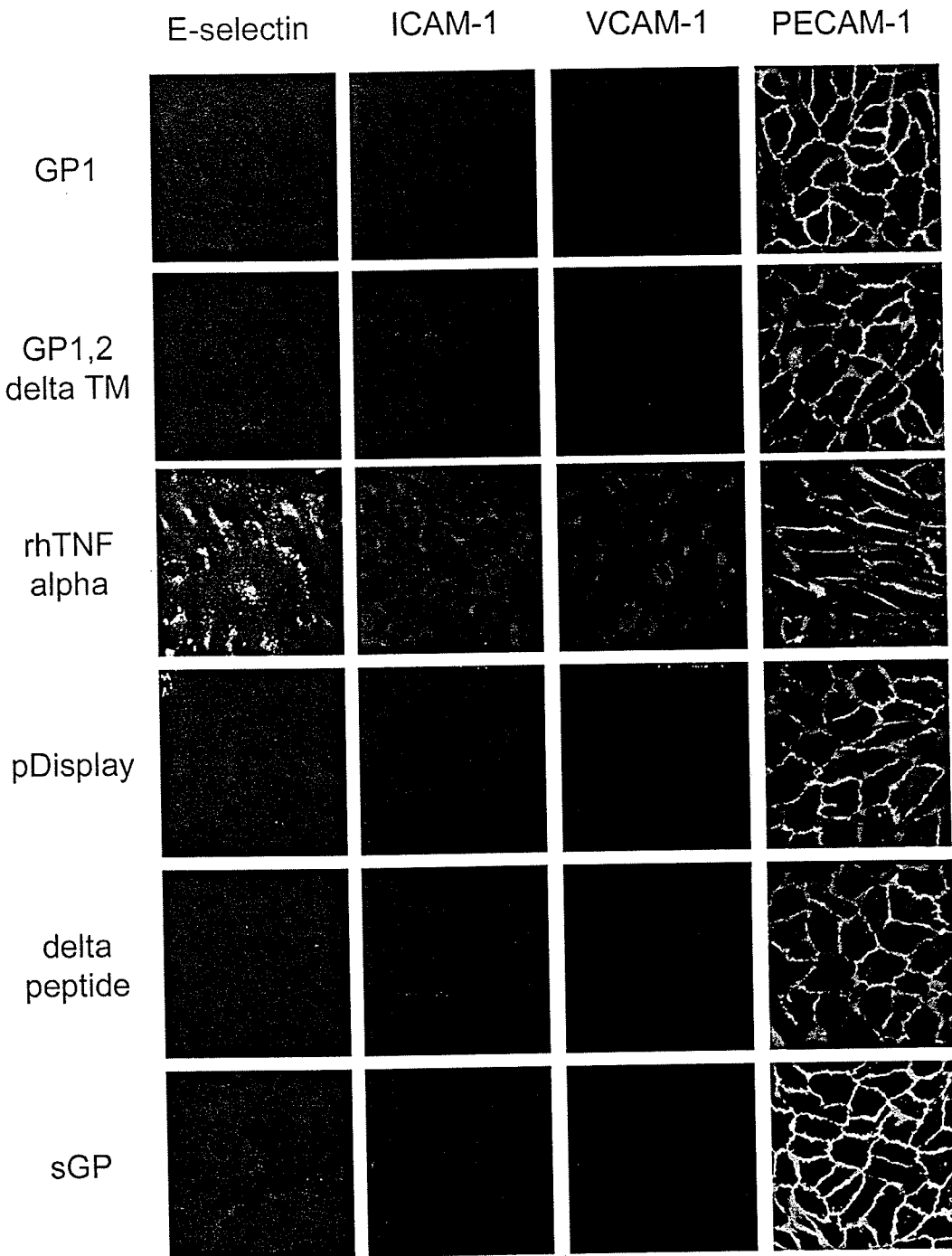


Figure 59. Activation of HUVECs. HUVECs were treated with soluble proteins at a concentration of 10ug/ml. After 6 h post-treatment cells were fixed, permeabilized and stained for E-selectin, ICAM-1, VCAM-1 and PECAM-1. Images acquired at 400X magnification.

(Figure 60)

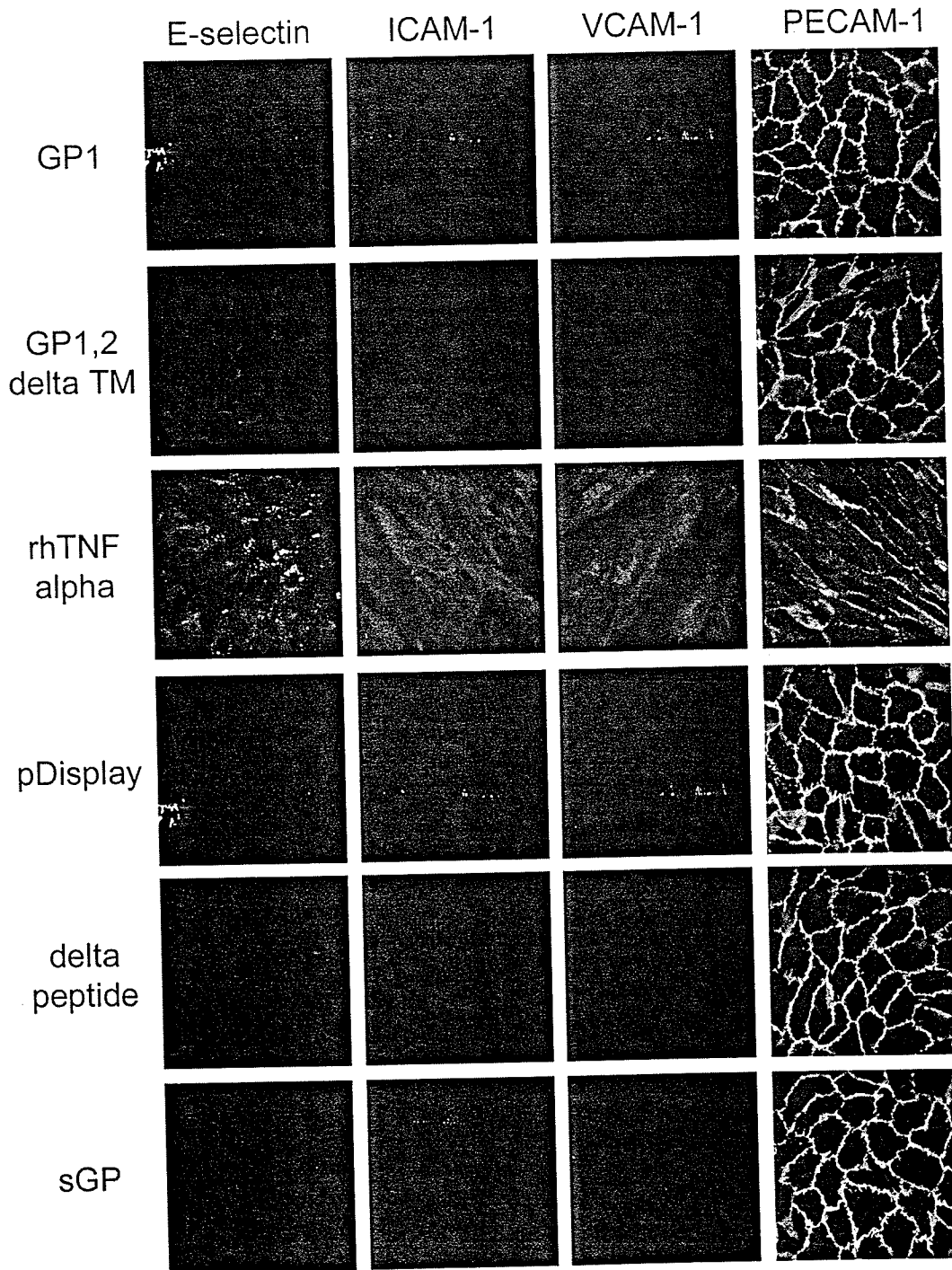


Figure 60. Activation of HUVECs. HUVECs were treated with soluble proteins at a concentration of 10ug/ml. After 12 h post-treatment cells were fixed, permeabilized and stained for E-selectin, ICAM-1, VCAM-1 and PECAM-1. Images acquired at 400X magnification.

(Figure 61)

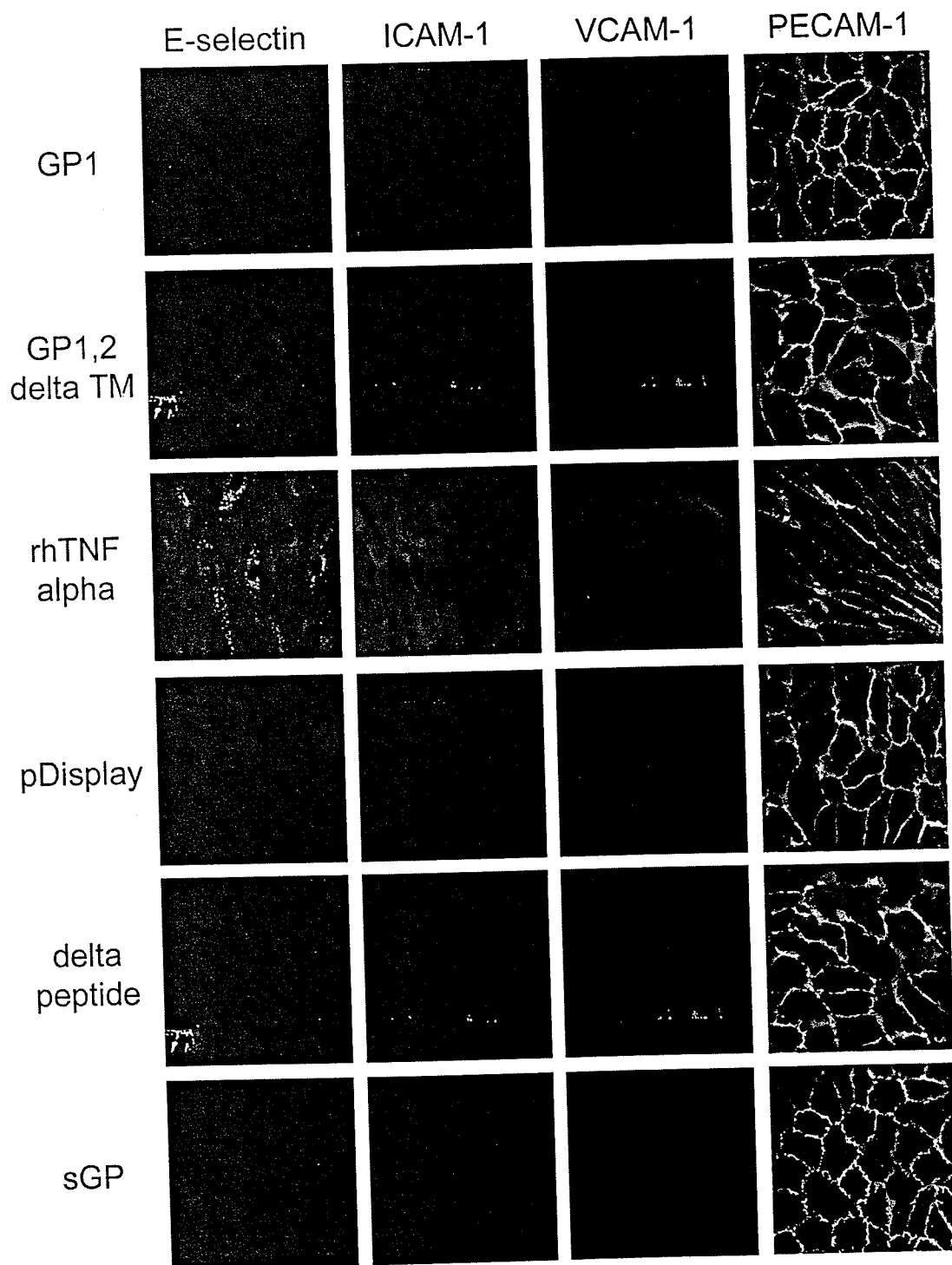


Figure 61. Activation of HUVECs. HUVECs were treated with soluble proteins at a concentration of 10ug/ml. After 24 h post-treatment cells were fixed, permeabilized and stained for E-selectin, ICAM-1, VCAM-1 and PECAM-1. Images acquired at 400X magnification.

(Figure 62)

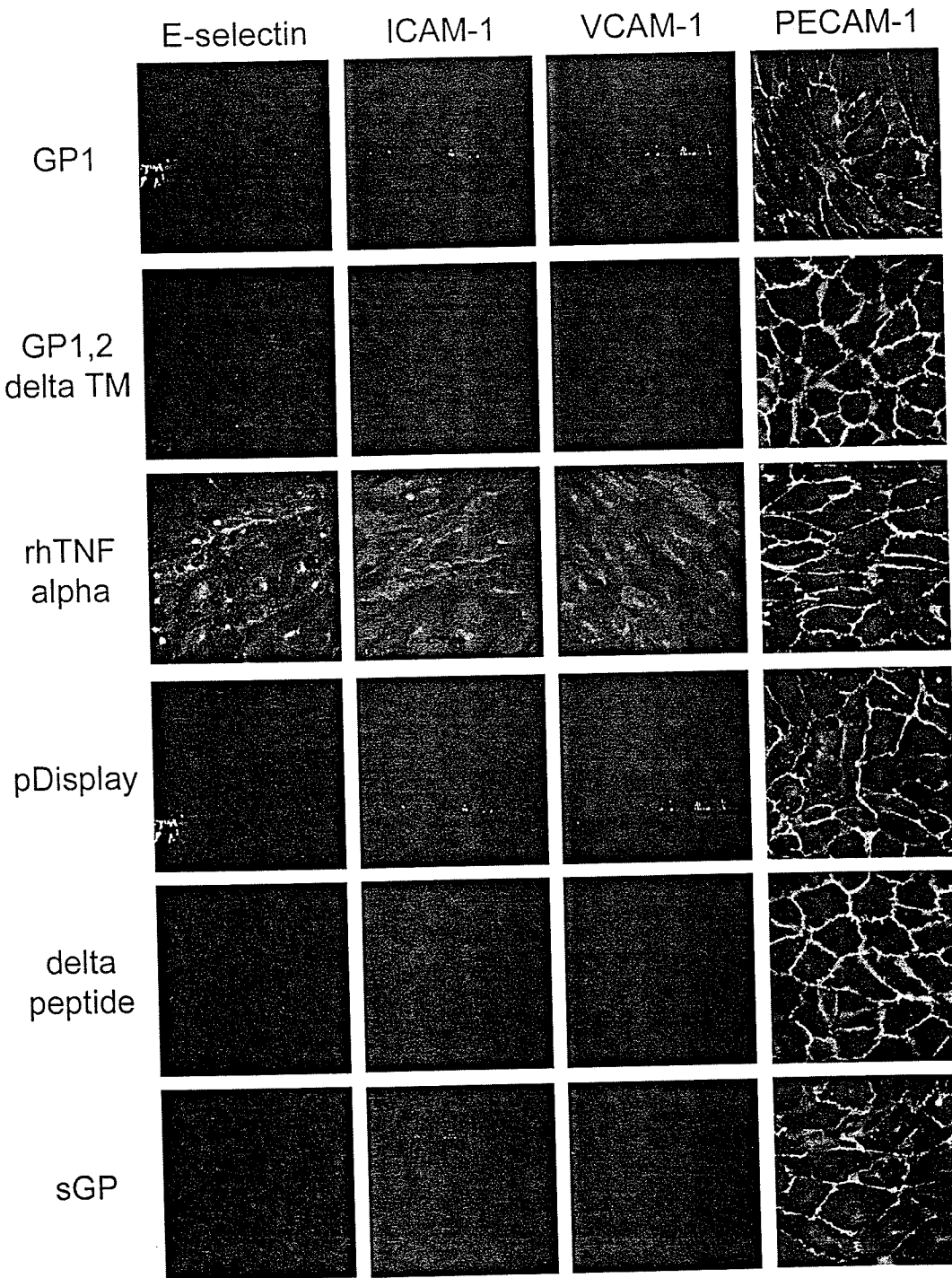


Figure 62. Activation of HUVECs. HUVECs were treated with soluble proteins at a concentration of 50ug/ml. After 6 h post-treatment cells were fixed, permeabilized and stained for E-selectin, ICAM-1, VCAM-1 and PECAM-1. Images acquired at 400X magnification.

(Figure 63)

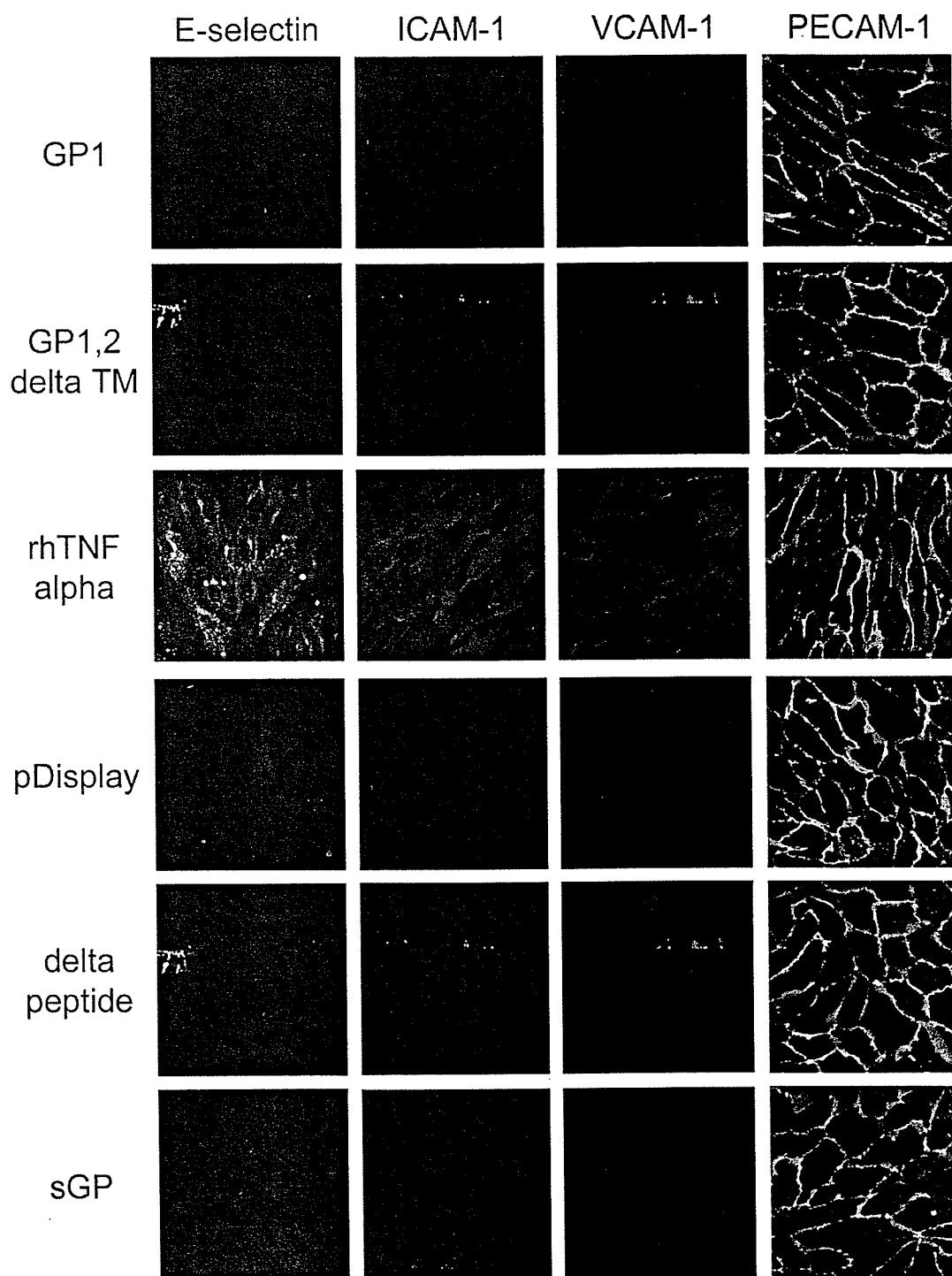


Figure 63. Activation of HUVECs. HUVECs were treated with soluble proteins at a concentration of 50ug/ml. After 12 h post-treatment cells were fixed, permeabilized and stained for E-selectin, ICAM-1, VCAM-1 and PECAM-1. Images acquired at 400X magnification.

(Figure 64)

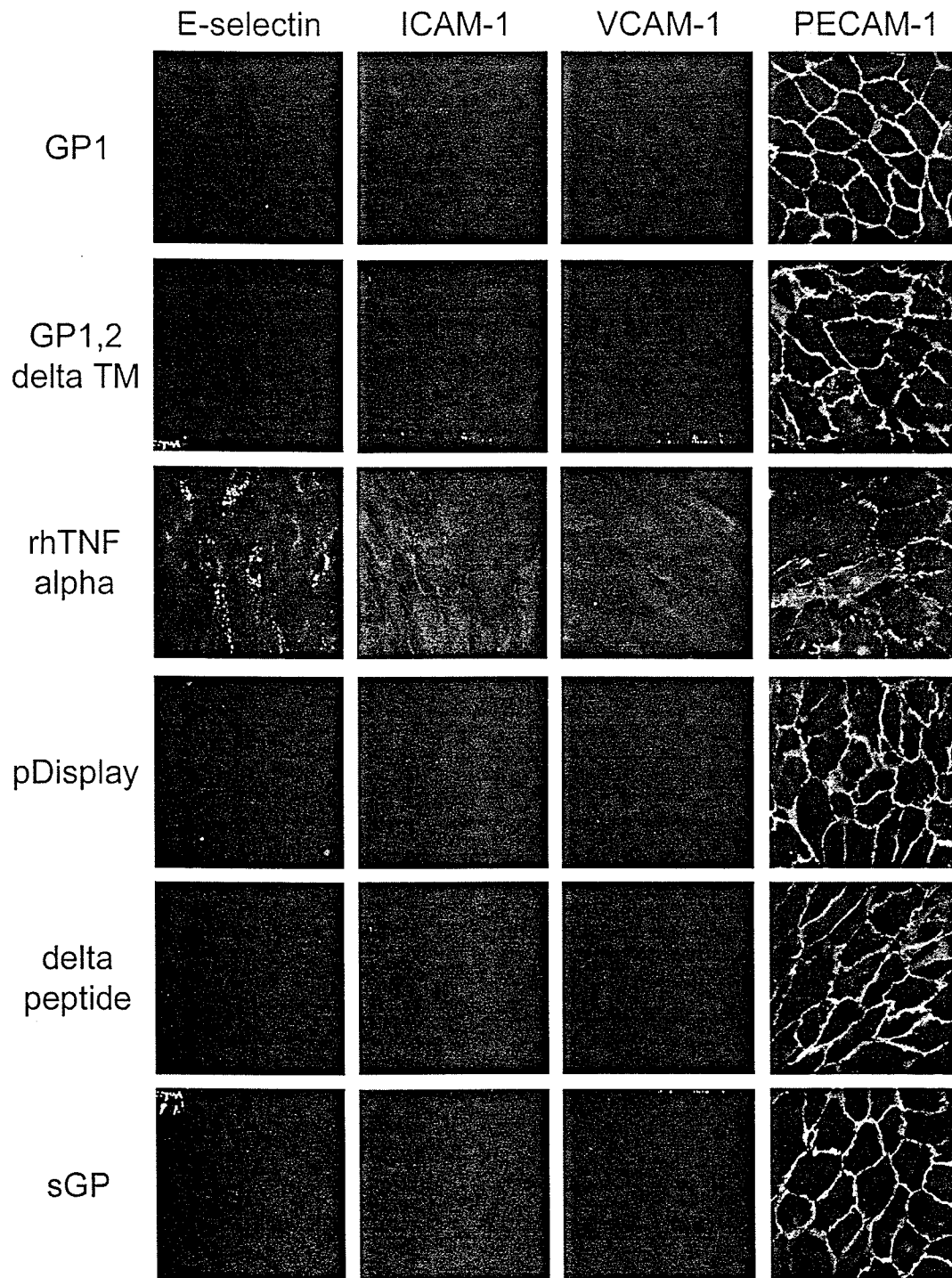


Figure 64. Activation of HUVECs. HUVECs were treated with soluble proteins at a concentration of 50ug/ml. After 24 h post-treatment cells were fixed, permeabilized and stained for E-selectin, ICAM-1, VCAM-1 and PECAM-1. Images acquired at 400X magnification.

(Figure 65)

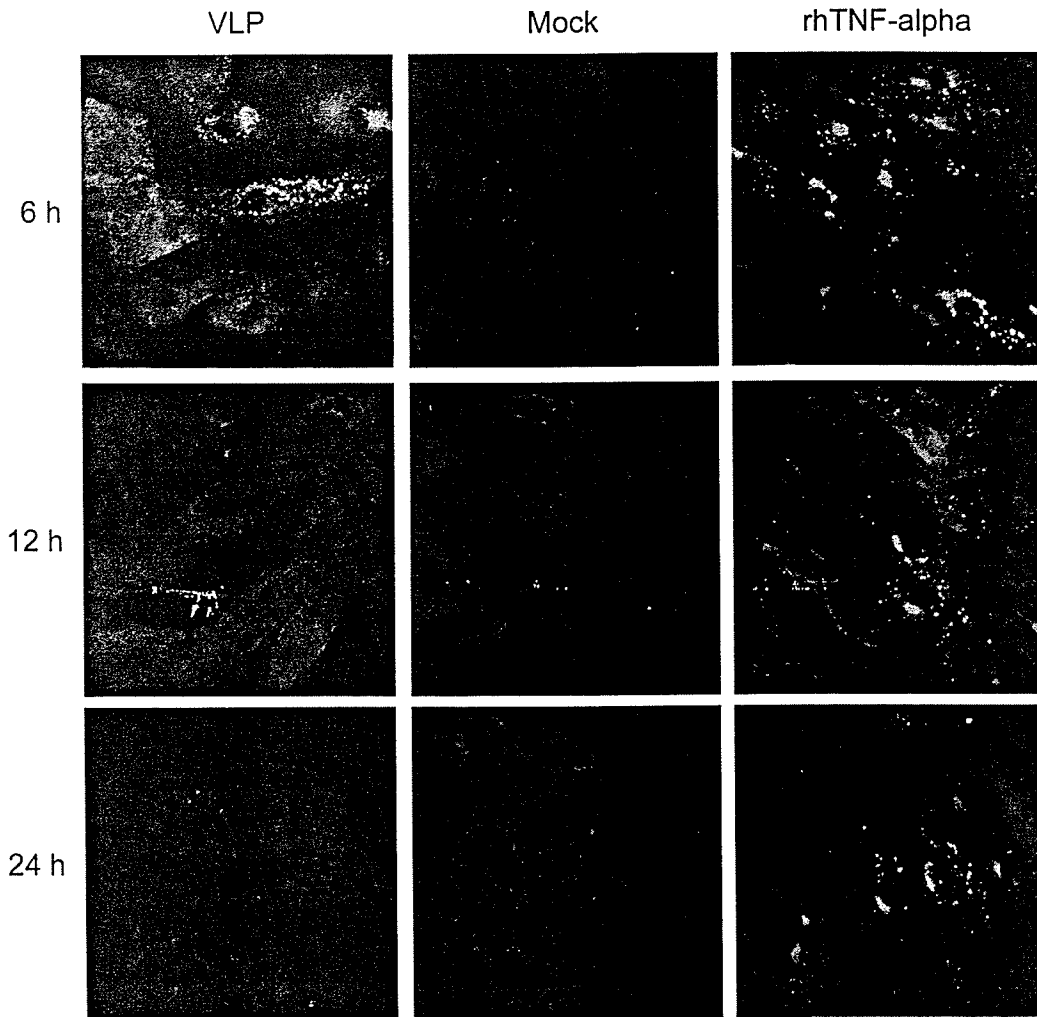


Figure 65. Upregulation of E-selectin by VLPs. HUVECs were treated with VLPs ('MOI' 10), mock or rhTNF-alpha (100ng/mL). Cells were fixed at 6, 12 and 24 hours post treatment and immunostained for E-selectin. Images acquired at 400X magnification.

(Figure 66)

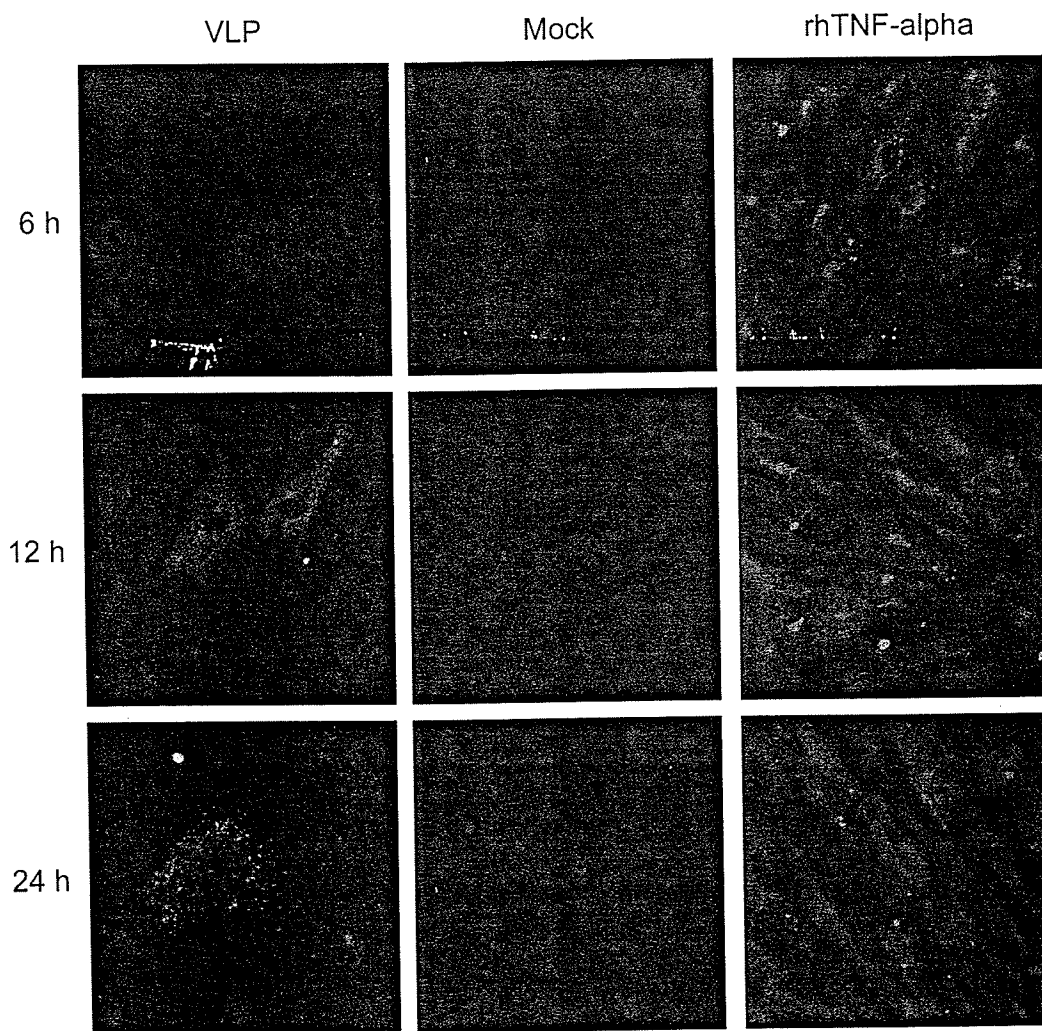


Figure 66. Upregulation of ICAM-1 by VLPs. HUVECs were treated with VLPs ('MOI' 10), mock or rhTNF-alpha (100ng/mL). Cells were fixed at 6, 12 and 24 hours post treatment and immunostained for ICAM-1. Images acquired at 400X magnification.

(Figure 67)

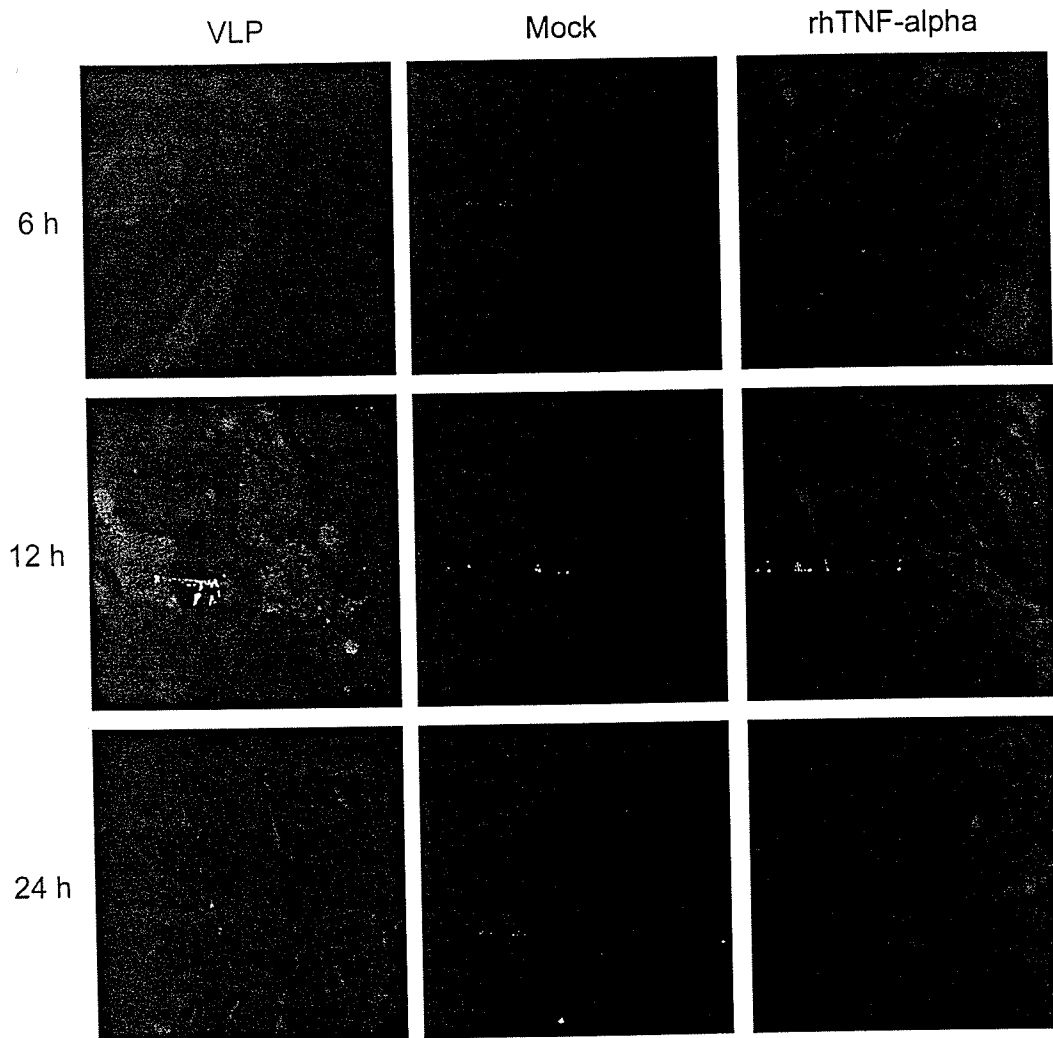


Figure 67. Upregulation of VCAM-1 by VLPs. HUVECs were treated with VLPs ('MOI' 10), mock or rhTNF-alpha (100ng/mL). Cells were fixed at 6, 12 and 24 hours post treatment and immunostained for VCAM-1. Images acquired at 400X magnification.

E Supporting data for VE-cadherin/actin staining of HUVECs

(Figure 68)

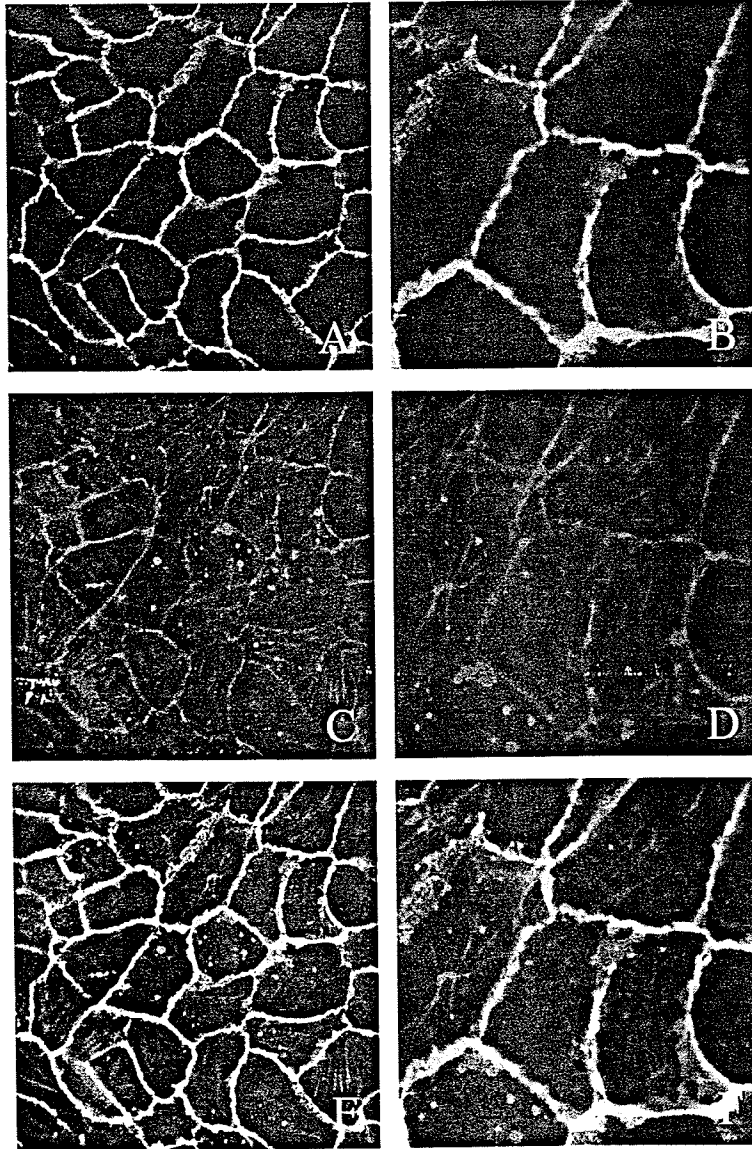


Figure 68. VEcadherin and rhodamine labelled phalloidin staining of HUVECs treated with 10ug/mL of GP1,2-delta-TM. Human umbilical vein endothelial cells (HUVEC) were treated with 10ug/mL of GP1,2-delta-TM for 24 hours. Cells were stained with antibodies to VE-cadherin (A) and shown at higher magnification in (B) or with rhodamine labelled phalloidin in (C) and higher magnification in (D). Images were merged to show distribution of cellular actin within cells in (E) and higher magnification in (F). Images were acquired at 400X magnification.

(Figure 69)

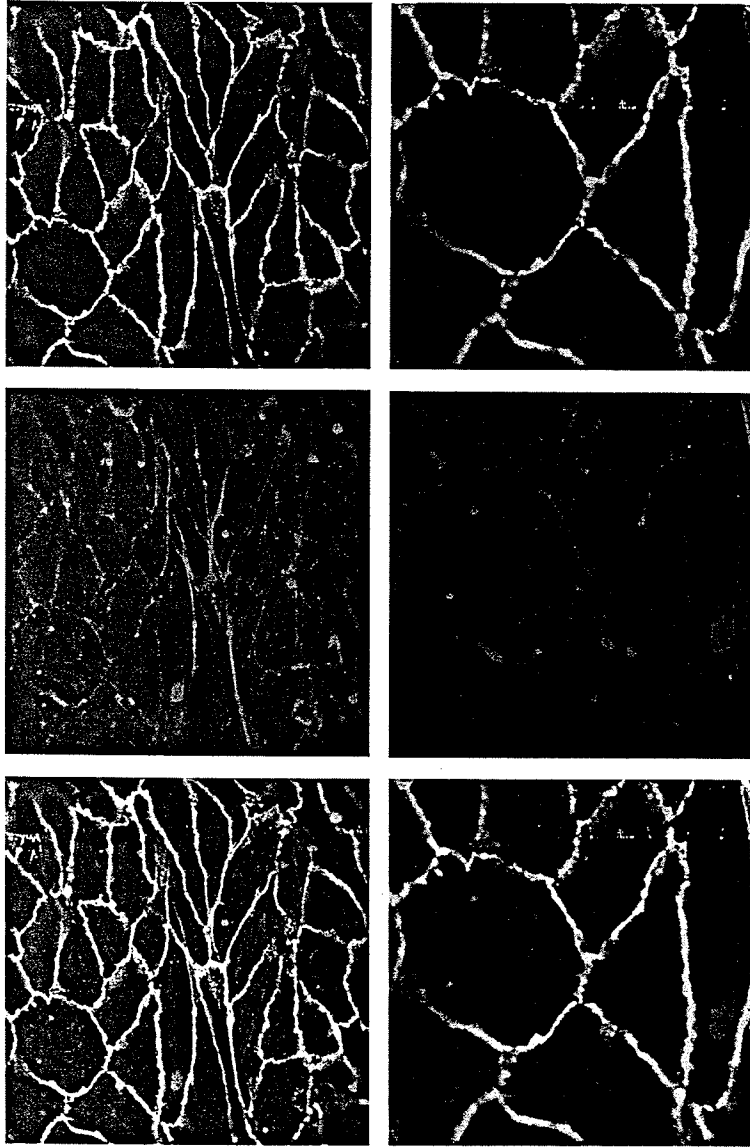


Figure 69. VEcadherin and rhodamine labelled phalloidin staining of HUVECs treated with 10ug/mL of delta peptide. Human umbilical vein endothelial cells (HUVEC) were treated with 10ug/mL of delta peptide for 24 hours. Cells were stained with antibodies to VE-cadherin (A) and shown at higher magnification in (B) or with rhodamine labelled phalloidin in (C) and higher magnification in (D). Images were merged to show distribution of cellular actin within cells in (E) and higher magnification in (F). Images were acquired at 400X magnification.

(Figure 70)

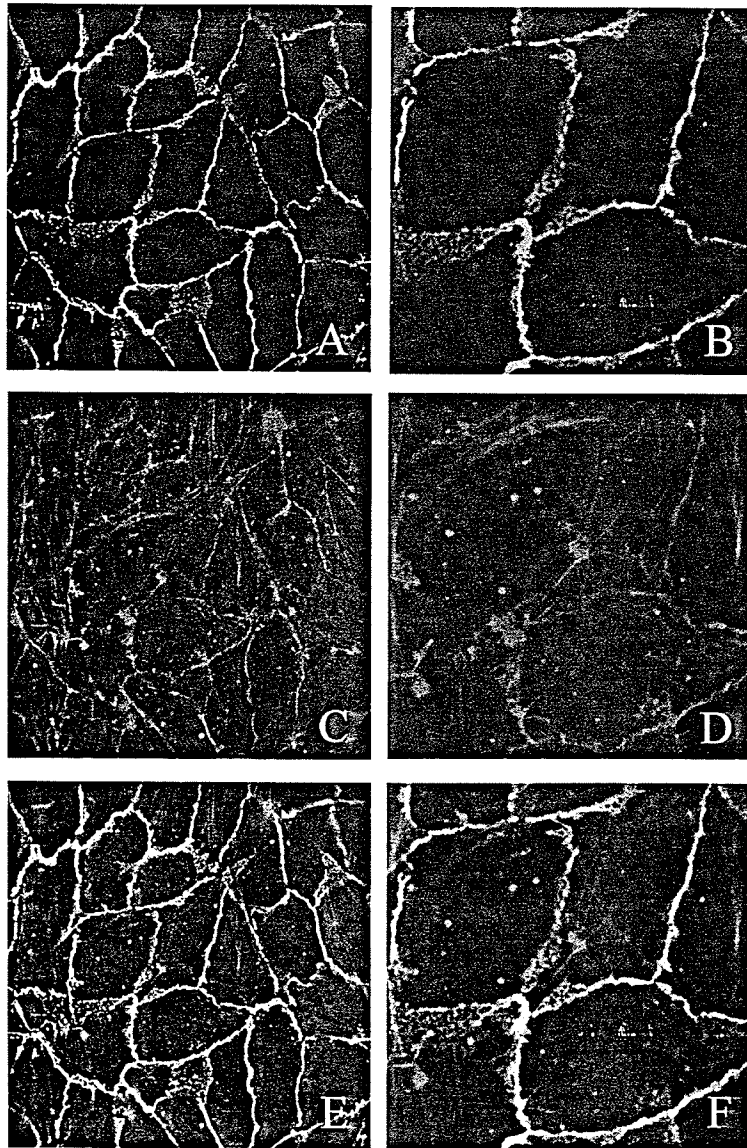


Figure 70. VEcadherin and rhodamine labelled phalloidin staining of HUVECs treated with 10ug/mL of GP1. Human umbilical vein endothelial cells (HUVEC) were treated with 10ug/mL of GP1 for 24 hours. Cells were stained with antibodies to VE-cadherin (A) and shown at higher magnification in (B) or with rhodamine labelled phalloidin in (C) and higher magnification in (D). Images were merged to show distribution of cellular actin within cells in (E) and higher magnification in (F). Images were acquired at 400X magnification.

(Figure 71)

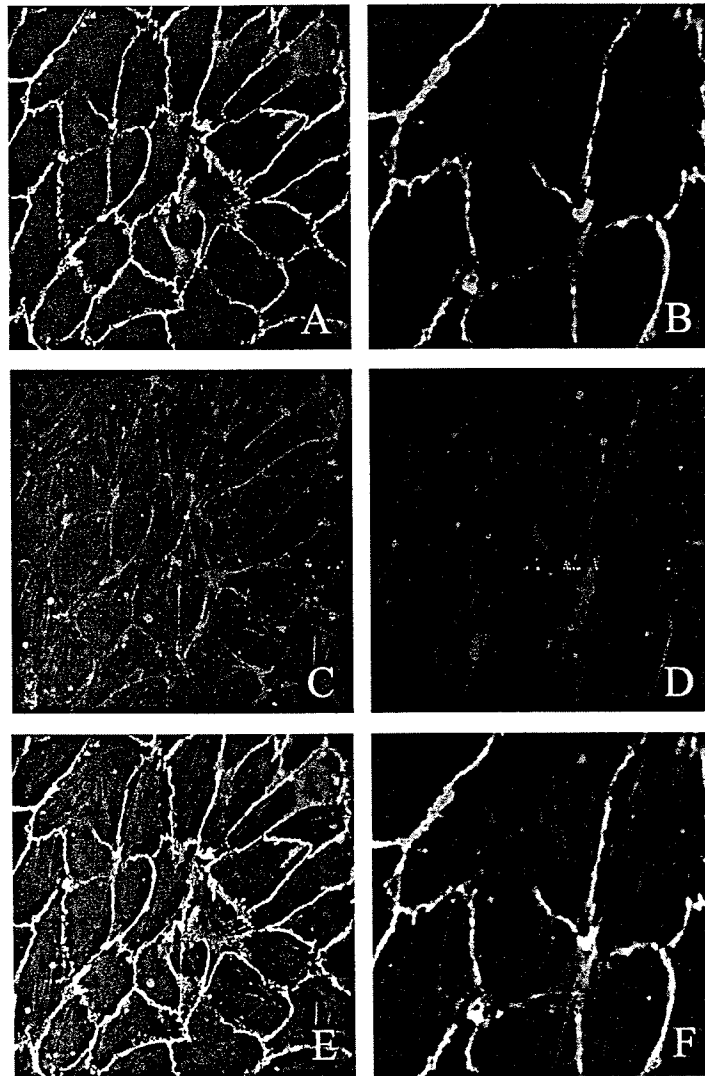


Figure 71. VEcadherin and rhodamine labelled phalloidin staining of HUVECs treated with 10ug/mL of sGP. Human umbilical vein endothelial cells (HUVEC) were treated with 10ug/mL of sGP for 24 hours. Cells were stained with antibodies to VE-cadherin (A) and shown at higher magnification in (B) or with rhodamine labelled phalloidin in (C) and higher magnification in (D). Images were merged to show distribution of cellular actin within cells in (E) and higher magnification in (F). Images were acquired at 400X magnification.

(Figure 72)

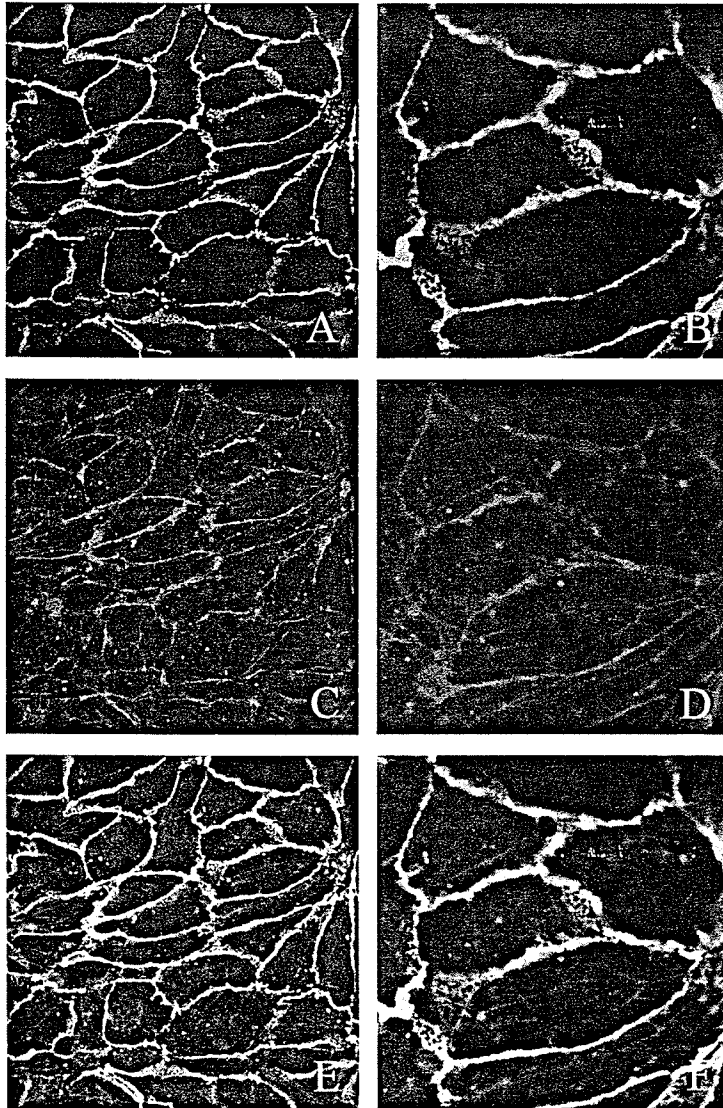


Figure 72. VEcadherin and rhodamine labelled phalloidin staining of HUVECs treated with 10ug/mL of pDisplay. Human umbilical vein endothelial cells (HUVEC) were treated with 10ug/mL of pDisplay for 24 hours. Cells were stained with antibodies to VE-cadherin (A) and shown at higher magnification in (B) or with rhodamine labelled phalloidin in (C) and higher magnification in (D). Images were merged to show distribution of cellular actin within cells in (E) and higher magnification in (F). Images were acquired at 400X magnification.

(Figure 73)

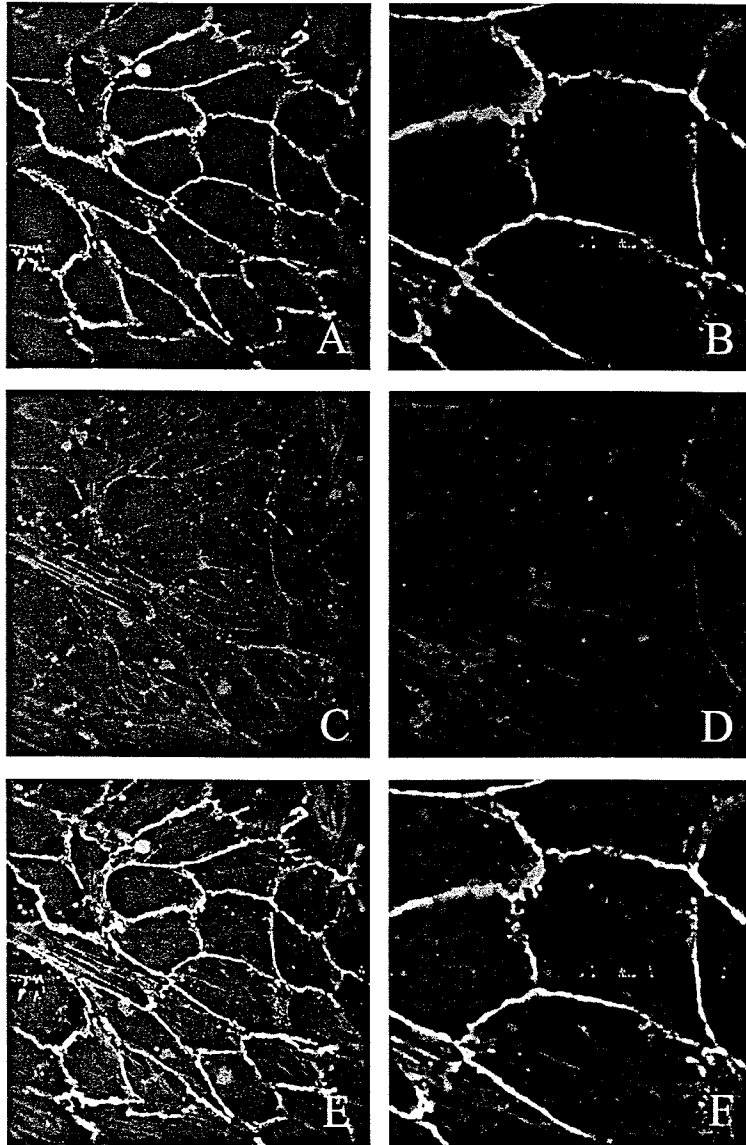


Figure 73. VEcadherin and rhodamine labelled phalloidin staining of HUVECs treated with 10ug/mL of HA peptide. Human umbilical vein endothelial cells (HUVEC) were treated with 10ug/mL of HA peptide for 24 hours. Cells were stained with antibodies to VE-cadherin (A) and shown at higher magnification in (B) or with rhodamine labelled phalloidin in (C) and higher magnification in (D). Images were merged to show distribution of cellular actin within cells in (E) and higher magnification in (F). Images were acquired at 400X magnification.

(Figure 74)

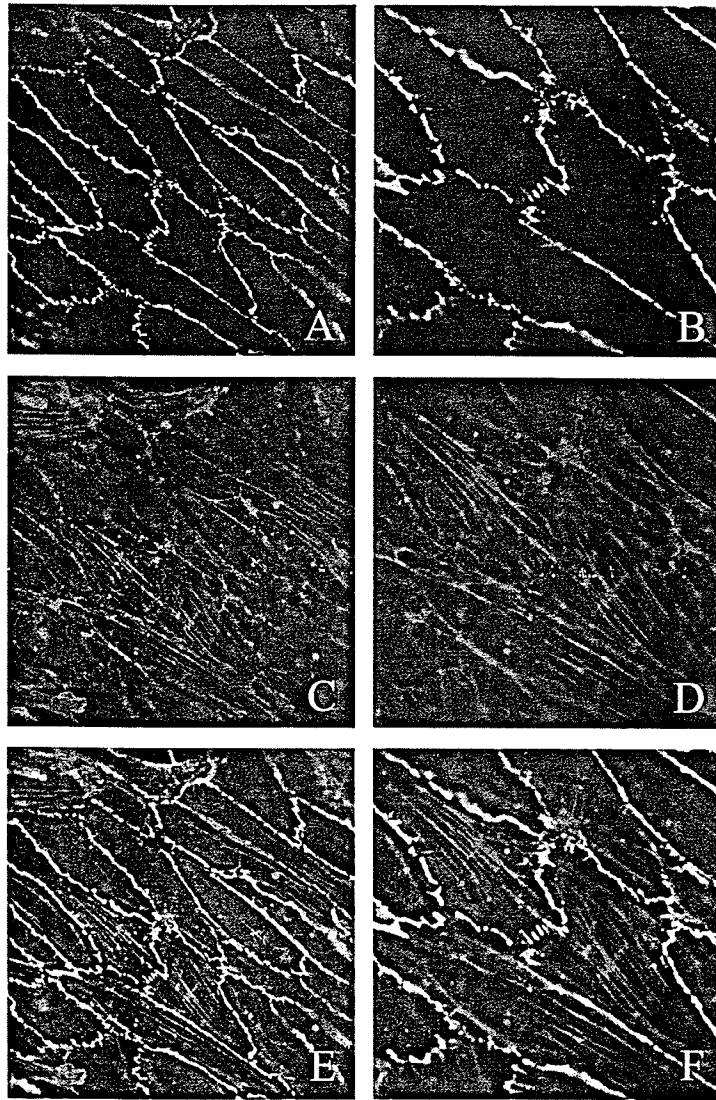


Figure 74. VEcadherin and rhodamine labelled phalloidin staining of HUVECs treated with 10ug/mL of rhTNF-alpha. Human umbilical vein endothelial cells (HUVEC) were treated with 10ug/mL of rhTNF-alpha for 24 hours. Cells were stained with antibodies to VE-cadherin (A) and shown at higher magnification in (B) or with rhodamine labelled phalloidin in (C) and higher magnification in (D). Images were merged to show distribution of cellular actin within cells in (E) and higher magnification in (F). Images were acquired at 400X magnification.

(Figure 75)

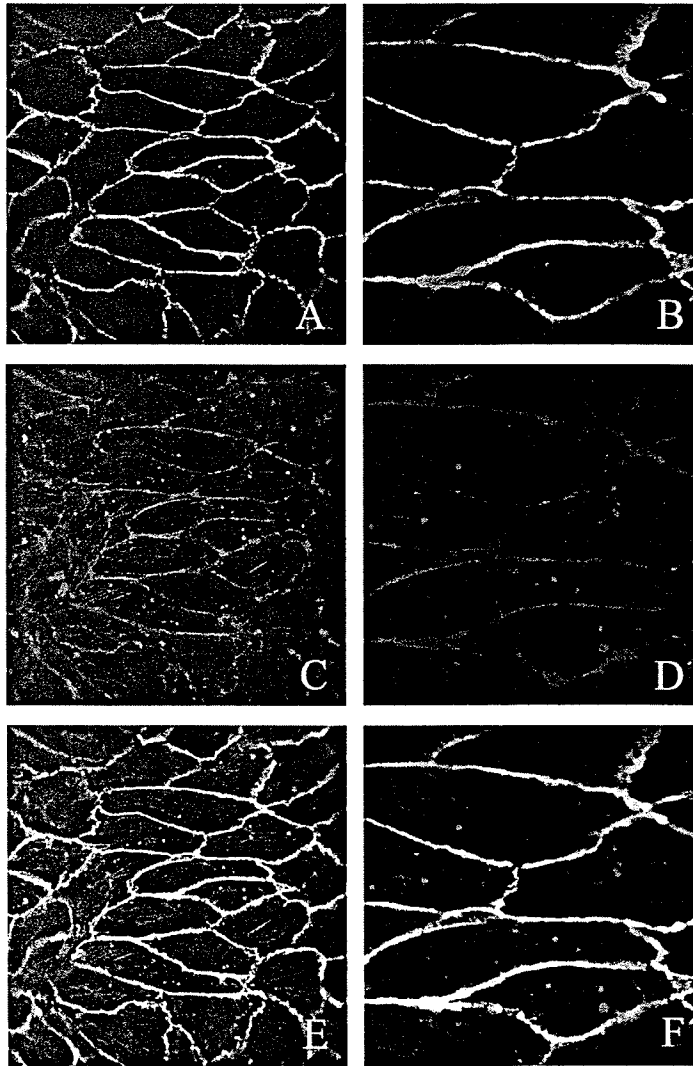


Figure 75. VEcadherin and rhodamine labelled phalloidin staining of untreated HUVECs. Untreated human umbilical vein endothelial cells (HUVEC) were incubated for 24 hours. Cells were stained with antibodies to VE-cadherin (A) and shown at higher magnification in (B) or with rhodamine labelled phalloidin in (C) and higher magnification in (D). Images were merged to show distribution of cellular actin within cells in (E) and higher magnification in (F). Images were acquired at 400X magnification.

(Figure 76)

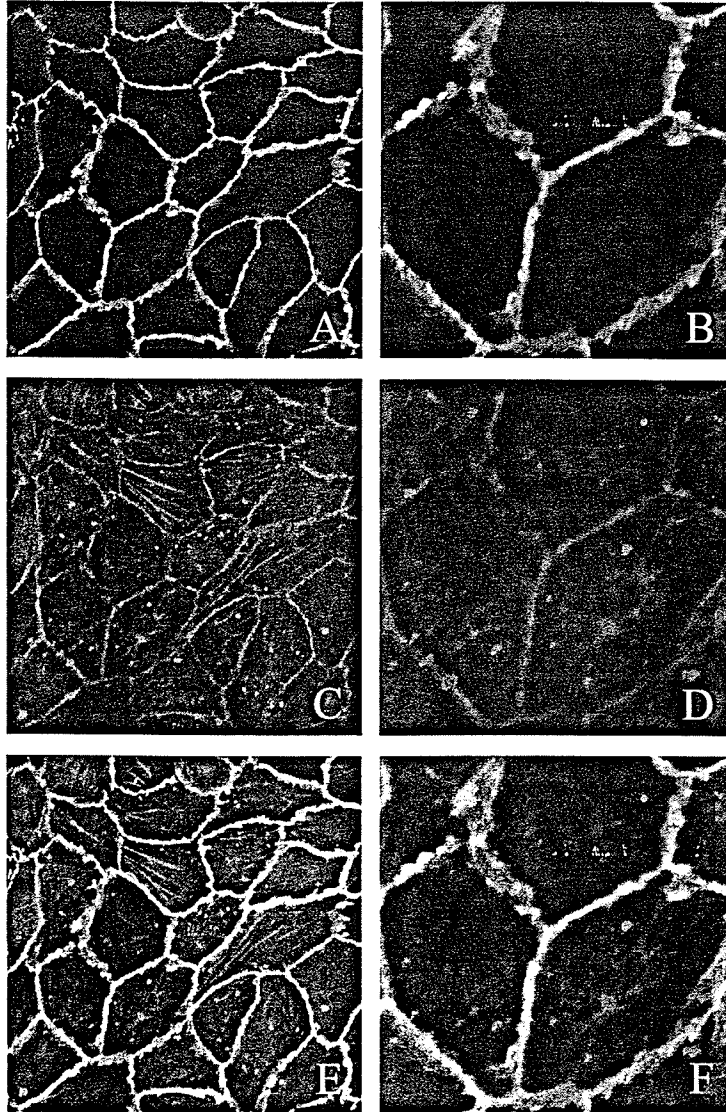


Figure 76. VEcadherin and rhodamine labelled phalloidin staining of HUVECs treated with 50ug/mL of GP1,2-delta-TM. Human umbilical vein endothelial cells (HUVEC) were treated with 50ug/mL of GP1,2-delta-TM for 24 hours. Cells were stained with antibodies to VE-cadherin (A) and shown at higher magnification in (B) or with rhodamine labelled phalloidin in (C) and higher magnification in (D). Images were merged to show distribution of cellular actin within cells in (E) and higher magnification in (F). Images were acquired at 400X magnification.

(Figure 77)

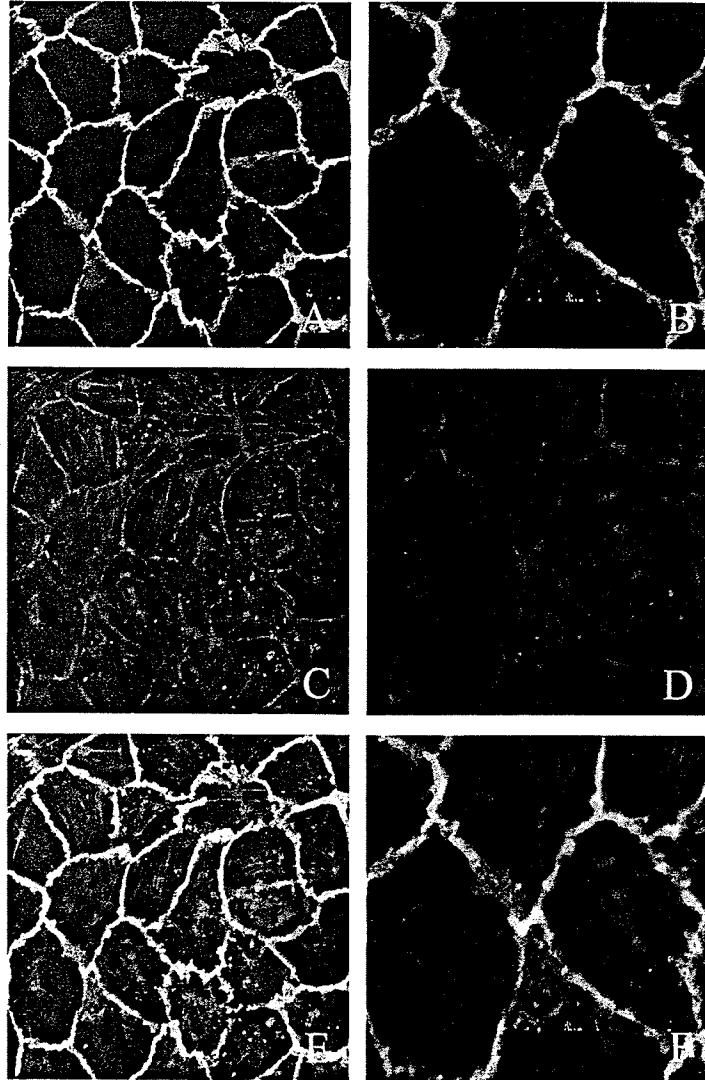


Figure 77. VEcadherin and rhodamine labelled phalloidin staining of HUVECs treated with 50ug/mL of delta peptide. Human umbilical vein endothelial cells (HUVEC) were treated with 50ug/mL of delta peptide for 24 hours. Cells were stained with antibodies to VE-cadherin (A) and shown at higher magnification in (B) or with rhodamine labelled phalloidin in (C) and higher magnification in (D). Images were merged to show distribution of cellular actin within cells in (E) and higher magnification in (F). Images were acquired at 400X magnification.

(Figure 78)

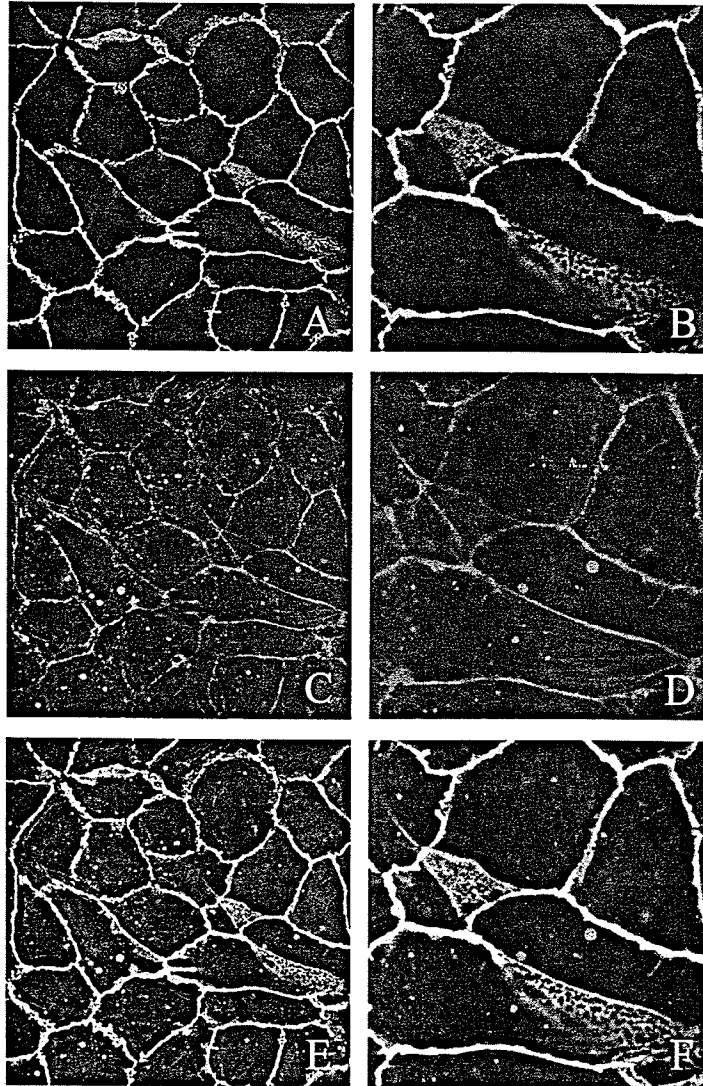


Figure 78. VEcadherin and rhodamine labelled phalloidin staining of HUVECs treated with 50ug/mL of GP1. Human umbilical vein endothelial cells (HUVEC) were treated with 50ug/mL of GP1 for 24 hours. Cells were stained with antibodies to VE-cadherin (A) and shown at higher magnification in (B) or with rhodamine labelled phalloidin in (C) and higher magnification in (D). Images were merged to show distribution of cellular actin within cells in (E) and higher magnification in (F). Images were acquired at 400X magnification.

(Figure 79)

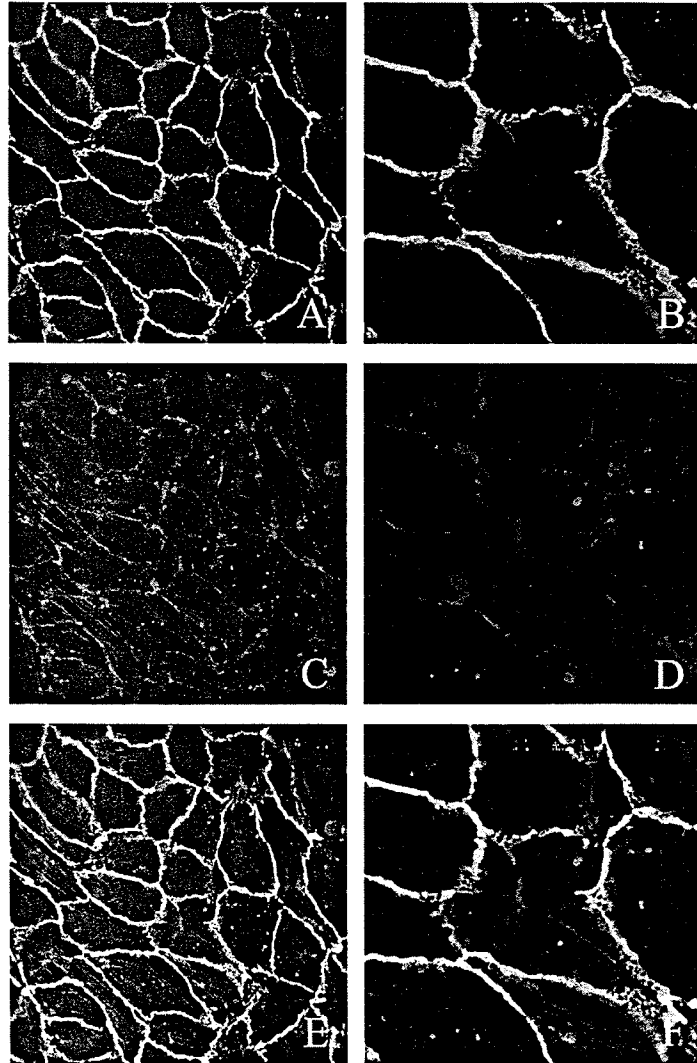


Figure 79. VEcadherin and rhodamine labelled phalloidin staining of HUVECs treated with 50ug/mL of sGP. Human umbilical vein endothelial cells (HUVEC) were treated with 50ug/mL of sGP for 24 hours. Cells were stained with antibodies to VE-cadherin (A) and shown at higher magnification in (B) or with rhodamine labelled phalloidin in (C) and higher magnification in (D). Images were merged to show distribution of cellular actin within cells in (E) and higher magnification in (F). Images were acquired at 400X magnification.

(Figure 80)

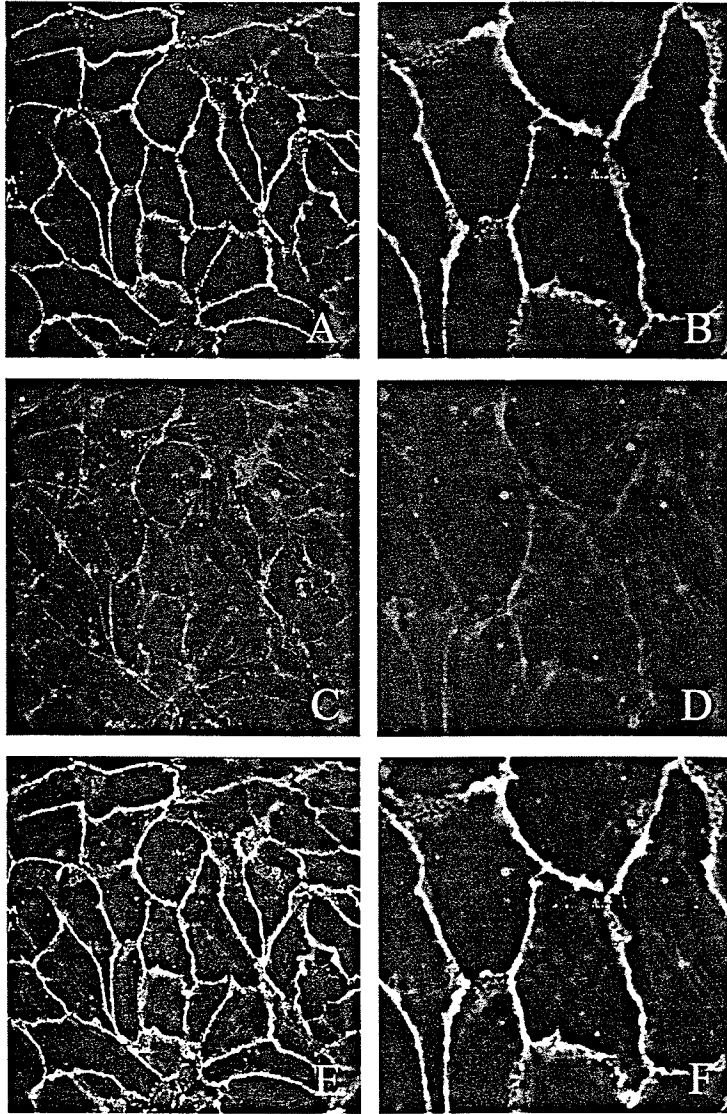


Figure 80. VEcadherin and rhodamine labelled phalloidin staining of HUVECs treated with 50ug/mL of pDisplay. Human umbilical vein endothelial cells (HUVEC) were treated with 50ug/mL of pDisplay for 24 hours. Cells were stained with antibodies to VE-cadherin (A) and shown at higher magnification in (B) or with rhodamine labelled phalloidin in (C) and higher magnification in (D). Images were merged to show distribution of cellular actin within cells in (E) and higher magnification in (F). Images were acquired at 400X magnification.

(Figure 81)

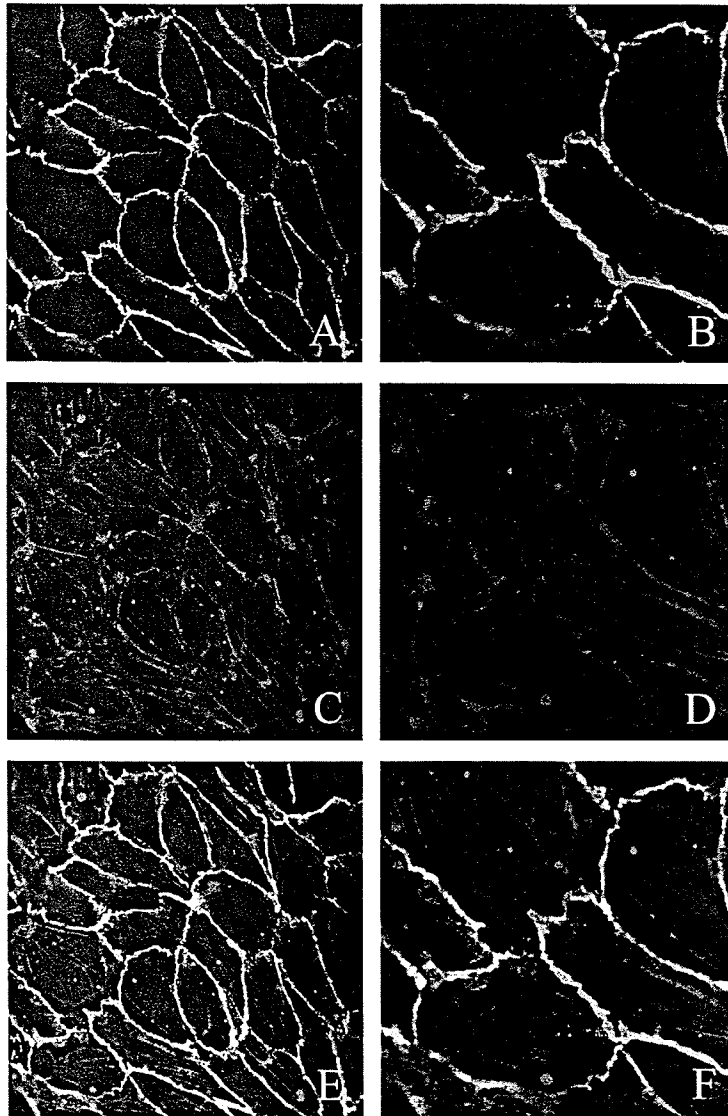


Figure 81. VEcadherin and rhodamine labelled phalloidin staining of HUVECs treated with 50ug/mL of HA peptide. Human umbilical vein endothelial cells (HUVEC) were treated with 50ug/mL of HA peptide for 24 hours. Cells were stained with antibodies to VE-cadherin (A) and shown at higher magnification in (B) or with rhodamine labelled phalloidin in (C) and higher magnification in (D). Images were merged to show distribution of cellular actin within cells in (E) and higher magnification in (F). Images were acquired at 400X magnification.

(Figure 82)

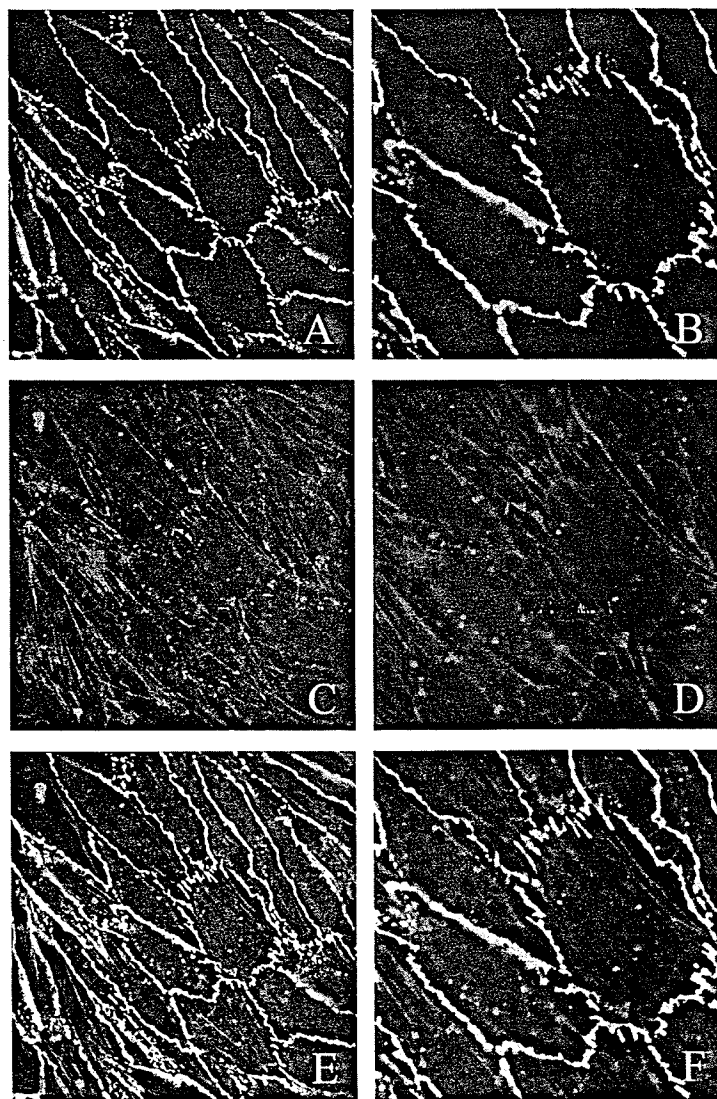


Figure 82. VEcadherin and rhodamine labelled phalloidin staining of HUVECs treated with 50ug/mL of rhTNF-alpha. Human umbilical vein endothelial cells (HUVEC) were treated with 50ug/mL of rhTNF-alpha for 24 hours. Cells were stained with antibodies to VE-cadherin (A) and shown at higher magnification in (B) or with rhodamine labelled phalloidin in (C) and higher magnification in (D). Images were merged to show distribution of cellular actin within cells in (E) and higher magnification in (F). Images were acquired at 400X magnification.

(Figure 83)

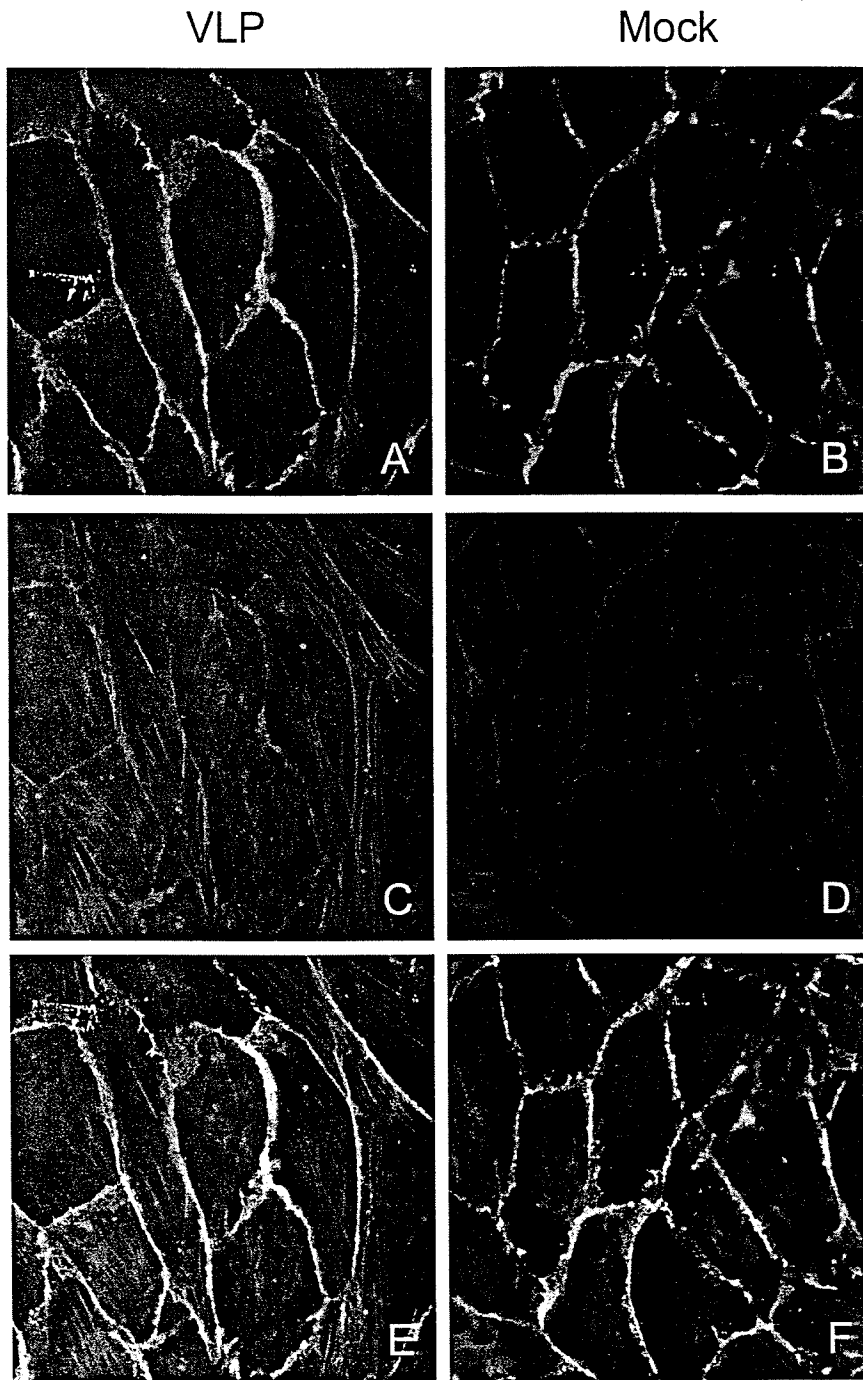


Figure 83. VEcadherin and rhodamine labelled phalloidin staining of HUVECs treated with VLPs or mock. Human umbilical vein endothelial cells (HUVEC) were treated for 24 hours. Cells were stained with antibodies to VE-cadherin (A & B) or with rhodamine labelled phalloidin in (C & D). Images were merged to show distribution of cellular actin within cells in (E & F). Images were acquired at 630X magnification.

(Figure 84)

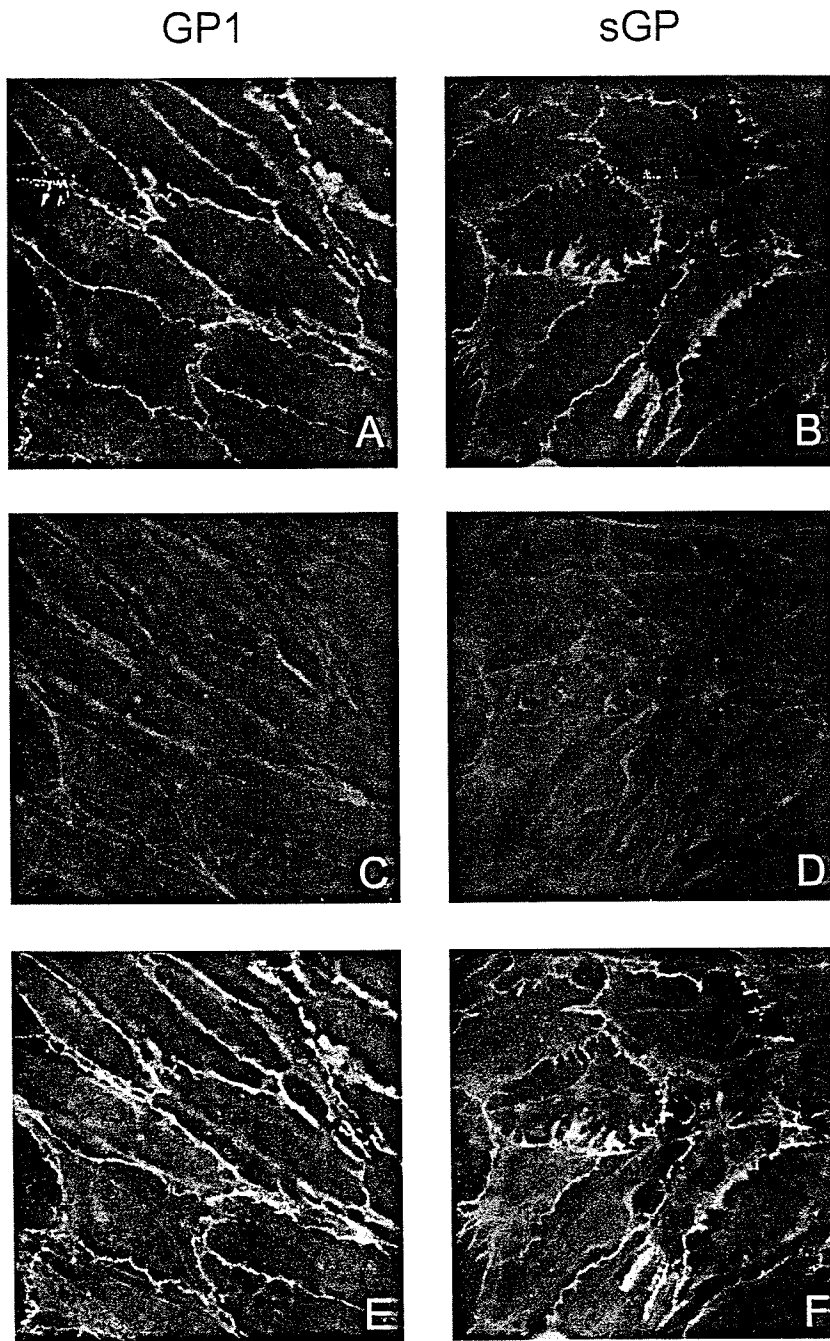


Figure 84. VECadherin and rhodamine labelled phalloidin staining of HUVECs treated with GP1 or sGP. Human umbilical vein endothelial cells (HUVEC) were treated for 1 hour. Cells were stained with antibodies to VE-cadherin (A & B) or with rhodamine labelled phalloidin in (C & D). Images were merged to show distribution of cellular actin within cells in (E & F). Images were acquired at 630X magnification.

(Figure 85)

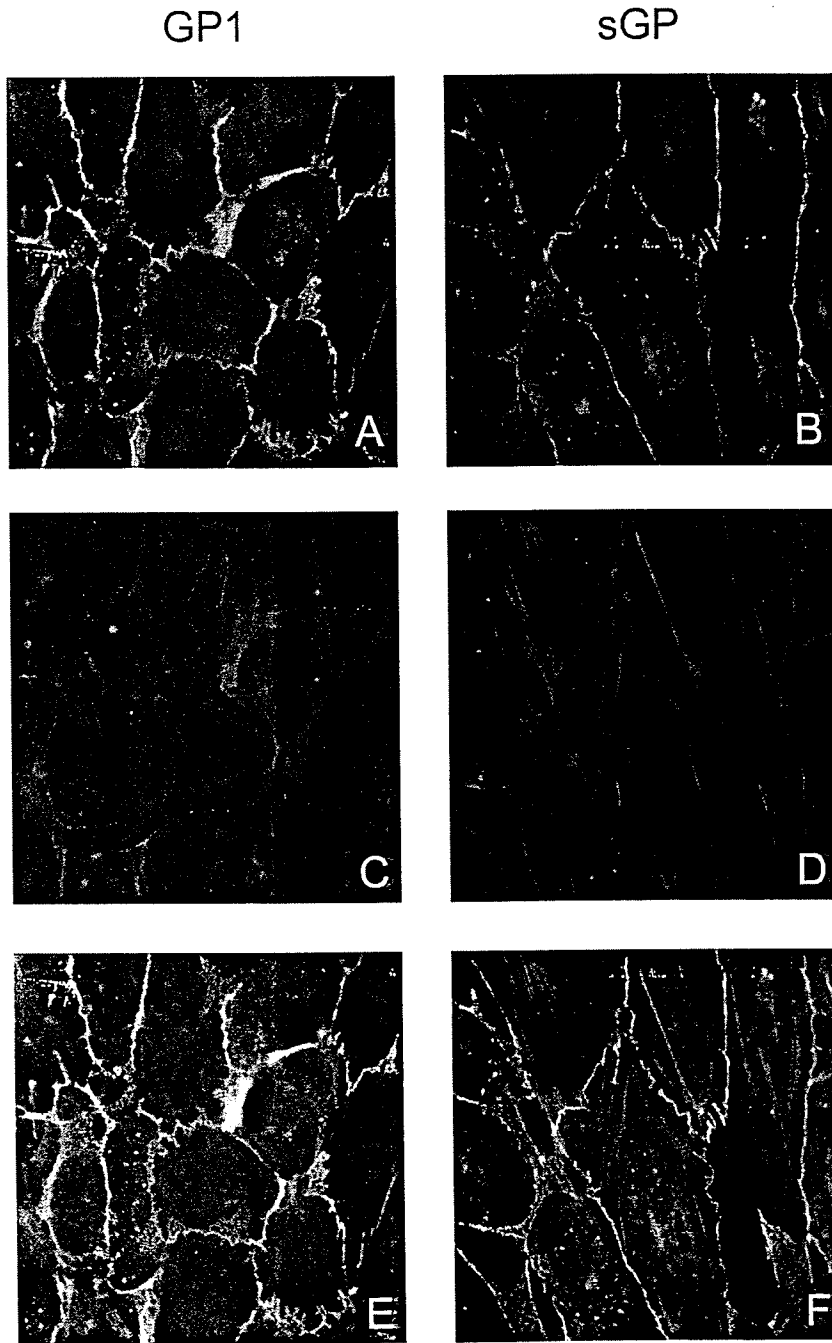


Figure 85. VEcadherin and rhodamine labelled phalloidin staining of HUVECs treated with GP1 or sGP. Human umbilical vein endothelial cells (HUVEC) were treated for 2 hours. Cells were stained with antibodies to VE-cadherin (A & B) or with rhodamine labelled phalloidin in (C & D). Images were merged to show distribution of cellular actin within cells in (E & F). Images were acquired at 630X magnification.